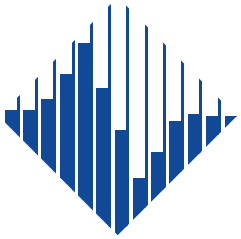

PACIFIC EARTHQUAKE ENGINEERING
RESEARCH CENTER

Cripple Wall Small-Component Test Program: Wet Specimens I

A Report for the "Quantifying the Performance of Retrofit of Cripple Walls and Sill Anchorage in Single-Family Wood-Frame Buildings" Project

Brandon Schiller
Tara Hutchinson
University of California San Diego

Kelly Cobeen
Wiss, Janney, Elstner Associates, Inc.

PEER Report 2020/16
Pacific Earthquake Engineering Research Center
Headquarters, University of California at Berkeley

November 2020

PEER 2020/16
November 2020

Cripple Wall Small-Component Test Program: Wet Specimens I

A Report for the "Quantifying the Performance of Retrofit of Cripple Walls and Sill Anchorage in Single-Family Wood-Frame Buildings" Project

Brandon Schiller

Tara Hutchinson

University of California San Diego

Kelly Cobeen

Wiss, Janney, Elstner Associates, Inc.

PEER Report No. 2020/16
Pacific Earthquake Engineering Research Center
Headquarters at the University of California, Berkeley

November 2020

ABSTRACT

This report is one of a series of reports documenting the methods and findings of a multi-year, multi-disciplinary project coordinated by the Pacific Earthquake Engineering Research Center (PEER and funded by the California Earthquake Authority (CEA). The overall project is titled "*Quantifying the Performance of Retrofit of Cripple Walls and Sill Anchorage in Single-Family Wood-Frame Buildings*," henceforth referred to as the "PEER–CEA Project."

The overall objective of the PEER–CEA Project is to provide scientifically based information (e.g., testing, analysis, and resulting loss models) that measure and assess the effectiveness of seismic retrofit to reduce the risk of damage and associated losses (repair costs) of wood-frame houses with cripple wall and sill anchorage deficiencies as well as retrofitted conditions that address those deficiencies. Tasks that support and inform the loss-modeling effort are: (1) collecting and summarizing existing information and results of previous research on the performance of wood-frame houses; (2) identifying construction features to characterize alternative variants of wood-frame houses; (3) characterizing earthquake hazard and ground motions at representative sites in California; (4) developing cyclic loading protocols and conducting laboratory tests of cripple wall panels, wood-frame wall subassemblies, and sill anchorages to measure and document their response (strength and stiffness) under cyclic loading; and (5) the computer modeling, simulations, and the development of loss models as informed by a workshop with claims adjustors.

This report is a product of *Working Group 4: Testing* and focuses on the first phase of an experimental investigation to study the seismic performance of retrofitted and existing cripple walls with sill anchorage. Paralleled by a large-component test program conducted at the University of California [Cobeen et al. 2020], the present study involves the first of multiple phases of small-component tests conducted at the UC San Diego. Details representative of era-specific construction, specifically the most vulnerable pre-1960s construction, are of predominant focus in the present effort. Parameters examined are cripple wall height, finish materials, gravity load, boundary conditions, anchorage, and deterioration. This report addresses the first phase of testing, which consisted of six specimens. Phase 1 including quasi-static reversed cyclic lateral load testing of six 12-ft-long, 2-ft high cripple walls. All specimens in this phase were finished on their exterior with stucco over horizontal sheathing (referred to as a "wet" finish), a finish noted to be common of dwellings built in California before 1945. Parameters addressed in this first phase include: boundary conditions on the top, bottom, and corners of the walls, attachment of the sill to the foundation, and the retrofitted condition. Details of the test specimens, testing protocol, instrumentation; and measured as well as physical observations are summarized in this report. In addition, this report discusses the rationale and scope of subsequent small-component test phases. Companion reports present these test phases considering, amongst other variables, the impacts of dry finishes and cripple wall height (Phases 2–4). Results from these experiments are intended to provide an experimental basis to support numerical modeling used to develop loss models, which are intended to quantify the reduction of loss achieved by applying state-of-practice retrofit methods as identified in *FEMA P-1100*, *Vulnerability-Base Seismic Assessment and Retrofit of One- and Two-Family Dwellings*.

ACKNOWLEDGMENT AND DISCLAIMER

ACKNOWLEDGMENT

This research project benefited from the interaction of many researchers and practitioners. In particular, the authors are grateful for the technical input and advice from all members of the PEER–CEA Project Team including Principal Investigator, Yousef Bozorgnia, Project Coordinator, Grace Kang, and members of the Working Groups, Jack Baker, Henry Burton, Greg Deierlein, Seb Ficcadenti, Bret Lizundia, Curt Haselton, Charlie Kircher, Thor Matteson, Frank McKenna, Vahid Mahdavifar, Silvia Mazzoni, Gilberto Mosqueda, Sharyl Rabinovici, Evan Reis, Chia-Ming Uang, John van de Lindt, Dave Welch, and Farzin Zareian. In addition, the authors are grateful for the technical input and advice from the Project Review Panel, which includes: Colin Blaney, Doug Hohbach, John Hooper, and Charlie Scawthorn.

The authors would also like to thank Dr. Chris Latham, Darren McKay, Noah Aldrich, Michael Sanders, Abdullah Hamid, Andrew Sanders, Sergio Suarez, Carla Tutolo, Derek McDanell, Edna Mariela, William Deeley, Selena Nichols, Armando Godoy-Velasquez, and all undergraduate students staffed at UC San Diego Powell Structural Labs for their continuous work in supporting the execution of the experimental program discussed herein.

DISCLAIMER

This research study was funded by the California Earthquake Authority (CEA). The support of the CEA is gratefully acknowledged. The opinions, findings, conclusions, and recommendations expressed in this publication are those of the authors and do not necessarily reflect the views of CEA, Pacific Earthquake Engineering Research Center (PEER), members of the Project Team, or the Regents of the University of California.

CONTENTS

LIST OF TABLES

LIST OF FIGURES

1 INTRODUCTION

1.1 DESCRIPTION OF PROJECT

This report is one of a series of reports documenting the methods and findings of a multi-year, multi-disciplinary project coordinated by the Pacific Earthquake Engineering Research Center (PEER) and funded by the California Earthquake Authority (CEA). The overall project is titled "*Quantifying the Performance of Retrofit of Cripple Walls and Sill Anchorage in Single-Family Wood-Frame Buildings*," henceforth referred to as the "PEER–CEA Project."

The overall objective of the PEER–CEA Project is to provide scientifically based information (e.g., testing, analysis, and resulting loss models) that measure and assess the effectiveness of seismic retrofit to reduce the risk of damage and associated losses (repair costs) of wood-frame houses with cripple wall and sill anchorage deficiencies as well as retrofitted conditions that address those deficiencies. Tasks that support and inform the loss-modeling effort are: (1) collecting and summarizing existing information and results of previous research on the performance of wood-frame houses; (2) identifying construction features to characterize alternative variants of wood-frame houses; (3) characterizing earthquake hazard and ground motions at representative sites in California; (4) developing cyclic loading protocols and conducting laboratory tests of cripple wall panels, wood-frame wall subassemblies, and sill anchorages to measure and document their response (strength and stiffness) under cyclic loading; and (5) the computer modeling, simulations, and the development of loss models as informed by a workshop with claims adjustors.

Within the PEER–CEA Project, detailed work was conducted by seven Working Groups, each addressing a particular area of study and expertise, and collaborating with the other Working Groups. The seven Working Groups are as follows:

Working Group 1: Resources Review

Working Group 2: Index Buildings

Working Group 3: Ground-Motion Selection and Loading Protocol

Working Group 4: Testing

Working Group 5: Analytical Modeling

Working Group 6: Interaction with Claims Adjustors and Catastrophe Modelers

Working Group 7: Reporting

This report is a product of the Working Group denoted in bolded text above.

The testing program of Working Group (WG) 4 focused on the first phase of an experimental investigation to study the seismic performance of existing[1] and retrofitted cripple walls with sill anchorage. Paralleled by a large-component test program conducted at University of California, Berkeley (UC Berkeley) [Cobeen et al. 2020], the present study involves the first of multiple phases of small-component tests conducted at University of California San Diego (UC San Diego).

1.2 BACKGROUND AND MOTIVATION OF THE STUDY

Single-family light-frame wood dwellings suffered extensive damage in previous earthquakes in California, notably the 1989 Loma Prieta earthquake and the 1994 Northridge earthquake. The 1989 Loma Prieta (M 6.9) was responsible for the causing significant structural damage to over 18,000 dwellings in the Bay Area, stretching from the San Francisco Marina District down to Watsonville. Over 500 dwellings were condemned and demolished in the aftermath; The Federal Emergency Management Agency (FEMA) estimated that the cost of physical damage was more than $6.7 billion. This estimate does not account for the long-term loss of business revenue, reallocation of resources, and many additional factors that likely increased the total cost by several times the initial FEMA estimate [Mahin 1991]. The 1994 Northridge earthquake (M 6.8) was responsible for even more extensive damage to structures given its proximity to the densely populated urban/suburban area of the San Fernando Valley located northwest of Los Angeles. It is estimated that the 1994 Northridge earthquake was responsible for an estimated $20 billion in damage to residential dwellings alone [Hall 1994]. The Earthquake Engineering Research Institute (EERI) [EERI 1996] reported that 56,119 residential units were damaged and of these, 29% or 16,269 units were red tagged. Figure 1.1 shows the number and distribution of red and yellow-tagged residential units reported by building inspectors. Many of the residential units affected by the Loma Prieta and Northridge earthquakes were single-family wood-frame dwellings built in or prior to the 1960s.

On August 24, 2014, the South Napa earthquake (M 6.0) caused damage to many single-family wood-frame dwellings throughout the area, which was alarming due to the earthquake being relatively moderate. Although most damage was non-structural, a large number of homes, predominately built pre-1950, suffered significant structural damage. Almost one in three houses built prior to 1950 received yellow or red tags from the city building department housing inspection [Rabinovici and Ofodire 2017].

[1] An important note regarding terminology: For the present report series, cripple walls in their "as-built" configuration are referred to as either "existing", "unretrofit", or "unretrofitted" cripple walls, all terms being synonymous. In addition, the terms "retrofit" and "retrofitted" are both used interchangeably to describe cripple walls to which sill anchorage and bracing have been added. No other types of seismic retrofit are considered in this Project, for instance chimney, roof, garage opening, or porch attachment changes. Additional information on terminology and definitions related to this Project can be found in a glossary appendix of the WG 7 Project Technical Summary [Reis 2020].

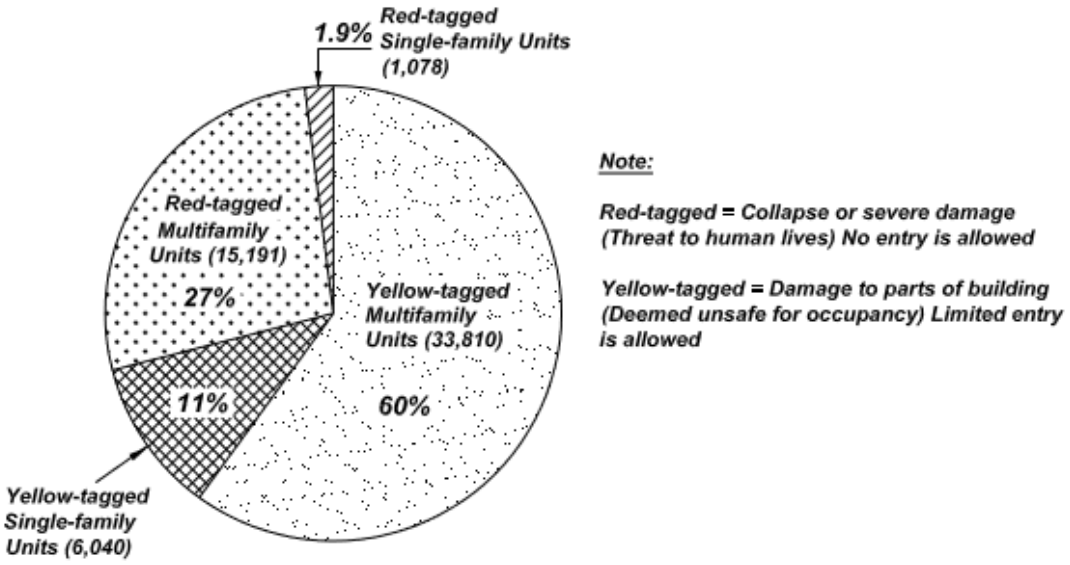

Figure 1.1 **Distribution of type of red- and yellow-tagged residential buildings in Los Angeles County following the 1994 Northridge earthquake (figure courtesy of EERI [1996]).**

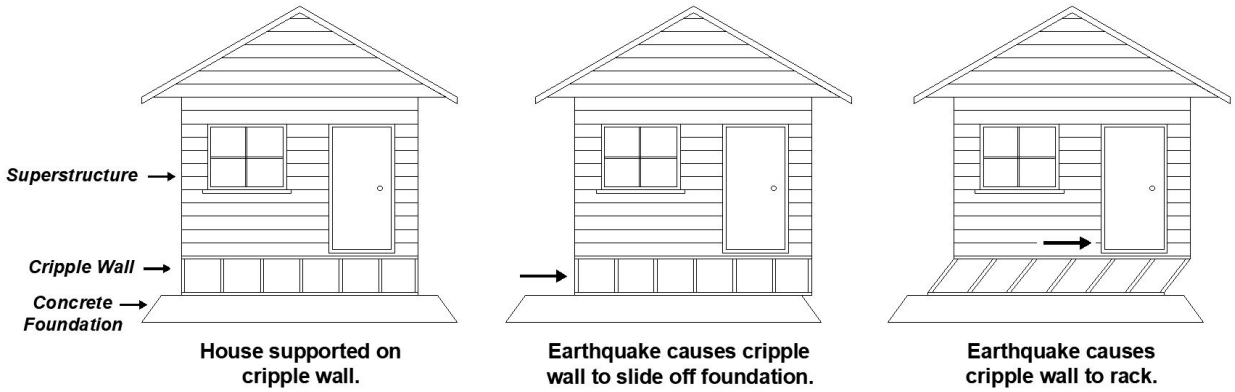

Figure 1.2 **Common earthquake induced failure modes of California's single-family wood-frame houses containing cripple walls.**

Older dwellings typically built prior to the 1960s and containing cripple walls and/or inadequate sill anchorage, suffered the most damage in these earthquakes. The primary culprit for damage was the "cripple wall," which is a short wood stud wall that encloses the crawl space under the first floor. Cripple walls are used to support a dwelling between its concrete foundation and the floor of the dwelling. These walls are usually 1–4 ft high (although cripple walls can be as tall as 6 ft) and are commonly used to: (a) provide a level surface for a house on uneven ground; (2) allow space to access utility lines; or create a workable basement area for a house. In older construction, cripple walls are covered with stucco or wood siding finishes, and often sheathed with wooden boards. They are responsible for carrying most of the gravity load of the house to the foundation. Importantly, cripple walls are commonly braced only by the finish materials, giving them little resistance to transfer lateral forces from the floors above the wall to the foundation,

such as would be imposed via inertial forces generated by an earthquake. In the event of high-intensity earthquake shaking, the unbraced cripple walls behave as a soft story, leading to the racking and collapse of the wall; see Figure 1.2. In addition to these weak cripple walls, many older homes contain limited or no anchorage of the foundation sill plate to the foundation. Due to this, common failure modes of single-family wood-frame dwellings during an earthquake also may include sliding of the house off of its foundation possibly leading to crushing and overloading to the cripple walls; see Figure 1.2.

In light of the failure modes of single-family dwellings common to both the 1994 Northridge and 1989 Loma Prieta earthquakes, there has been emphasis on retrofitting susceptible wood-frame dwellings. Retrofit methods include installation of oriented strand board (OSB) or plywood to the interior of the cripple walls, as well as addition of anchorage bolts to the sill, and attaching additional plates and/or framing angles to allow for the transfer of lateral load from the upper floors to the foundation. While the retrofitting methodology is understood and continues to be refined by FEMA-issued document, *FEMA P-1100 Vulnerability-Base Seismic Assessment and Retrofit of One- and Two-Family Dwellings* [FEMA 2018], the performance of retrofitted houses in the event of high-intensity shaking has limited experimental documentation. In addition, the performance of cripple wall finishes, such as stucco, wooden siding, and wood sheathing, in the event of high-intensity shaking has observed limited experimental investigation. Finally, while studies have been performed on cripple walls, they have focused on cripple walls 4 ft in height or less. While most cripple walls fall within this range, there are still a substantial portion of walls with heights more than 4 ft tall.

As another major seismic event is imminent in California, preparing the housing stock for such an event is of concern. California's major fault, the San Andreas Fault, has shown an ability to produce an 8.0+ magnitude earthquake. In 2008, the USGS modeled a 7.8 earthquake on the southern San Andreas Fault and estimated that the damage of such an event would cause around 1800 deaths and $213 billion in economic loses [Perry et al. 2008]. Due to this, the need to retrofit and ensure that dwellings are prepared for such an event is crucial.

1.3 FIELD OBSERVATIONS OF PAST CRIPPLE WALL FAILURES

There has been extensive documentation of the damage to single-family wood-frame dwellings due to the failure of cripple walls and inadequate sill anchorage through reconnaissance reports performed by EERI [Hall 1994], the Pacific Earthquake Engineering Research Center (PEER), the National Center for Earthquake Engineering Research (NCEER), and other institutions. This includes even recent earthquakes. For example, Figure 1.3 shows an example of a home with a collapsed cripple wall caused by the 2014 South Napa earthquake [Kang and Mahin 2014]. This house was built with ~2-ft-tall cripple walls and finished with wooden horizontal siding boards. The displacement of the entire house appears to be in excess of a foot. It can be seen that the cripple wall contained no lateral bracing to resist the inertial forces of the upper floor subjected to shaking. This large displacement led to a clear change in the elevation of the house relative to the doorstep, in addition to skewing of the patio railing. Consequently, the utility lines and piping suffered major damage as a result of the lateral and vertical displacements. Regardless of the state of the upper story of the house, there would be a significant repair costs associated with repositioning the house,

rebuilding the cripple wall, and replacing the nonstructural components inside and surrounding the house.

Figure 1.4 shows a foundation anchorage failure as a result of the 2019 Ridgecrest earthquake [Cobeen 2019]. In this case, the shaking caused sliding between the house and the foundation. In addition to the foundation anchorage failure at the cripple wall, the superstructure shows large cracks extending up the face of the stucco on the front of the house (note that these may not be as visible in the photograph at the present print scale). Besides these cracks and the foundation anchorage failure, the house appears to be relatively undamaged.

Due to the known seismic hazards associated with the low lateral capacity of an unbraced cripple wall, retrofitting methods have been developed and practiced for decades. One of the most commonly prescribed retrofits is installation of structural wood panels on the interior of the cripple wall, i.e., within the accessible crawl space. These panels are fastened with closely spaced nails along the edge and face. Damage statistics from single-family wood-frame houses from the 1989 Loma Prieta, 1994 Northridge, and 2014 South Napa earthquakes have shown the effectiveness of this simple and relatively inexpensive retrofit solution. For example, Figure 1.5(a) shows a one-story home in Alameda, California, built in the 1920s with a cripple wall as tall as 6 ft [Anderson-Niswander 2015]. The age of the house, height of its cripple wall, and location of the house make it extremely susceptible to catastrophic damage in the event of a near-field earthquake, like the 1989 Loma Prieta earthquake. Figure 1.5(b) shows cripple wall bracing utilized on the interior face of the cripple wall within this home, which is intended to minimize its potential for structural damage. While there are many examples of the benefits of retrofitting, an interesting direct comparison was noted by an architect who owned two identical homes in Santa Cruz, one retrofitted and one as-built and thus not retrofitted. During the 1989 Loma Prieta earthquake, the unretrofitted house's cripple wall collapsed, causing the house to shift laterally off of its foundation. The cost of repair for the house was $260,000 while the cost of repair for the retrofitted house was $5000 and included only cosmetic and nonstructural repair [Cook 2006].

Figure 1.3 **A view of a cripple wall collapse on an as-built house (top left), damage to the utility lines and gutter pipe (bottom left), and displacement as well as elevation change of the homes entrance stairs (top right) and patio railing (bottom right), 2014 Napa earthquake, Napa, California (image courtesy of Kang and Mahin [2014]).**

Figure 1.4 **Partial foundation anchorage failure at the cripple wall of a stucco house in Trona, California (image courtesy of Cobeen [2019]), 2019 Ridgecrest earthquake, Ridgecrest, California.**

(a)

(b)

Figure 1.5 **A 1920s one-story home in Alameda, California, with 6-ft-tall cripple walls finished with stucco over horizontal sheathing: (a) view of the front of the house; and (b) plywood panels providing lateral bracing on the interior of the cripple wall [photos courtesy of Anderson-Niswander [2015]).**

1.4 GUIDELINES FOR DESIGN AND RETROFIT OF CRIPPLE WALLS

1.4.1 FEMA Plan Set

Although there are examples such as those above of homeowners taking initiative to brace their cripple walls, formal guidelines to implement retrofits on unbraced cripple walls [IBHS 1995] were developed following the 1989 Loma Prieta and the 1994 Northridge earthquakes. Most recently, however, following the 2014 South Napa earthquake, FEMA developed a *Plan Set for Earthquake Strengthening of Cripple Walls in Wood-Frame Dwellings*, coined the *FEMA Plan Set*; these guidelines offered pre-engineered retrofit solutions to be used by contractors and homeowners [FEMA 2015]. Within these plans, seismic retrofitting of cripple walls consists of adding wood structural panels to the interior face of the cripple wall. These panels are attached with a prescribed nailing scheme and work to brace the cripple wall. Blocking plates are nailed to the sill plate allowing for an area to nail the wood panels. In addition to bracing of the cripple wall itself, inadequate sill anchorage is improved by adding or replacing deteriorated anchor bolts connecting the sill plate to the foundation. Finally, framing angles and post caps are installed to securely transfer the lateral loads from the first-floor diaphragm to the cripple wall. For taller cripple walls and two-story houses, the addition of tie-downs at each end of wood panels are used. A typical retrofit layout from the *FEMA P-1100* plan set is shown in Figure 1.6.

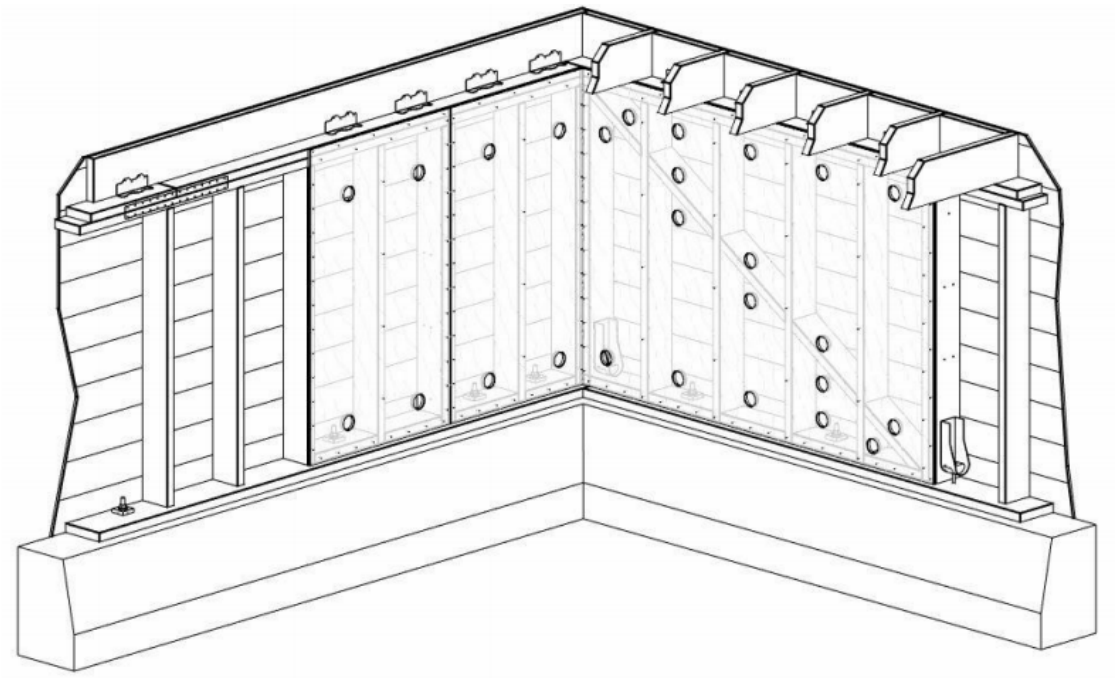

Figure 1.6 Retrofitted cripple wall corner from the FEMA Plan Set (image courtesy of FEMA [2015]).

1.4.2 Recent ATC-110 and *FEMA P-1100* Guidelines

The Applied Technology Council (ATC) 110 project—*Development of a Pre-Standard for Seismic Retrofit of One- and Two-Family Light Frame Dwellings*—provides recent criteria for the retrofit of cripple wall-supported dwellings [ATC 2014]. This guideline was adopted in the present project to assist in providing experimental evidence of the performance of a modern set of retrofit guidelines. During Phase 1 of the present CEA project, ATC-110 had yet to publish their finalized design guidelines but have since published "*FEMA P-1100 Vulnerability-Base Seismic Assessment and Retrofit of One- and Two-Family Dwellings*, [FEMA 2018]. The retrofit design used in Phase 1 of this experimental program closely resembles the finalized design criteria recommended in *FEMA P-1100*. In later phases of the test program, the FEMA plan set was available and adopted.

1.5 PREVIOUS RESEARCH

Previous earthquakes in California have shown that some residential wood-frame homes have suffered extensive damage due to the poor performance of cripple walls and sill anchorage. In light of this, research on the performance of retrofitted and unretrofitted cripple walls has been performed, but the range of test parameters remains limited, given the possible range of construction conditions. For example, following the 1989 Loma Prieta earthquake, two testing programs were initiated at the University of California Irvine (UC Irvine) that focused on the response of level cripple walls [Sheperd and Delos-Santos 1991; Steiner 1993]. Later, following the 1994 Northridge earthquake, the Consortium of Universities for Research in Earthquake Engineering (CUREE) and California Institute of Technology, under the auspices of the CUREE-Caltech Woodframe Project, performed a more extensive investigation of the seismic performance of wood-frame components and systems. Within this program, a testing effort was undertaken at the University of California Davis (UC Davis) that focused on the response of retrofitted and unretrofitted, level and stepped cripple walls [Chai et al. 2002]. In addition, the UC Davis tests endeavored to evaluate the behavior of stucco on wood-frame cripple walls. Subsequently, UC San Diego conducted a series of tests with support from the California Earthquake Authority and CUREE aimed at better understanding of the cyclic behavior of wood-frame walls to improve modeling techniques through implementation of boundary conditions that more accurately represented one and two-story houses [Arnold et al. 2003].

Outside of these efforts, very little experimental data is available that documents the seismic performance of cripple walls. Note: although many testing programs have been performed on wood-framed shear walls in general, the height-to-length of such walls typically ranges from 1 to 2 or more, which is considerably different from cripple walls, which have much smaller aspect ratios (in the range of 0.125 to 0.5). For smaller aspect ratios, the lateral response tends to be shear dominated, which is not the common case for full-height walls. Moreover, cripple walls tend to be less than 6 ft in height; while shear walls are on the order of 8 ft or taller. The following sections will summarize the most relevant results obtained from past testing programs, with a focus on those conducted specifically on cripple wall-sized specimens

1.5.1 Tests by Sheperd and Delos-Santos

The work of Sheperd and Delos-Santos [1991] is among the earliest test programs, which involved testing of seven 2-ft-tall × 16-ft-long level cripple walls (height-to-length aspect ratio of 0.125). This program examined the effectiveness of three retrofitting techniques applied to the interior of the cripple walls. The walls were all constructed with construction grade Douglas Fir and firmly anchored to the floor. The studs were toe-nailed into the bottom plate with 4–8d nails. The top plate was connected to the studs with 2–10d nails, and an additional top plate was connected to the top plate with a 16d nail at 16 in. on center. A uniform vertical load of 300 lbs/ft was applied to the upper top plate of the wall using sandbags. Reverse cyclic lateral loading was imposed to the upper top plate with increasing magnitude, followed by a monotonic push to failure. Five of the seven walls underwent retrofitting, while the remaining two remained "as-built." No exterior finishes were applied to any wall. Three retrofitting schemes were investigated, namely:

1. Two cripple walls were retrofitted by bracing four 1 × 6 nominal planks laid diagonally at a slope of 26° from the horizontal to the wall studs. The braces were attached to the studs and to the top and bottom plates with 2–10d nails.
2. One cripple wall was retrofitted by fastening five Simpson MST68 steel straps to the wall studs. The steel straps were 12-gauge, 2.06 in. wide and 48 in. long. Holes were drilled in the straps to allow for 2–10d nails to fasten the straps to studs.
3. Two cripple walls were retrofitted with plywood sheathing over the entire span of the cripple wall. The panels were 1/2-in.-thick (nominally) CDX plywood attached with 10d nails at 4 in. on center spacing along the edges and over the field.

Figure 1.7 shows the lateral load versus lateral displacement envelope curves for the seven cripple walls tested. The envelopes developed for the two as-built cripple walls show that these walls were very flexible. Maximum lateral loads achieved were 650 lbs and 700 lbs at lateral displacements of 0.988 in. and 0.954 in., respectively. This corresponds to a 4.1% and 4.0% drift ratio at peak load, respectively. Failure of the "as-built" cripple walls was attributed to the pullout of the toenails attaching the studs to the top and bottom plates.

All three of the retrofit schemes imposed on the cripple walls showed significant increases in the lateral stiffness and strength of the cripple walls compared with their "as-built" counterparts. By far the most effective retrofitting method in terms of increasing lateral strength and stiffness was the addition of plywood structural panels along the interior face of the cripple wall. Both of the plywood braced cripple walls achieved a peak lateral force of 20,000 lbs (an increase of over 2800% compared with the unretrofitted specimen), at lateral displacements of 0.96 in. and 1.06 in. or about a 4% drift ratio at peak load. This constitutes an increase in secant stiffness between about 20–40 times that of the as-built walls, depending on the displacement amplitude of interest. Cripple walls retrofitted with diagonal 1 × 6 planks showed a 30 times increase in peak-to-peak secant lateral stiffness at like force targets, and the cripple wall retrofitted with Simpson MST68 steel straps showed almost a 20 times increase in peak-to-peak secant lateral stiffness at like force targets, again compared with a bare frame cripple wall.

Failure of the plywood retrofitted cripple walls was attributed to slipping of the nails securing the plywood when the frame distorted as a parallelogram while the sheathing panel remained undeformed. For timber bracing, final failure involved gouging and splitting of the timber braces and the top and bottom plates. The use of steel straps proved to be the weakest of the retrofit schemes, which exhibited failure in the form of the steel strap buckling early in the test and with the nails pulling out on the studs and nail-heads shearing off on the straps.

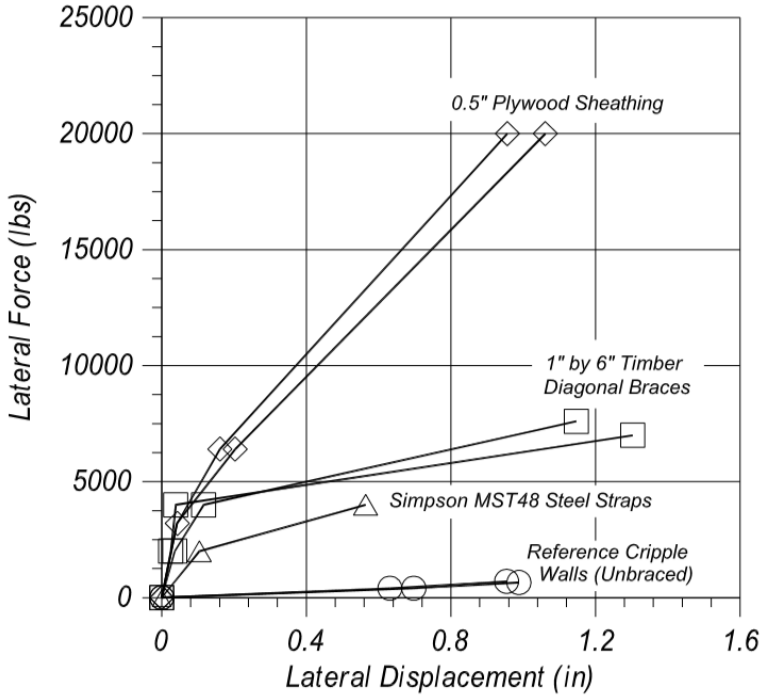

Figure 1.7 **Lateral load-deflection results from testing of [Sheperd and Delos-Santos 1991] five retrofitted and two "as-built" 2-ft-tall × 16-ft-long cripple walls (figure courtesy of Chai et al. [2002]).**

1.5.2 Tests by Steiner

A follow-up testing program on cripple wall retrofitted with wood structural panels was conducted at UC Irvine. Steiner performed tests on five level cripple walls retrofitted with 3/8-in.-thick (nominal) plywood and oriented strand board (OSB) [Steiner 1993]. The 3-ft tall × 6-ft long walls presented a much larger height-to-length aspect ratio than the Sheperd and Delos-Santos [1991] tests (0.5 compared with 0.125). The variables selected for these tests were the type of structural wood panel (plywood and OSB), the panel layout (a single panel with continuous nailing and a split-panel with blocking at mid-height), and driving of the nails (flush to the panel face and 60% of the nails overdriven 3/16 in.). No exterior finishes were attached to the cripple walls. The testing matrix is shown in Table 1.1, and the layout of the panels on the cripple walls is shown in Figure 1.8.

Table 1.1 Test matrix for level cripple walls tested by Steiner [1993].

Specimen	Parameters
1	Single panel without blocking- 3/8 in.-thick CDX plywood
2	Single panel without blocking- 3/8 in.-thick OSB
3	Split panel with blocking- 3/8 in.-thick CDX plywood
4	Split panel with blocking- 3/8 in.-thick OSB
5	Split panel with blocking- 3/8 in.-thick OSB and 60% of nails overdriven by 3/16 in.

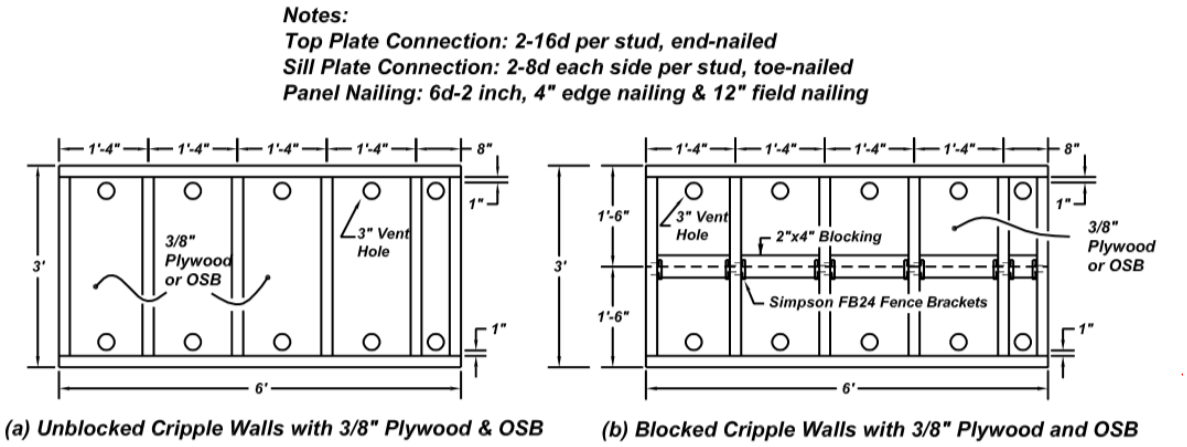

Figure 1.8 Wood structural panel layout with and without block tested by Steiner [1993] (figure courtesy of Chai et al. [2002]).

Unlike the Sheperd and Delos-Santos tests, the framing consisted of salvaged lumber from older homes. This required pre-drilling of the salvaged lumber to nail pieces together. The nailing pattern for framing and wood panel connection is indicated in Figure 1.8. Note: the use of 6d nails is uncommon in practice (generally 8d nails are used). The vertical load imposed was a 233 lbs/ft and uniformly distributed along the top of the wall using a concrete block. A servo-controlled hydraulic actuator imposed increasing magnitude lateral loads to the top plate of the wall at a frequency of 0.5 Hz.

The lateral load versus lateral deflection envelopes of the five tests are shown in Figure 1.9. Results show that the use of CDX plywood versus OSB in bracing walls caused little difference in the lateral response of the braced cripple walls, with exception being the unblocked frame braced with 3/8-in.-nominally-thick OSB that was stiffer than the other specimens but achieved a lower peak strength. The envelopes of the unblocked plywood cripple wall and the blocked OSB cripple wall were very similar, showing that the split-panel arrangement caused little difference in the lateral response of the cripple walls. Even with using smaller nails (6d versus 8d) for panel attachment, the primary cause of failure for the cripple walls was attributed to splitting of the sill plate. The specimen with 60% of the nails overdriven achieved the lowest peak strength, with a lateral strength reduction of around 20% compared with its counterpart, the unblocked frame braced with 3/8-in.-thick OSB and flush nails.

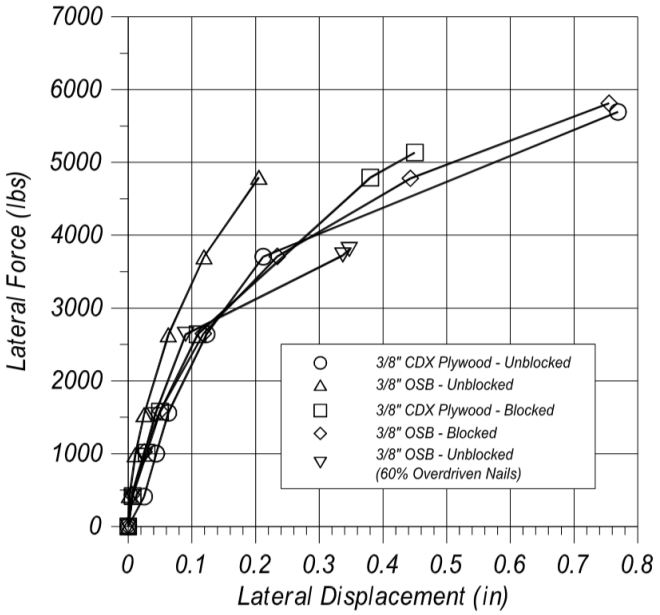

Figure 1.9 Lateral strength envelopes for five level cripple walls tested by Steiner [1993] (figure courtesy of Chai et al. [2002]).

1.5.3 Tests by Chai, Hutchinson, and Vukazich

As part of the CUREE-Caltech Woodframe Project, UC Davis conducted a testing program in 2002 involving 28 level and stepped, retrofitted and unretrofitted cripple walls [Chai et al. 2002]. Of the 28 specimens, 13 were level cripple walls either 2 ft or 4 ft in height and 12 ft in length, with height-to-length aspect ratios of 0.167 and 0.33, respectively. The remaining specimens were stepped cripple walls and thus not pertinent to the present effort. Besides cripple wall height and application of retrofit, the other parameters investigated of the level specimens were vertical load level, with and without stucco finish, percentage of bracing, and loading histories. The testing matrix for the 13 level cripple walls is shown in Table 1.2.

Two bracing percentages, defined as the length of the braced cripple wall divided by the nominal length of the cripple wall, were considered in the testing program. The two percentages of bracing evaluated were 66% and 100%. For the 66% bracing scheme, the middle 4 ft length of the cripple wall was not braced. Two vertical loads were implemented, namely 100 lbs/ft and 450 lbs/ft. These were meant to mimic the typical gravity load of a one- or two-story house, respectively. The lighter vertical load was used in combination with the 66% bracing, and the heavier vertical load was used in combination with the 100% bracing. The loading histories used were developed for the CUREE-Caltech Woodframe Project by Krawinkler et al. [2001]. The loading protocol was a deformation-controlled, quasi-static cyclic protocol representing near-fault and ordinary ground motions. The loading protocol for ordinary ground motions represented a probability of exceedance of 10% in 50 years, whereas the loading protocol for near-fault ground motions represented a probability of exceedance of 2% in 50 years. Unlike previous tests, the use of stucco as an exterior cripple wall finish was investigated. Construction details of the level cripple walls can be seen in Figure 1.10.

Table 1.2 **Test matrix for thirteen level cripple walls test performed at UC Davis within the CUREE-Caltech Woodframe Project [Chai et al. 2002].**

Specimen number	Wall height (ft)	Stucco (finish)	Bracing %	Gravity (lbs/ft)	Loading history
M	2	No	100	450	Monotonic
1	2	No	100	450	Ordinary
2	2	Yes	100	450	Ordinary
3	2	Yes	100	450	Near-fault
4	2	No	66	100	Ordinary
5	2	Yes	66	100	Ordinary
6	2	Yes	66	100	Near-fault
7	4	No	100	450	Ordinary
8	4	Yes	100	450	Ordinary
9	4	Yes	100	450	Near-fault
10	4	No	66	100	Ordinary
11	4	Yes	66	100	Ordinary
12	4	Yes	66	100	Near-fault

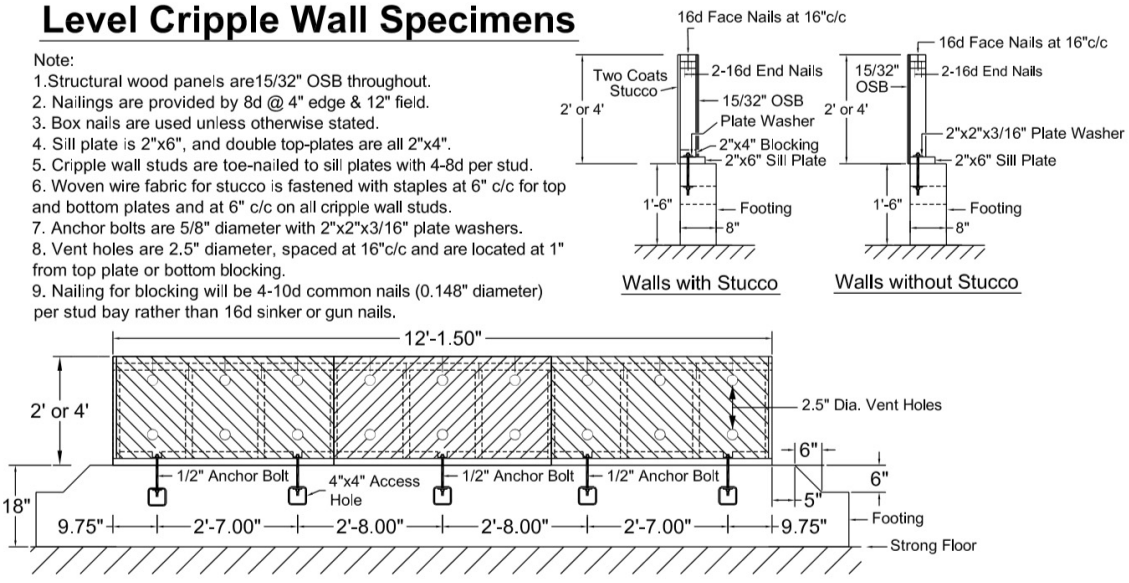

Figure 1.10 **Level cripple wall details tested at UC Davis within the CUREE-Caltech Woodframe project [Chai et al. 2002].**

Framing for the level cripple walls used #2 Douglas Fir besides the sill plate, which was pressure-treated Hemp Fir. Studs were connected to the sill plate with 4–8d toe-nails and connected to the top plate with 2–16d box nails per stud. An additional top plate was attached with a 16d nails at 16 in. on center. Wood structural panels were 15/32-in. OSB and attached with 8d nails at 4 in. spacing on edge and 12 in. spacing over the field. A two-layer stucco (scratch and brown

coat) was applied to eight of the cripple walls. Details on the installation of the stucco can be seen in Figure 1.11. The stucco consisted of a mixture of Type I-II cement and plaster sand without lime or expansive additives. Compressive strengths of the stuccos varied from 1880–2810 psi. The brown coat was applied five days after the scratch coat, and both were kept moist for two to three days following their application.

The lateral load was applied using a servo-controlled horizontal actuator attached to a stiff steel beam. An additional wood beam was fastened to the upper top plate allowing for the OSB panels to have unimpeded rotation. The loading was displacement controlled, pseudo-static reversed cyclic at a rate of 0.01 to 0.02 in/sec. The first test performed was a monotonic push of a 2-ft-tall cripple wall carrying a constant vertical load of 450 lbs/ft; see Figure 1.12. This test was used as to define the reference displacement to be imposed on the remaining 27 specimens, per the CUREE-Woodframe testing protocol [Krawinkler et al. 2001].

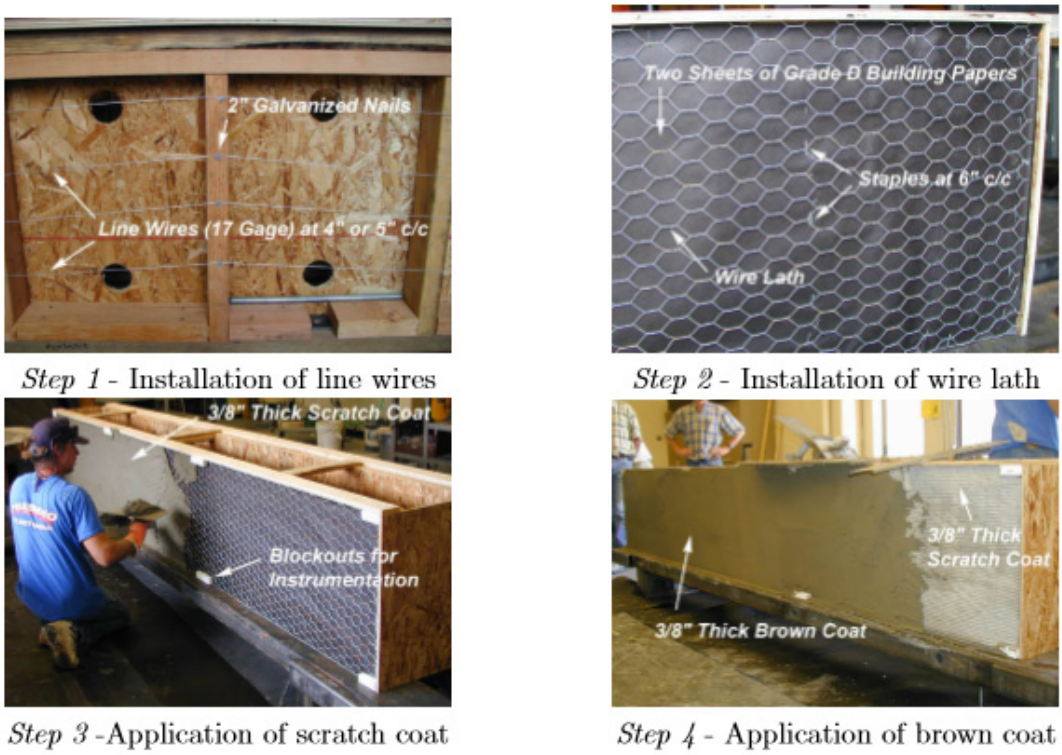

Figure 1.11 **Stucco installation and details from tests performed at UC Davis within the CUREE-Caltech Woodframe project [Chai et al. 2002].**

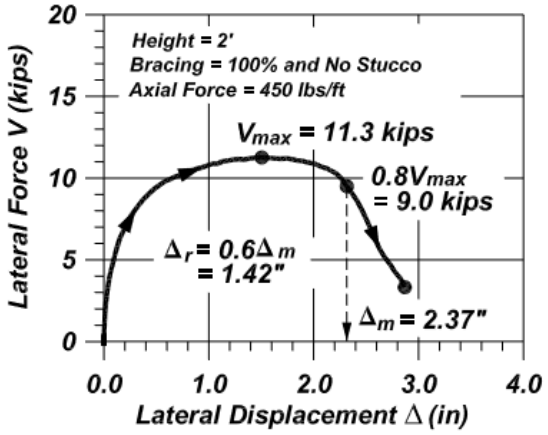

Figure 1.12 Reference displacements from the monotonic tests of a 2-ft-tall level cripple wall: tests performed at UC Davis within the CUREE-Caltech Woodframe project [Chai et al. 2002] (specimen M, per Table 1.2).

Results from these tests indicate that the influence of the two different load protocols had minimal effect on the lateral response of the cripple walls, noting less than a 10% increase in lateral strength for a near-fault test protocol compared with the ordinary motion protocol (per Krawinkler et al. [2001]). Cripple walls with OSB exhibited damage in the form of the OSB panels tearing along the edges and corners as the frame deformed as a parallelogram. For tests with a lighter vertical load, significant uplift of the walls studs and sheathing occurred, leading to splitting of the sill plate. Minor uplift also occurred for the heavier vertical load cases.

Figure 1.13 shows the lateral force versus lateral displacement response of two pairs of 2-ft-tall cripple walls with and without stucco finishes. One pair had 450 lbs/ft of vertical load and 100% bracing (Specimens 1 and 2), and the other pair had 100 lbs/ft of vertical load and 66% bracing (Specimens 4 and 5). For both pairs of specimens, the stucco contributed 0.35–0.36 kips per linear foot (plf) to peak strength. In the case of 4-ft-tall cripple walls, with and without stucco finishes, the stucco contributed 0.43–0.50 kips plf. Between all level and stepped cripple walls tested, the addition of a stucco finish accounted for about a 15% increase in capacity when compared with design recommendations from Section 8.4.10.2 of *FEMA-273* [FEMA 1997] stating that:

> *"Stucco has a yield capacity of approximately 350 pounds per linear foot. This capacity is dependent on the attachment of the stucco netting to the studs and the embedment of the netting in the stucco."*

Since this yield capacity is 80% of the ultimate capacity, these suggestions resulted in an ultimate capacity increase of 440 lbs plf, which were observed to be in line with that measured for the stucco-finished specimens. Figure 1.14 shows the lateral strength contribution of stucco for all cripple walls tested. The 2-ft-tall specimens show stucco strength contributions around 80 lbs plf less than the *FEMA-273* recommendations, while the 4-ft-tall specimens show a range of stucco strength contributions within the *FEMA-273* recommendations.

For the 2-ft-tall level cripple walls, the drift ratio at peak strength ranged from 4.3% to 6.3% in the push and pull directions of loading. In the case of 4-ft-tall level cripple walls, the drift ratio at peak strength ranged from 2.3% to 4% in the push direction and from 1% to 4% in the pull

direction. The lower end values were noted from the lighter vertical load specimens where the sill plate split early in the test due to the pronounced uplift of the wall at the sill plate. Cracking in the stucco was minimal for level cripple walls as it tended to move as a rigid unit with detachment precipitating from bottom edge staples.

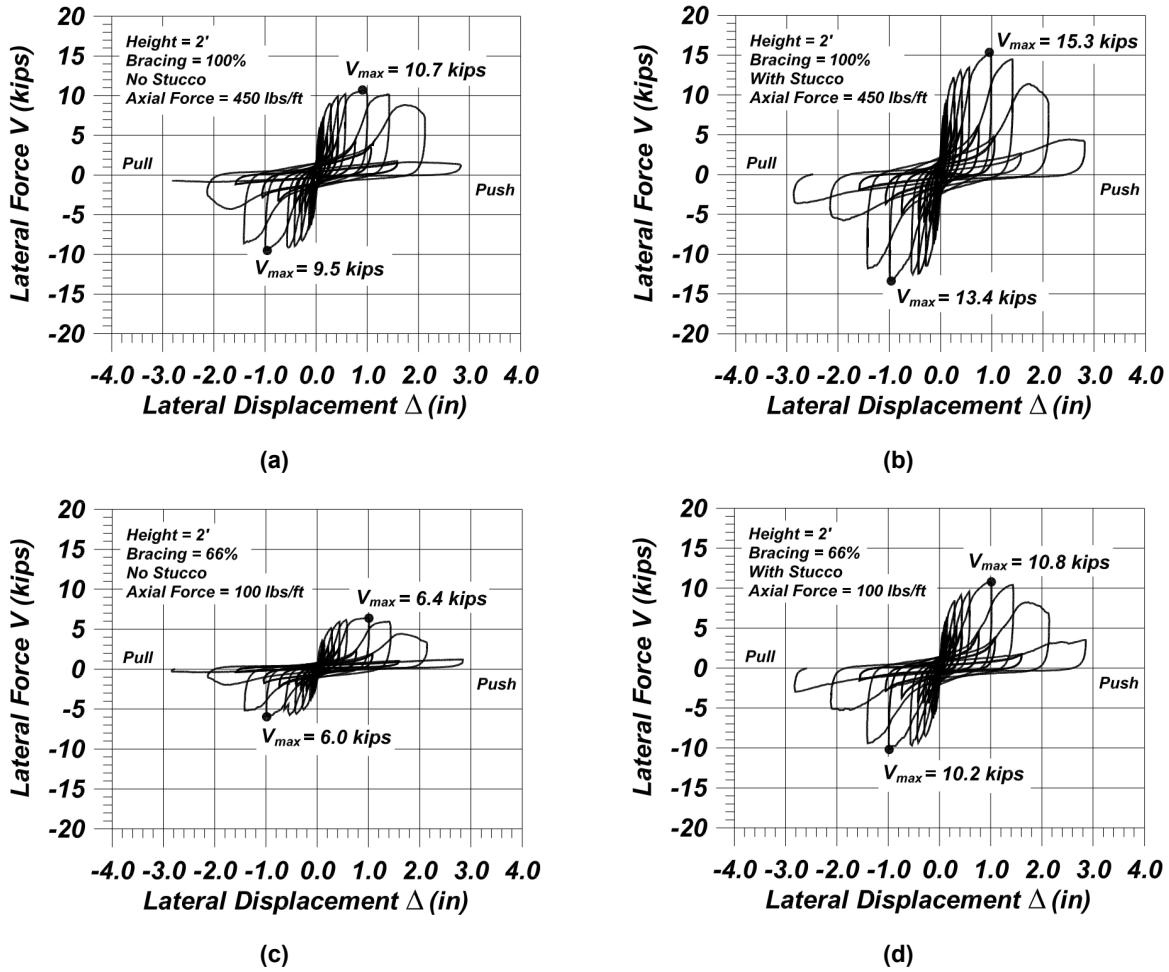

Figure 1.13 **Lateral force–lateral displacement response of pairs of 2-ft-tall cripple walls with and without stucco finishes (tests performed at UC Davis within the CUREE-Caltech Woodframe project) [Chai et al. 2003]: (a) Specimen 1; (b) Specimen 2: (c) Specimen 4; and (d) Specimen 5.**

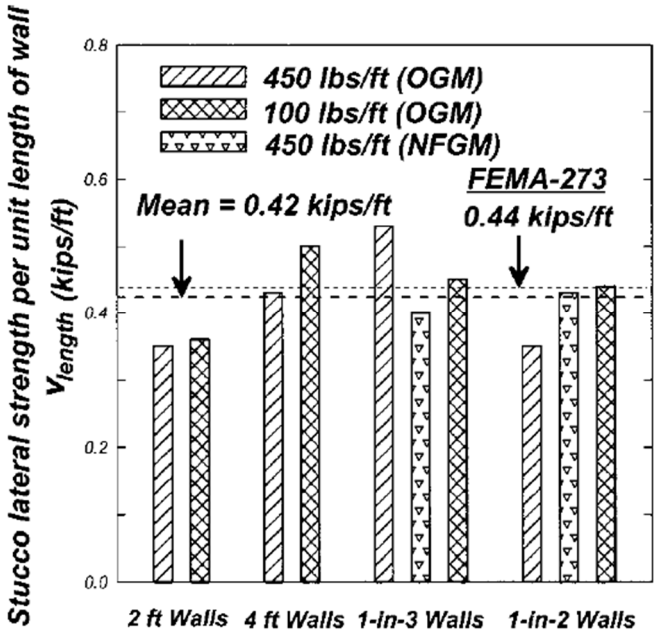

Figure 1.14 **Lateral strength contribution for walls with stucco finish (tests performed at UC Davis within the CUREE-Caltech Woodframe project) [Chai et al. 2003].**

1.5.4 Tests by Arnold, Uang, and Filiatrault

Following the CUREE-Caltech Woodframe project, a series of tests were performed at UC San Diego with support from the CEA to investigate the cyclic response of wood-frame walls having boundary conditions consistent with the first level walls of two-story structures [Arnold et al. 2003]. These tests were performed on 8-ft-tall × 16-ft-long shear walls (height-to-length aspect ratio of 0.5) with stucco exterior finishes and gypsum wallboard interior finishes. These tests are pertinent to the present research program as one goal was to understand the options for capturing continuity of the wall from floor to floor and at its ends. To investigate the influence of wall-end boundary conditions and seek the optimum construction method for the test specimens to mimic the behavior of walls as installed within a two-story dwelling, various boundary conditions were implemented; see Figure 1.15. The testing matrix is shown in Table 1.3, and the layout of the shear walls in shown in Figure 1.16.

At the top of each wall, the furring nail configuration connecting the stucco to the framing consisted of two rows of furring nails at 3-in. spacing on center along a 2 × 8 wooden loading plate and the upper top plate. The use of a denser furring nail spacing was intended to mimic the continuity of stucco extending from the first to the second floor of an actual home. The stucco used was a 7/8 in., three-coat application, i.e., 3/8-in. brown coat, 3/8-in. scratch coat, and 1/8-in. finish coat, with compressive strengths of 2200, 1600, and 380 psi, respectively. In addition, typical corner construction was used at the specimen ends with the purpose of simulating intersecting walls in an actual home.

These boundary conditions were developed following results from a previous study done at UC San Diego by Gatto and Uang [2002] as a part of the CUREE-Caltech Woodframe Project.

This study focused on the response of a series of 8-ft-tall square frames with different sheathing configurations, loading protocols, and loading rates. Stucco was considered in two tests and was attached with 1-1/4-in.-wide crown staples at 6 in. on center along framing members. The shear walls contained no corners and no dense fastening arrangement of the stucco at the top of the walls.

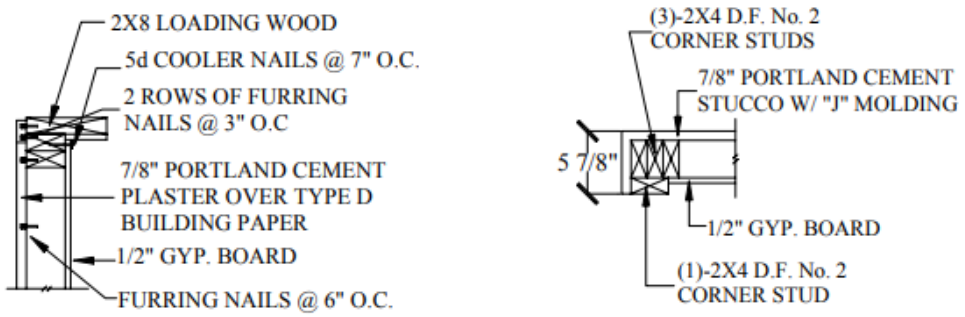

Figure 1.15 **Top and corner boundary condition details of shear walls tested by Arnold et al. [2003]: (a) top plate section; and (b) plan view of corner stud construction.**

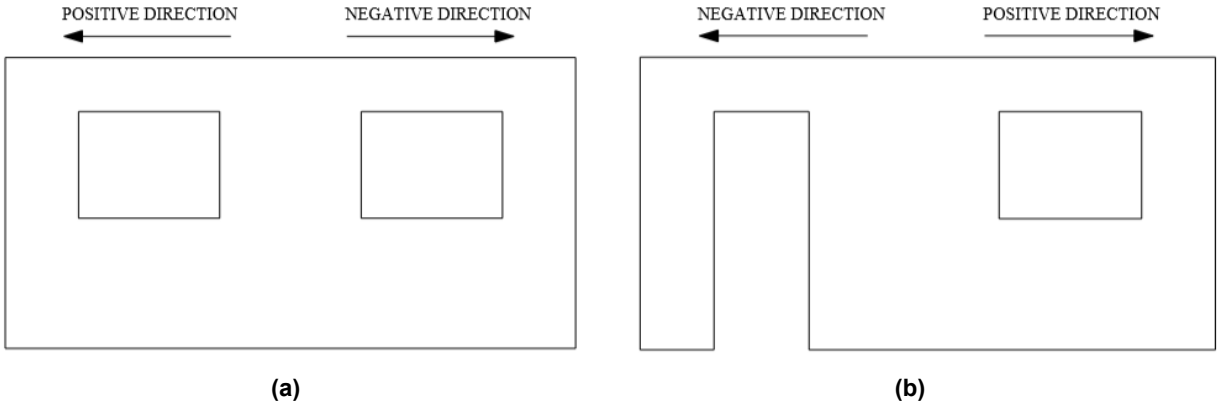

Figure 1.16 **Loading direction and stucco finish layout of shear walls tested by Arnold et al. [2003]; (a) stucco layout for Specimens 2 and 3; and (b) stucco layout for Specimens 2 and 4.**

Table 1.3 **Testing matrix for tests by Arnold et al. [2003].**

Test no.	Specimen designaton	Openings	Testing method
1	1	Two windows	CUREE protocol to failure
	2	One window, one door	
2	3	Two windows	CUREE protocol to failure, 4-stage testing
	4	One window, one door	

The loading protocol implemented was consistent with that of tests done by Chai et al. [2002] per the CUREE-Caltech Woodframe Project. The load implementation was displacement controlled, with cyclically reversed static loading applied with a servo-controlled actuator placed at one-third of the wall's height. A 450 lbs/ft vertical load, typical of a two-story home, was imposed, with three-point loads on a steel loading beam attached to a 1/2-in. section of plywood resting on the 2 × 8 wooden loading plate. Details of the test setup are shown in Figure 1.16. The implementation of a denser furring nail-spacing and built-up corner resulted in a response stiffer and stronger than test specimens absent the enhanced boundary conditions used in the Gatto and Uang [2002] study. Thus, it was believed that should continuity be envisioned in the scenario under consideration, it is worthwhile to consider enhancing an individual specimen's boundary conditions. This aspect of detailing was evaluated during Phase 1 of the test program specific for cripple walls and is discussed in greater detail in the present report.

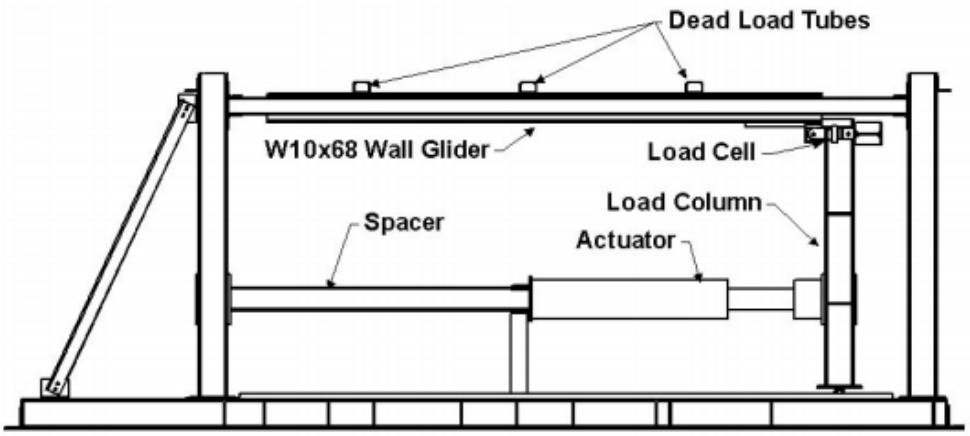

Figure 1.17 Testing frame setup for tests by Arnold et al. [2003].

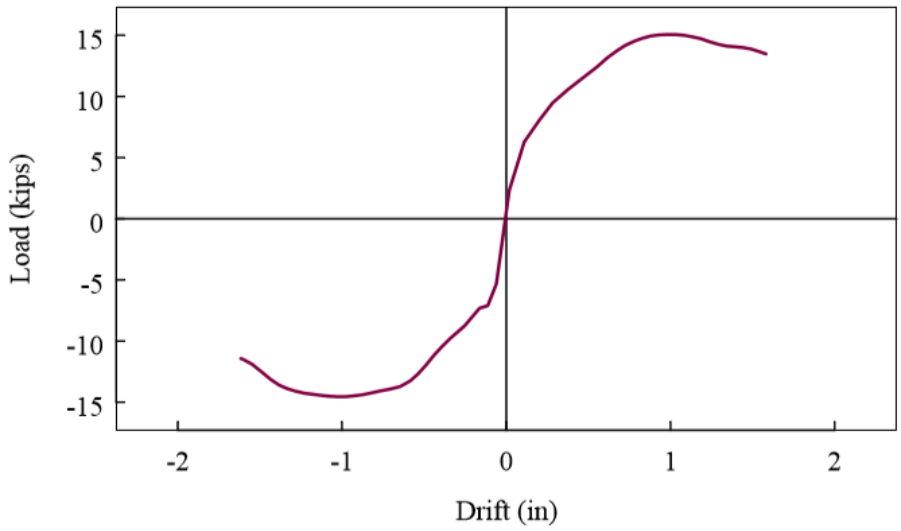

(a) Specimen 1

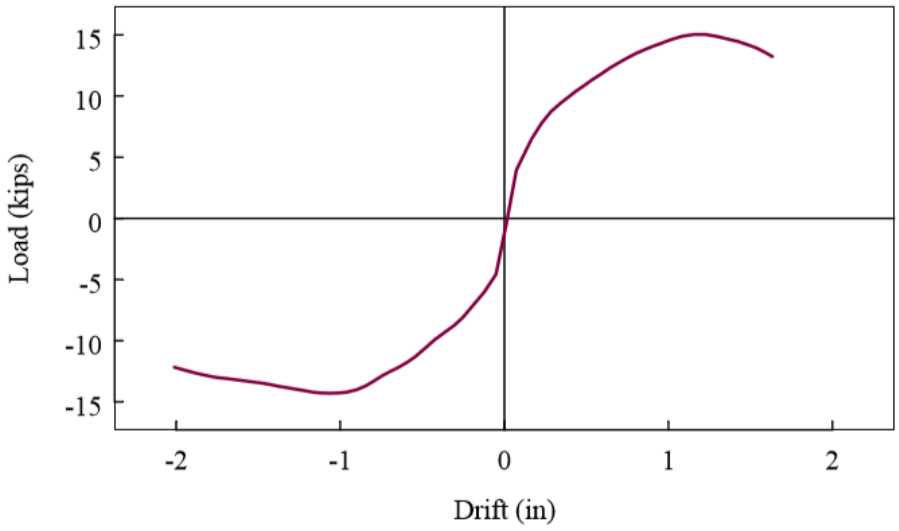

(b) Specimen 2

Figure 1.18 Lateral force –lateral displacement envelope for Specimens 1 and 2 of tests by Arnold et al. [2003]; (a) Specimen 1 and (b) Specimen 2.

1.6 SCOPE OF THIS STUDY AND ORGANIZATION OF REPORT

To augment the current understanding of cripple wall behavior, in this work, four phases of full-scale component tests on model cripple walls were performed. A consistent wall length, framing plan, and foundation setup were utilized for each testing regimen. It is envisioned that results from this experimental program will provide numerical modelers with useful response data to develop larger models of housing units to determine with confidence whole-dwelling seismic performance. Termed the *Cripple Wall Small-Component Tests*, the present program concentrates on characterizing the load-deflection behavior of level cripple walls, both unretrofitted (i.e., as-built) and retrofitted, using the *FEMA P-1100* guidelines. The program consists of 28 tests conducted in

four distinct phases. Test variables included cripple wall finishes, boundary conditions, height, and retrofitted or unretrofitted conditions. The cripple wall finishes were driven by common styles of finishes observed in various eras of California housing construction. The experimental program contains many similarities with the UC Davis CUREE testing program, while expanding on the database of knowledge derived from the prior level cripple wall tests. The current report is the first in a series of four reports, presenting findings from the first phase of these tests. Subsequent reports will document Phases 2–4. This report is organized as follow:

- Chapter 2 presents the details of the overall four-phased testing program performed including the test variables and the justification for their selection. The test matrix for Phase 1 is specifically described. Subsequently, the testing setup and loading protocol utilized for Phase 1 are described. Finally, the protocol for collecting data from all tests and documenting damage to the cripple walls is discussed;
- Chapter 3 describes the specific details of each specimen within test Phase 1. In addition, a visual documentation of the construction of the cripple walls is provided. The strategy for the test setup is presented. Finally, the layout of instrumentation used to acquire data for each test is presented;
- Chapter 4 presents the results of each specimen tested in Phase 1. Included in these results is the load-deflection response of each specimen. Plots of other important measurements such as anchor bolt load, relative displacement measurements, distortion within panel segments of the wall specimens, and vertical displacement of the wall are also presented;
- Extensive documentation of the physical damage to each cripple wall specimen is provided in Chapter 5. Visually documented damage is correlated with key attributes of the measured load-deflection curves is provided in Chapter 4; and
- Finally, Chapter 6 provides concluding remarks regarding observations from the Phase 1 test program.

2 SCOPE OF OVERALL TEST PROGRAM

2.1 OVERALL PEER–CEA (WORKING GROUP 4) TEST PROGRAM

The experimental program within the PEER–CEA Project was executed at UC San Diego and UC Berkeley: (1) UC San Diego's program consisted of testing only cripple-wall assemblies denoted as the *small-component testing program*; and (2) UC Berkeley tested cripple wall and first-floor assemblies, denoted as the *large-component testing program* [Cobeen et al. 2020]. Scaling of results from the small-component tests was undertaken to capture results for similarly detailed specimens from test results of the large-component tests [Cobeen et al. 2020]. In addition, UC Berkeley tested load path connections between the foundation sill plate and the foundation, and between the cripple wall top plate and the floor framing above. Finally, UC Berkeley tested combined materials in occupied stories. These tests were intended to characterize the hysteretic behavior of walls with both interior and exterior finishes.

2.2 UC SAN DIEGO SMALL-COMPONENT TEST PROGRAM

The small-component test program at UC San Diego was divided into four phases, with six–eight specimens tested per phase. Subdividing the program into multiple phases allowed analysis of one phase of test results to aid in the design of subsequent phases. In addition, this resulted in a manageable number of full-scale specimens within the laboratory space. Each of the test phases considered a similar theme, allowing for meaningful comparisons amongst specimens within a particular phase, and yet were complimentary to other phases for cross comparison upon completion of subsequent phases. The scope and purpose of each testing phase is as follows:

- *Phase 1.* The first phase of testing contained six cripple wall specimens. Each of the cripple walls were 2 ft tall and finished on their exterior face with stucco installed over horizontal lumber sheathing. In addition, a uniform vertical load of 450 lbs/ft was applied to each specimen. Parameters amongst specimens in this phase included: the specimens boundary conditions, anchorage conditions, and existing or retrofit detailing. By controlling the exterior finish, height, and applied vertical load, the results of the Phase 1 tests work offered insight into the importance of the boundary conditions (ends, top, and bottom) of the wall on the performance of the specimens. In addition, one of the cripple walls was constructed with a wet set sill, a previously untested type of anchorage. Lastly, two of the cripple walls were identical, with one being an existing condition and the other being a retrofitted condition. The details of these specimens, including boundary conditions variability, retrofit design, and wet set sill

construction, is discussed in Chapter 3 of the present report. All results from Phase 1 are presented in the current report;

- *Phase 2.* The second phase of testing contained eight cripple wall specimens. Six of the cripple walls were 2 ft tall, and two of the cripple walls were 6 ft tall. Similar to Phase 1, all wall specimens were subjected to 450 lbs/ft of vertical load. The boundary conditions remained the same for all specimens. The walls differed from each other in exterior finishes, height, and retrofit condition. The eight walls were grouped in four identical pairs of existing and retrofitted walls. All specimens had sill plates attached to the foundation with anchor bolts. The main focus of Phase 2 was to document the performance of dry, or non-stucco, exterior finish materials. One pair of walls was finished with T1-11 wood structural paneling, one pair was finished with shiplap horizontal lumber siding over diagonal lumber sheathing, and the final two pairs were finished with shiplap horizontal lumber siding. The two pairs with horizontal siding differed in height, one pair being 2 ft tall and the other being 6 ft tall. These tests provided insight regarding the performance of dry-finished specimens, with emphasis on understanding the failure mechanisms associated with short and tall cripple walls. In addition, the results of four retrofitted walls built upon knowledge gained in Phase 1 regarding the effectiveness of the *FEMA P-1100* prescriptive retrofit [Schiller et al. 2020b];
- *Phase 3.* The third phase of testing also consisted of eight specimens. These specimens were each 2 ft tall and had the same boundary conditions imposed on the top and ends of the cripple walls. There were three pairs of identical walls that only differed in their retrofit condition. A uniform vertical load of 450 lbs/ft was consistently applied for all specimens. Key parameters differing among the specimens in this phase included the exterior finish details and the bottom of specimen boundary conditions. Pairs of cripple walls with stucco over horizontal lumber sheathing, stucco over diagonal lumber sheathing, and stucco over framing were tested. One cripple wall was constructed with a wet set sill plate. Results of these three pairs of tests examined the performance of differing wet or stucco exterior finishes, as well as provide additional results regarding the performance of the *FEMA P-1100* prescriptive retrofit [Schiller et al. 2020c]; and
- *Phase 4.* The final phase of testing consisted of six specimens. All wall specimens were detailed with the same boundary conditions. Two pairs of identical 6-ft-tall cripple walls were tested, both existing and retrofitted. Two walls were detailed with stucco over framing exterior finishes, while the other two utilized T1-11 wood structural panel exterior finishes. Two of the six specimens were 2 ft tall. One of these had stucco over horizontal lumber sheathing and was loaded with a monotonic push. The other cripple wall had shiplap horizontal sheathing over diagonal lumber sheathing and was tested with a light uniform vertical load of 150 lbs/ft. Results from this phase investigated the effect of height on the performance of the cripple wall and the *FEMA P-1100* prescriptive retrofit. In addition, the effect of a light vertical load and a monotonic push loading protocol was evaluated [Schiller et al. 2020c].

While there were four phases of testing, the reporting of each phase was not strictly organized based on the testing phase. Nonetheless, four reports are available to summarize the UC San Diego's small-component test program. The present (first) report and the third report focus on wet specimens, i.e., specimens with stucco exterior finishes (i.e., Phase 3 and a portion of phase 4). The second report focuses solely on dry specimens, i.e., specimens finished with wood absent stucco (i.e., Phase 2 and a portion of Phase 4). The final (fourth) report presents a cross comparison of specimens, with both wet and dry finishes [Schiller et al. 2020d]. These reports are as follows:

- Report 1: Cripple Wall Small-Component Test Program: Wet Specimens I [Schiller et al. 2020(a)];
- Report 2: Cripple Wall Small-Component Test Program: Dry Specimens [Schiller et al. 2020(b)];
- Report 3: Cripple Wall Small-Component Test Program: Wet Specimens II [Schiller et al. 2020(c)]; and
- Report 4: Cripple Wall Small-Component Test Program: Comparisons [Schiller et al. 2020(d)]

2.3 DETERMINING TEST VARIABLES

Within the PEER–CEA Project, a working group was organized to analyze and define representative "Index Buildings" and their variants [Reis et al. 2020]. This effort, under the auspices of WG2, significantly guided the design of the small-component test program. The Index Buildings described have variants formulated based on three criteria:

1. Parameters have a significant effect on the seismic response of the building.
2. Parameters have a statistically significant presence in the California housing stock.
3. Amount of damage reduction possible resulting from the seismic retrofit of the cripple wall is dependent upon the presence of the variant.

For each of the variants considered, the determination of whether it had a significant effect on the seismic response of the building and whether the amount of damage reduction due to a specific retrofit strategy is dependent on the presence of the variant was evaluated based on information from ATC-110 [ATC 2014], the CUREE-Caltech Index Building Report [Reitherman and Cobeen 2003], and expert opinions from members of this PEER–CEA Project. Resources used to determine what parameters have a statistically significant presence in the California housing stock included data provided by the CEA, the U.S. Department of Housing and Urban Development [NAHB 1994; 2004], and the ATC-110 project [2014]. Further narrowing of the selection is attributed to the CUREE Index Building Report [Reitherman and Cobeen 2003], which refined the criteria for selecting variants stating that while many variants may satisfy the above conditions, they cannot be included in the test program because of the follow reasons:

- A variant may have a significant impact on building performance, but it cannot practically be discovered by owners or insurance agents when writing a policy; and

- Variants such as construction quality, code enforcement and adoption, trade practices, availability of materials, and quality of inspection are likely to lead to differences in expected performance but may not be quantified or cataloged.

Ultimately, a variant must be observable in order to be quantified with fragility and damage functions. A primary variant considered by all loss modelers is the age of the home. The age of a house is an observable variant, which sheds light on many of the variants dismissed above and has been found to have a strong correlation to the performance of the house [Mahin 1991; Hall 1994; EERI 1996; and Rabinovici 2017]. To allow for reasonable categorization, the age of housing construction considered in this project was discretized into vintages, namely: Pre-1945, 1945–1955, and 1956–1970. These eras were selected based on the common construction practices of their time, whereby one era offered notable differences from another. Note that era delineation does not correlate with the number of houses constructed. Houses built after 1970 were assumed to primarily use plywood sheathing extending to the foundation and were typically built on slabs and, thus, do not contain cripple walls. For these reasons, post-1970 houses have conditions that would not trigger the need for seismic retrofits prescribed in this program. The other primary variant considered by a loss modeler is the number of stories of the house. This also has a direct impact on the seismic performance of a house. Both of these are easily quantifiable and drive the determination of the variables examined in the test program.

Secondary variants within the Index Buildings, as defined by WG2, are the finish on the house, presence and height of a cripple wall, presence and spacing of anchor bolts, building weight, cripple wall slope differential, room or house over garage, and presence of a retrofit. All of these fulfill the two criteria affecting the seismic performance of a house and having a significant presence in the California housing stock. For the scope of this test program, the parameters included within the test matrix are derived from the Index Building variants and include various boundary conditions affecting the performance of a cripple wall. Thus, the variables of particular focus are:

- *Existing and retrofit conditions.* Cripple walls are either constructed "as-built" (denoted herein as *existing*) or retrofitted following the *FEMA P-1100* prescriptive retrofit guidelines;
- *Height of cripple wall.* Cripple walls are either 2 ft or 6 ft in height. All cripple walls tested were level, i.e., this program did not consider cripple walls on hillsides, which are often constructed with slope or stepped cripple walls;
- *Vertical Load.* Two different vertical load levels were used, namely light = 150 lbs/ft and heavy = 450 lbs/ft;
- *Anchorage.* Two cases of anchorage exist: sill anchor bolts and wet set sill plates. For sill anchor bolts, spacing between the bolts was set at 64 in. on center to simulate the existing sill anchorage, which was observed to be very sparse in pre-1970 constructed dwellings. Retrofitted cripple walls have anchor bolt spacing prescribed by *FEMA P-1100*;
- *Exterior Finish.* The finish of the cripple wall contained the most variability in the present test program. As noted, both wet (or stucco) and dry (or non-stucco) exterior finishes were used. Wet exterior finishes included stucco over framing, stucco over horizontal lumber sheathing, and stucco over diagonal lumber

sheathing. Dry exterior finishes include shiplap horizontal lumber siding, shiplap horizontal lumber siding over diagonal lumber sheathing, and T1-11 wood structural panels; and

- *Boundary Conditions.* Various boundary conditions on the top, bottom, and ends of the cripple walls were implemented in the test program. Descriptions of the boundary conditions is discussed in Chapter 3.

2.4 JUSTIFYING TEST VARIABLE RANGE AND SELECT DETAILING ASPECTS OF SMALL CRIPPLE WALL SPECIMENS

As noted, the choice of variables to be implemented into this test program were derived from variants in the Index Buildings, as defined by WG2 of the overall PEER–CEA Project. The range of these test variables was developed through careful and continued consultation amongst the Project Team, a peer review panel, and the CEA. Related studies also aided in guiding the test variable range. The logic for selecting the range in each test variable type is provided below.

- *Cripple Wall Height.* Previous studies have been performed on cripple walls ranging from 2 ft to 4 ft [Sheperd and Delos-Santos 1991; Steiner 1993; and Chai et al. 2002]. The majority of cripple walls in the California housing stock are 4 ft or less in height. There are, however, a significant number of houses containing cripple walls in excess of 4 ft, yet no experimental data exist to document the performance of such taller cripple walls. In a housing survey study of 633 homes following the 2014 South Napa earthquake, 8.8% of the houses surveyed contained a cripple wall taller than 4 ft. Importantly, the presence of taller cripple walls was greater for houses built pre-1950. It was found that 21.3% of the houses built pre-1950 were constructed with cripple walls in excess of 4 ft [Rabinovici 2017]. In addition, according to the 2000 US Census, 32.6% of the housing stock in California was built prior to 1960 [U.S. Census Bureau 2000]. Thus, a significant number of houses in California, primarily old homes, have cripple walls taller than 4 ft. While taller cripple walls, with larger height-to-length aspect ratios, are similar to wood-frame shear walls, in older homes they typically do not have interior finishes like wood-frame shear walls, which are a part of the living areas of the house. Unlike shorter cripple walls that are dominated by a shear mode, taller cripple walls may be more flexural or mixed-mode (flexure-shear) dominated. Moreover, taller walls are more likely to uplift under lateral loading. Given that this phenomenon is not well understood, it was determined that a wall height of 6 ft should be considered in select specimens;
- *Vertical Load*. The use of various vertical load cases is important to document to model one and two-story houses accurately as well as those considered of light or heavy construction. Therefore, two vertical load cases, 150 lbs/ft and 450 lbs/ft, were implemented in the present test program. A uniform vertical load of 150 lbs/ft represents the gravity load of a one-story house construction using light construction materials, while a uniform vertical load of 450 lbs/ft represents the gravity load of a two-story house constructed using heavy

construction materials. These vertical loads were derived from the ATC-110 project Median Home definition [ATC 2014] as well as the CUREE Index Building Report [Reitherman and Cobeen 2003]. The vertical load a cripple wall experiences during lateral loading plays a major role in the seismic behavior of the wall; and

- *Anchorage.* Two types of anchorage were considered in this testing program: (1) sill plates anchored with 1/2-in. bolts and (2) wet set sill plates. The most common condition found in California houses is sill plates connected to the foundation with anchor bolts, which have been cast in the foundation concrete. Herein, the anchor bolt spacing is set at 64 in. on center for unretrofitted houses. While many older houses in California contain no anchor bolts or spacings greater than 64 in. on center, the goal of this testing program was to evaluate the performance of the cripple wall as opposed to forcing the wall into total failure, i.e., the sliding of the wall from its supporting foundation. As such, minimal anchorage was implemented to assure failure occurred within the actual cripple wall.

In pre-1945 construction, wet set sills were common practice in California housing construction. Although this condition is not extremely prevalent, there is no information on the performance of wet set sill attachment of the cripple wall. As such, wet set sill anchorage was chosen as a variant for the testing program.

Regarding the detailing adopted for the anchorage: when present, it is noted that the National Design Specification for Wood Construction [AWC 2018] requires that bolt holes be oversized by 1/16 in.; however, this was not found to be common practice due to the skill and attention it required the builder to invest in matching up framing and foundation. In its characterization of the Index Buildings, WG2 estimated that only 10% of anchor bolt holes were properly sized, 40% were 1/16 in. to 1/4 in. oversized, and 50% were more than 1/4 in. oversized [Reis et al. 2020]. Thus, the choice was made to use a 1/4 in. oversize as a middle-of-the-road approach.

- *Exterior Finish.* The exterior finishes examined across the testing program were horizontal siding, horizontal siding over diagonal sheathing, stucco over horizontal sheathing, stucco over diagonal sheathing, stucco only (i.e., directly over framing), and T1-11 wood structural panels. Horizontal siding, horizontal siding over diagonal sheathing, and the various stucco configurations are commonly seen in California housing stock during the various eras of construction considered herein. In contrast, T1-11 structural panels gained popularity post-1960. Note: the most common finishes in California are stucco and horizontal siding. From the *CEA South Napa Home Impact Study* [Rabinovici 2017], 24.9% contained horizontal siding and 55.6% contained stucco of the 633 houses surveyed. Both finishes are commonly seen not only in the San Francisco Bay Area but in Los Angeles County, surrounding counties, and other parts of California. These two types are by far the most predominant finishes in California. Amongst the sheathing types, the most common type noted was horizontal sheathing due to its ease of construction; however, with higher-end construction practices, diagonal sheathing was

preferred. For example, in the San Francisco Bay Area, approximately 80% of houses containing sheathing have it installed horizontally. In California, the approximate distribution of sheathing types on houses is 40% containing no structural sheathing (exterior cladding including stucco, siding, plywood, or others), 40% containing horizontal sheathing, and 20% containing diagonal sheathing [Reis et al. 2020]. While other styles of siding do exist, such as diagonal siding, they do not have a significant enough presence to be deemed necessary to be included in the program; and

- Sheathing boards utilized California homes in the era under consideration, ranged in width from 6 in. to 12 in., with 6 in. or 8 in. in width being the most common. Thus, diagonal and horizontal sheathing used herein were 1 × 6 nominal members (3/4 in. × 5-1.2 in.) made from Douglas Fir. Adopting the original 1927 UBC codes, 8 in. or narrower sheathing boards were fastened with 2–8d (0.131 in. × 2-1/2 in.) common nails at each stud. For boards wider than 8 in., 3–8d common nails were used [ICBO 1927]. To the authors' knowledge, a recommendation for connection of sheathing to sill plates was lacking in the UBC. Therefore, in the present study, the bottom sheathing board (1 × 6 member) was attached with one nail to the stud and one nail in-line and attached to the sill plate. This resulted in a 16 in. on center nailing to the sill plate. Diagonal sheathing was placed at 45° angles with the horizontal foundation.

2.5 LOADING PROTOCOL

As part of this PEER–CEA Project, WG3 undertook the task of developing a testing protocol for use across the testing programs at both UC Berkeley and UC San Diego [Zareian and Lanning 2020]. Since the protocol was common to both the UC Berkeley and UC San Diego studies, it is discussed here in the context of the overall WG4 effort. Specific nuances relative to the various phases of testing will be discussed later. Similar to previously developed testing protocol available in the literature (e.g., Krawinkler et al. [2001]), the protocol developed involved imposition of a forward-ordered cyclic reversed quasi-static loading, with increasing amplitudes of lateral displacement. The loading protocol can be seen in Figure 2.1. The loading protocol is intended to cover a wide range of deformation sequences and amplitudes as to provide a full assessment of the behavior of each specimen in one experiment. Two objectives for the cripple wall experiments were used for its development:

1. Using experimental results for assessing and adjusting cripple wall analytical models to be used in system level nonlinear time-history analysis.
2. Using experimental results for the development of component fragility curves covering a wide a range of damage states associated with the cripple wall behavior.

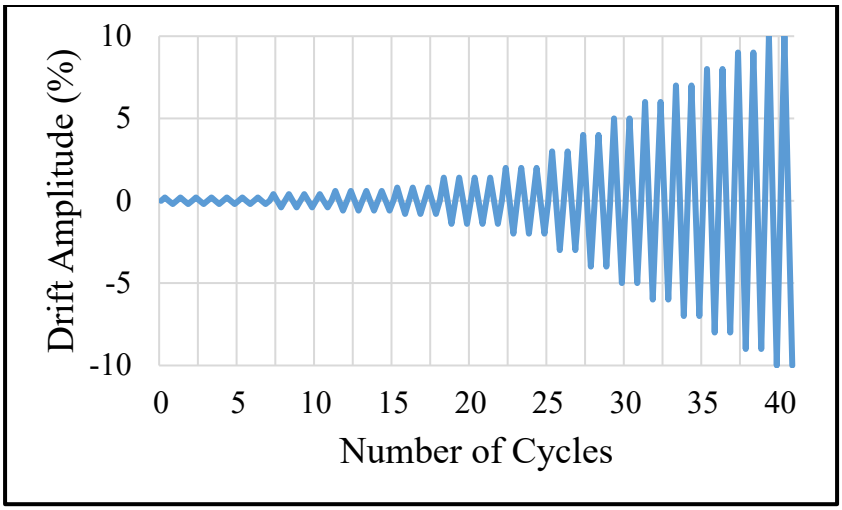

Figure 2.1 **Deformation-controlled loading protocol for cripple wall experiments (after Zareian and Lanning [2020]).**

The displacement imposed at each grouping of drift amplitudes is taken as relative to the height of the cripple wall being tested and is referred to as drift amplitude. Drift amplitude is equal to the imposed displacement divided by the height of the cripple wall and is expressed as a percentage. Each drift level contains an equal displacement push and pull up to the specified displacement, followed by trailing cycles of the same amplitude. This contrasts with the protocol of the CUREE-Caltech project, where trailing cycles were reduced in amplitude to 75% that of their primary cycles. The amount of cycles per drift level is variable but decreases as the amplitude of the imposed displacement increases. Table 2.1 summarizes the loading protocol used for 2-ft-tall cripple walls.

The loading rate was kept slow, allowing for continued monitoring of the damage progression to the specimen. It was back calculated by defining the time per full cycle as either 30 or 60 sec. As a result, the rate of loading generally increased as the displacement amplitudes increased. The loading time per cycle was increased for taller cripple walls specimens to assure that the loading rate was maintained less than 0.39 in/sec (1 cm/sec). The loading rate during this test program was not considered a variable.

Additional rules were imposed during testing to ensure consistency across different specimens. For example, once the specimen realized a loss greater than 60% of its measured lateral strength, the imposed amplitude of drifts was increased at a rate of 2% per drift level rather than 1%.; see Table 2.1, which articulates a continuous drift amplitude increase of 1% after reaching 2%. If a 60% loss in lateral strength was not realized, the imposed increase in drift level remained at 1% per cycle grouping. The criteria for ending a test was when it reached an 80% loss in lateral strength. If this did not occur, a monotonic push of the cripple wall was performed following attainment of a lack in change of post-peak strength (despite increasing drift amplitudes imposition). For all tests, these criteria were met between 12–13% drift. The monotonic push typically was conducted to a drift of 20%, with possible exceptions due to instrumentation or other test fixture constraints.

Table 2.1 Example of loading protocol used for 2-ft-tall cripple wall tests.

Cycle group no.	Drift (%)	Amplitude (in.)	No. of cycles per group	Loadig rate (in./sec)	Time per cycle (sec)	Total time per cycle group (sec)
1	0.2	0.048	7	0.0064	30	210
2	0.4	0.096	4	0.0128	30	120
3	0.6	0.144	4	0.0192	30	120
4	0.8	0.192	3	0.0256	30	90
5	1.4	0.336	3	0.0448	30	90
6	2	0.48	3	0.064	30	90
7	3	0.72	2	0.096	30	60
8	4	0.96	2	0.128	30	60
9	5	1.2	2	0.16	30	60
10	6	1.44	2	0.192	30	60
11	7	1.68	2	0.224	30	60
12	8	1.92	2	0.256	30	60
13	9	2.16	2	0.288	30	60
14	10	2.4	2	0.16	30	120
15	11	2.64	2	0.176	60	120
16	12	2.88	2	0.192	60	120
17	13	3.12	2	0.208	60	120
18	14	3.36	2	0.224	60	120
19	15	3.6	2	0.24	60	120
20	Mono	5	--	0.333	60	60

3 SPECIMEN DETAILS, TEST SETUP, AND INSTRUMENTATION

3.1 OVERVIEW

The focus of this chapter is on the details of the cripple wall specimens, test setup, and testing instrumentation for Phase 1 of the program, where various boundary conditions, retrofit, and anchorage conditions were selected as primary specimen variables. The boundary conditions affected the top, bottom, and ends of the cripple wall specimens. In this regard, testing in Phase 1 examined the effects of these boundary conditions on the performance of the cripple walls to guide the selection of boundary conditions in subsequent testing phases. All specimens were constructed with a stucco overlaying horizontal lumber sheathing exterior finishes, emulating detailing of pre-1945 era dwellings. Table 3.1 summarizes the variables for specimens within the test matrix of Phase 1. Note that the baseline finish condition was consistent across specimens and is denoted in subsequent reports as S+HSh.

Table 3.1 Test matrix for Phase 1. All specimens in Phase 1 were 2 ft tall, with stucco finish over horizontal sheathing (S+HSh), emulating detailing of the pre-1945 era, and subjected to a cyclic loading protocol.

Specimen	Test no. (date)	Existing or retrofit	Anchorage	Top BC	Bottom boudary condition	Test date
A-1	4	E	S (64 in.)	A	a	1/26/2018
A-2	3	E	S (64 in.)	B	a	1/18/2018
A-3	6	E	S (64 in.)	C	a	2/2/2018
A-4	1	E	S (64 in.)	B	b	12/18/2017
A-5	5	R	S (32 in.)	B	a	1/31/2018
A-6	2	E	WS	B	b	2/22/2017
		Retrofit	Wet set sill plate or retrofit	Case A, C		

Notes: E = existing, R = retrofit, S = anchor bolt spacing, WS = wet sill plate, BC = boundary condition, uppercase letters = top boundary conditions, lowercase letters = bottom boundary condition. Bottom boundary condition c and d were not implemented until Phase 3 of testing [Schiller et al. 2020(c)].

3.2 SPECIMEN DETAILS

3.2.1 Framing and Retrofit Details

All six cripple wall specimens in Phase 1 were nominally 2 ft high and 12 ft long; see Figure 3.1. Minor differences in height were attributed to different boundary conditions and the presence of an anchored sill plate versus a wet set sill plate. The height of the cripple wall was measured from the base of the sill plate to the top of the uppermost top plate. For the case of the embedded wet set sill plate, the height of the cripple wall was measured from the top of the footing to the top of the uppermost top plate. Framing members were constructed with #2 Douglas Fir, with the exception of the wet set sill plate, which was construction-grade redwood. Wall studs and top plates were 2 × 4 nominal members, and sill plates were 2 × 6 nominal members. All stud bays were 16 in. on center. Studs were connected to the sill plate and top plate with 2-16d (0.165-in. diameter) common nails per stud. Additional top plates were connected with 16d common nails staggered at 16 in. on center. All of the lumber used was tested for moisture content. Upon procurement of lumber, the moisture content was between 14–24% for the Douglas Fir (studs, sill plates, top plates, and sheathing boards) and 5% for the redwood sill plate. The moisture contents were documented before testing as well and were in the range of 4–12% for all wood. The loss of moisture can be attributed mostly to moisture being removed during the stucco curing process. All moisture content readings are summarized in Appendix A.1.

The details for the framing of cripple walls can be seen in Figure 3.1. Note that anchor bolt spacing shown in this figure applies to the unretrofitted cases, and small variations exist in the framing details, which are dependent on the various boundary conditions imposed on the cripple walls. These variations and additional details regarding the nailing and dimensioning will be discussed in detail later in this chapter.

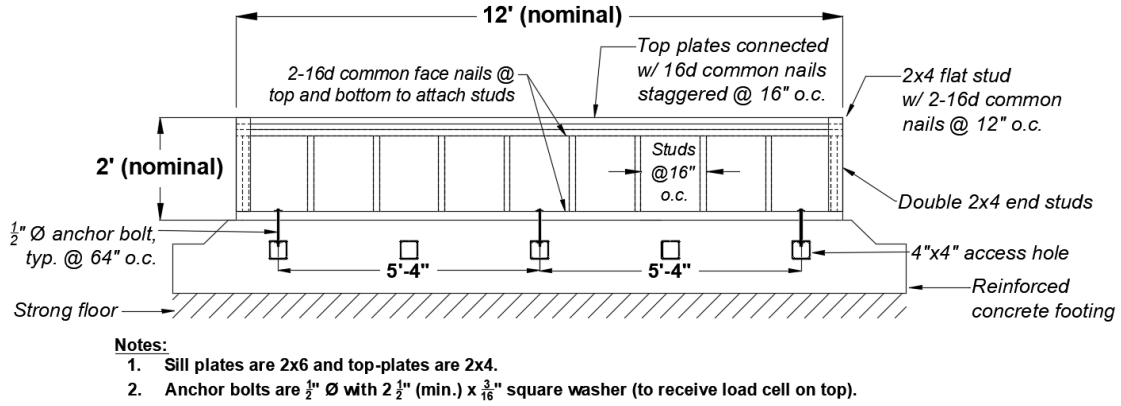

Figure 3.1 Elevation of framing details of the interior face of the 2-ft-tall cripple wall Phase 1 test specimens. Note: the specimen height and length vary slightly due to modifications in the boundary conditions, which was a variable in Phase 1.

Anchor bolts used were all 1/2-in.-all-thread F1554 Grade 36 straight rods with nuts and washers at both ends. To allow for ease in removal of the specimen, the anchor bolts were not cast in the foundation per se. Instead, the concrete footings were cast with 4 in. × 4 in. access holes to allow for the anchor bolts to be tightened and switched out if damaged during a test. The access holes were spaced 32 in. apart to allow for the prescribed 32 in. on center and 64 in. on center spacing of anchor bolts. The footings were cast with poured-in-place concrete, with a 28-day compressive strength target of 8 ksi. The rebar arrangement and details of the footing is shown in Figure 3.2. Anchor bolt holes were oversized 1/4 in., which is a common building practice in California as it facilitates ease of construction. Square washers (2 in. × 2 in. × 3/16 in. overlaid with spherical washers) were used at the anchor bolt connection at the sill plate, allowing for placement of 10-kip donut load cells intended to measure the tensile force in the anchor bolts during testing. Conventional nuts and washers were used at the bottom anchor bolt connection within the 4 in. × 4 in. access hole. The load-cell configuration can be seen in Figure 3.3.

The primary resistance to sliding during imposition of lateral load to the specimen comes from the frictional resistance at the interface of the sill plate and the foundation, and the bearing of the anchor bolt on the sill plate. By oversizing the anchor bolt holes, the cripple walls have less resistance to sliding. Because sliding of the walls was a key metric for certain specimens prior to development of bearing between the anchor bolt within its hole, both the global lateral displacement response and the relative lateral displacement responses are presented in Chapter 4. The global lateral response includes the displacement of the cripple wall and the sliding of the sill plate, while the relative lateral response only considers the displacement of the actual cripple wall structure.

The details for the framing of retrofitted cripple walls from Phase 1 can be seen in Figure 3.4. In this application, three 15/32-in.-thick × 4-ft-long plywood structural panels were used to brace the interior face of the cripple wall. A 1/8-in. gap was left between each panel and flat stud at each end to allow for expansion of the panels. No gap was left between the plywood and the sill plate as these are commonly installed by resting on the sill. Additional 2 × 4 blocking was attached to the sill plate with 4–10d (0.148-in.-diameter) common nails per stud bay. Studs (2 × 4) were added to each end, and two 4 × 4 studs were added within the interior to allow for an area for the plywood to be nailed to. These extra studs were toe-nailed with 2–8d (0.131-in.-diameter) common nails at top and bottom. The plywood panels were connected to the framing with 8d common nails at 4 in. on center at the edges and 12 in. on center over the field. A 3/4-in. gap was left between the edge nails and the edge of the plywood. This was done to ensure that each nail was attached to the center of the stud, top plate, or blocking plate. With the addition of plywood structural panels, the anchor bolt spacing was reduced from 64 in. on center to 32 in. on center.

Note: the retrofit design used in this testing phase was consistent with the current recommendations per ATC-110, which was in a preliminary publication state at the time of execution of the Phase 1 tests. These recommendations were modified after the completion of this testing phase, and an updated design was incorporated in each retrofitted cripple wall thereinafter. The primary difference between the retrofit design in Phase 1 and the retrofit design used in subsequent testing phases involved the use of a finer edge nailing pattern; 4 in. on center spacing was utilized as opposed to 3 in. on center spacing in subsequent phases, and the use of five anchor bolts versus seven anchor bolts in the present case versus the later test phases. Photographs showing the details of the retrofit are shown in Section 3.5.

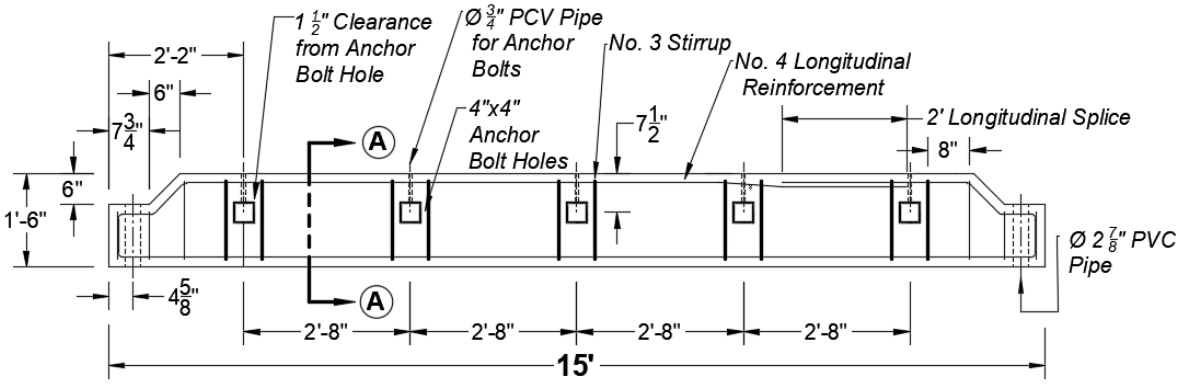

Note:

1. **All concrete cover is 1-1/2".**

(a)

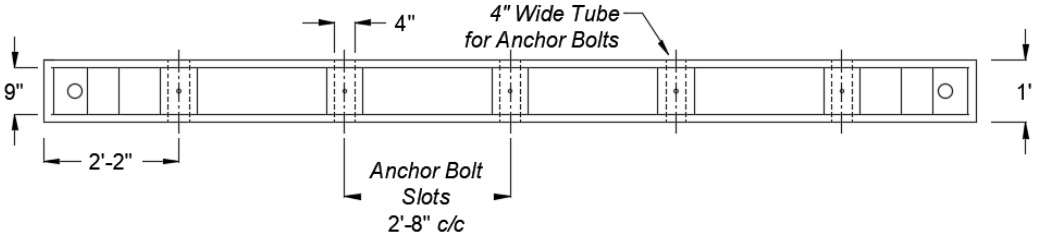

(b)

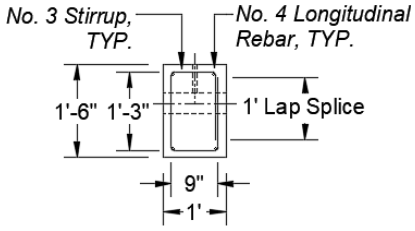

(c)

Figure 3.2 Concrete footing details for cripple wall tests: (a) elevation; (b) plan view; and (c) Section A-A.

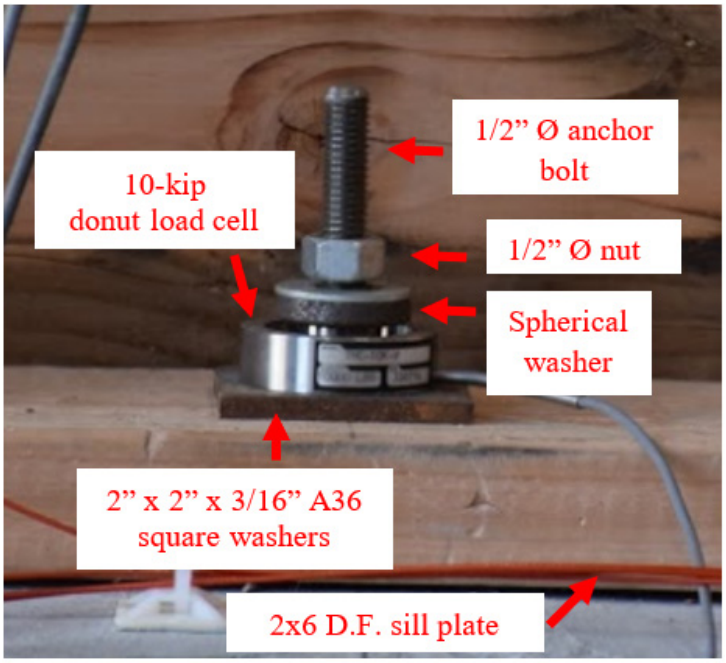

Figure 3.3 Load cell and square plate washer for anchor bolts.

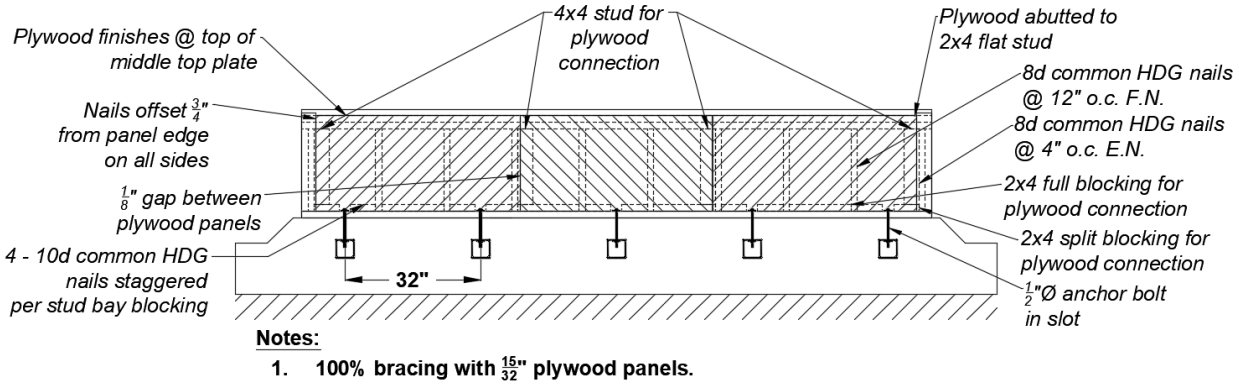

Figure 3.4 Specimen A-5 elevation of the interior face of the retrofitted cripple wall framing details.

3.2.2 Boundary Conditions

Framing details of the specimens were dependent upon the boundary conditions. Boundary conditions were split into two categories, top and bottom boundary conditions. The top condition also affected the end of the specimens, whereas the bottom boundary condition only involved modifications to the bottom detailing of the specimens. Specific details associated with each variation are presented below.

3.2.2.1 Top Boundary Conditions

The top boundary conditions implemented were intended to examine the effects of enhanced top plates and built-up end framing (corners), including C-shaped walls (i.e., built-up corners with a wall return), and, in particular, to compare with the response of walls tested by Chai et al. [2002], which did not contain enhanced top plates or corners. In addition, at the top of the cripple walls variations in furring nail arrangements connecting the stucco to the framing were implemented with the purpose of simulating stucco continuity into the floor above as done in tests by Arnold et al. [2003]. Unlike the bottom boundary conditions, top boundary conditions affect the framing details of each specimen. The test program consisted of three top boundary conditions, denoted as A, B, and C. The description of these boundary conditions and the framing details for each condition are described below.

Top Boundary Condition "A"

Top boundary condition-A was similar to the specimen details used in the CUREE-Caltech Woodframe Project at UC Davis by Chai et al. [2002]. These specimens were cripple walls framed with two 2 × 4 top plates connected with 16d common nails at 16 in. on center; see Section 3.2.1. Studs were 16 in. on center and connected to the lower 2 × 4 top plate and 2 × 6 sill plate with 2–16d common nails per stud, top and bottom; Figure 3.5 shows the framing details. Figure 3.6 shows details for stucco and sheathing attachment, and the nailing pattern. The purpose of incorporating this boundary condition into the testing program was to provide a basis of comparison to the CUREE tests performed at UC Davis. Only one cripple wall was tested with this configuration. Figure 3.7 provides photographs of this boundary condition.

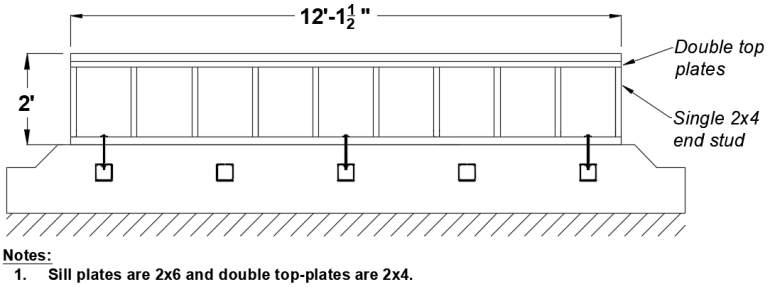

Figure 3.5 Framing detail elevation for top boundary condition A.

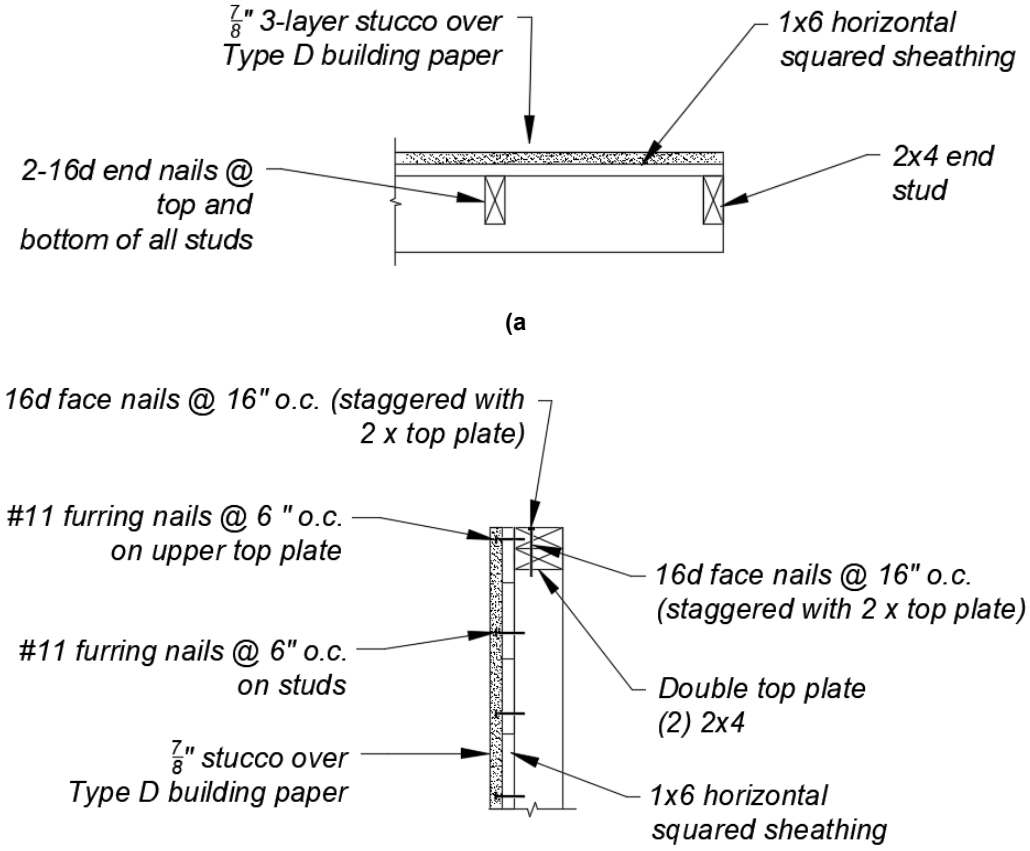

Figure 3.6 **Corner and top of wall details for stucco over horizontal sheathing for top boundary condition A: (a) plan view detail; and (b) top of wall detail.**

(a) (b)

Figure 3.7 Specimen A-2 isometric corner views showing top boundary condition A details: (a) north exterior corner; and (b) south interior corner.

Top Boundary Condition "B"

Top boundary condition B contained built-up corners (ends) as well as an additional top plate. The built-up wall ends are typical to those seen in California houses at re-entrant corners (corners where return walls would be present). These simulated corners contained two 2 × 4 studs instead of a single 2 × 4 stud and an additional 2 × 4 flat stud abutted against the interior side of the framing; see Figure 3.9 for details of the corner construction as well as the stucco and sheathing arrangement. The additional top plate was provided to allow for a denser furring nail arrangement at the top of the cripple wall, which was intended to simulate the increased stiffness provided by the continuity of the stucco running from the cripple wall into the upper story of the house. This framing detail and furring nail spacing was akin to the CUREE-Caltech Woodframe Project testing done at UC San Diego by Arnold et al. [2003]. Figure 3.8 shows an elevation view of this boundary condition; Figure 3.9 shows framing details; and Figure 3.10 provides photographs of the boundary condition. The prescribed nailing pattern for the furring nails was two rows of #11 × 1-1/2 in. (0.121-in. diameter) connected to the uppermost top plate and the middle top plate at 3 in. on center. Along the edges and the studs, #11 × 1-1/2 in. furring nails were attached at 6 in. on center, and along the sill plate; the same furring nails were attached with three nails per stud bay or 5-1/3 in. on center. Top boundary condition B was selected as the baseline top boundary condition for the entire testing program.

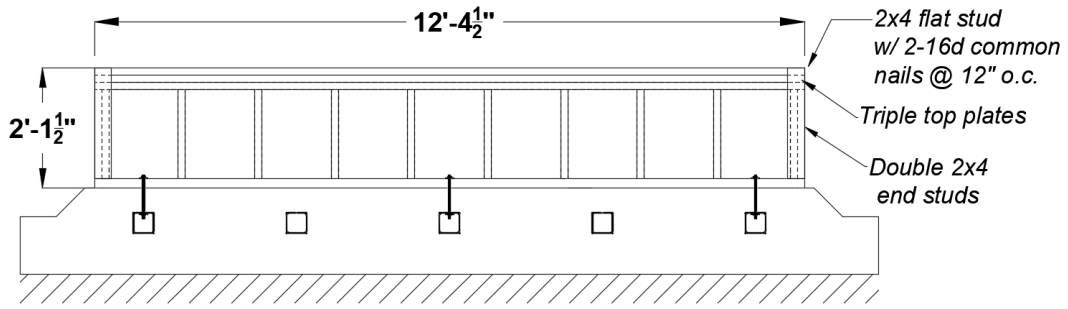

Notes:
1. **Sill plates are 2x6 and top-plates are 2x4.**

Figure 3.8 **Elevation of framing details for top boundary condition b and top boundary condition c.**

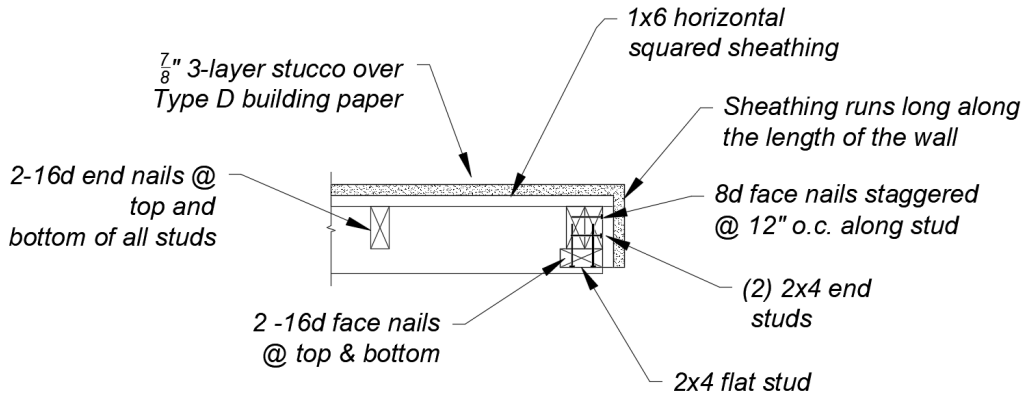

(a)

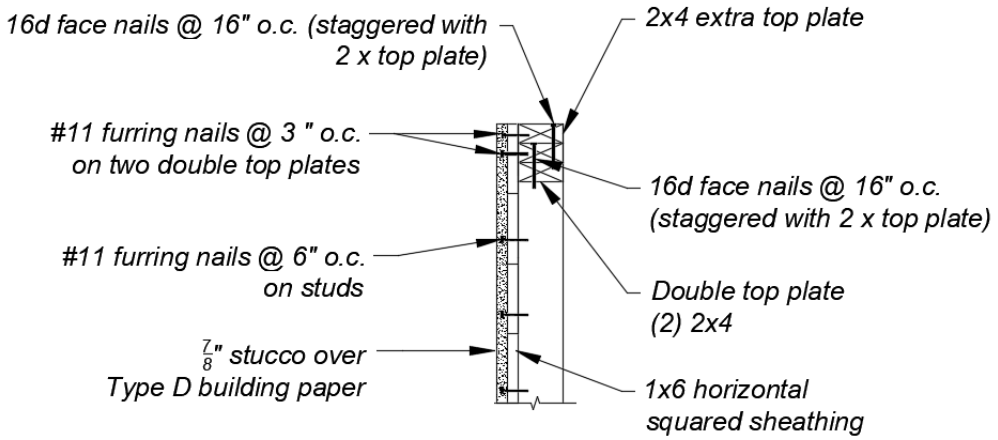

(b)

Figure 3.9 **Corner and top of wall details for stucco over horizontal sheathing: (a) plan view detail of top boundary condition B; and (b) top of wall detail for top boundary condition B and top boundary condition C.**

(a) (b)

Figure 3.10 Specimen A-2 isometric corner views showing top boundary condition B details: (a) south exterior corner; and (b) south interior corner.

Top Boundary Condition "C"

Top boundary condition C contained the same detailing at the top of the wall and stucco and sheathing attachment details as top boundary condition B; however, this boundary condition incorporated a return wall at each end, effectively resulting in a C-shaped wall specimen. The purpose of the return wall was to determine if the detailed end conditions adopted in top boundary condition B sufficiently contributed to the response of the wall considering the presence of a return wall. The return walls were 2 ft long on both ends of the specimen. The first stud bay was 16 in. on center, and the second was 8 in. on center. The return wall corners were framed with two 2 × 4 studs; the return wall was tied down with two anchor bolts, one within each stud bay; see Figure 3.11 for details of the corner construction. Figure 3.12 provides photographs of this boundary condition. Only one specimen was constructed with top boundary condition C.

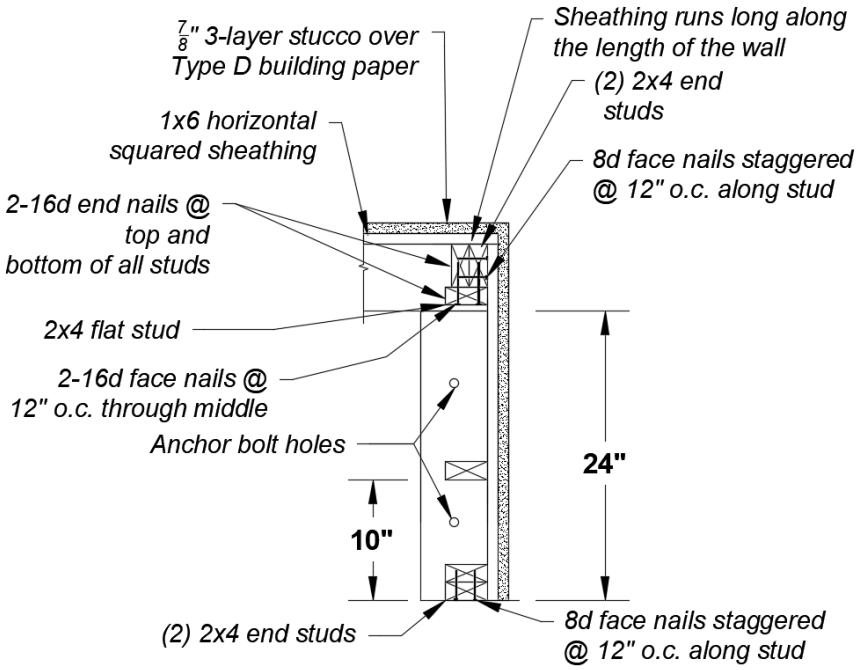

.

Figure 3.11 Plan view detail of corner and top of wall details for stucco over horizontal sheathing for top boundary condition C.

(a)

(b)

Figure 3.12 **Specimen A-3 showing top boundary condition C details: (a) interior elevation; and (b) isometric view of north exterior corner.**

3.2.2.2 Bottom Boundary Conditions

The bottom boundary conditions primarily affect the placement of the cripple walls on the footing. In addition, the bottom boundary conditions incorporated the use of a wet set sill in lieu of the typical sill plate with anchor bolts, as well as finish attachment meant to mimic deterioration of finishes at the base of a home commonly seen in older California homes. Variations in placement of the walls on the footings were meant to determine the effect of finishes bearing on the concrete compared to finishes overhanging the footing. In the latter, the finish is unimpeded and can rotate freely as the walls move. The more common condition in California is to have finishes outboard of their footing, but a number of houses with finishes bearing on their foundation remain. Bottom boundary conditions were denoted with lower case letters to avoid confusion with the top boundary conditions. Phase 1 of testing utilized four different bottom boundary conditions, denoted as bottom boundary condition "a", "b", "c", and "d". The description and details of each of these boundary conditions are presented below.

Bottom Boundary Condition "a"

Bottom boundary condition "a" pertains to instances when there is a combined exterior finish. This boundary condition orientated the cripple wall so that the siding or stucco overhung the face of the footing while the sheathing (if present) remained bearing on the foundation; see Figure 3.13. Typically, houses in California containing sheathing behind siding have both the siding and sheathing overhanging the footing, allowing them both to rotate freely as the cripple wall deforms; but there are a significant number of houses that only have the siding or stucco overhanging with the sheathing material remaining bearing on the foundation. This is attributed to the difficulty in construction of applying stucco from the cripple wall to the base of the footing when overhanging sheathing boards produce a 3/4-in. to 7/8-in. gap between the face of the footing and the face of the sheathing; see Figure 3.14.

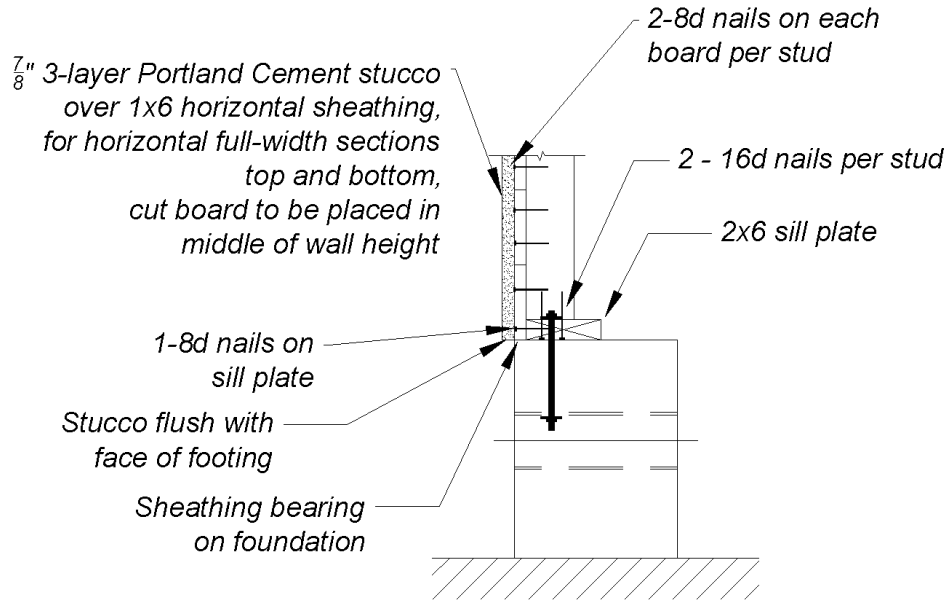

Figure 3.13 Bottom of the wall detail for stucco over horizontal sheathing for bottom boundary condition "a".

(a) (b)

Figure 3.14 Specimen A-1 showing bottom boundary condition details: (a) south exterior corner; and (b) south corner bottom.

Bottom Boundary Condition "b"

Bottom boundary condition "b" also pertained to combined exterior finishes. This configuration had both the siding or stucco and sheathing material bearing on the top of the foundation, where the bottom nailing of the sheathing was attached to the middle of the sill plate (if a sill plate exists). In the case of a wet set sill plate, the bottom nail of the sheathing was attached to the stud instead of the sill plate due to the lack of member depth available to attach to the sill plate. In the case of either wet set sill or typical sill on foundation, the furring nails were nailed to the sill plate. Details of bottom boundary condition "b" can be seen in Figure 3.15 for both the wet set sill plate and the typical sill plate. While this is not the most common condition in California houses, it still occurs in older dwellings. Moreover, the bearing of the stucco on the concrete inhibits the stucco from rotating freely as the cripple wall deforms, producing a significantly different response than the boundary condition, where the exterior finishes overhang the face of the foundation and can freely rotate as the cripple wall deforms. Figure 3.16 shows this boundary condition with a typical sill plate, and Figure 3.17 shows photographs of the same bottom boundary condition with a wet set sill plate.

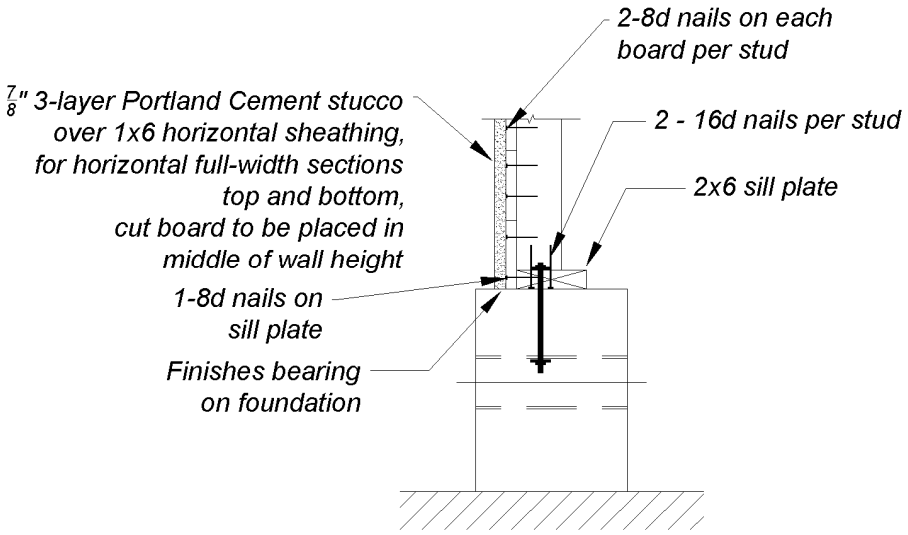

(a)

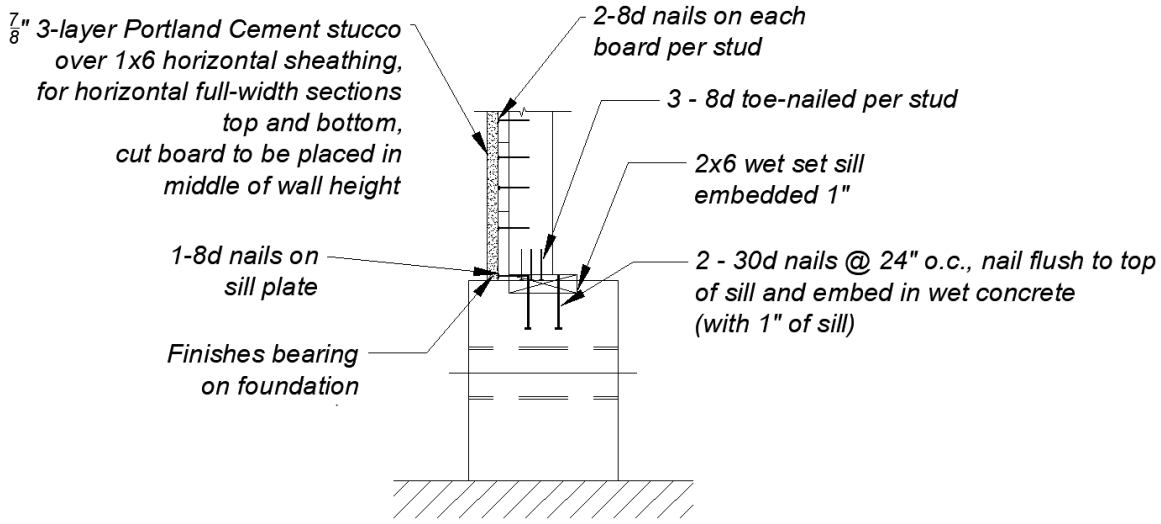

(b)

Figure 3.15 Bottom of the wall detail for stucco over horizontal sheathing for bottom boundary condition "b": (a) typical sill plate; and (b) wet set sill plate.

(a) (b)

Figure 3.16 Specimen A-4 showing bottom boundary condition “b” details: (a) north exterior corner; and (b) north exterior corner bottom.

(a)

(b)

(c)

Figure 3.17 **Specimen A-6 showing corner details for bottom boundary condition "b" with a wet set sill plate: (a) north exterior corner; (b) south interior corner; and (c) interior face.**

Bottom Boundary Condition "c"

Bottom boundary condition "c" orientated the cripple wall so that all exterior finishes were an outboard of foundation. This is the same whether there was a combined finish material or only the presence of a siding or stucco finish. Regardless of a single or combined finish material, the first layer of material attached to the framing was flush with the face of the footing; see Figure 3.18. Although it is a common condition in California homes to have the stucco extending down the face of the footing to the ground, in older homes this stucco has often deteriorated, with little bond left between the stucco and the foundation. Bottom boundary condition "c" emulates the condition where there is no bond between the stucco and foundation by having the stucco terminate at the top of the foundation. With this boundary condition, all finish materials were able to rotate freely as the cripple wall deformed. Note: this condition was tested in both a typical sill on foundation and a wet set sill configuration. Figure 3.19 provides photographs of this boundary condition. Note: the bottom boundary condition "c" was tested in Phase 3 [Schiller et al. 2020(c)], however, for completeness of the overall test program, it is described in this report.

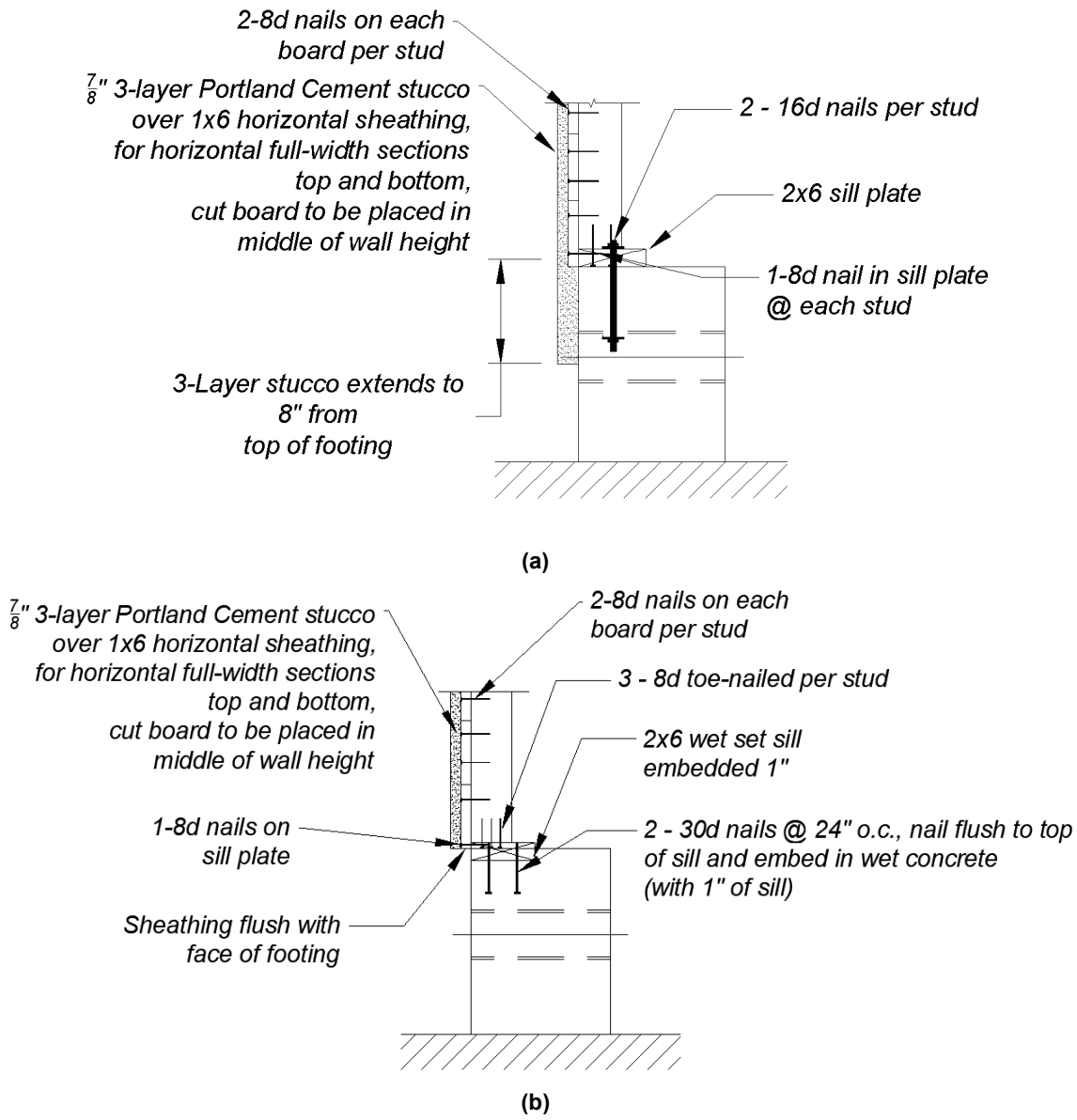

Figure 3.18 **Bottom of the wall detail for stucco over horizontal sheathing: (a) for bottom boundary condition "c"; and (b) a wet set sill plate for bottom boundary condition "c".**

(a)

(b)

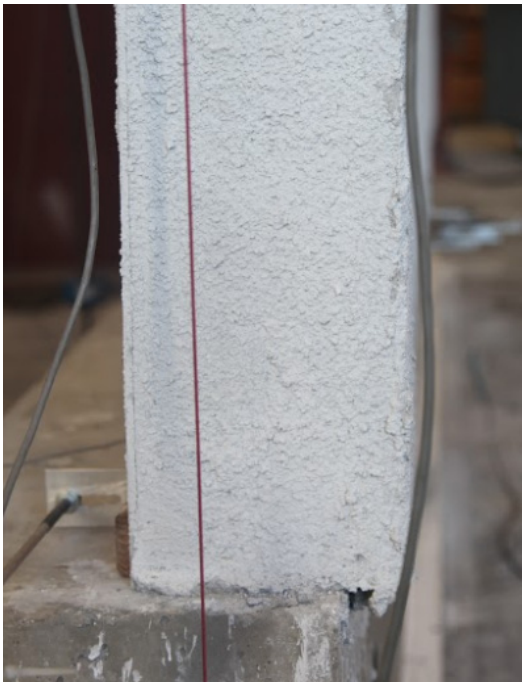

(c)

Figure 3.19 **Corner views showing bottom boundary condition “c” detail: (a) south corner exterior; (b) south interior corner; and (c) north corner bottom.**

Bottom Boundary Condition "d"

Bottom boundary condition "d" pertained to cripple walls with stucco only or stucco over sheathing exterior finish. This boundary condition was similar to bottom boundary condition "c" except that the stucco was extended down the face of the footing. It is believed that this also a very common condition in California houses where the foundation stem wall is extended above grade. In this scenario, home builders would often extend the stucco to meet the soil grade, rather than terminate it at the base of the sill plate. As seen in Figure 3.20, the tail extension of the stucco ran 8 in. down the face of the foundation. This inevitably created a thicker patch of stucco when sheathing is present in the finish, as it is also an outboard of the foundation; see Figure 3.21. As with bottom boundary condition "c", bottom boundary condition "d" was not tested in the first phase of testing. It was tested in Phase 3 [Schiller et al. 2020(c)]; for completeness of the overall test program, it is described herein.

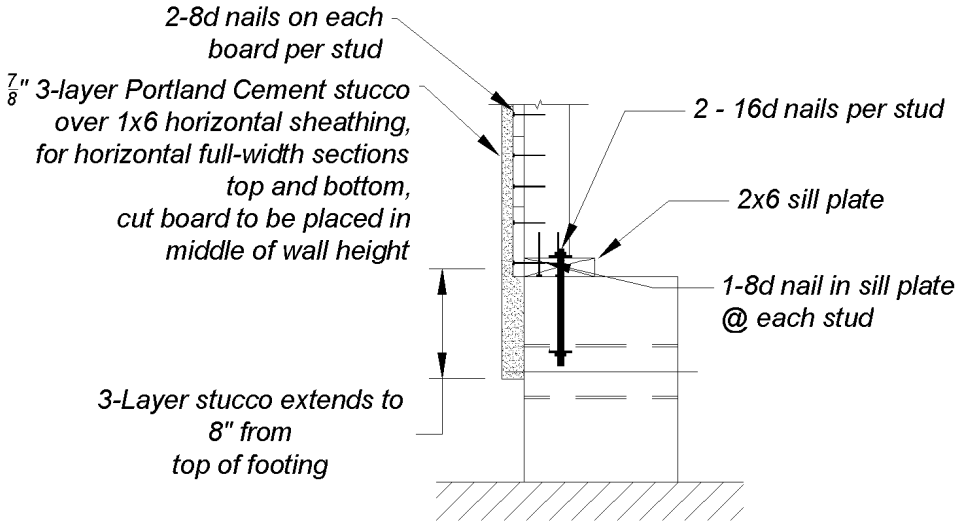

Figure 3.20 Bottom of the wall detail for stucco over horizontal sheathing for bottom boundary condition "d".

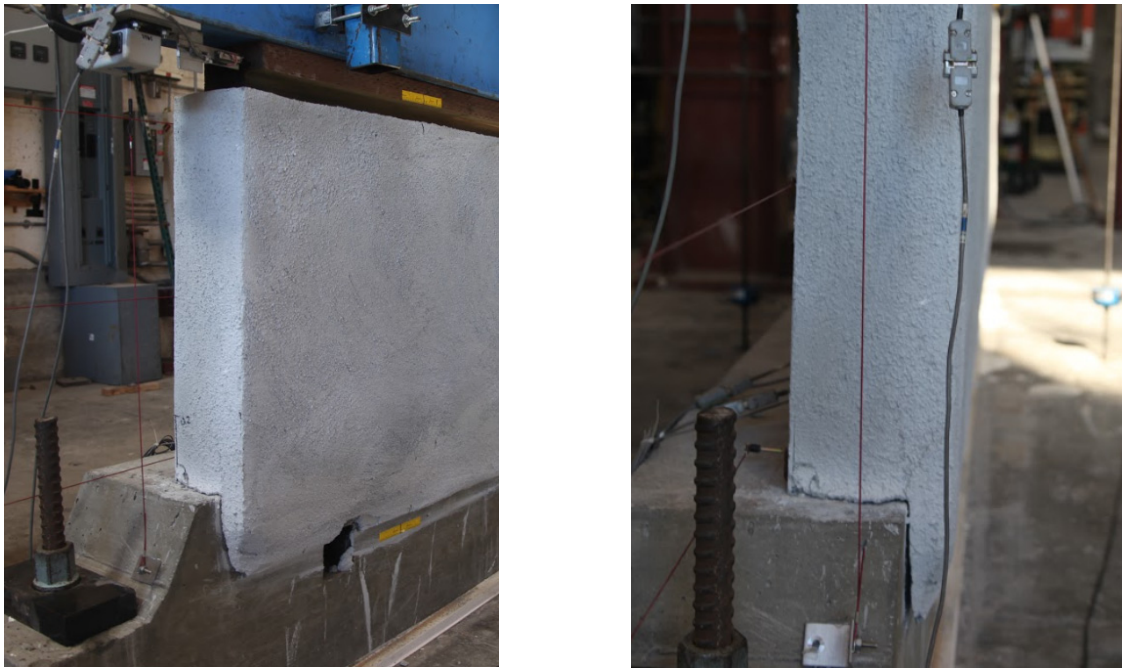

(a) (b)

Figure 3.21 Specimen A-2 showing corner views with bottom boundary condition "d": (a) south exterior corner; and (b) bottom of south corner.

3.3 WET SET SILL PLATE

Although not as common as a traditional sill plate placed atop a foundation and tied down with anchor bolts, wet set sill plates have a statistically significant presence in California homes, especially in older construction. No information is available on the performance of wet set sill plates. Traditionally, wet set sill plates are 2 × 4 or 2 × 6 wood sill plates placed or set-in foundations when it is being poured; see Figure 3.22. The sill is usually prepared prior to the pour with a series of nails, potentially offering additional load transfer. In these tests, the wet set sill used was construction-grade redwood 2 × 6 with 2–30d nails driven through the sill at 24 in. center-to-center spacing along the board length. The nailed side was set in the wet foundation to offer additional resistance to movement of the sill plate. Details of the wet set sill and the construction procedure in shown in Figure 3.23. A view of the wet set sill plate used in Specimen A-6 is shown in Figure 3.24.

Figure 3.22 Specimen A-6 sill plate being wet set into the footing.

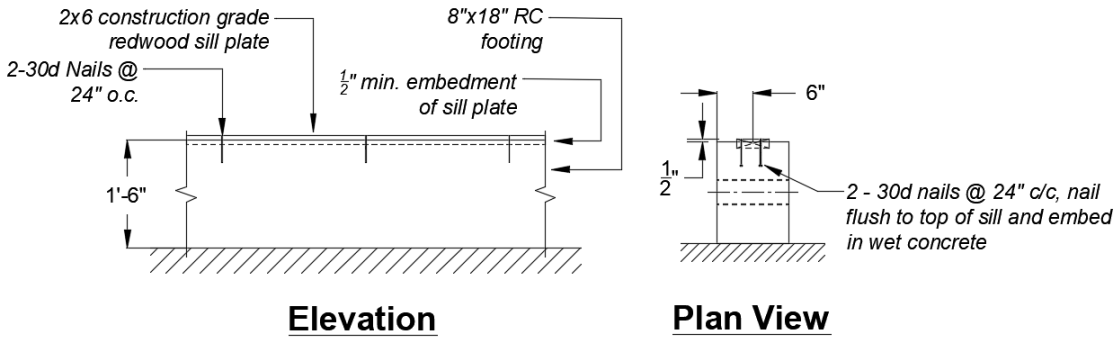

Notes:

1. **Set form w/ plywood or 1x8 sheathing material to 19" tall by 12" wide.**
2. **2x6 Construction Grade Redwood wet set sills are cut to desired length.**
3. **Trowel in wet concrete to fit the form.**
4. **Check the level on top and width of form.**
5. **Place a center line in the wet concrete to form alignment for wet set sill.**
6. **Embed the protruding nails into the concrete so that the sill is embedded 1".**
7. **Check level of sill and use flat head hammer to make adjustments.**
8. **Add additional bracing/blocking as needed to keep form while curing.**
9. **Chisel away excess concrete as need be.**

Figure 3.23 Wet set sill plate view and construction procedure.

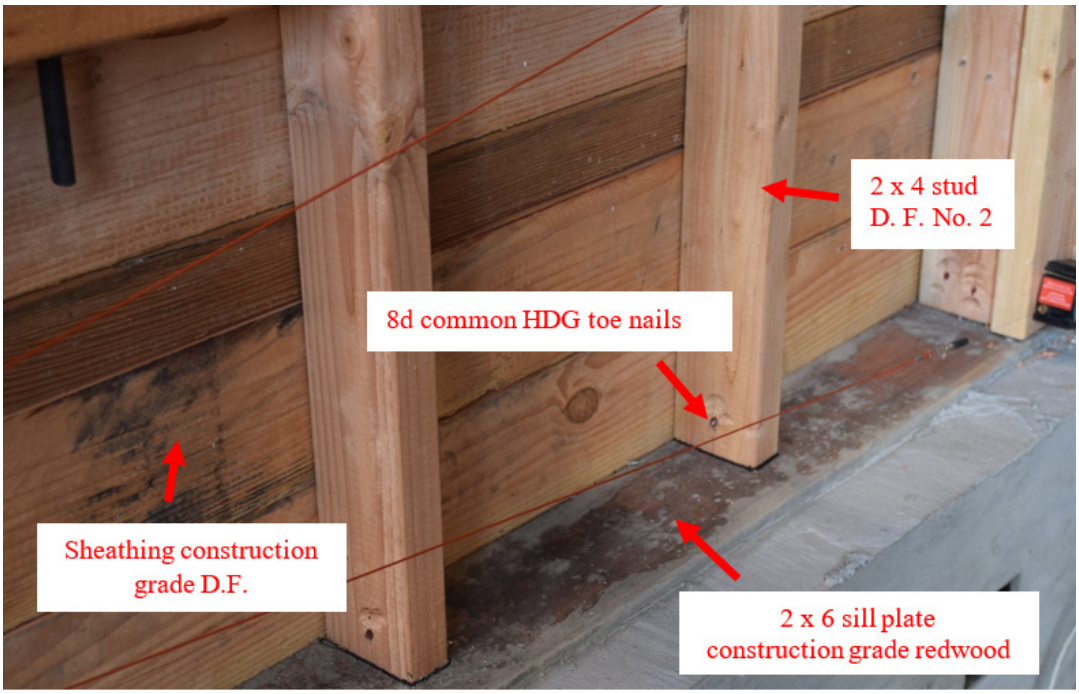

Figure 3.24 Specimen A-6 wet set sill plate.

3.4 INSTALLATION OF FINISHES

Each of the six cripple walls tested in Phase 1 of the program contained a stucco finish over horizontal sheathing boards. For consistency, the same details, materials, and contractor were used for the application of the stucco, and the same details and materials were used for the application of the sheathing. Sheathing boards used were 1 × 6 nominals (7/8 in. #11 × 1-1/2 in. 5-1/2 in.) construction-grade Douglas Fir. Full boards were placed at the top and bottom of each wall. A 1/8-in. gap was placed between each board to allow for expansion. The middle sheathing board was cut to match the required dimension to fit in the middle of the wall; see Figure 3.25. Boards along the front face of the cripple walls extended 3/4 in. beyond the outer stud to allow for the boards at the corners to abut to them. An example of this can be seen Figure 3.26, showing the C-shaped cripple wall (top boundary condition C). All sheathing boards, besides the middle board, were attached with 2–8d common nails per stud. The middle board was attached with 1–8d common nail per stud. At the ends of each wall where two studs were present, the sheathing boards were only nailed to the outermost stud.

In order to mimic the increased strength and stiffness a cripple wall would have due to the continuity of the stucco running from the cripple wall past the floor diaphragm, an extra top plate was added to the cripple walls to allow for an additional row of furring nails to be attached. These details were previously discussed in the sections discussing top boundary conditions. Five of the six walls contained this dense furring nail arrangement, denoted as either top boundary condition B or top boundary condition C, while the last wall was constructed with the furring nail arrangement described in top boundary condition A. The furring nail arrangement can be seen in Figure 3.27. The furring nails used were #11 × 1-1/2-in. (0.121-in.-diameter) nails with 1/4-in. wads to allow for proper separation between the metal reinforcement and the sheathing boards.

This is in compliance with 1946 UBC, which specifies that nails should be no less than 4d nails (1-1/2-in. × 0.109-in.-diameter), furred 1/4-in. with a vertical spacing of 6 in. on center [ICBO 1946]. The metal reinforcement used was a 17-gauge, galvanized, hexagonal wire mesh. This metal reinforcement meets the requirements of the 1946 UBC, which states that metal reinforcement shall be galvanized and not be thinner than 18-gauge wire with openings no less than 3/4 in. and no greater than 2 in. [ICBO 1946]. A single layer of Grade D building paper was fastened to the sheathed walls using 3/8-in. staples along the studs, top plate, and sill plate. The building paper is meant to act as a moisture barrier between the stucco finish and the horizontal sheathing.

The stucco used for the exterior finish consisted of three layers of stucco, typical of pre-1945 construction. The total thickness of the stucco was 7/8 in., with a 3/8-in-thick scratch coat, 3/8-in.-thick brown coat, and a 1/8-in.-thick finish coat. The mix design used for each coat was derived from the UBC [1943] as well as recommendations from the Portland Cement Association stucco guidebook [Portland Cement Association 1941]. The scratch coat and brown coat both consisted of one-part Type I Portland cement to three-parts fine aggregate and 1/5-part hydrated lime. The fine aggregate was a plastering sand, which was well graded and clean with 70–90% passing through a No. 8 sieve. The hydrated lime met the ASTM C207-06 standard [ASTM 2006]. The finish coat consisted of one-part Type I Portland cement to three-parts fine aggregate, and 3/5 parts hydrated lime. Clean water was added to each mixture until the plaster became workable. The amount of water required was largely left at the discretion of the stucco contractor who targeted a workable mix. Note: the in-place water/cement ratio ranged from 0.5 to 0.55.

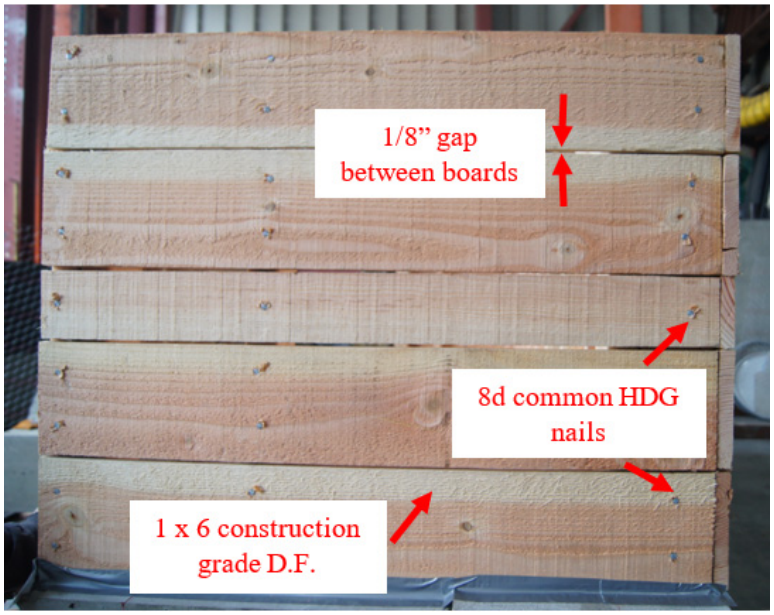

Figure 3.25 **Specimen A-3 horizontal sheathing board arrangement at the wall return for the C-shaped cripple wall.**

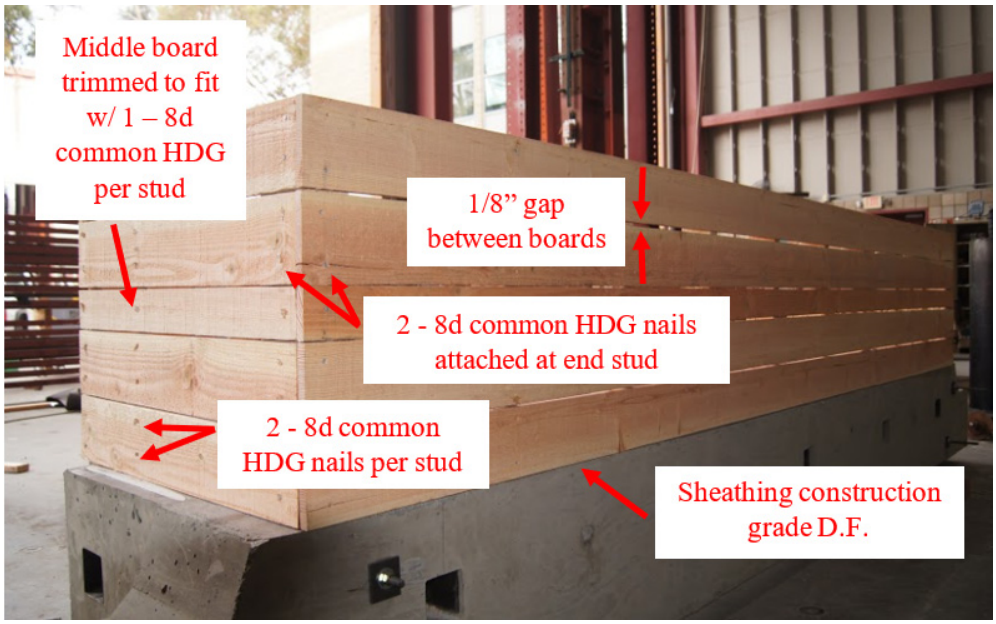

Figure 3.26 **Specimen A-3 sheathing applied to the C-shaped cripple wall.**

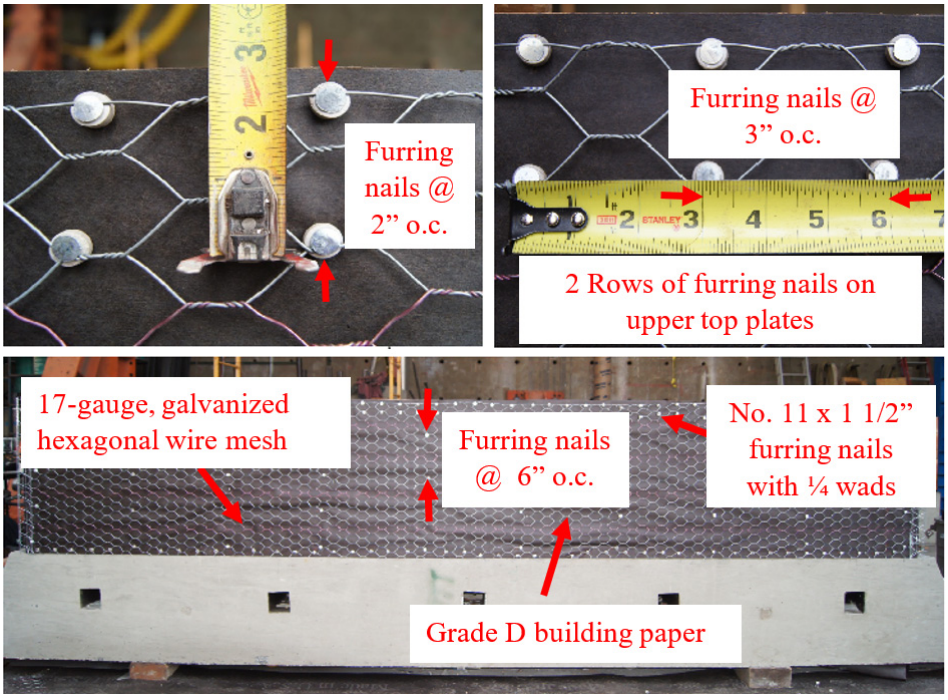

Figure 3.27 **Cripple wall with metal reinforcement and furring nails attached over building paper.**

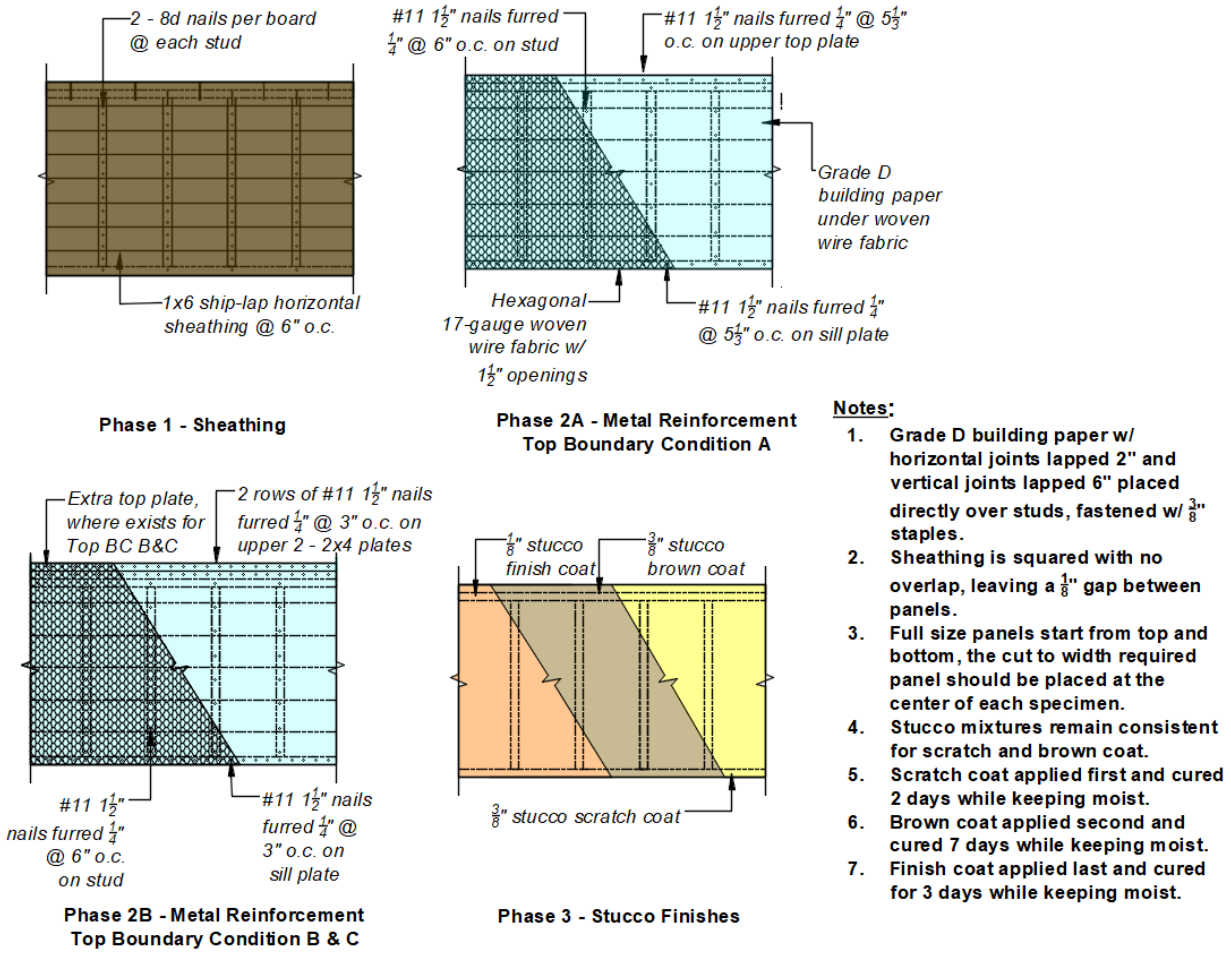

Figure 3.28 Elevation of construction sequence of stucco over horizontal sheathing.

The construction sequence for application of the stucco and sheathing can be seen in Figure 3.28; photographs of the process are provided in Figure 3.29. The process was as follows: Following installation of the horizontal sheathing overlaid by building paper, a 3/8 in.-thick stucco scratch coat was applied onto the building paper and metal reinforcement. Once the scratch coat was applied, the walls were covered and kept moist for 48 hours. After four days, a 3/8-in.-thick brown coat was applied, and the walls covered and kept moist for 72 hours. The brown coat was given seven days to cure before the finish coat was applied. The finish coat was a 1/8-in.-thick smooth troweled finish. The walls were covered and kept moist for three more days to allow for the finish coat to cure. Small (2 in. × 4 in.) cylinders were used to take samples of each coat of stucco. The compressive strength of the scratch coat was 1000 psi on the date of the first test (21 days after application), 1100 psi on the date of the second test (25 days after application), and 1235 psi on the date of the third test (62 days after application). Compressive strengths of the brown coat were 920 psi after 17 days, 1100 psi after 21 days, and 1250 psi after 58 days, and compressive strengths of the finish coat were 450 psi after 10 days, 640 psi after 14 days, and 720 psi after 51 days. These dates correspond to the testing of the first three walls. The lower strength of the finish coat is attributed to the increase volume of hydrated lime in the coat. A summary of the compressive strengths of the stucco is provided in Appendix A.2.

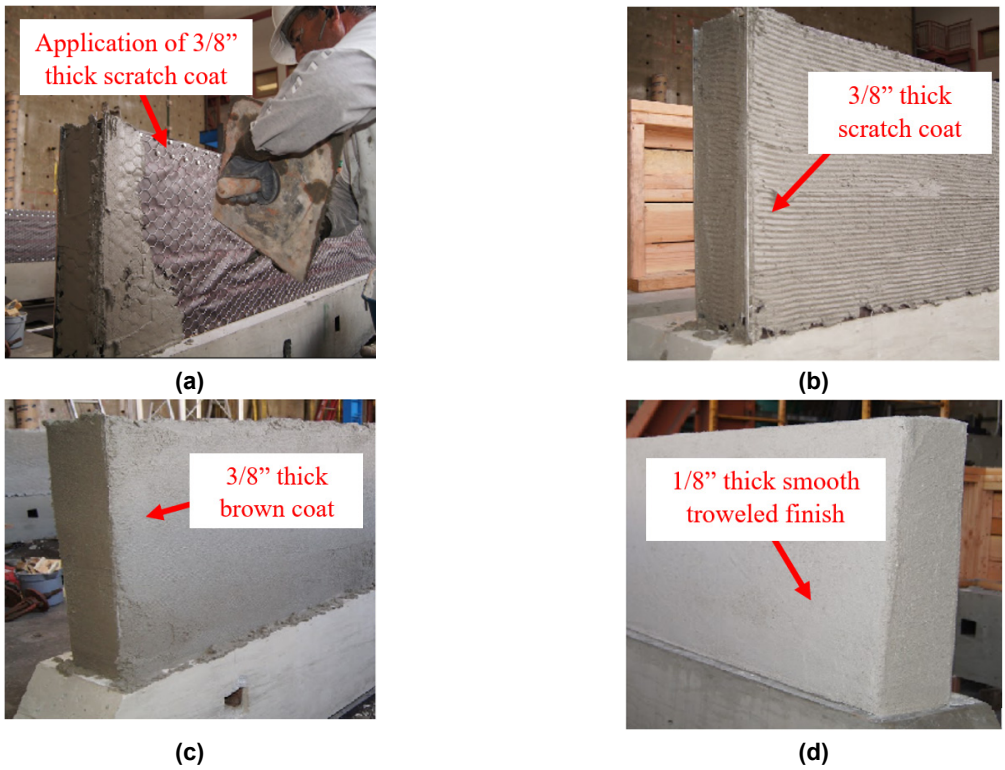

Figure 3.29 **Installation of stucco: (a) applying scratch coat; (b) final scratch coat; (c) final brown coat; and (d) final finish coat.**

3.5 INSTALLATION OF RETROFIT

Only one of the six cripple walls tested in Phase 1 incorporated a retrofit. This wall, Specimen A-5, was identical to Specimen A-2; however, it was retrofitted according to engineering calculations following ATC-110 design guidelines for houses designated as "heavy construction" [ATC 2014]. The retrofit design calculations are provided in Appendix A.3. The retrofit involved fully sheathing the interior face of the cripple wall with 15/32-in. plywood. Prior to sheathing, 2 × 4 blocking was attached to the sill plate with 4–10d common nails per stud bay. Additional 2 × 4 studs were toe-nailed in with 2–8d common nails on the top and bottom at each end of the wall, and two 4 × 4 studs were toe-nailed in with 2–8d common nails on the top and bottom in the interior of the cripple wall at each interior third. The addition of studs and blocking plates were used to allow the plywood panels to be nailed to the cripple wall. Figures 3.30 (a) and (b) show the interior of the framing before the application of plywood. The plywood was placed in three 4-ft sections, fully sheathing the interior face of the wall. Panels were attached with 8d common nails at 4 in. on center along the edges and 12 in. on center along the field. A 1/8-in. gap was provided between panels to allow for expansion, and the nails were placed 3/4 in. from the panel edge to prevent nails from tearing through the panel edges. Details of the plywood panel attachment for Specimen A-5 can be seen in Figure 3.31.

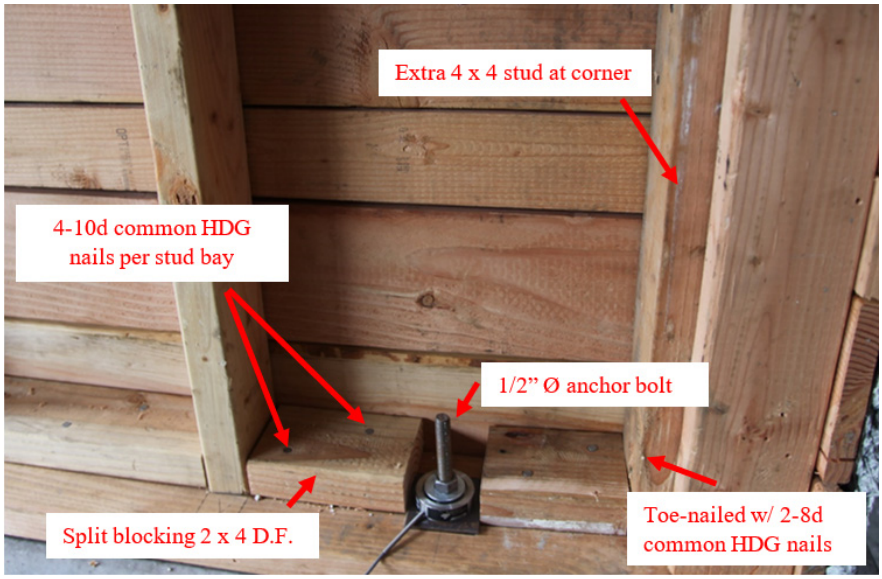

(a)

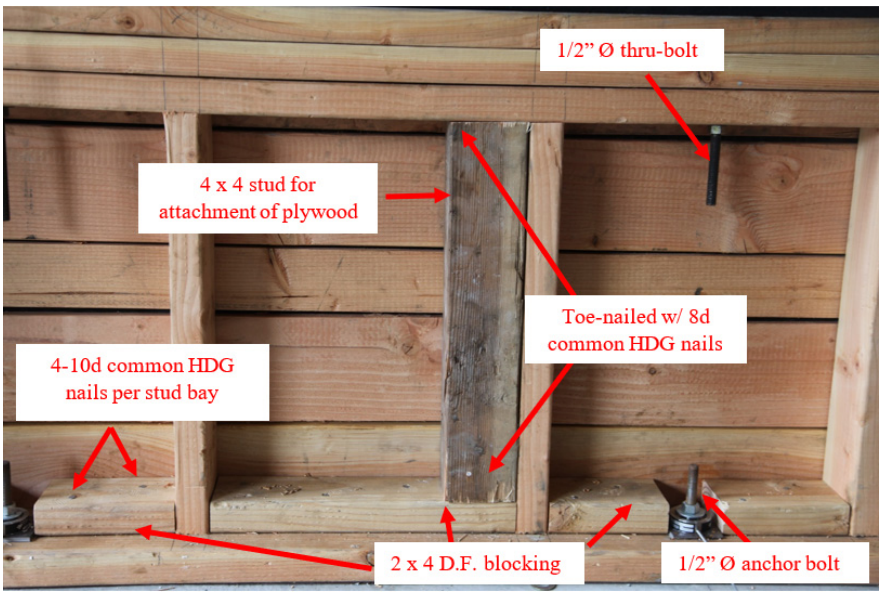

(b)

Figure 3.30 **Specimen A-5 retrofit framing details prior to plywood placement: (a) framing face corner retrofit detail; and (b) framing face interior retrofit detail.**

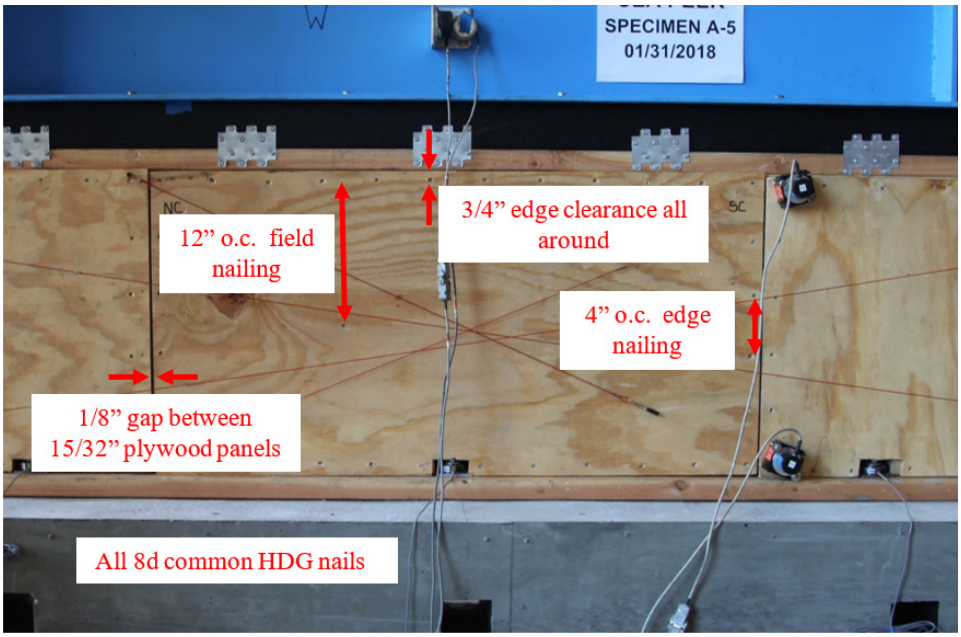

Figure 3.31 Specimen A-5 retrofit plywood panel attachment.

3.6 TEST SETUP

Figures 3.32(a) and (b) show a plan and elevation view of the typical test setup. Complementary photographs of these setups are shown in Figure 3.33(a) and (b). The same test setup was used for all cripple walls in Phase 1. The lateral load was applied with a 48 in. (total) stroke, servo-controlled, hydraulic horizontal actuator capable of imposing 50 kips. The actuator was mounted to a strong wall using an actuator mounting plate, with its weight carried via a link chain back to the reaction wall so as to not impose a vertical load on the cripple wall. The lateral force was transferred from the actuator to the cripple wall with a stiff steel beam (W12 × 26 section). To allow for uninhibited movement of the finishes and plywood panels (present in the retrofitted walls only) during testing, a 4 × 4 laminated wood beam was used as a spacer between the steel beam and the uppermost top plate of the cripple wall. This also facilitated ease of assembly of the specimens. Details of the connection of the steel beam, laminated wood beam, and cripple wall framing can be seen in Figure 3.34. The connection from the steel beam to the laminated wood beam was made with pairs of 3/8 in.-diameter × 3-1/2-in.-long lag bolts at 16 in. on center spacing, connected from the bottom flange of the steel beam top of the wood beam. The laminated wood beam was selected to be sufficiently thick as to preclude connection between the lag bolts and the cripple wall top plates. The cripple wall specimens were connected to the laminated wood beam using 1/2-in.-diameter × 7-1/2-in.-long Grade 2 steel thru bolts at 32 in. on center spacing. Note that the length of these bolts was modified when an additional top plate was utilized over the two 2 × 4 top plates (top boundary condition B and top boundary condition C). These bolts were countersunk into the laminated wood beam and fastened with nuts and washers at the bottom of the lowermost top plate.

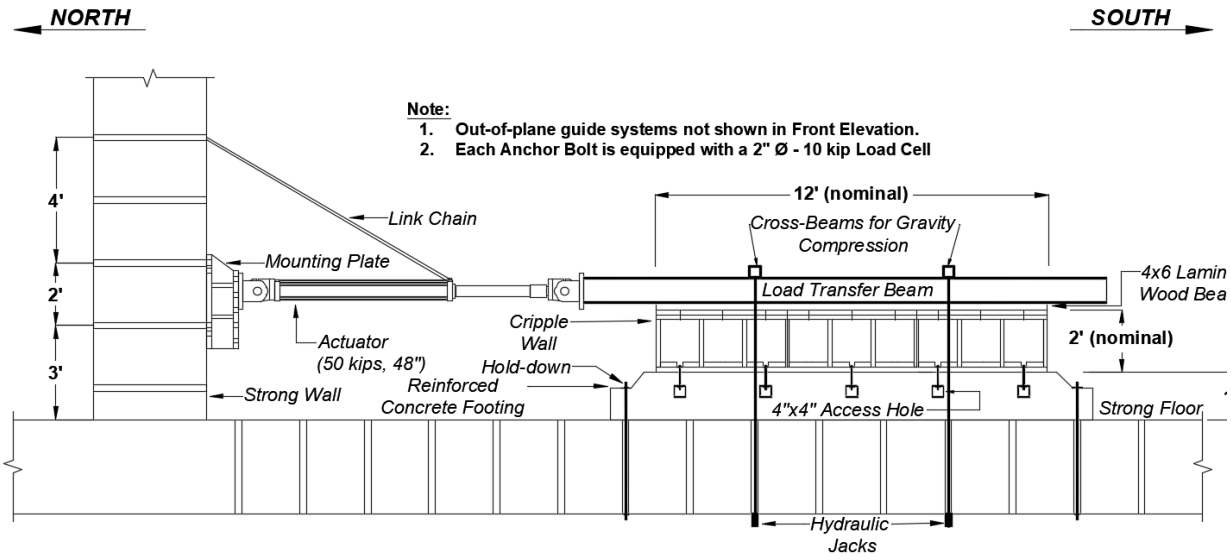

(a)

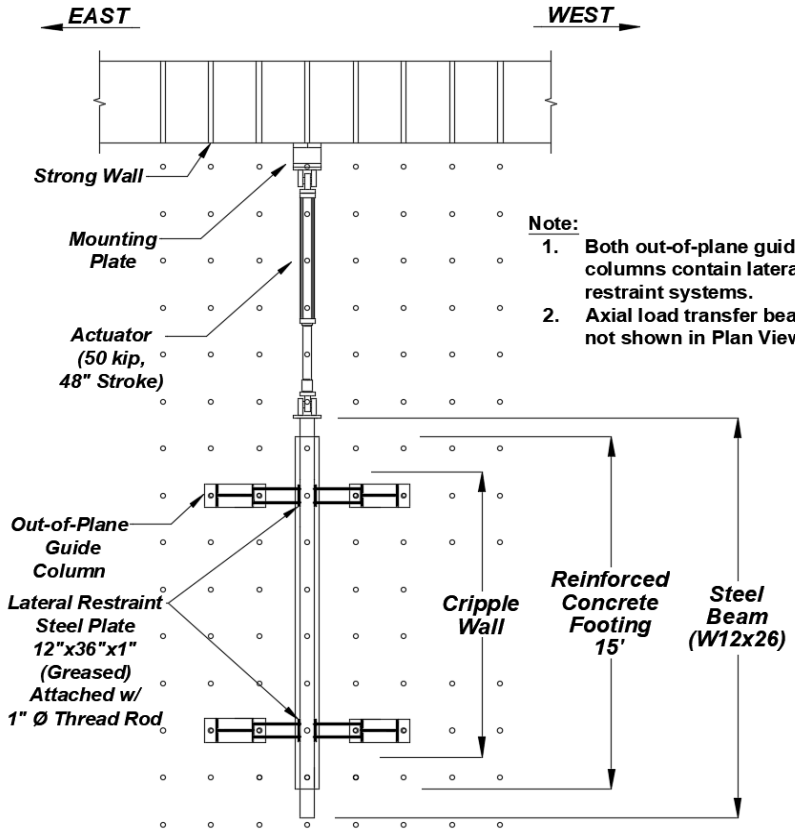

(b)

Figure 3.32 Test setup for 2-ft-tall cripple walls: (a) elevation of basic test setup; and (b) plan view of basic test setup.

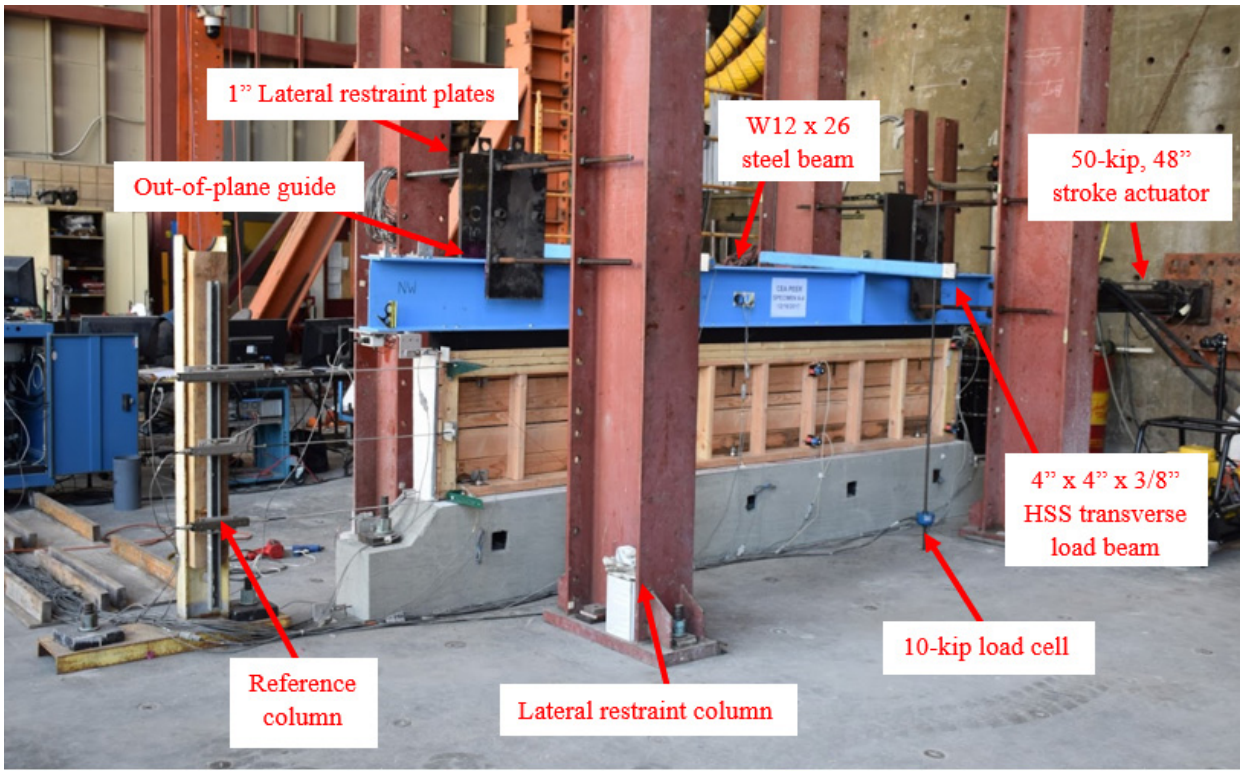

Figure 3.33 Photographs of the test setup for 2-ft-tall cripple walls during Phase 1.

The wood framing for individual specimens was assembled on the laboratory floor. Because all specimens were constructed with a stucco finish for this phase, the wood framing was erected vertically onto an individual concrete footing, and the stucco finish applied. This was intended to minimize pretest damage and simplify the installation process. The footings were fastened to the strong floor with a rod at each end, each tensioned to 50 kips. Once the cripple wall and footing were in place, the laminated wood beam and steel beam were attached. After these beams were attached, the actuator was attached with four 1-in.-diameter bolts. Subsequently, two 4 × 4 × 3/8-in. HSS sections were placed transversely at three points along the specimen to apply vertical load to the steel beam. Each transverse HSS beam had a 1/2-in.-diameter all-thread rod attached at each end, which were attached to hydraulic jacks at the base of the strong floor. The hydraulic jacks applied the desired vertical load to each specimen. The location of the transverse beams is shown in Figure 3.31(a). The choice of location for applying the loads was meant to apply a uniformly distributed gravity load on the full length of the cripple wall specimen. Note: although additional point loads would have increased the uniformity of the load distribution, they would have also increased the complexity significantly. In addition, the stiff W12 × 26 lateral transfer beam was deemed sufficient to nominally result in a uniform load application. Each thread rod at the HSS transverse beam load locations was equipped with a 10-kip load cell used to monitor the applied vertical load during testing.

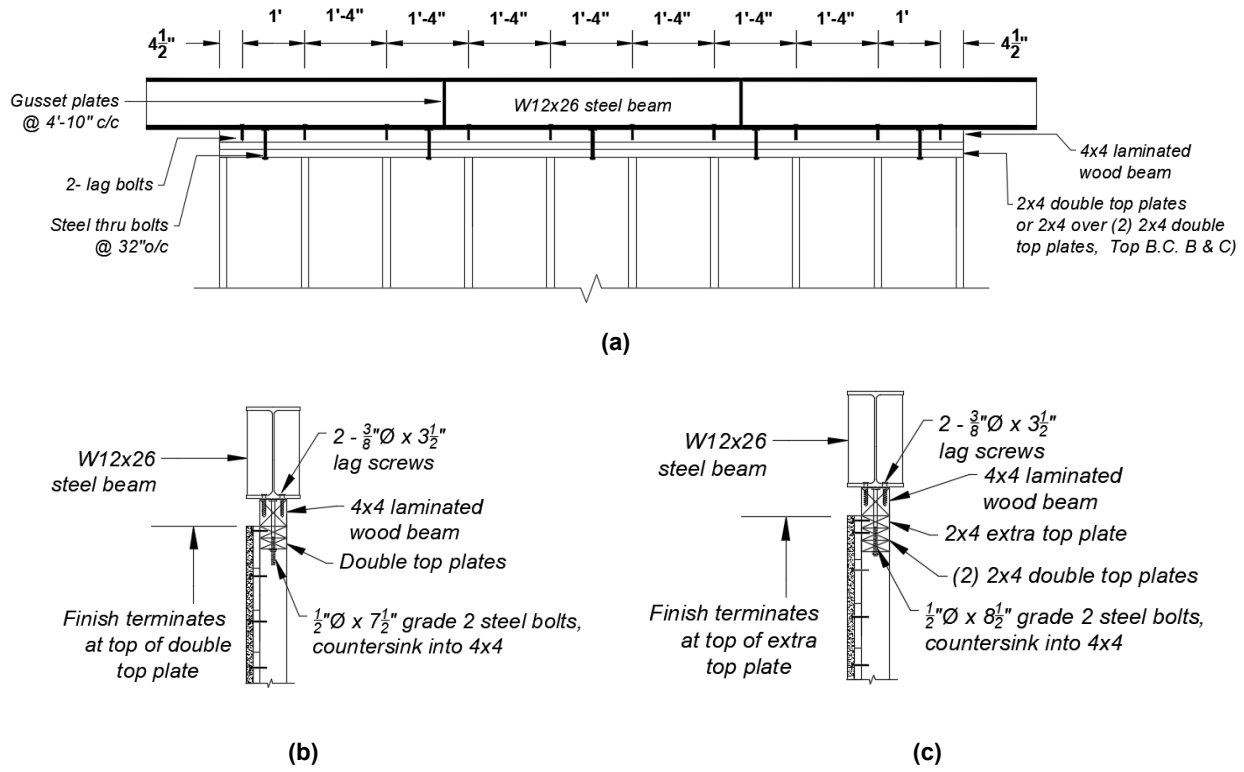

Figure 3.34 **Steel beam connections: (a) elevation of steel beam connection; (b) top of wall detail for stucco over horizontal sheathing for top boundary condition A; and (c) top of wall detail for stucco over horizontal sheathing for top boundary condition B and top boundary condition C Horizontal steel beam to cripple wall connection details.**

Each of the walls tested in Phase 1 was subjected to a constant uniform vertical load of 450 lbs/ft (5400 lbs total). The cumulative weight of the steel transfer beam, laminated wood transfer beam, and the transverse vertical loading beams coupled with the use of a pair of hydraulic jacks tied to the bottom of the strong floor was used to achieve this target vertical load. Note: 400 lbs of the target 5400 lbs (450 plf case) were available via the weight of the lateral steel and wood-laminated transfer beams; thus, the transverse HSS assembly required applying an additional 1250 lbs per point load location. The necessary vertical load required of the hydraulic jacks was 1.25 kips each for a total of 5 kips. Due to eccentricity of the walls when constructed with bottom boundary condition "c", the applied loads measured did not "pencil out" to 1.25 kips each. Loads ranged from 1.15 kips to 1.40 kips for each hydraulic jack, resulting in 4.8 kips to 5.0 kips for the sum of all hydraulic jacks. For bottom boundary condition "a" and bottom boundary condition "b", there were negligible differences in the applied load at each jack.

Before any loads were applied to the cripple wall, steel plates were fastened to the sides of the steel transfer beam so that both the top and bottom flange of the steel beam were around 1/16 in. from the face of the steel plate. Once the desired position was achieved, the steel plates were fastened into position to the out-of-plane guide columns; see Figures 3.32 and 3.33. The steel plates were greased, and a gap was left between the steel plate and the steel transfer beam so as to not

impose any artificial loads via friction force at the contact interface of the plates and beam. The purpose of implementing an out-of-plane guide system was to ensure that the imposed displacement during testing was only in-plane.

Once the vertical load was applied to the test setup, the anchor bolts were tensioned. For two tests, each anchor bolt was tensioned to about 4 kips. The subsequent two tests reduced the tension to 1 kip. The anchor bolt tension load was relaxed in the last test to emulate a hand-tight condition; thus, the target was selected to be 200 lbf. This became the standard level of tension for all subsequent tests. Once the anchor bolts were tensioned, a bias of all instrumentation including the actuator load and displacement was applied, and all values were recorded before and after the bias. At this point the application of lateral cyclic loading would commence.

3.7 INSTRUMENTATION

Extensive measurements of displacements, rotations, and loads were performed on each cripple wall specimen. Each specimen had slight variations in instrumentation depending on its boundary conditions and retrofitting condition. Figure 3.34 shows the instrumentation details for Specimen A-5, a retrofitted 2-ft-tall cripple wall. The complete instrumentation details for all the cripple wall specimens are available in Appendix B.1. Note: between 35–40 channels of instrumentation were utilized for the test specimens in Phase 1. In addition, digital video cameras were arrayed around the specimen to provide between three to four views.

The overall response of the cripple wall was characterized using displacements measured by displacement transducer LP01. Sensor LP01, along with transducers LP02 and LP03, were connected to a stationary reference column tied down to the strong floor. Sensor LP01 was attached to the middle of the middle top plate (upper top plate for top boundary condition A), 23-1/4 in. from the top of the concrete footing and measured the total displacement at the top of the cripple wall. Sensor LP02 was attached to the middle of the cripple wall at a height of 12 in. from the top of the footing. This intermediate displacement transducer was used to capture the deflected shape of the cripple wall. Sensor LP03 was attached to the middle of the sill plate and used to measure the absolute displacement of the sill plate. By taking the difference between LP01 and LP03, the relative displacement of the cripple wall could be determined (neglecting sill displacement relative to the foundation). Details of these transducers can be seen in Figure 3.34(a). A photograph of the placement of LP01-LP03 is shown in Figure 3.35.

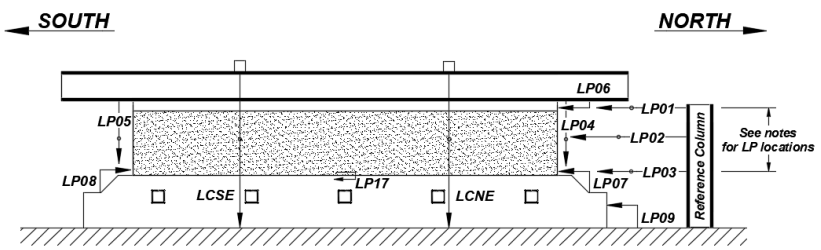

Notes:
1. LP01, LP02, and LP03 measure lateral displacement with LP01 attached to middle of second top plate, LP02 attached to middle of stud, and LP03 attached to middle of sill plate.
2. LP04 and LP05 measure the uplift at each end of the wall.
3. LP06 monitors the slip between the horizontal transfer beam and the upper top plate.
4. LP07 and LP08 monitor the slip between the footing and the sill plate.
5. LP09 monitors the slip of the footing.
5. LCNE and LCSE monitor the axial load on the East Side of the wall.
6. LP17 monitors displacement of stucco relative to the footing.

(a)

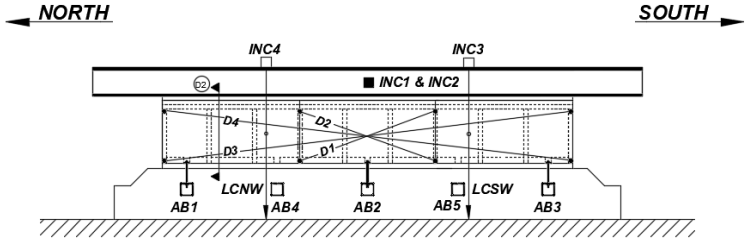

Notes:
1. AB1-AB5 are instrumented with 2" Ø Donut Load Cells measuring uplift loads.
2. Pairs of strength potentiometers are mounted on framing studs or plywood panels for retrofit cases.
3. INC1 measures longitudinal rotation of load transfer beam. INC2 measures the transverse rotation of the load transfer beam.
4. INC3 and INC4 measure the rotation of the transverse beams where axial load is applied.
5. LCNW and LCSW monitor the axial load on the West Side of the wall.

(b)

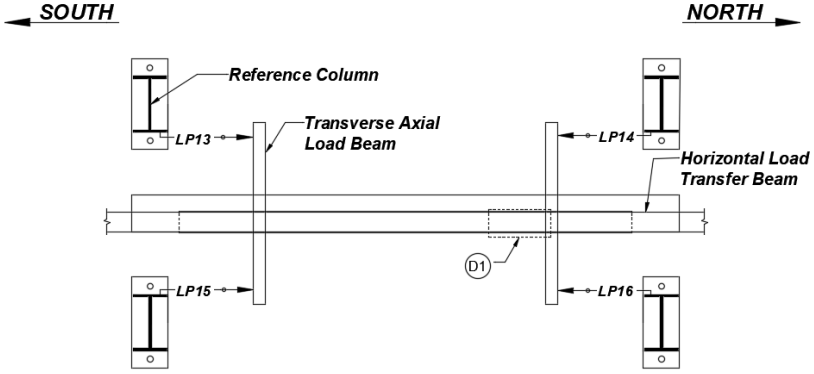

Notes:
1. LP13 - LP16 monitor the displacement of the transverse axial load beams.

(c)

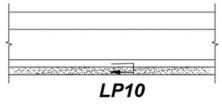

Notes:
1. LP10 monitors the differential displacement between the stucco and the siding.

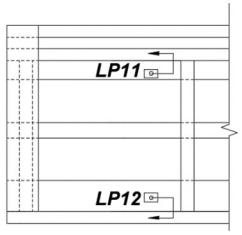

Notes:
1. LP11 and LP12 monitor the siding slip.

(d)

Figure 3.35 **Specimen A-5 instrumentation details for the retrofitted 2-ft-tall cripple wall: (a) instrumentation elevation view of the stucco finish face; (b) instrumentation elevation for the framing face (note that AB4 and AB5 only active when the specimen incorporated a retrofit); (c) instrumentation plan view; and (d) instrumentation details for the stucco detachment and siding.**

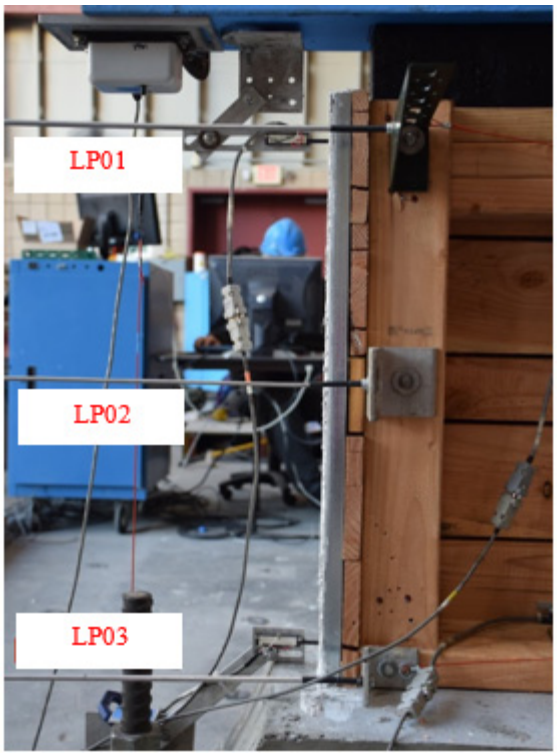

Figure 3.36 Placement of displacement transducers LP01 – LP03 on a 2-ft-tall cripple wall.

Local deformations of the cripple wall were also obtained. For retrofitted cripple walls, plywood panel deformations of the interior panel and all three panels were taken with two pairs of diagonal displacement transducers denoted as D1–D4. For unretrofitted cases, the diagonal transducers were fastened to the framing on the top and bottom of studs for the interior transducers and the flat corner studs for the outer transducers (excepting top boundary condition A, which had the outer displacement transducers fastened to the top and bottom of the outer studs). The location of these diagonal transducers is shown in Figure 3.34(b). The inner diagonal transducers, D1 and D2, characterized the distortion of the middle four feet of the wall (or the middle plywood panel) when the cripple wall was retrofitted. For the retrofitted cases, the shear distortion of the middle panel was smaller than the resolution of the displacement transducers. The outer diagonal transducers, D3 and D4, characterized the overall distortion of the entire cripple wall.

Uplift of the cripple wall was measured at each end with displacement transducers LP04 and LP05; see Figure 3.34(a). For the 2-ft-tall cripple walls, uplift measurements were out of the resolution range of the transducers. This is not expected to be the case with 6-ft-tall cripple wall specimens. The slip between the steel transfer beam and the uppermost top plate was measured by LP06. Note: even if slip between steel transfer beam and top plate occurred, it did not affect the amount of displacement imposed on the cripple wall specimen as that is controlled by LP01, which is attached to the cripple wall itself; LP07 and LP08 are displacement transducers attached to the corners at each end of the cripple wall. These transducers worked to calculate the displacement of the stucco at each corner. At higher displacement amplitudes, these transducers would be removed as the corners of the wall would crush against the footing, and the readings would become inaccurate. The slip between the footing and the strong floor was monitored with LP09; no slip occurred between footing and the strong floor in any of the tested walls.

On the top of the cripple wall, a displacement transducer, LP10, was implemented to monitor the displacement between the stucco finish and the top horizontal sheathing board; see Figure 3.26(d). On the interior face of the cripple wall, transducer LP11 monitored the slip between the top horizontal sheathing board and the lowermost top plate; LP12 monitored the slip between the bottom horizontal sheathing board and the sill plate. On the finish face of the cripple wall, LP17 measured the displacement between the bottom of the stucco finish and the footing. The combination of these aforementioned transducers allowed for the displacement between the framing, sheathing, and finish to be independently characterized.

Four additional transducers, LP13–LP17, were attached to the out-of-plane guide columns and measured the displacement of the transverse vertical load beams at each end. Two inclinometers, denoted as INC3 and INC4, were attached to the east end of the transverse vertical load beams to measure rotations of the beams during loading. Each transverse load beam was tensioned through a thread rod and a hydraulic jack fastened under the strong floor. Each thread rod was connected to a 10-kip load cell to monitor the vertical load imposed. These load cells are shown in Figure 3.34(a) and (b) and labeled according to their cardinal directional position (i.e., LCNW for the northwest load cell). The use of these four displacement transducers, two inclinometers, and four load cells works not only monitored the vertical load applied to the specimen but also helped to determine the lateral load imposed due to the horizontal component of the displacing vertical load. This artificial horizontal load component is taken out of the lateral responses of each cripple wall.

The tension in each anchor bolt was measured with a 10-kip donut load cell. These load cells monitored the uplift forces in the cripple wall; see Section 3.2 for details on the setup of these load cells. Finally, two inclinometers, INC1 and INC2, were used to measure the rotation of the horizontal load transfer beam along the longitudinal and transverse axis of the loading direction.

Minor variations in the instrumentation of select cripple wall specimens were implemented depending on its boundary condition and/or retrofit condition. The largest variation in instrumentation occurred with the testing of Specimen A-3, the C-shaped cripple wall. Complete instrumentation details for all cripple walls can be found in Appendix B.1.

3.8 DIGITAL VIDEO CAMERAS

For each test, extensive high-resolution digital photographs and video documentation were taken to document the pre-test, during testing, and post-test state of each cripple-wall specimen. During testing, photographs were taken at the push and the pull of the first cycle for each drift level as well as at the end of the last cycle of the drift level for the 0.2%–1.4% drift amplitudes. Five to six cameras were used to capture the live motion of the cripple wall during testing. Figure 3.37 shows the locations of each of the cameras used to record an individual specimen. Two of the cameras were live-web cameras with views of the framing and finish faces of the cripple wall. These tests recorded continuously. During video processing, the recordings of the webcams were edited and overlaid with the loading protocol as well as the lateral force–lateral displacement hysteresis of the cripple wall. The other three to four cameras captured various angles of the walls deemed most important to help understand the specimen's behavior during testing. The framing face and finish face as well as the ends of the cripple walls were often recorded with these cameras because the video resolution of these cameras is higher than that of the webcams. All of the cripple walls would

bear on the foundation at their ends, which caused these areas to accumulate more significant damage than the framing or finish faces, especially at low drift amplitudes.

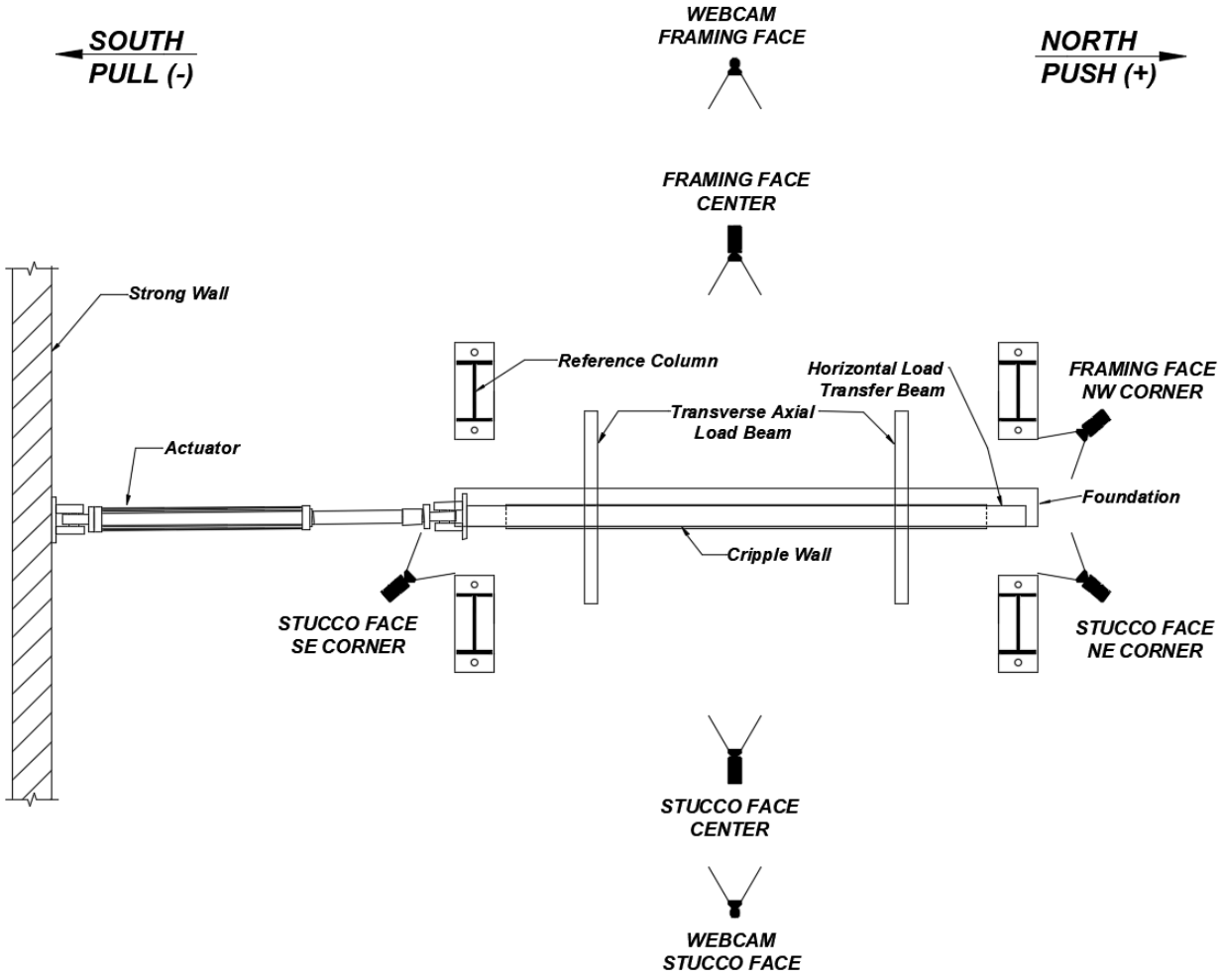

Figure 3.37 Plan view of typical camera layout.

3.9 LOADING PROTOCOL

The loading protocol for each test varied slightly depending on the rate of post-peak strength degradation of the individual specimen. As noted in Section 2.4, all cripple walls underwent the same loading protocol until the specimen realized a loss greater than 60% of its measured lateral strength. At this point in the protocol, the following and each subsequent drift level was increased by 2%, rather than 1%. If the 60% loss in strength did not occur, each drift level would remain at an increase of 1% per cycle grouping. The loading protocol would progress until an 80% loss in strength was realized. At this point, a monotonic push would be conducted, typically to a global drift of 20%. The amplitude of the monotonic push might vary slightly depending on instrumentation constraints. The loading protocol as stated was precluded for Specimens A-4 and

A-5. Specimen A-4, which was tested first, did not have a monotonic push initiated at the end of the loading protocol because this step in the testing protocol was implemented later in the test protocol regime. During testing of Specimen A-5, the actuators displacement control measurement sensor was obstructed, causing the cripple wall to displace further than the targeted displacement (around 13% drift instead of the target 9% drift). This caused significant damage to the cripple wall, and the accuracy of the displacement sensor to be lost. Therefore, the results of the test discussed are up to the end of the 7% drift cycle level. Figure 3.36 shows the loading protocol for Specimen A-1, and Table 3.2 gives details of the loading protocol. Details of the loading protocols for each test specimen can be seen in Appendix A.4.

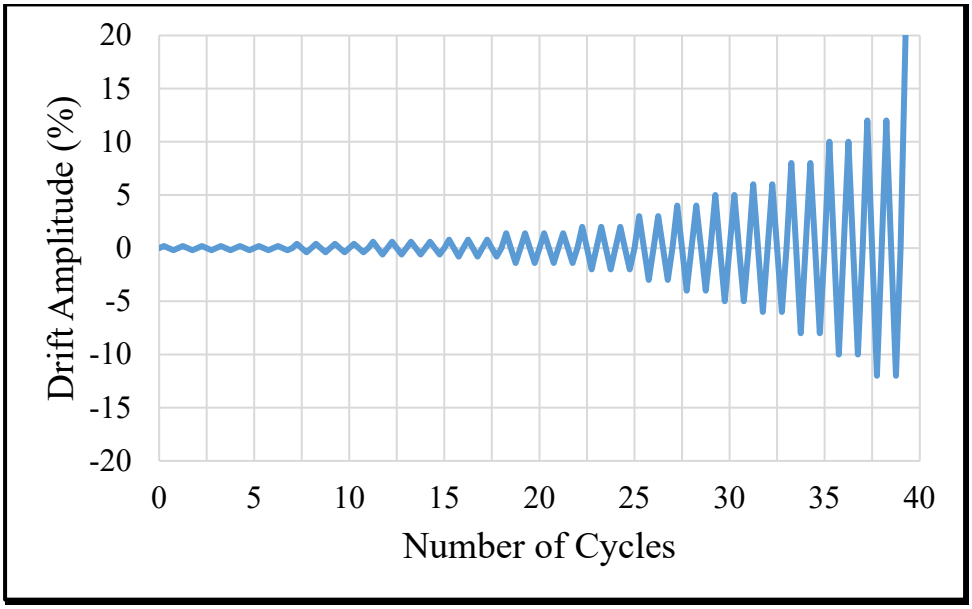

Figure 3.38 Specimen A-1 loading protocol.

Table 3.2 Specimen A-1 example of loading protocol.

Cycle group no.	Drift (%)	Amplitude (in.)	No. of cycles per group	Loading rate (in./sec)	Time per cycle (sec)	Total time per cycle group (sec)
1	0.2	0.048	7	0.0064	30	210
2	0.4	0.096	4	0.0128	30	120
3	0.6	0.144	4	0.0192	30	120
4	0.8	0.192	3	0.0256	30	90
5	1.4	0.336	3	0.0448	30	90
6	2	0.48	3	0.064	30	90
7	3	0.72	2	0.096	30	60
8	4	0.96	2	0.128	30	60
9	5	1.2	2	0.16	30	60
10	6	1.44	2	0.192	30	60
11	8	1.92	2	0.256	30	60
12	10	2.4	2	0.16	60	120
13	12	2.88	2	0.192	60	120
14	Mono	5.0	--	0.333	60	60

4 TEST RESULTS

4.1 OVERVIEW

This chapter presents the results of reversed cyclic response of the six cripple walls tested in Phase 1. The key parameters of this testing program are the boundary conditions and the retrofit condition of the cripple walls. The loading protocol, vertical load, height, length, and finish of the cripple walls remained constant for all six specimens. As stated in the previous chapter, each cripple wall has a nominal length of 12 ft and nominal height of 2 ft. Each wall was subjected to a vertical load of 450 lbs/ft, mimicking the gravity load of a typical two-story house, and all walls were finished with stucco over horizontal lumber sheathing.

Each individual cripple wall considered a single parameter variation, while the remaining parameters were consistent with other specimens. This was done to ensure that the impact of the varied parameter on the response of the wall could be readily determined by cross-comparing the response of multiple specimens. Table 4.1 presents the unique variable for each specimen. In addition, a pseudo-name was assigned to each of the specimens for the purposes of clarity in the presentation of the results.

Table 4.1 Variable parameters for each cripple wall tested and specimen pseudo-names.

Specimen name	Test no.	Unique variables tested	Specimen pseudo-name
A-1	4	Top boundary condition A[1]	Top A
A-2	3	Top boundary condition B[2]	Top B
A-3	6	Top boundary condition C[3]	Top C
A-4	1	Bottom boundary condition D[4]	Bottom b
A-5	5	Retrofit	Retrofit
A-6	3	Wet set sill plate	Wet set

[1] CUREE tests at UC Davis boundary condition, no built-up ends
[2] Top boundary condition B (built-up ends)
[3] Return wall, C-shaped wall
[4] All finishes bearing on foundation

4.2 LATERAL FORCE–DISPLACEMENT RESPONSE

This section presents the global lateral force-displacement response of each of the specimens tested in Phase 1. The presentation includes photographs of each specimen, followed by the lateral force-displacement hysteresis (Figures 4.1 through 4.17). Note: both global total and global relative displacement are presented, where the relative displacement accounts for the displacement of the cripple wall only and ignores the displacement between the foundation and the sill plate. In addition, secondary axes were incorporated in each plot to present the lateral load plf of wall length and the drift ratio (i.e., displacement/cripple wall height). The maximum lateral load in the positive and negative directions are identified in each hysteresis. Discussing the individual hysteresis is useful, and a cross-comparison amongst the various specimens is presented, with particular emphasis on eliciting the impact of the varied parameters. In this regard, a cross-comparison of all specimens is provided first. Next, the effect of individual parameters considered in the Phase 1 matrix is discussed.

4.2.1 Summary of Response of All Specimens in Phase 1

Figure 4.18 compares the lateral strength plf of wall in the push and pull direction for all six cripple walls in Phase 1; Figures 4.19 and 4.20 show the global and relative drift ratios, respectively, at lateral strength in both directions. Important information on the response can be found in the pre-lateral strength and post-lateral strength behavior; therefore, Figure 4.22 provides a generic monotonic response to illustrate the selected pre- and post- strength values shown in subsequent figures. Figure 4.23 compares the relative drift ratio of each specimen at 80% of the pre-lateral strength. Figure 4.23 compares the relative drift ratio of each wall at 40% of the post-lateral strength (i.e., 40% residual strength). Note that in Figure 4.23, Specimen A-5 is not presented as the test did not follow the loading protocol to achieve 40% post-lateral strength. During testing, the displacement control measurement was disturbed, causing the displacement during one cycle to be much larger than what was logical. Finally, Figure 4.24 shows the initial secant stiffness for all six specimens. Note: the secant stiffness is defined as the slope from the origin to a point on the pre-strength portion of the envelope curve that is equal to 80% of the maximum lateral load for the relative displacement response.

With respect to the comparison of lateral strength shown in Figure 4.18, it is worth noting that for Specimens A-1 through A-5, the lateral strength in the push direction was 5–15% larger in the push direction than the pull direction. This can be attributed the walls being initially loaded in the push direction, resulting in damage on the walls before they were loaded in the pull direction. The exception to this trend was Specimen A-6, which was constructed with a wet set sill. The strength in the pull direction being larger than in the push direction is possibly due to the orientation of the toe-nailed connection between the studs and the wet set sill plate, which had one nail toe-nailed pointing in the push direction and two nails toe-nailed point in the pull direction.

Figures 4.19 and 4.20 indicate that four of the six cripple walls showed significant differences in the global and relative displacement response of the walls due to the displacement of the sill plate relative to the foundation. The cripple wall with the wet set sill plate did not have any differences in its global and relative response as its sill plate was confined on all sides by concrete, thus preventing any sill displacement. No damage to the concrete surrounding the wet set sill was observed during the testing of this specimen. Specimen A-1 exhibited no significant

difference between the global and relative response due to the low lateral strength of the wall, i.e., its lateral strength was not large enough to overcome the frictional resistance between the bottom of the sill and the top of the concrete foundation.

Cross comparing all specimens considering both the push and pull directions, the lateral strength occurred between 3% and 5% global drift. On the low end of the spectrum, Specimen A-1, which contained top boundary condition A (no wrap around finish condition and fewer furring nails on the top plate) attained its strength in the push and pull direction at 3% global drift. Likewise, this specimen attained the lowest lateral strength in both the push and pull directions. This may be attributed largely to the reduced number of furring nails on the top plate. Top boundary condition A prescribed one row of furring nails connected to the upper top plate at a spacing of three furring nails per stud bay, whereas top boundary condition B and top boundary condition C contained an additional top plate allowing for two rows of furring nails to be connected at 3 in. spacing on the middle and upper top plate. The stucco finish of Specimen A-1 pulled away from the furring nails much more easily and at a lower drift amplitude than those specimens with a denser furring nail arrangement. In addition, unlike the other specimens that had finishes wrapped around their ends, Specimen A-1 had no finish material to bear on the concrete foundation and no continuity of stucco wrapping around the corner. These attributes also contributed to the lower lateral strength and lower global drift at strength.

Specimen A-6, which contained a wet set sill plate and top boundary condition B, also reached its lateral strength in the push direction at 3% drift; however, it had a larger drift capacity in the pull direction where it attained lateral strength at 4% drift. While the drift at strength in the push direction is the same amplitude as Specimen A-1, the lateral strength was 62% greater in the push direction and 93% greater in the pull direction. The reasoning for the difference in strength is attributed to the top boundary condition-B used in Specimen A-6 compared with the top boundary condition A used in Specimen A-1. Furthermore, as shown in Figure 4.17 in a comparison of the global drift at peak in the push direction of Specimen A-6 and Figures 4.5, 4.6, 4.9, and 4.12 showing the relative drift at peak in the push direction of Specimens A-2–A-5, the peak strength occurred at nearly the same drift amplitude. This was to be expected because the greatest attributor to the lateral response of the cripple walls is the furring nail spacing, which is the same for Specimens A-2 through A-6.

4.2.2 Effect of Top Boundary Condition

A comparison between Specimens A-2 and A-3 highlights the effects of top boundary condition B and top boundary condition C on the lateral response of the cripple walls. The furring nail arrangement at the top of the cripple walls is identical for the two boundary conditions, but top boundary condition B wraps the stucco approximately 4 in. around the ends of the cripple wall, while top boundary condition C contains a return wall on each end effectively forming a C-shaped wall. Each return wall added an additional two feet of wall length, with two anchor bolts to the typical corner used in top boundary condition B. Notably, the lateral responses for both specimens were similar; see Figures 4.5 and 4.8. Interestingly, Specimen A-2, which did not contain the return wall, carried slightly larger strength in both directions, albeit by a small margin: 747 plf to 735 plf kips in the push direction and 714 plf to 680 plf in the pull direction. In the push direction, the peak strength occurred at a 5% drift ratio for Specimen A-2 compared with 4% for Specimen A-3; in the pull direction, the peak strength occurred at 4% for Specimen A-2 and 3% for Specimen

A-3. For Specimen A-2, from 3% to 5% drift, the strength increased from 714 plf to 747 plf when being pushed; the strength fluctuated from 695 plf to 714 plf to 646 plf when being pulled. For Specimen A-3, from 3% to 4% drift, the strength increased from 727 kips to 735 plf in the push direction and decreased from 680 plf to 663 plf in the pull direction.

If the same cripple walls were to be tested again, their strength in both directions might occur at the same drift amplitude. The results do not indicate that the cripple wall containing a return wall was significantly stiffer than the cripple wall without the return wall. A comparison of their initial secant stiffnesses, shows that the cripple wall with a return wall was 23.4% stiffer in the push direction but 6.1% softer in the pull direction. The higher strength and nominally similar initial stiffness in the cripple wall without return walls compared with the cripple wall with return walls are contrary to the trend that would have been expected. It would have been expected that the wall return would provide some additional strength and stiffness to the cripple wall. Nonetheless, it is evident that the addition of out-of-plane wall sections had an insignificant effect on the in-plane performance of the cripple wall.

4.2.3 Effect of Wet Set Sill

Similar to Specimen A-6, Specimen A-4 contained the same top and bottom boundary conditions but utilized a typical sill plate with anchor bolts instead of a wet set sill plate. In the push direction, the lateral strength of Specimen A-4 was 1000 plf, which was 27% stronger than Specimen A-6 with the wet set sill plate. In the pull direction, the lateral strengths were much closer: 871 plf for Specimen A-4 and 1000 plf for Specimen A-6, amounting to a 9% increase in the lateral strength; see Figures 4.11 and 4.17. These strengths occurred at 5% drift in both directions as opposed to the 3–4% drift for the wet set sill condition. Looking at the relative drift, however, the strengths occurred at drift ratios of 3.9% in the push direction and 3.5% in the pull direction, which is more consistent with the response of Specimen A-6. This cripple wall may be anticipated to be the strongest amongst the unretrofitted cripple walls tested in this phase due to bottom boundary condition “b”, which has the horizontal sheathing boards and the stucco finish bearing on the concrete. The additional bearing of finish in this case provided substantial increased resistance. Unlike other specimens in this phase, the rotation of the stucco was prohibited by the foundation and could only move out-of-plane, thereby forcing the furring nails to pull out of the studs or stucco to rip away from the furring nails as the wall displaced.

The reduced capacity of Specimen A-4 compared with Specimen A-6 is likely due to the nailing condition of the framing. In Specimen A-4, 2–16 common nails were end-nailed from the sill plate to the stud whereas in Specimen A-6, 3–8d common nails were toe-nailed to connect the sill plate to the studs, which is a much weaker condition. Finally, a comparison between Specimen A-4 with Specimen A-2 (which is the same as Specimen A-2 except for having bottom boundary condition “a” whereby the stucco finish outboard from the footing), Specimen A-4 had a 34% and 22% increase in strength in the push and pull directions, respectively.

4.2.4 Effect of Retrofit

When comparing specimens that differ only in their retrofitted condition (Specimen A-2 and A-5), it was found that the addition of the prescribed ATC-110 [FEMA 2018] retrofit increased the strength from 747 plf to 2033 plf in the push direction and 714 plf to 1926 plf in the pull direction.

This amounts to a 174% increase in strength in the push direction and a 170% increase in the pull direction. A comparison of the global drift at peak strengths is similar for the two specimens, 5% for the retrofitted wall and 4–5% for the unretrofitted wall; see Figures 4.5 and 4.14. An examination of the relative drifts at peak strength demonstrates that the retrofitted wall, Specimen A-5, had a relative drift ratio of 3.6% at peak in the push direction and a relative drift ratio of 2.8% in the pull direction compared with 4.3% and 3.1%, respectively, for the unretrofitted cripple wall; see Figures 4.6 and 4.15. Also worth noting is the increase in initial stiffness associated with the addition of the retrofit. Finally, there was an average increase of 104% in the secant stiffness, which is attributed to the addition of the plywood structural panels.

(a)

(b)

(c)

(d)

Figure 4.1 **Specimen A-1 pre-test photographs for top boundary condition A and bottom boundary condition "a": (a) exterior elevation; (b) interior elevation; (c) south exterior corner; and (d) south interior corner.**

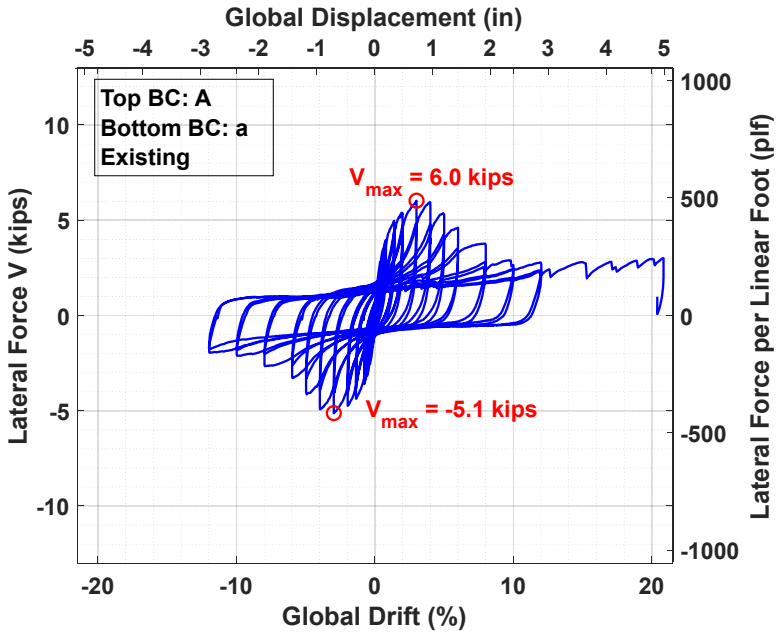

Figure 4.2 **Specimen A-1 lateral force versus *global* lateral drift and displacement hysteresis.**

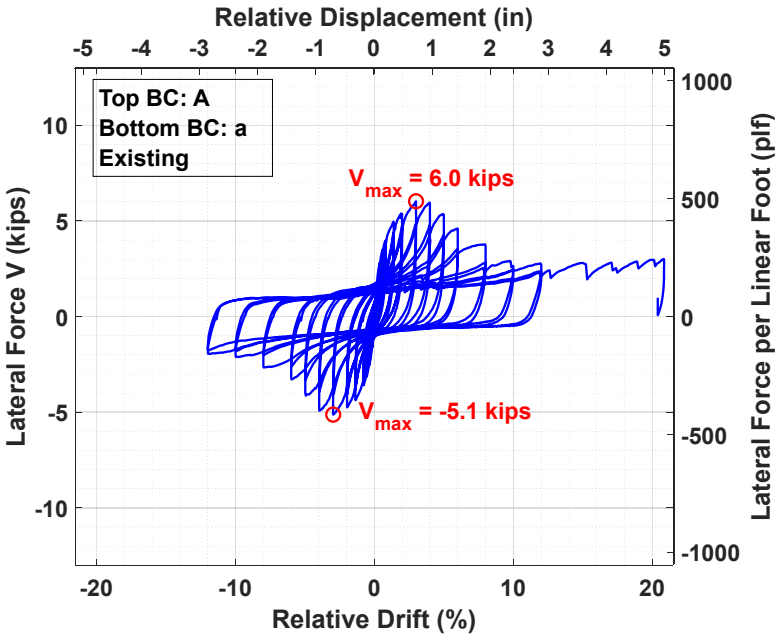

Figure 4.3 **Specimen A-1 lateral force versus *relative* lateral drift and displacement hysteresis.**

(a)

(b)

(c)

(d)

Figure 4.4 **Specimen A-2 pre-test photographs, top boundary condition B and bottom boundary condition "a": (a) exterior elevation; (b) interior elevation; (c) south exterior corner; and (d) south interior corner.**

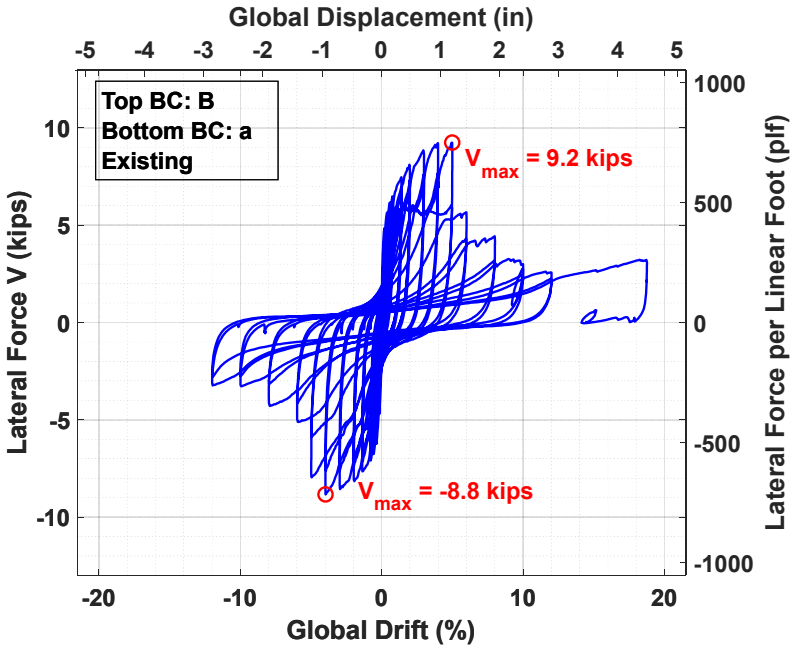

Figure 4.5 Specimen A-2 lateral force versus *global* lateral drift and displacement hysteresis.

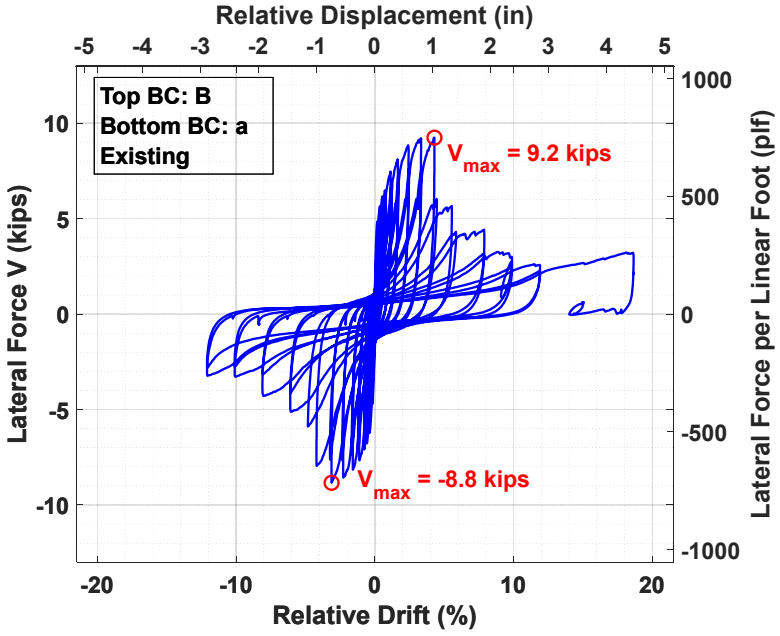

Figure 4.6 Specimen A-2 lateral force versus *relative* lateral drift and displacement hysteresis.

(a)

(b)

(c)

(d)

Figure 4.7 **Specimen A-3 pre-test photographs, top boundary condition C and bottom boundary condition "a": (a) exterior elevation; (b) interior elevation; (c) south exterior corner; and (d) south interior corner.**

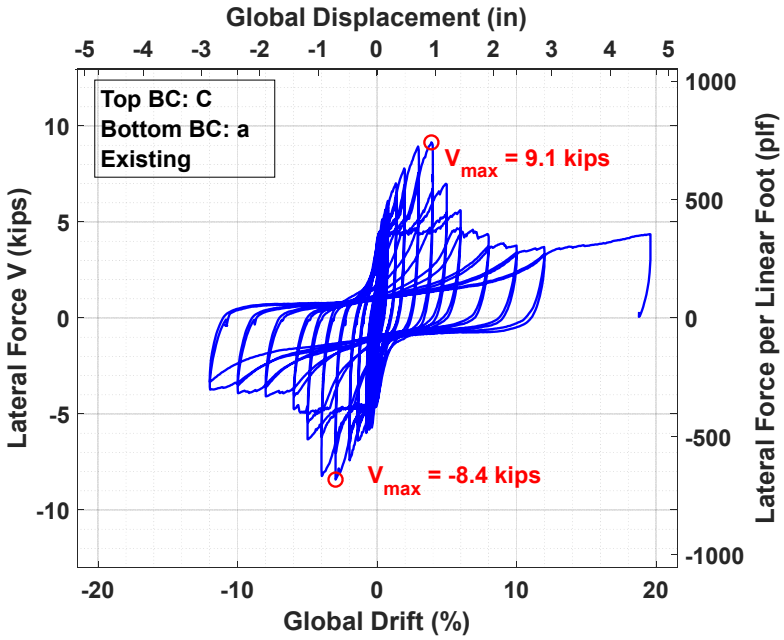

Figure 4.8 **Specimen A-3 lateral force versus *global* lateral drift and displacement hysteresis.**

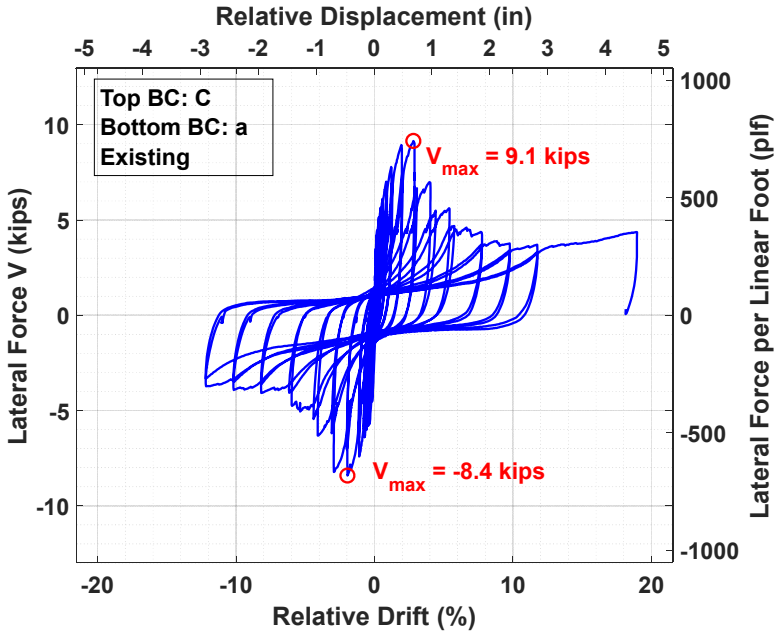

Figure 4.9 **Specimen A-3 lateral force versus *relative* lateral drift and displacement hysteresis.**

(a)

(b)

(c)

(d)

Figure 4.10 **Specimen A-4 pre-test photographs, top boundary condition B\ and bottom boundary condition "b": (a) exterior elevation; (b) interior elevation; (c) north exterior corner; and (d) north interior corner.**

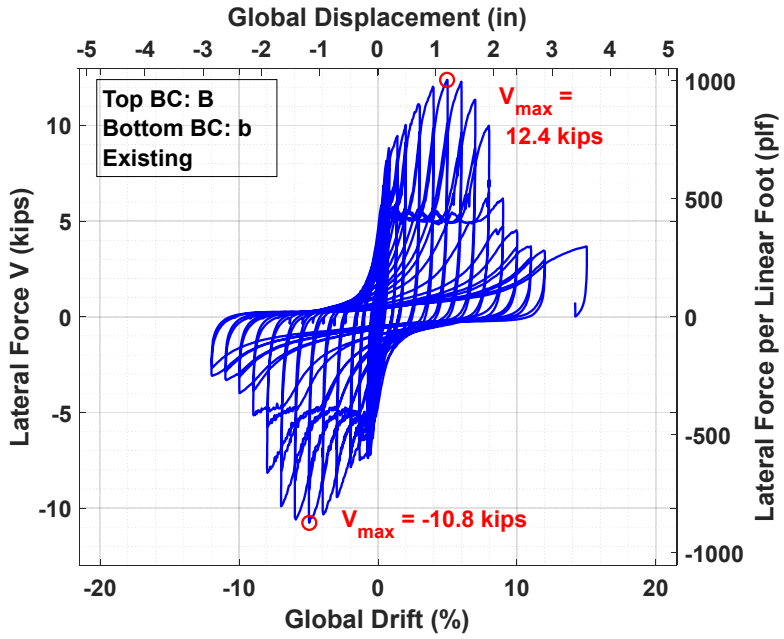

Figure 4.11 **Specimen A-4 lateral force versus *global* lateral drift and displacement hysteresis.**

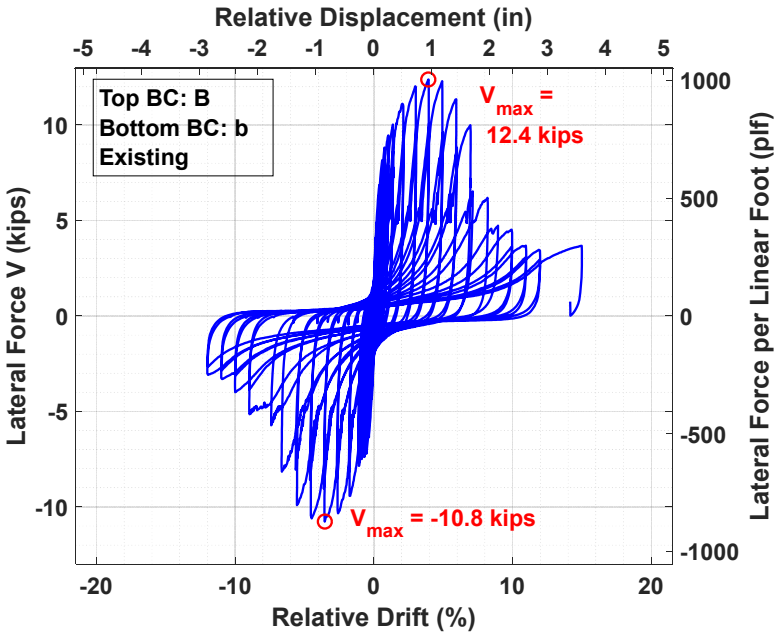

Figure 4.12 **Specimen A-4 lateral force versus *relative* lateral drift and displacement hysteresis.**

(a)

(b)

(c)

(d)

Figure 4.13 **Specimen A-5 (retrofitted) pre-test photographs, top boundary condition B and bottom boundary condition "a": (a) exterior elevation; (b) interior elevation; (c) north exterior corner; and (d) south interior corner.**

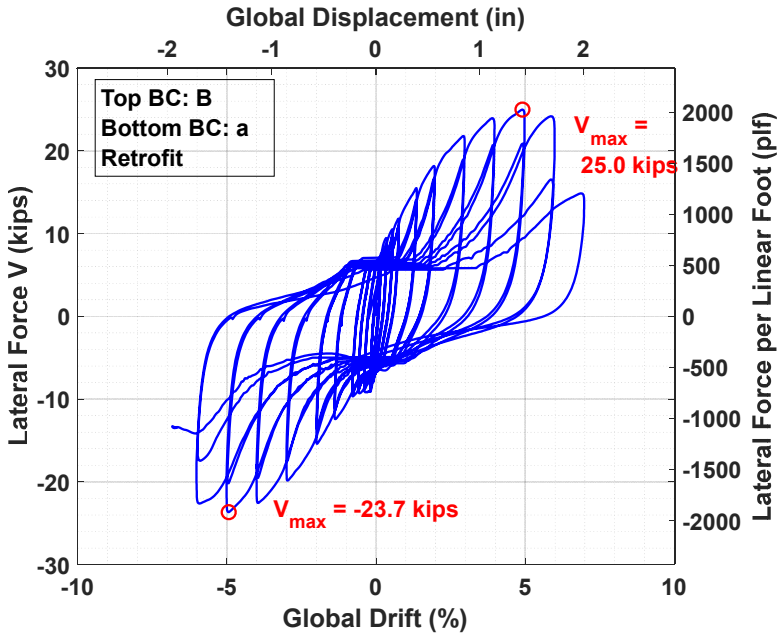

Figure 4.14 **Specimen A-5 lateral force versus *global* lateral drift and displacement hysteresis.**

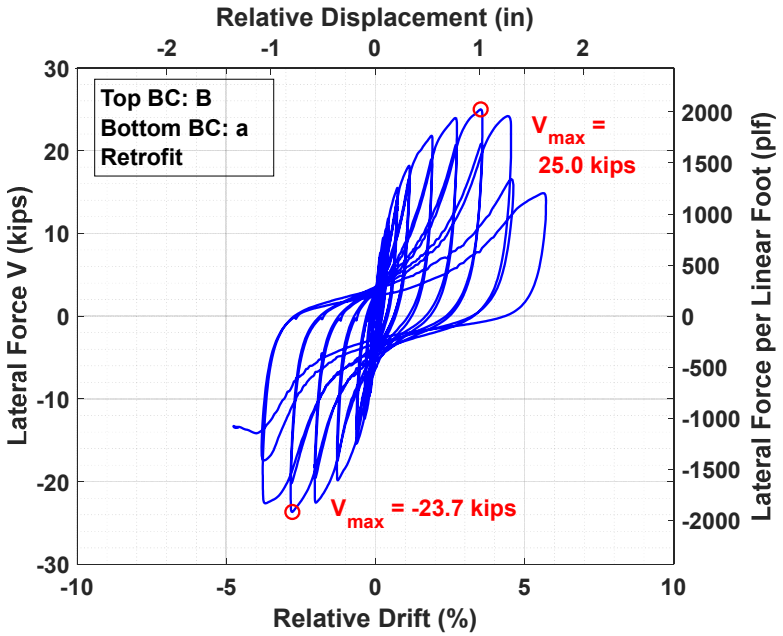

Figure 4.15 **Specimen A-5 lateral force versus *relative* lateral drift and displacement hysteresis.**

(a)

(b)

(c)

(d)

Figure 4.16 **Specimen A-6 (wet sill plate) pre-test photographs, top boundary condition B and bottom boundary condition "b": (a) exterior elevation; (b) interior elevation; (c) north exterior corner; (d) and south interior corner.**

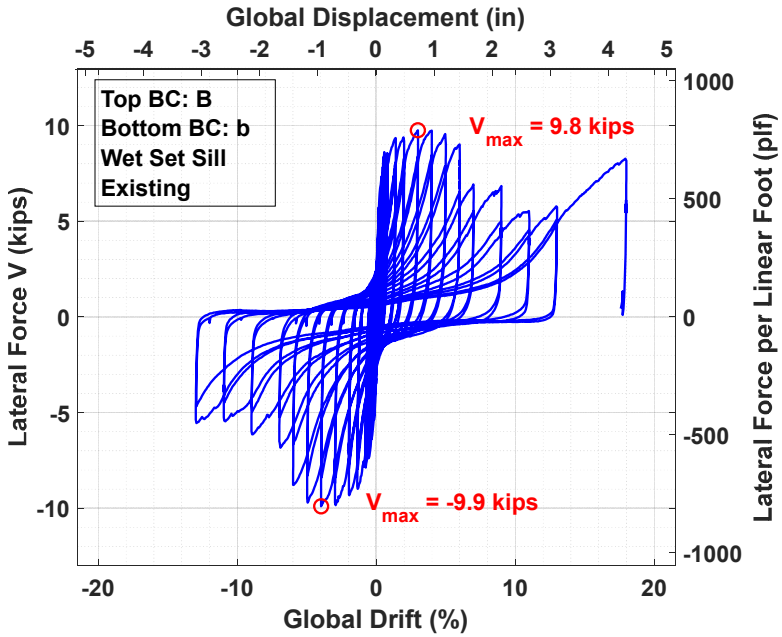

Figure 4.17 Specimen A-6 lateral force versus *global* lateral drift and displacement hysteresis; note that for this specimen, wet set sill, and global and relative drift are identical.

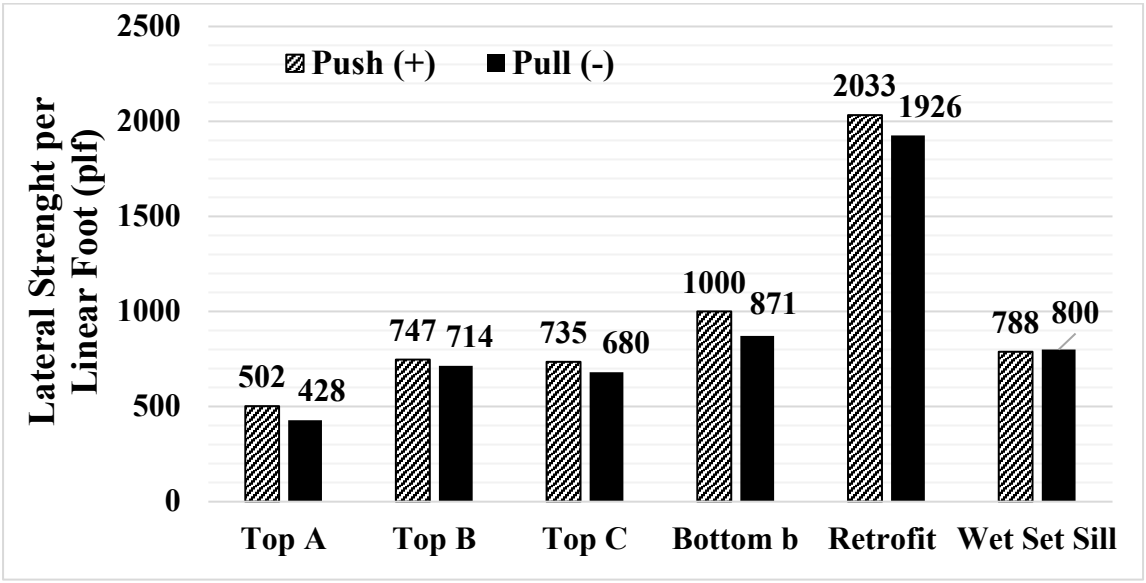

Figure 4.18 Comparison of lateral strength per linear foot of cripple walls.

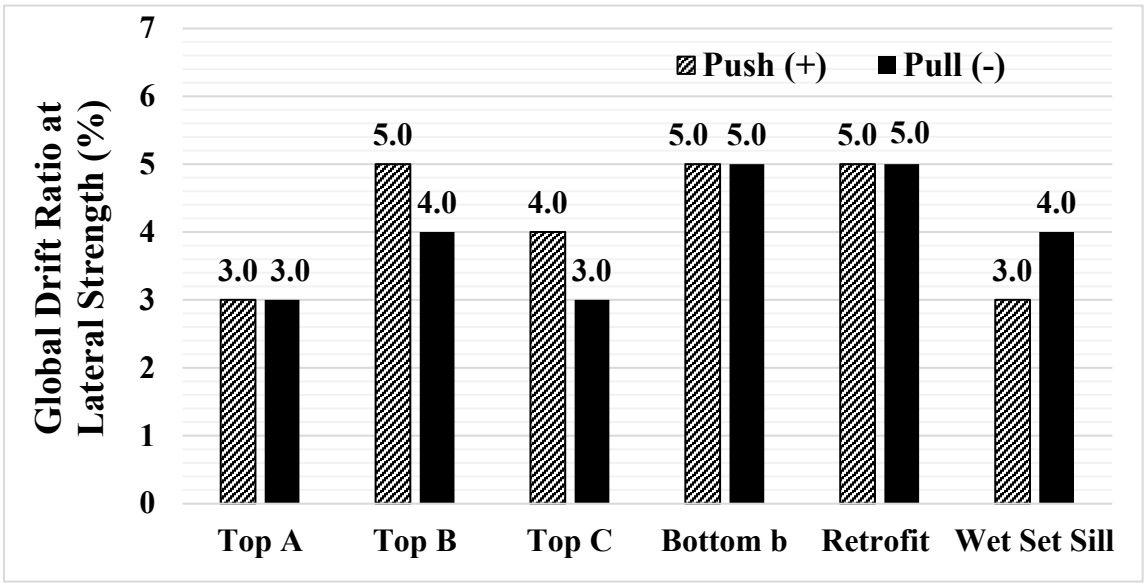

Figure 4.19 Comparison of *global* drift ratio at lateral strength.

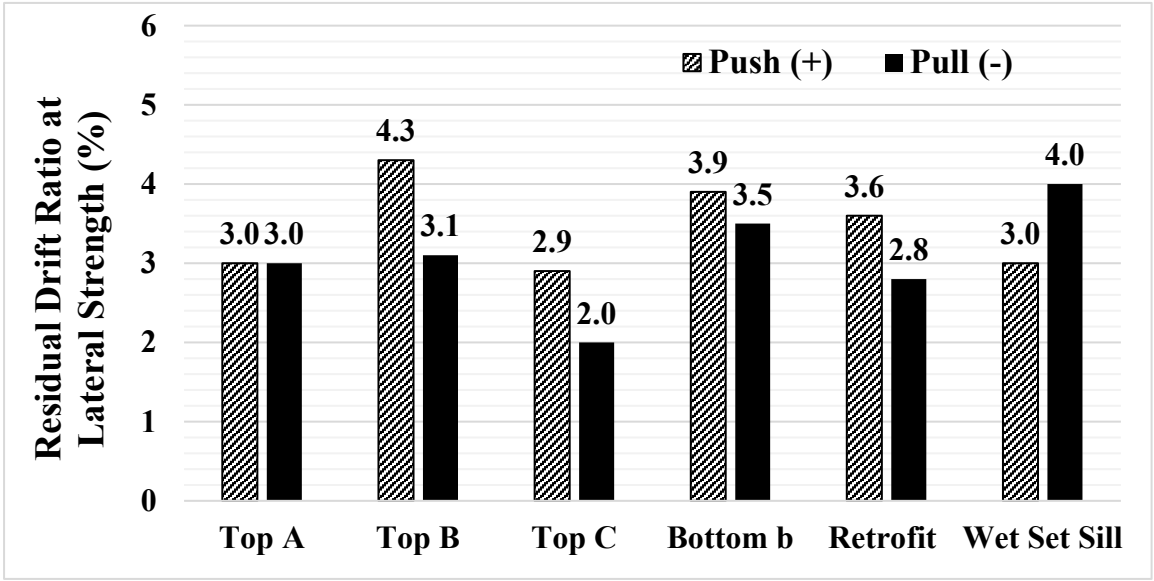

Figure 4.20 Comparison of *relative* drift ratio at lateral strength.

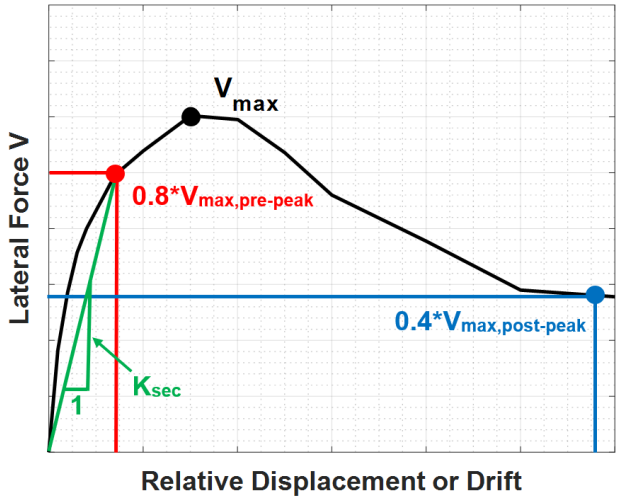

Figure 4.21 **Schematic defining key parameters cross-compared amongst specimens in Phase 1; initial secant stiffness, relative drift at 80% lateral strength (pre-strength), and relative drift at 40% lateral strength (post-strength) from an envelope of the response.**

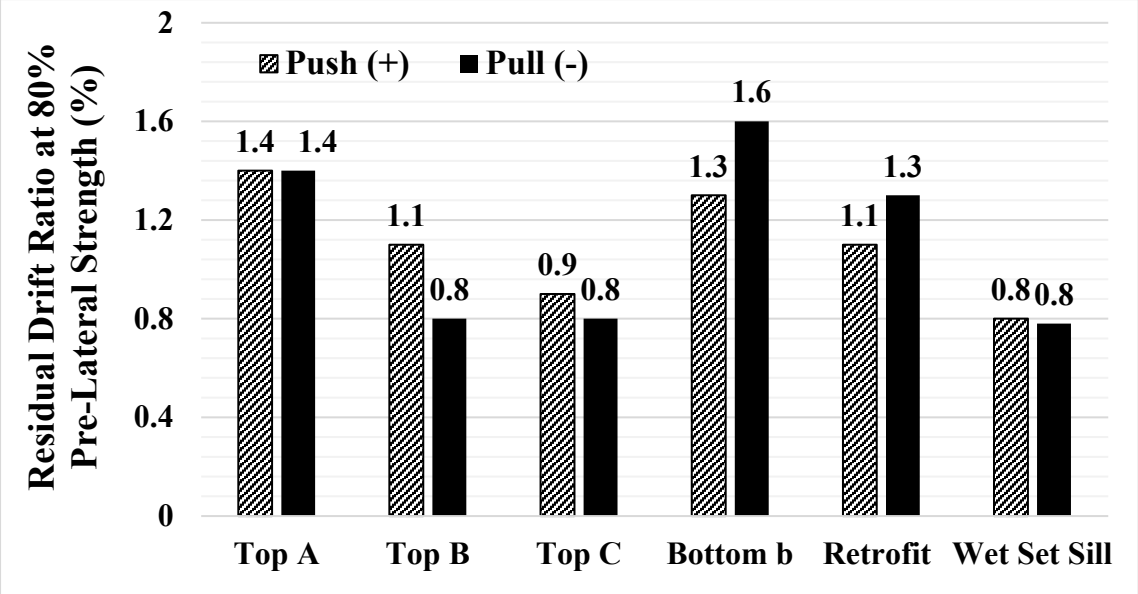

Figure 4.22 **Comparison of *relative* drift ratio at 80% pre-lateral strength ($0.8V_{max}$).**

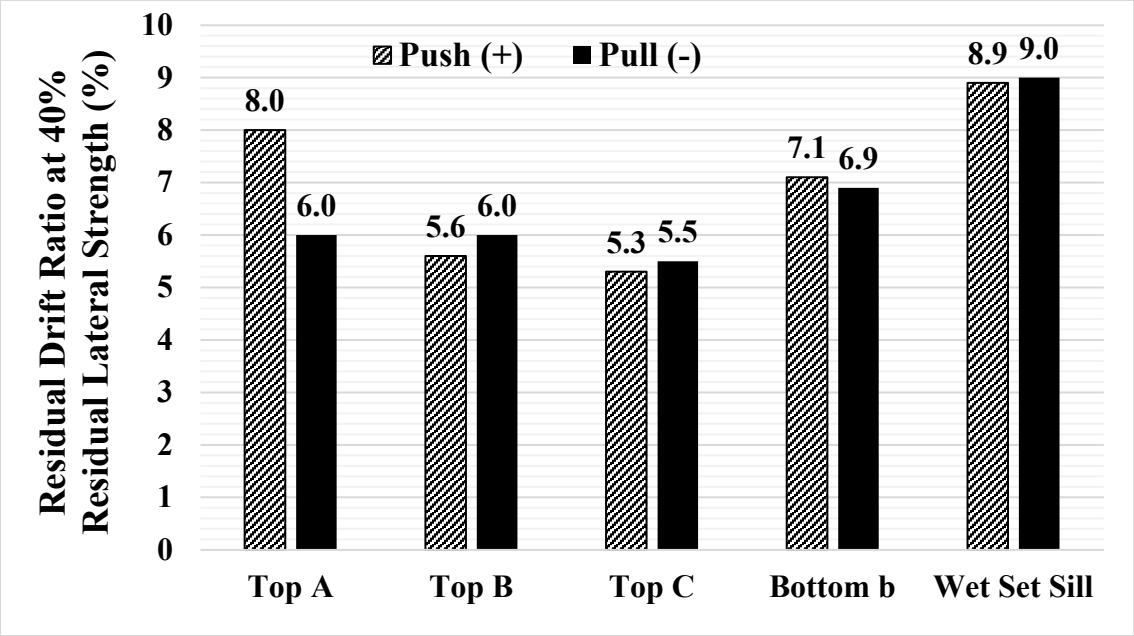

Figure 4.23 Comparison of *relative* drift ratio at 40% post-lateral strength ($0.4V_{max}$).

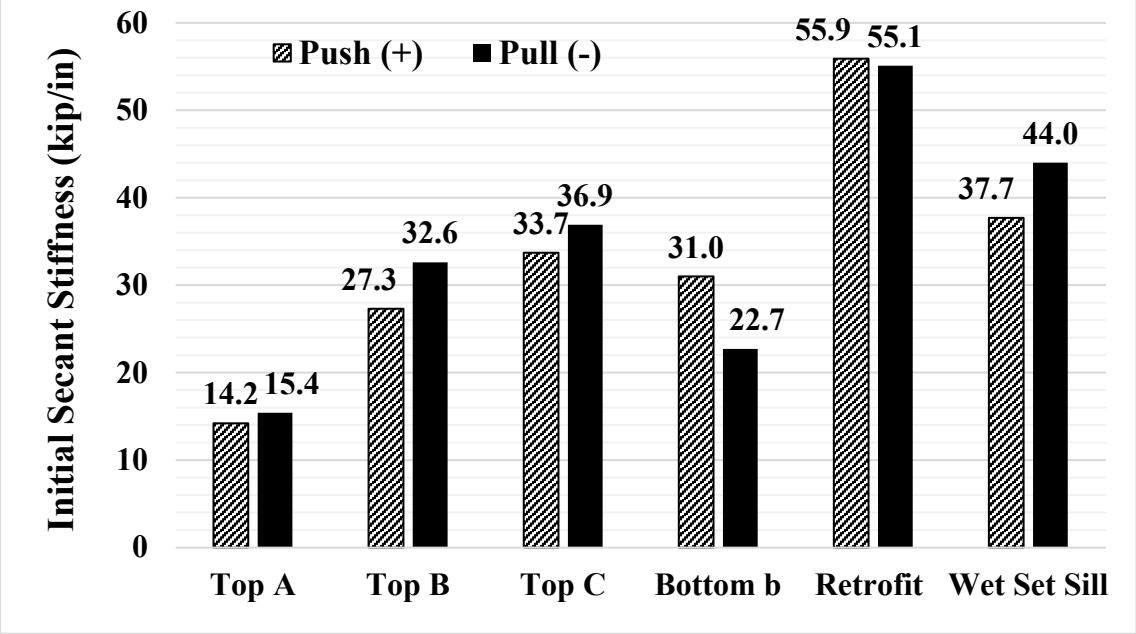

Figure 4.24 Secant stiffness for *relative* drift at 80% pre-lateral strength.

4.3 SILL PLATE DISPLACEMENT RELATIVE TO FOUNDATION

In addition to the lateral response, it is important to characterize the contributions to displacement of the wall. As shown in the figures in Section 4.2, often the global response (including the combined sliding of the sill plate and displacement of the cripple wall structure) differs dramatically from the relative response (displacement of the cripple-wall structure only). For all

cripple walls tested in Phase 1, the anchor bolt holes were oversized by 1/4 in. This common construction practice in California wood-frame construction alleviates the precision needed to frame walls, ultimately leading to quicker construction schedules and is prone to fewer mistakes. Because the anchor bolt holes were oversized, there was less resistance to sliding of the sill plate on the foundation, as the anchor bolts do not resist the sliding at first. The resistance to this sliding will initially come from the frictional resistance between the bottom of the sill plate and the top of the foundation. Through a static analysis, the initiation of sliding can be estimated knowing the normal force provided by the weight of the cripple wall and the imposed vertical load, and the coefficient of friction between wood and concrete; see Section 4.3.1. It should be noted, however, that the concrete footings are finished using a smooth steel trowel, which may not necessarily emulate older construction practices.

Of the six cripple walls tested, four underwent considerable displacements of the sill plate relative to the foundation during loading. The two cripple walls that did not have any relative displacement or had negligible relative displacement occur were Specimen A-1 and Specimen A-6. For Specimen A-1, the lateral load carried by the cripple wall during testing was not enough to overcome the frictional resistance keeping the cripple wall in place. In the other tests, sliding of the sill plate began after around 6 kips of lateral load were applied to the wall. Given that the maximum lateral load achieved by Specimen A-1 was 6 kips, negligible displacements were measured. For Specimen A-6, no displacement of the sill plate occurred due to the wet set sill condition (unique to this specimen). Since the wet set sill plate was embedded in the concrete during the pouring of the foundation and 30 penny nails (6-in. nails) along the sill plate (which were also embedded into the concrete), there was a much higher resistance to sliding than the frictional resistance between the sill plate and the concrete foundation.

Figures 4.25–4.32 show the displacement of the sill plate relative to that of the foundation versus drift, and the relative displacement of the sill plate to the foundation versus lateral load for Specimens A-2 through A-5. The amount of sill plate movement is given in terms of displacement (inches) and drift (percentage). The sill relative drift is defined as the movement of the sill plate relative to the foundation divided by the height of the wall. This value is used to relate the difference between the global drift and the relative drift throughout the test. Note: Specimen A-1 and A-6 do not have plots as there was no displacement of the sill plate relative to the foundation. It would be expected that cripple walls with larger load capacities would exhibit greater displacement, which is generally the trend. The standout exception to this trend is a comparison between Specimen A-2 and Specimen A-3, which differ in their top boundary conditions, namely, Specimen A-2 has top boundary condition B and Specimen A-3 has top boundary condition C.

Recall the difference between these two boundary conditions: top boundary condition C has a return wall on each end of the cripple wall, effectively making the cripple wall C-shaped, while top boundary condition B does not have this extended return wall. While the sill displacement is comparable in the pull direction, 0.21 in. for Specimen A-2 compared to 0.25 in. for Specimen A-3, there is a considerable difference in the push direction, 0.17 in. for Specimen A-2 compared to 0.26 in. for Specimen A-3. The difference between the two is likely due to the drilling locations of the anchor bolt holes. It is difficult to construct walls where all the anchor bolts align in the direct center of the anchor bolt holes, which is why anchor bolt holes are oversized in construction. For Specimen A-2, one of the anchor bolts was resting against the edge of the anchor bolt during the installation of the cripple wall frame on the foundation. Because of this, there was less slack in the anchor bolt hole and the sill plate exhibited larger resistance to

moving, resulting in displacement. All other cripple walls underwent an amount of sill-plate displacement that increased with increased lateral load imposed. In all cases except Specimen A-3, the displacement of the sill plate relative to the foundation was greater in the pull direction than the push direction. This is due to the cripple walls initially being loaded in the push direction.

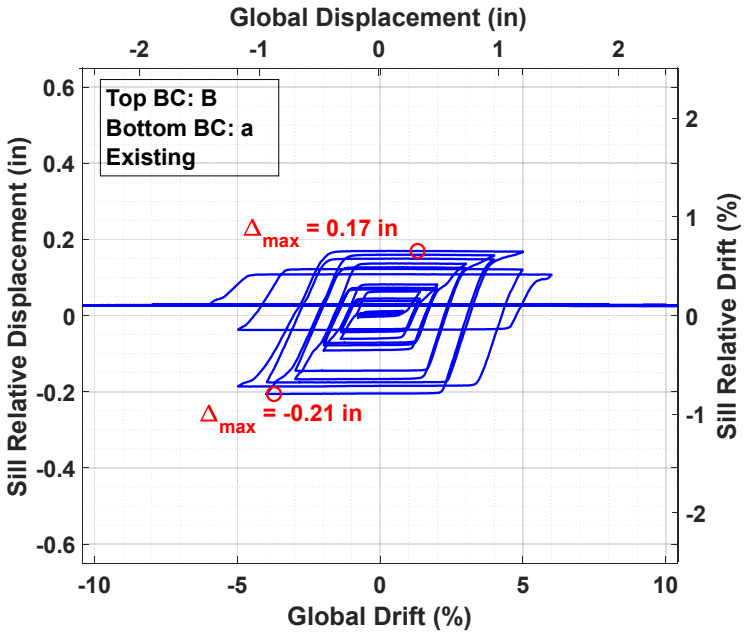

Figure 4.25 **Specimen A-2 sill plate to foundation relative displacement versus *global* drift.**

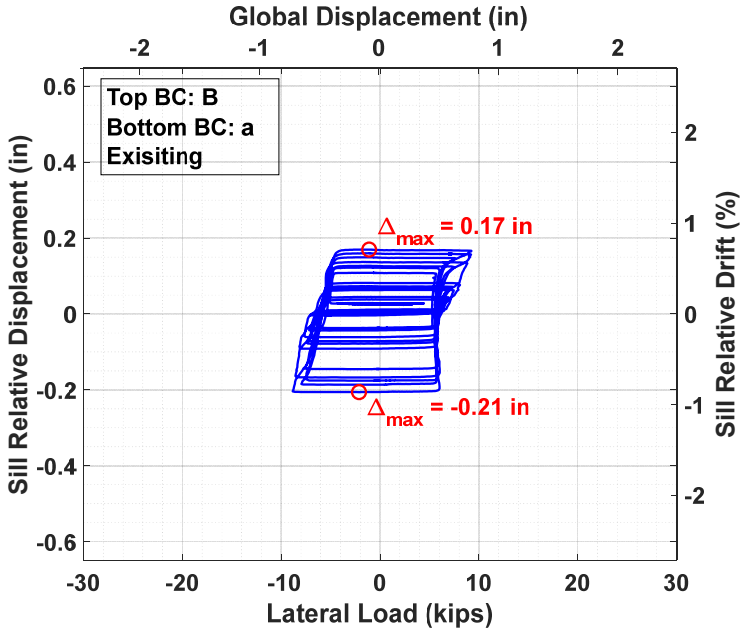

Figure 4.26 **Specimen A-2 sill plate to foundation relative displacement versus lateral strength.**

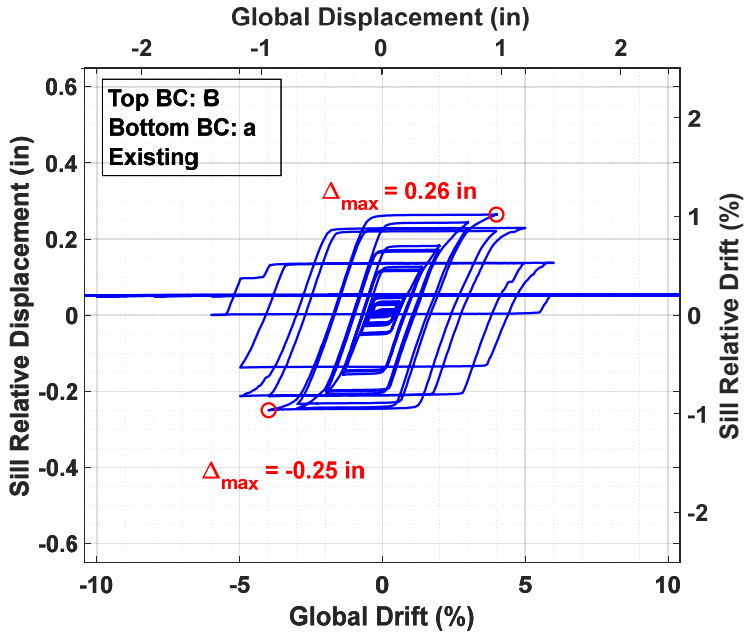

Figure 4.27 Specimen A-3 sill plate to foundation relative displacement versus *global* drift.

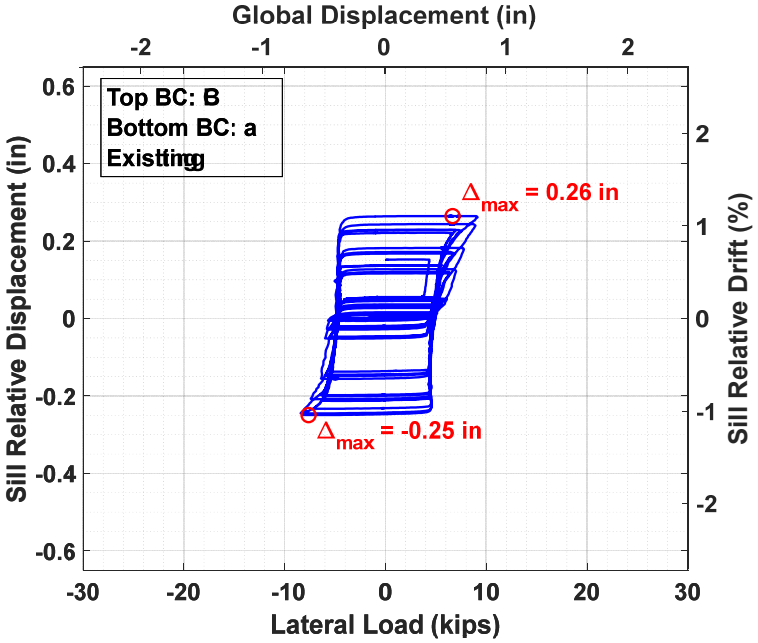

Figure 4.28 Specimen A-3 sill plate to foundation relative displacement versus lateral strength.

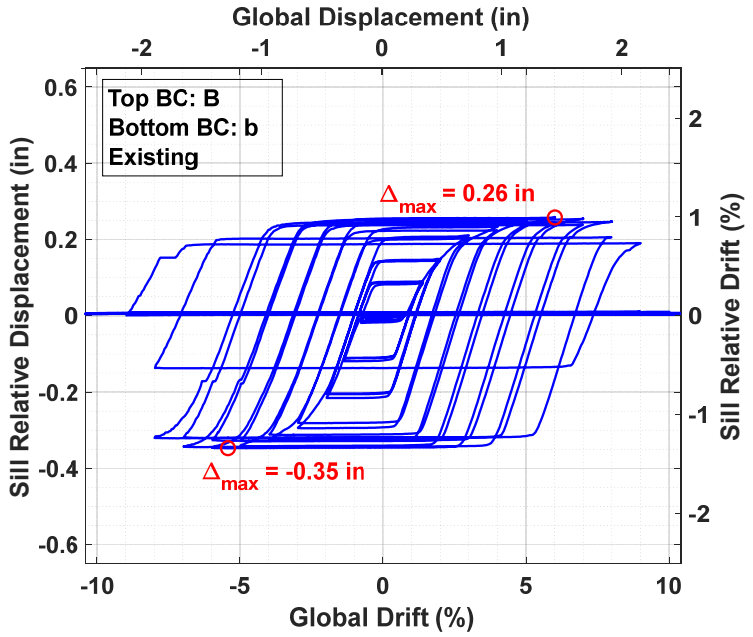

Figure 4.29 Specimen A-4 sill plate to foundation relative displacement versus *global* drift.

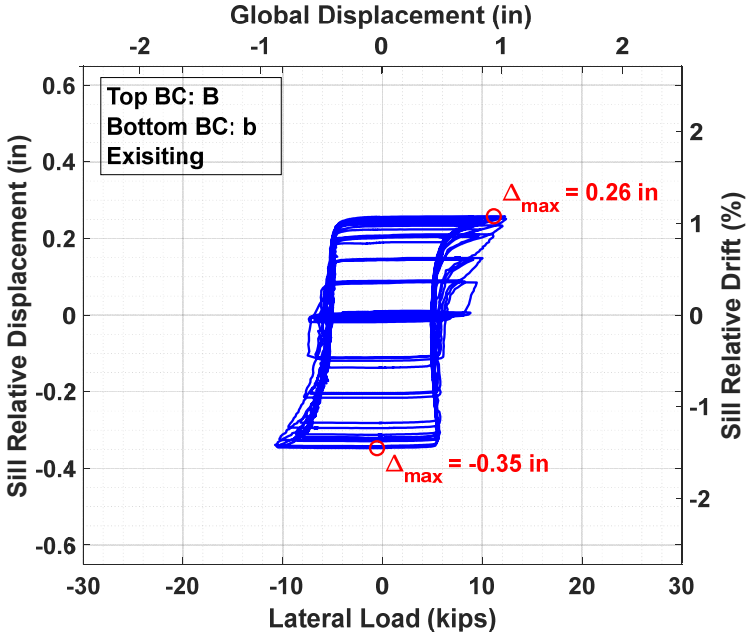

Figure 4.30 Specimen A-4 sill plate to foundation relative displacement versus lateral strength.

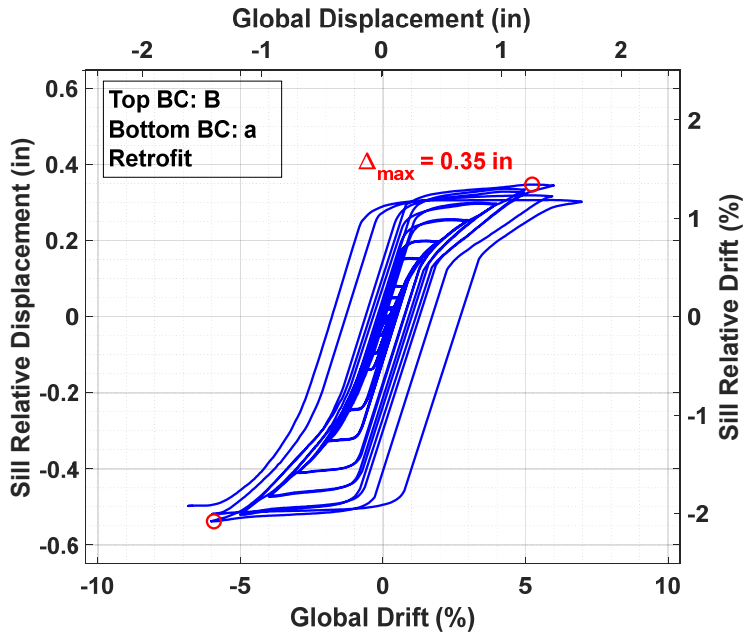

Figure 4.31 Specimen A-5 sill plate to foundation relative displacement versus *global* drift.

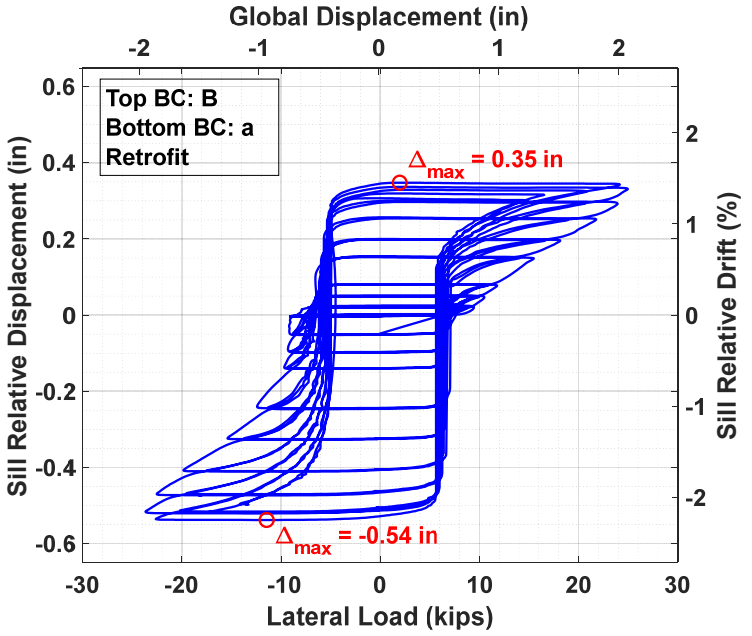

Figure 4.32 Specimen A-5 sill plate to foundation relative displacement versus lateral strength.

4.3.1 Sill Plate to Foundation Friction

The global and relative response in many of the test varied significantly due to the displacement of the sill plate relative to the foundation. For sliding of the sill plate along the foundation to occur, the load imposed on the cripple wall must overcome the frictional force between the sill plate and foundation. This frictional force is dependent on the weight of the cripple wall, the vertical load on the cripple wall, and the tensile forces in the anchor bolts fastening the sill plate to the foundation. Figure 4.33 gives a visual of the difference between the global and relative response, and the associated frictional force, thus preventing the cripple wall from displacing relative to the sill plate. Since the normal force and the lateral force are known, the coefficient of friction between the cripple wall sill plate and the foundation can be estimated by using the following equation:

$$V = \mu N$$

where V = the lateral load, N = the normal force, and μ = the static coefficient of fraction.

$$\therefore \mu = V/N \, .$$

The vertical load for all specimens is 450 plf or 5.5 kips. The weight of the cripple walls varies depending on the construction details and density of the lumber. Higher moisture content in the lumber equates to a slightly heavier specimen. The amount of material used for all cripple walls that exhibited displacements of the sill plate relative to the foundation was equal (with the exception of the cripple wall with the return walls). For the other cripple walls, the weight was approximately 0.45 kips and 0.65 kips for Specimen A-3, which had return walls at both ends. Therefore, the total weight of the cripple wall and the vertical load was 5.95 to 6.15 kips.

The anchor bolts were tensioned to different values that range from 0.2-kips to 4.5-kips. The amount of lateral load imposed to initiate sliding also varied. These variations can be attributed to the different tension in anchor bolts from test to test and the anticipated range in static coefficient due to nominal material interface variability. Accounting for the variations in anchor bolt tensions, the static coefficient of friction between the sill plate and the foundation for all specimens is shown in Table 4.2, which excludes Specimens A-1 and A-6 because these cripple walls did not experience any displacement of the sill plate relative to the foundation. Specimen A-1 did not have sufficient strength to overcome the frictional resistance between the sill plate and the foundation. Specimen A-6 had a wet set sill plate, which did not displace during testing. In addition, Specimen A-4 is not considered in this table due to the initial anchor bolt loads being around 4.5 kips, which is significantly larger than any of the other specimens considered. The average static coefficient of friction for all specimens that exhibited displacement of the sill plate relative to the foundation is approximated to be 0.62 with a range of values from 0.59 to 0.66. The static coefficient of friction between dry wood and concrete has been measured as 0.62 [Aira et al. 2014].

Table 4.2 Static coefficient of friction calculations.

Specimen	Total vertical load (kips)	Total anchor bolt loads (kips)	Frictional force (kips)	μ_{static}
A-2	5.95	3.1	5.7	0.63
A-3	6.15	0.5	4.5	0.68
A-4	5.95	5.2	6.6	0.59
Average static coefficient of friction = 0.63				

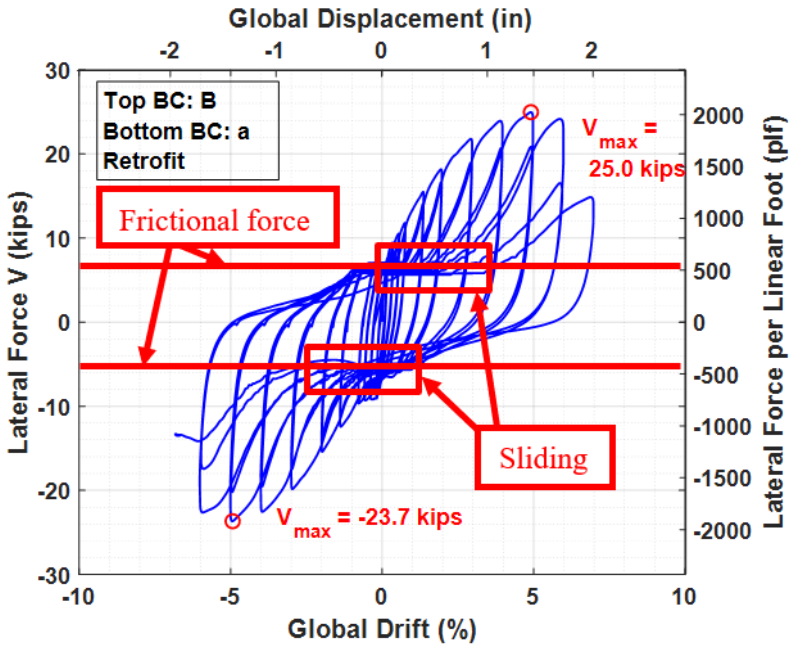

(a)

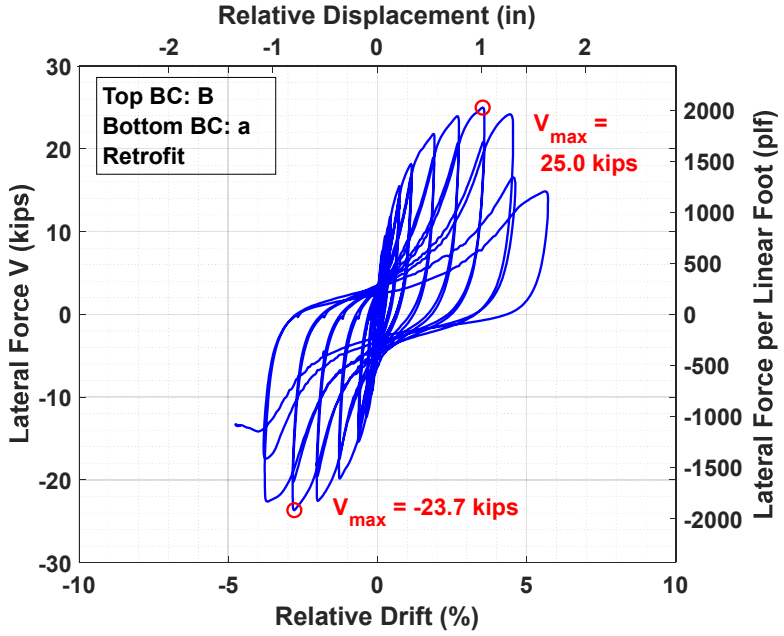

(b)

Figure 4.33 **The frictional force between the sill plate and foundation: (a) *global* response; and (b) *relative* response.**

4.4 ANCHOR BOLT LOADS

To measure the tension developed in each anchor bolt, 10-kip donut load cells were placed on top of the square plate washers. For unretrofitted cripple walls, three anchor bolts spaced at 64 in. on center were used. Figure 4.35 shows the anchor bolt layout for these cripple walls. For retrofitted cripple walls, additional anchor bolts were added per the ATC-110 retrofit guidelines, with spacing at 32 in. on center; see Figure 4.36. Specimen A-3, the cripple wall with a return wall, contained two additional anchor bolts on each return wall. A plan view of the anchor bolt layout can be seen in Figure 4.37.

For Specimens A-1 and A-4, the first two tests of cripple walls with anchor bolts, the anchor bolts were tensioned between 4 and 5 kips. This was reduced to tensioning of around 1 kip per anchor bolt for Specimens A-2 and A-5. Specimen A-3, the last cripple wall tested in Phase 1, began with around 0.2 kips of tension in each anchor bolt, which became the standard tensioning for all tests in subsequent phases. This was meant to mimic a hand-tightened amount of tension commonly observed in the field for older homes. Due to the increased amount of tension in the anchor bolts, the peak anchor bolt loads were higher than those that started with less tension; however, the difference between initial anchor bolt loads and peak anchor bolt loads was not necessarily higher for anchor bolts with higher initial tension. In addition, it was observed from the sill-slip analysis that the increased anchor bolt loads did not have a large effect on the sliding of the cripple wall.

Table 4.3 shows the tension applied to each anchor bolt prior to the start of the test. Table 4.4 shows the maximum anchor bolt loads experienced during testing. Table 4.5 shows the anchor bolt loads experienced by the cripple walls at the peak load (i.e., at strength) in the push direction, and Table 4.6 shows the anchor bolt loads at the peak load in the pull direction. The difference between peak anchor bolt loads and the initial anchor bolt are shown in Tables 4.7 and 4.8 for peak push load and peak pull load, respectively. It was assumed that there would be more tension in Anchor Bolt 3 (AB3) when the cripple walls were loaded in the push direction due to the uplift at the south end of the cripple wall; therefore, it was assumed there would be smaller amplitude tensile forces in the anchor bolt on the north end (AB1). The opposite would hold true for loading in the pull direction, a higher tension in AB1 than in AB3. This trend held true for all cripple walls except Specimen A-1.

For Specimen A-1, the loads on all three anchor bolts remained relatively consistent, regardless of the direction of loading; see Figure 4.37 with a plot of the anchor bolt loads versus global drift. The small deviations in anchor bolt tension for Specimen A-1 can be attributed to the low-strength capacity of the cripple wall. There was negligible uplift in the cripple wall throughout the entire test, which led to minimal fluctuations in anchor bolt loads.

As a point of comparison, Figure 4.38 shows the anchor bolt loads versus global displacement for Specimen A-4, which was the other cripple wall to have anchor bolts tensioned between 4 and 5 kips. Note the 110% increase in tension for AB1 at peak pull loading and a 61% increase in tension in AB3 at peak push loading. The load capacity of Specimen A-4 was double that of Specimen A-1, and the end uplift of Specimen A-4 was appreciable, both leading to the anchor bolt loads following the expected trend.

The largest percent increase in tension from initial anchor bolt tension occurred with Specimen A-3, the only cripple wall to have anchor bolts initially tensioned to 0.2 kips. By the end

of the tests, when the cripple walls were at rest, the anchor bolt loads were reduced from their initial loads due to the relaxation of the anchor bolts caused by cyclic loading. Plots of all anchor bolt loads versus global drift are available in Appendix C.1.

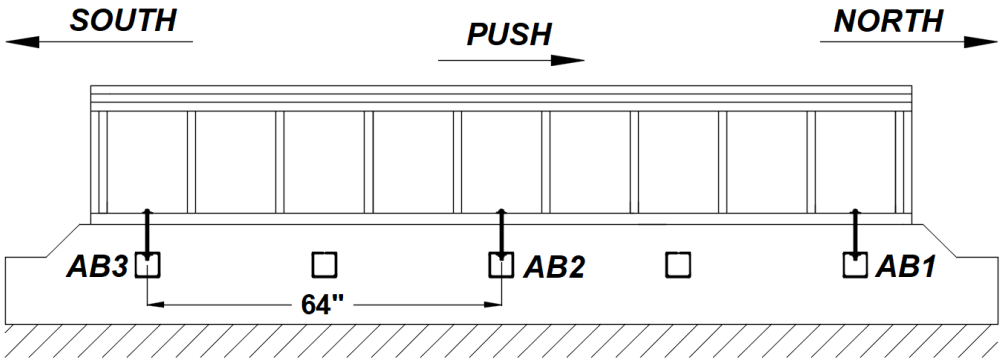

Figure 4.34 **Anchor bolt layout for unretrofitted cripple walls (for all specimens except Specimens A-5 and A-3).**

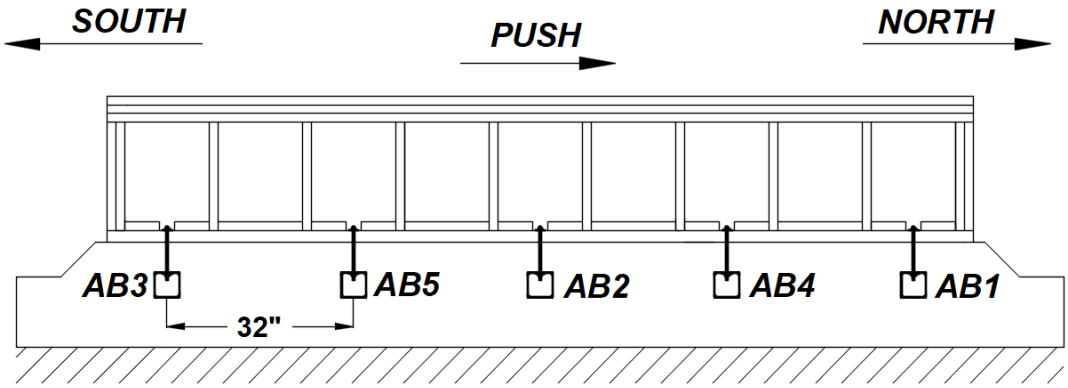

Figure 4.35 **Specimen A-5 anchor bolt layout for retrofitted cripple walls.**

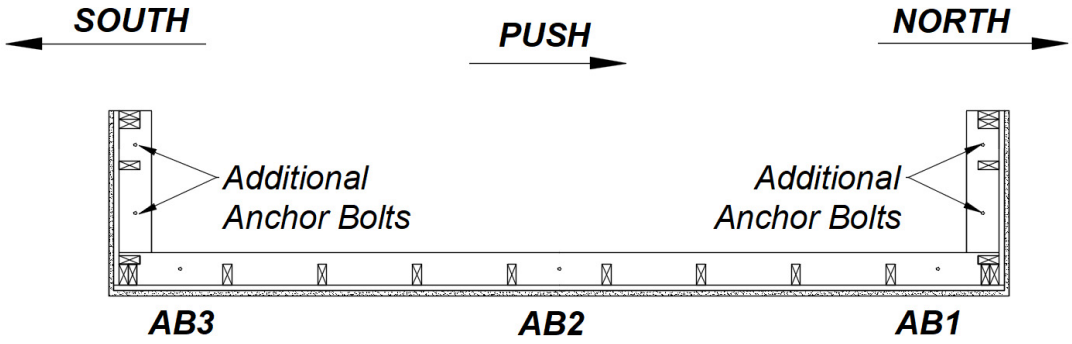

Figure 4.36 **Specimen A-3: plan view anchor bolt layout.**

Table 4.3 Initial anchor bolt tension (kips).

Specimen	South		Center	North	
	AB3	AB5	AB2	AB4	AB1
A-1	4.24		4.24		4.39
A-2	0.97		1.10		1.07
A-3	0.16		0.17		0.17
A-4	4.82		4.93		4.68
A-5	0.95	1.10	1.02	1.06	1.10

Table 4.4 Maximum anchor bolt loads (kips).

Specimen	South		Center	North	
	AB3	AB5	AB2	AB4	AB1
A-1	4.24		4.32		4.50
A-2	1.30		1.82		2.03
A-3	0.84		0.69		1.06
A-4	8.29		5.63		9.88
A-5	3.64	2.72	2.31	3.36	3.32

Table 4.5 Anchor bolt load at peak load in the *push* loading direction (kips).

Specimen	South		Center	North	
	AB3	AB5	AB2	AB4	AB1
A-1	4.12		4.06		4.50
A-2	1.20		0.91		0.96
A-3	0.79		0.68		0.24
A-4	7.77		1.37		5.84
A-5	3.55	2.65	2.01	1.39	1.55

Table 4.6 Anchor bolt load at peak load in the *pull* loading direction (kips).

Specimen	South		Center	North	
	AB3	AB5	AB2	AB4	AB1
A-1	4.05		3.53		4.29
A-2	0.75		1.82		2.03
A-3	0.76		0.41		1.06
A-4	7.31		5.56		9.85
A-5	0.71	2.58	2.09	3.23	1.55

Table 4.7 Difference in anchor bolt loads at peak *push* load to initial anchor bolt loads (kips).

Specimen	South		Center	North	
	AB3	AB5	AB2	AB4	AB1
A-1	-0.1		-0.2		0.1
A-2	0.2		-0.2		-0.1
A-3	0.6		0.5		0.1
A-4	2.9		-3.6		1.2
A-5	2.6	1.6	1.0	0.3	0.4

Table 4.8 Difference in anchor bolt loads at peak *push* load to initial anchor bolt loads (kips).

Specimen	South		Center	North	
	AB3	AB5	AB2	AB4	AB1
A-1	-0.2		-0.7		-0.1
A-2	-0.2		0.7		1.0
A-3	0.6		0.2		0.9
A-4	2.5		0.6		5.2
A-5	-0.2	1.5	1.1	2.2	0.4

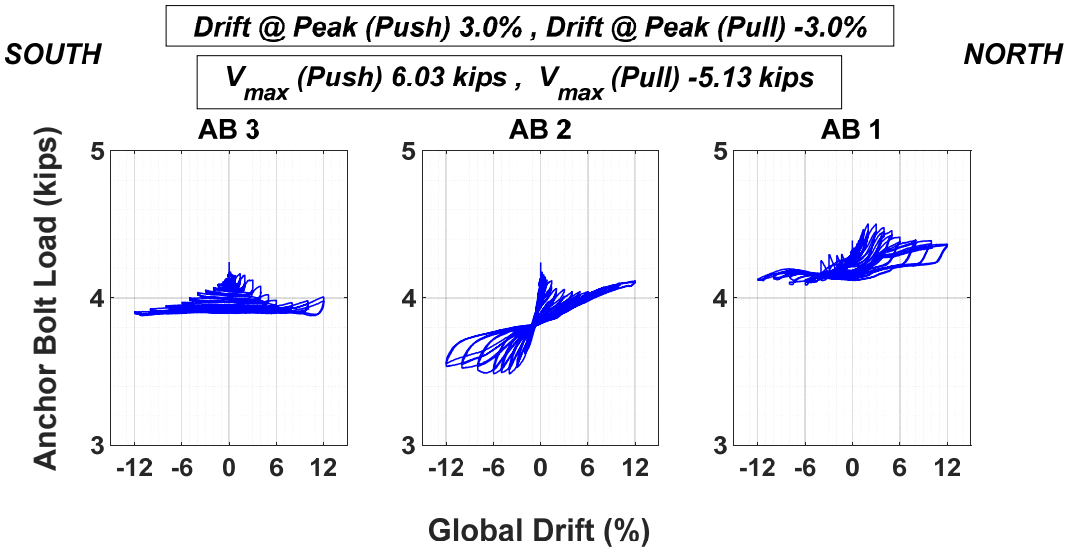

Figure 4.37 Specimen A-1 (top boundary condition A): anchor bolt tensile loads versus global drift.

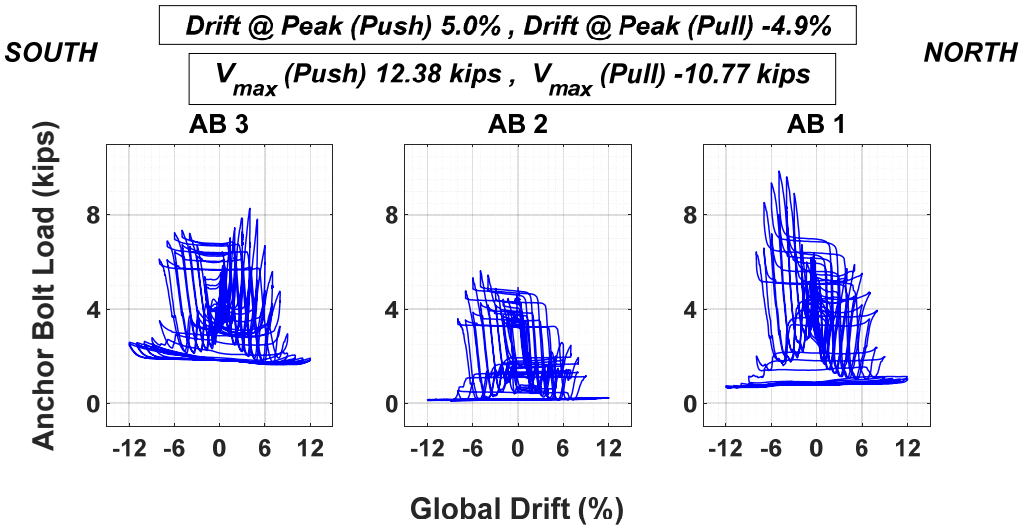

Figure 4.38 Specimen A-4 (bottom boundary condition "b"): anchor bolt tensile loads versus global drift.

4.5 DIAGONAL MEASUREMENTS

Two sets of potentiometers were used for measuring the displacement across the diagonal of the cripple wall. One pair of potentiometers measured the distortion across the entire cripple wall, while the other pair measured the distortion of the middle third of the cripple wall. The purpose of these measurements was to determine the amount of shear distortion within the cripple wall. These measurements were used to determine if the applied lateral displacement could be resolved using the diagonal and end uplift measurements. Figure 4.39 shows the linear potentiometers used to calculate the resolved lateral displacement of the cripple wall. Figure 4.40 shows how the resolved lateral displacements from diagonal and uplift measurements were derived.

Figures 4.41 through 4.48 show the relative drift versus the relative drift resolved from the diagonal and uplift measurements for Specimen A-1, A-2, A-3, and A-5. Figures 4.41, 4.43, 4.45, and 4.47 overlay the resolved lateral drifts from the inside diagonals on the left and the resolved lateral drifts from the outside diagonals on the right for Specimen A-1, A-2, A-3, and A-5, respectively. Figures 4.42, 4.44, 4.46, and 4.48 overlay the resolved lateral drifts from the diagonals running from the bottom north end of the wall to the top south end of the wall on the left, and the resolved lateral drifts running from the top north end of the wall to the bottom south end of the wall on the left for Specimen A-1, A-2, A-3, and A-5, respectively. As a reference, all of these figures include a green line indicating the measured relative drift plotted against itself.

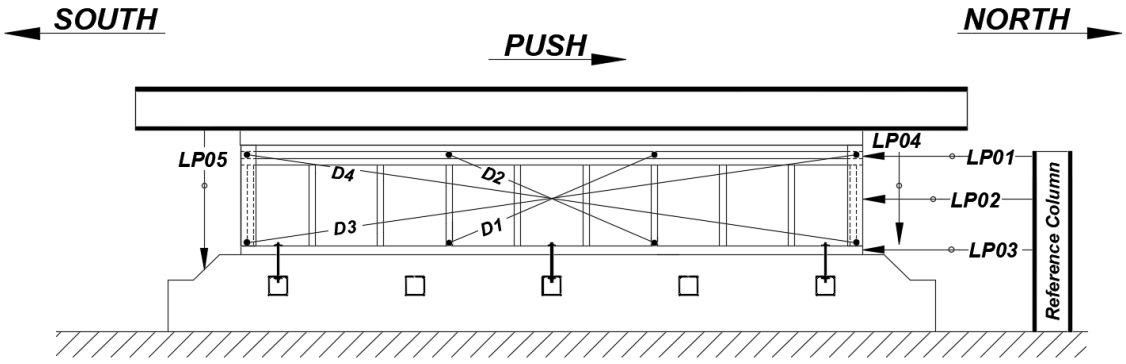

Figure 4.39 Diagonal, end uplift, and lateral displacement potentiometer schematic.

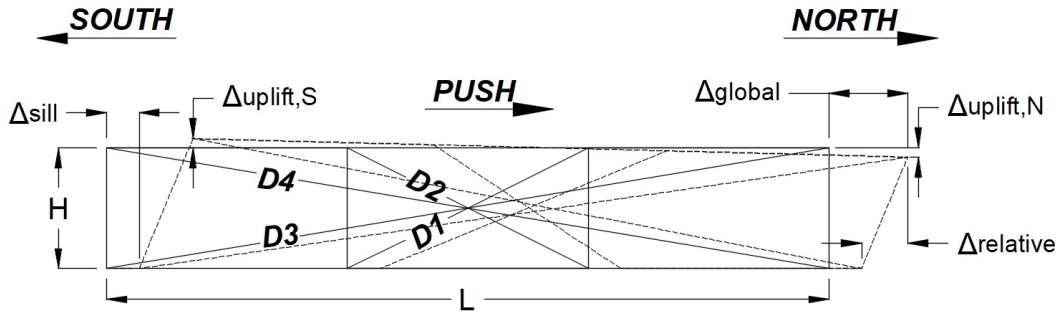

Figure 4.40 Deformed cripple wall with measurements used for resolving lateral displacement from diagonal and uplift measurements.

These cripple walls were chosen because they only differ in their top boundary conditions and the addition of a retrofit scheme (Specimen A-2 versus Specimen A-5). Specimen A-2, the unretrofitted cripple wall, had resolved relative drift values within 1.4% drift of the measured relative drift. The difference tended to be less than that. On average between push and pull loading, the relative drift resolved from the inside diagonals differed by 0.68% relative drift and the relative drift resolved from the outside diagonals differed by 0.73% relative drift. These values increased for the differences between the measured relative drift and resolved relative measurements from the inside diagonals for the retrofitted cripple wall, with an average difference of 2.3%, while the difference for the measured relative drift and resolved relative drift of the outside diagonals was 0.6% relative drift. This shows that the addition of the plywood panels for the retrofit reduced the shear distortion through the interior of the cripple wall where the panels were attached.

Overall, the resolved relative displacements from the outside diagonal measurements were closer to the measured relative displacements than those of the inside diagonal measurements. The resolved relative drifts from the outside diagonal measurements for cripple walls with top boundary condition B (Specimens A-2, A-4, A-5, and A-6) were all within the range of 0% to 2.2% relative drift difference. The cripple walls with top boundary condition A (Specimen A-1) and top boundary condition C (Specimen A-3) were within the range of 1.3% to 2.6% relative drift difference. The same trend was not exhibited for the inside diagonal measurements, as there was no trend between the top boundary conditions and the difference resolved relative drift and measured relative drift. Specimen A-5, the retrofitted cripple wall, showed the largest difference between resolved relative drift from the inside diagonal measurements and outside diagonal measurements, which demonstrated that the addition of plywood panels reduced the amount of shear distortion through the interior of the cripple wall. For the resolved relative drifts of the inside diagonal measurements, the measured relative drift was always greater than the resolved in the push direction and was always less than the resolved in the pull direction. This could be attributed to the cripple walls initially being pushed when displaced. The same trend was exhibited for the cripple walls with top boundary condition A and top boundary condition C for the resolved relative drifts of the outside diagonal measurements. For cripple walls with top boundary condition B, there was no definitive trend, only a smaller difference between the measured relative drift and the resolved relative drift.

Overall, the differences between the resolved relative drifts from the outside diagonal measurements and the inside diagonal measurements were similar, within a range of 0% to 1.8% except for Specimen A-5, the retrofitted cripple wall, which had resolved relative drift measurements from the inside diagonals in the range of 1.4% to 2.6% relative drift. All of the measured relative drift versus resolved relative drift from the diagonal and uplift measurement responses; the calculations to determine uplift and distortion measurements can be found in Appendix C.2.

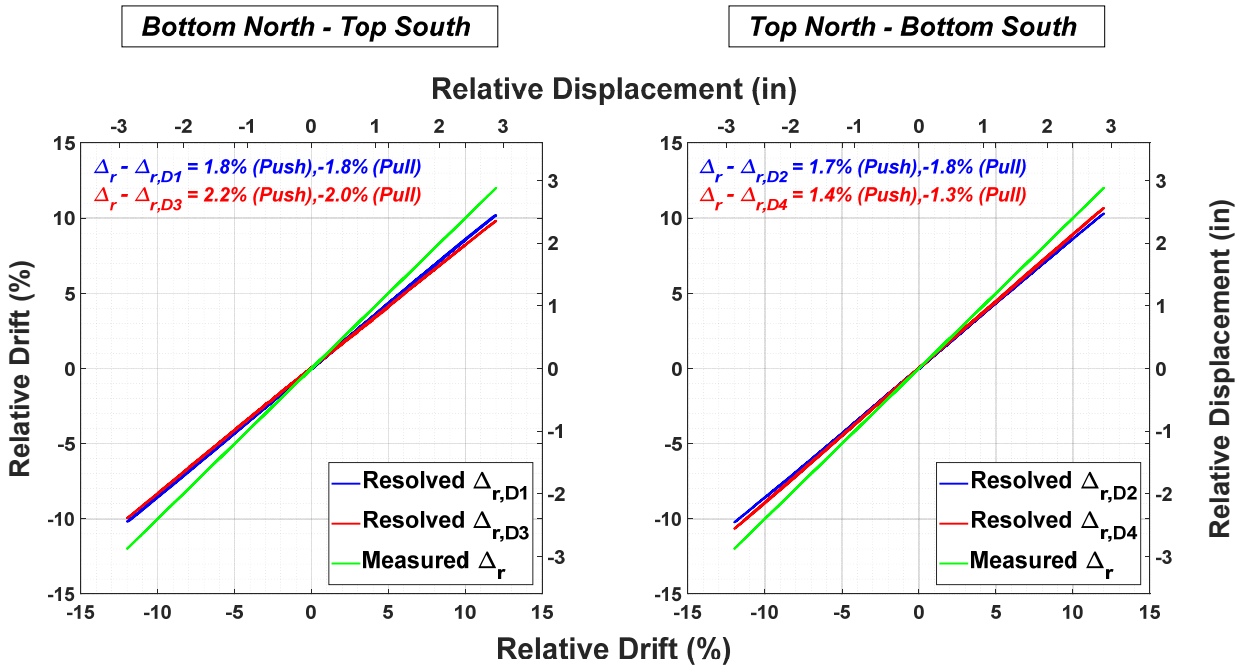

Figure 4.41 Specimen A-1 (unretrofitted, top boundary condition A): resolved *relative* drift from diagonal measurements in one direction versus measured *relative* drift.

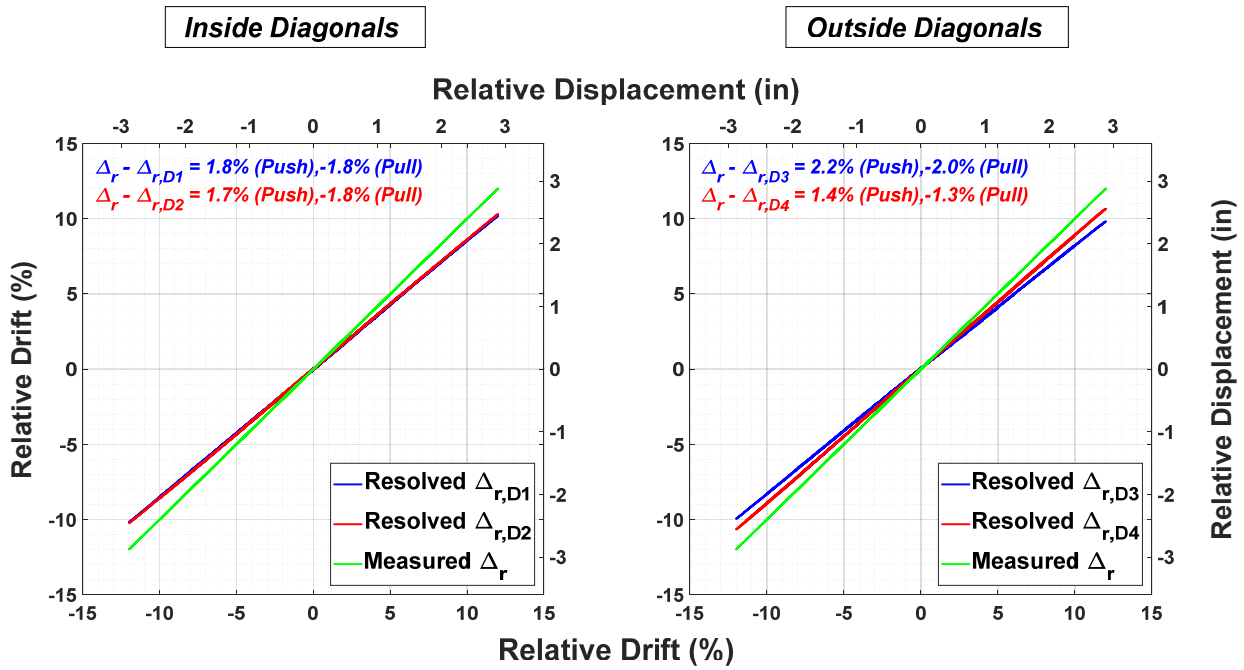

Figure 4.42 Specimen A-1 (unretrofitted, top boundary condition A): resolved *relative* drift from diagonal measurements (outside and inside diagonals) versus measured *relative* drift.

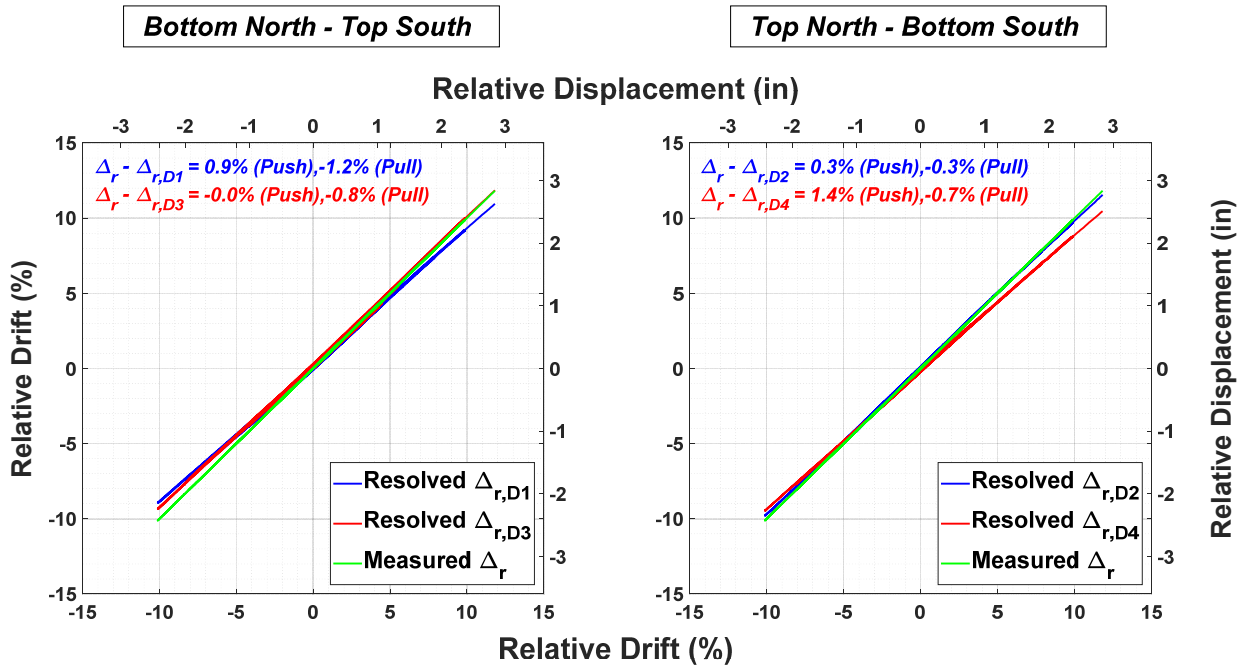

Figure 4.43 Specimen A-2 (unretrofitted, top boundary condition B): resolved *relative* drift from diagonal measurements in one direction versus measured *relative* drift.

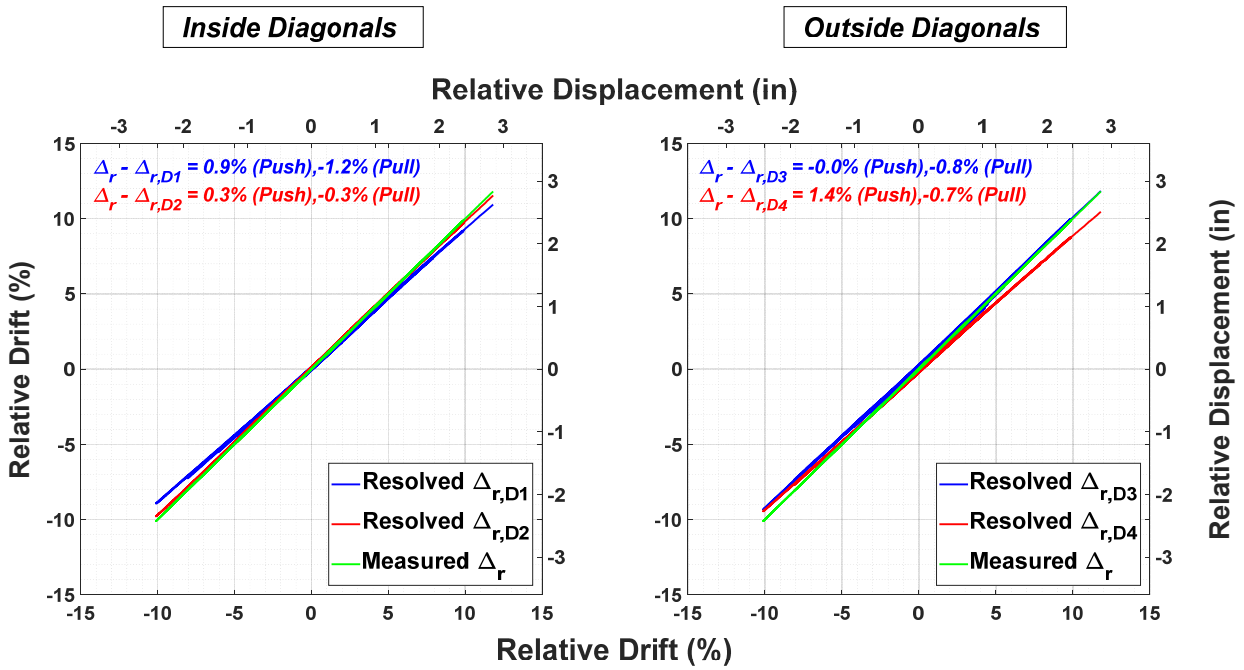

Figure 4.44 Specimen A-2 (unretrofitted, top boundary condition B): resolved *relative* drift from diagonal measurements (outside and inside diagonals) versus measured *relative* drift.

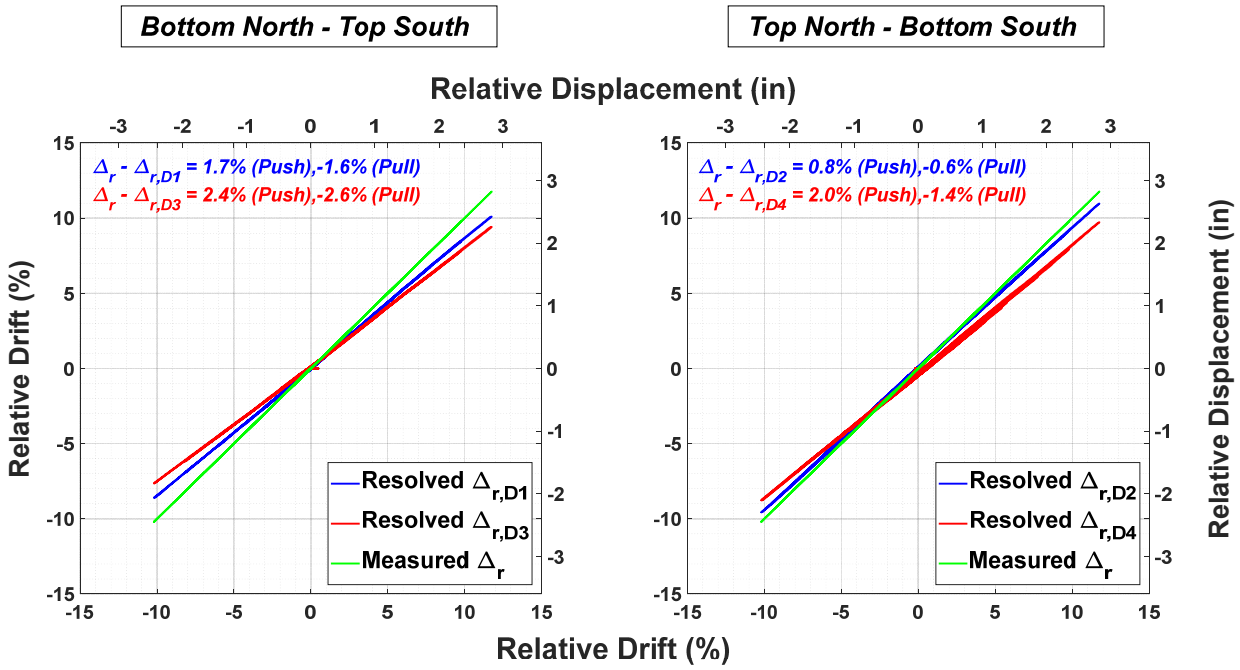

Figure 4.45 Specimen A-3 (unretrofitted with top boundary condition C): resolved *relative* drift from diagonal measurements in one direction versus measured *relative* drift.

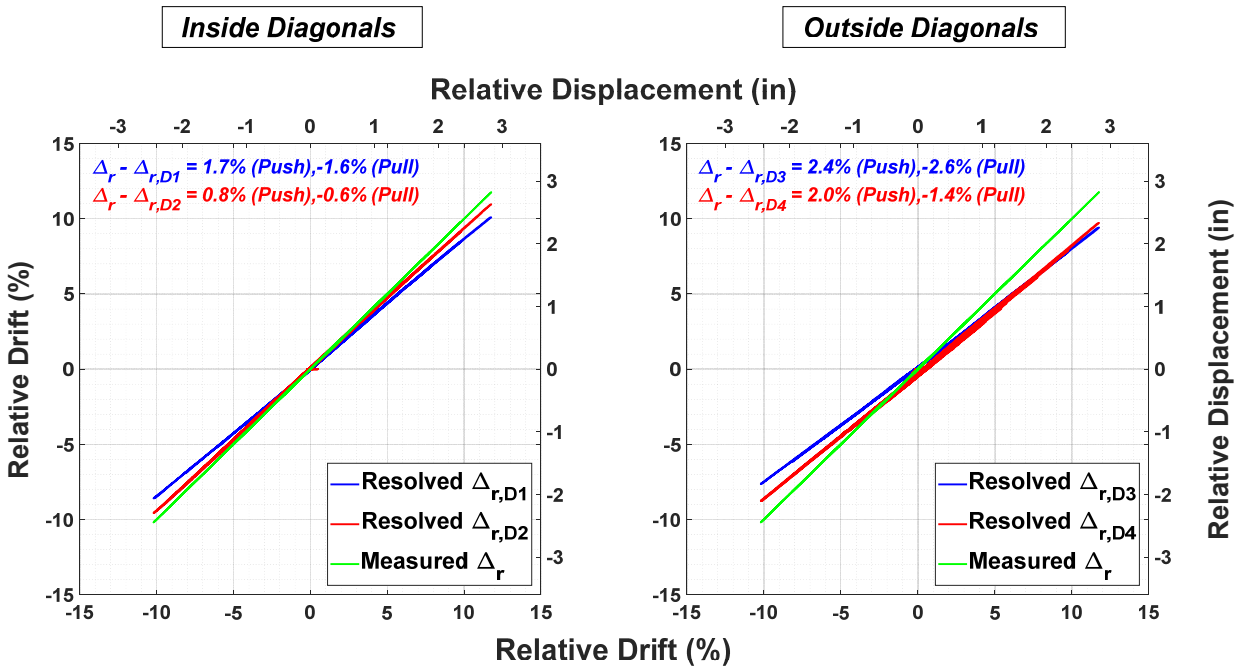

Figure 4.46 Specimen A-3 (unretrofitted, top boundary condition C): resolved *relative* drift from diagonal measurements (outside and inside diagonals) versus measured *relative* drift.

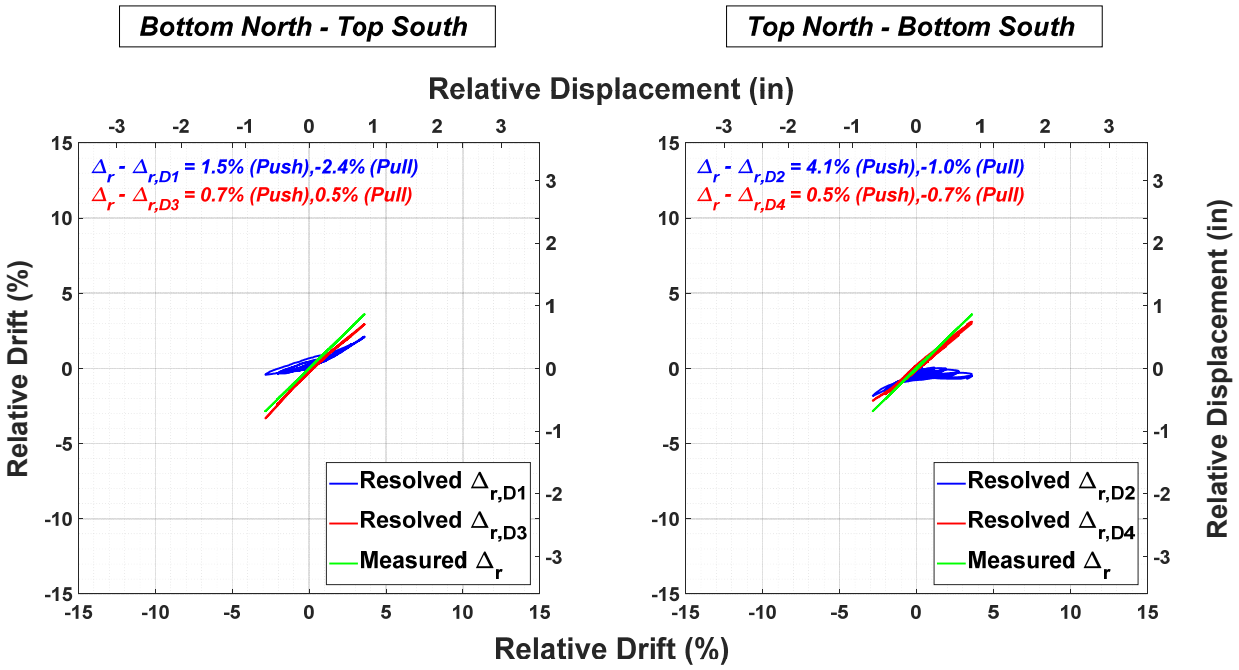

Figure 4.47 Specimen A-5 (retrofitted, top boundary condition B): resolved *relative* drift from diagonal measurements in one direction versus measured *relative* drift.

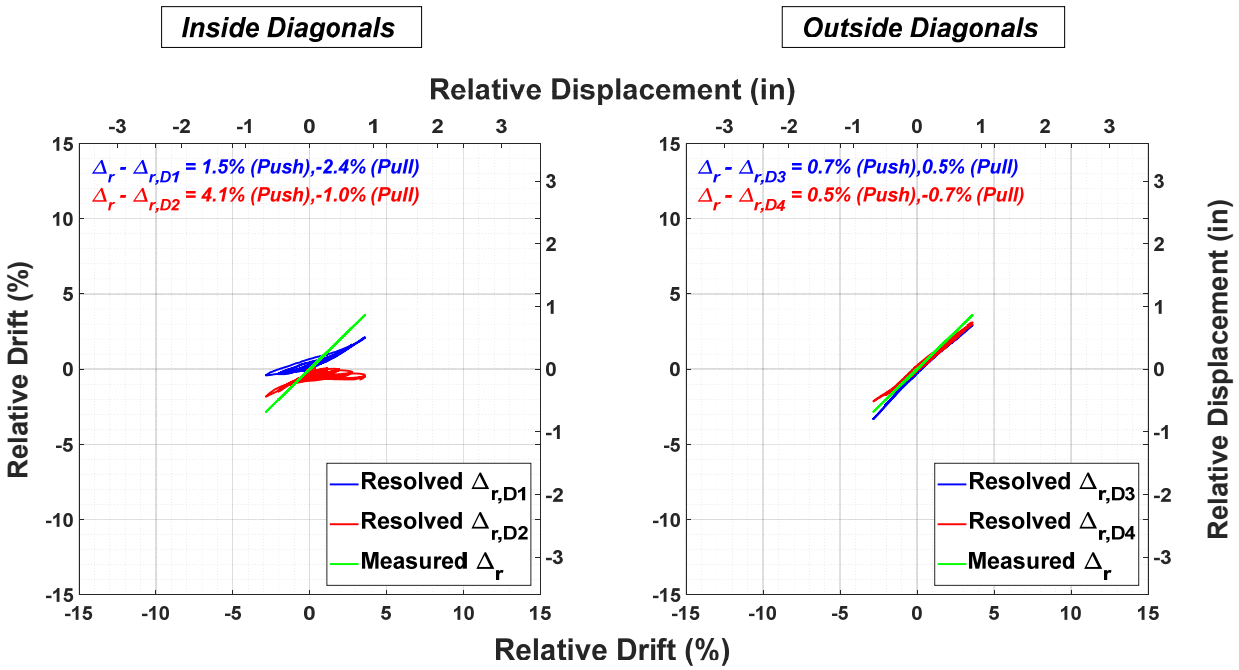

Figure 4.48 Specimen A-5 (retrofitted, top boundary condition B): resolved *relative* drift from diagonal measurements (outside and inside diagonals) versus measured *relative*.

4.6 UPLIFT MEASUREMENTS

Two linear potentiometers were used to measure the uplift at both ends of the cripple wall. These potentiometers were attached to the foundation and the steel load transfer beam. The calculations for determining the uplift of the cripple walls are discussed in Section 4.5, as the uplift measurements were factored into calculating the resolved relative displacement from the diagonal measurements. Table 4.8 summarizes the maximum uplift measurement at each end of the wall for all specimens. All of the cripple walls exhibited uplift when being displaced except Specimen A-1, which was the weakest cripple wall and did not contain a built-up corner. While Specimen A-1 had up to 0.06 in. of uplift (at the south end), this occurred when the cripple wall was at zero displacement. When displaced, the rotation of the studs and compression of the studs into the sill provided a minor reduction in the height of the cripple wall at both ends (-.10 in. in both directions). Figures 4.49 and 4.50 show the end uplift versus relative drift response for Specimens A-2 and A-5, respectively. The difference between these two cripple walls was the addition of the retrofit for Specimen A-5, which caused a 172% increase in lateral load capacity in the push direction and a 170% increase in lateral load capacity in the pull direction. The dramatic increase in strength also resulted in an increased uplift at the ends of the cripple wall for the retrofitted specimen. The largest measured uplift for the unretrofitted cripple wall was 0.42 in. when pushed compared with 0.33 in. for the retrofitted cripple wall. In the pull direction, the maximum end uplift was 0.31 in. for the unretrofitted cripple wall compared with 0.30 in. for the retrofitted cripple wall. The uplift response for the cripple walls was close to symmetric. All of the end uplift versus relative drift responses can be seen in Appendix C.3.

Table 4.9 End uplift measurements.

Specimen no.	South-end uplift (in.)	North-end uplift (in.)
A-1	0.06	0.01
A-2	0.02	0.03
A-3	0.22	0.07
A-4	0.36	0.27
A-5	0.3	0.33
A-6	0.42	0.31

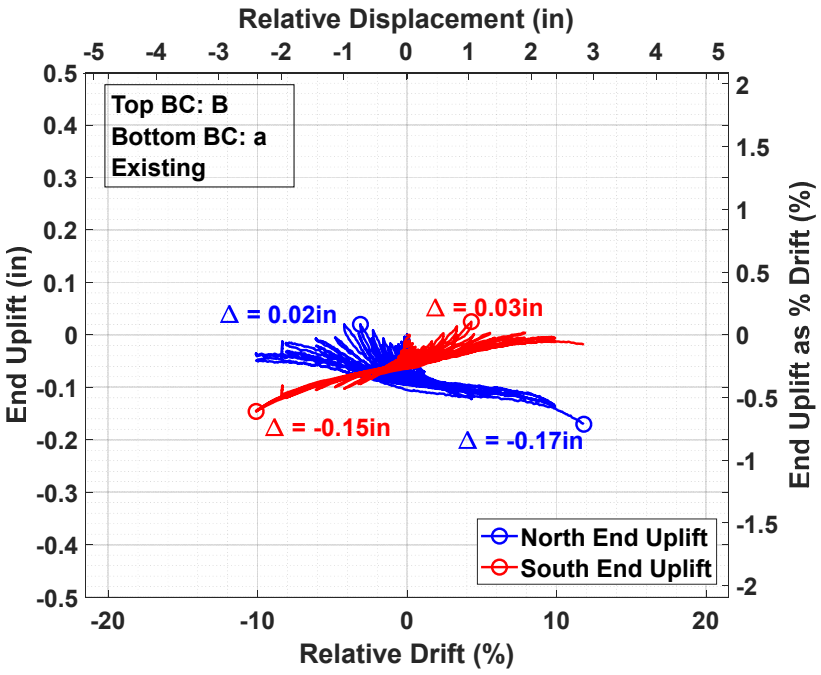

Figure 4.49 Specimen A-2 end uplift versus *relative* drift.

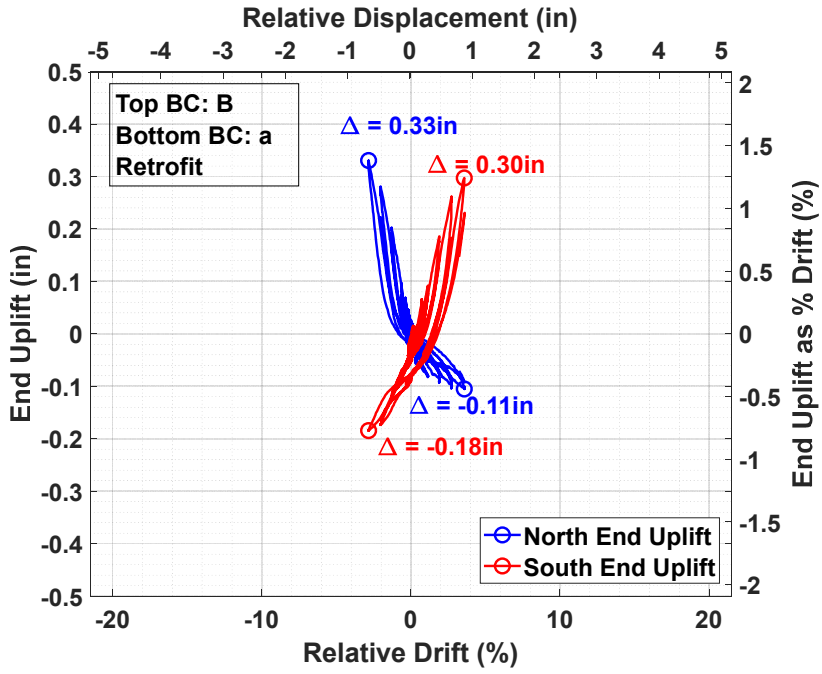

Figure 4.50 Specimen A-5 end uplift versus *relative* drift.

4.7 COMPARISON OF RETROFITTED CRIPPLE WALLS

A major goal of this project was to quantify the effectiveness of retrofitting cripple walls. In Phase 1, one cripple wall was retrofitted. The retrofitting of cripple walls is intended to address vulnerabilities in the connection of the cripple wall to the framing above, the cripple wall framing itself, and the foundation sill plate anchorage to the foundation. This involves adding connectors to improve the connection from the cripple wall to the framing above, adding wood structural panels to the interior framing of the cripple wall to strengthen the cripple wall, and installing additional anchor bolts to increase the sliding resistance of the dwelling. For taller cripple walls (typically 4 ft or greater), tie-downs are installed to increase the uplift capacity of the dwelling. For purposes of this testing program, connectors used to improve connection from the cripple wall to the framing above were not implemented as only cripple wall components were tested.

The design guidelines for retrofitting in this project come from the ATC-110 project [FEMA 2018]. Since *FEMA P-1100* guidelines had not yet been finalized, the retrofitted cripple wall did not strictly follow these guidelines. For later phases of testing, the *FEMA P-1100* prescriptive design provisions were used for the retrofit design. The main differences between the two retrofit designs were the number of additional anchor bolts and the spacing of the nailing attaching the plywood to the cripple wall framing. In this phase, Specimen A-5 contained an additional two anchor bolts, decreasing the anchor bolt spacing from 64 in. on center to 32 in. on center. In addition, the plywood panels were fastened with 8-penny hot dipped galvanized nails at 4 in. on center. Complete details of the retrofit design for Specimen A-5 can be found in Section 3.6.

Overall, although the retrofit dramatically increased the lateral strength and initial stiffness of the cripple wall, it caused a decrease in its drift capacity. The addition of the retrofit accounted for a 172% increase in lateral load in the push direction and a 170% increase in lateral load in the pull direction. The secant stiffness associated with drift at 80% strength increased by 105% in the push direction and by 70% in the pull direction. The drift at lateral strength decreased with the addition of the retrofit when considering the relative drift. Specimen A-2, the unretrofitted cripple wall, attained strength at 5% global drift and 4.3% relative drift in the push direction and 4% global drift and 3.1% relative drift in the pull direction. Specimen A-5, the retrofitted cripple wall, attained strength at 5% global drift and 3.6% relative drift in the push direction, and 5% global drift and 2.8% relative drift in the pull direction. An overlay of the lateral force–lateral displacement response hysteresis for the global response is shown in Figure 4.51 and the relative response is shown in Figure 4.52.

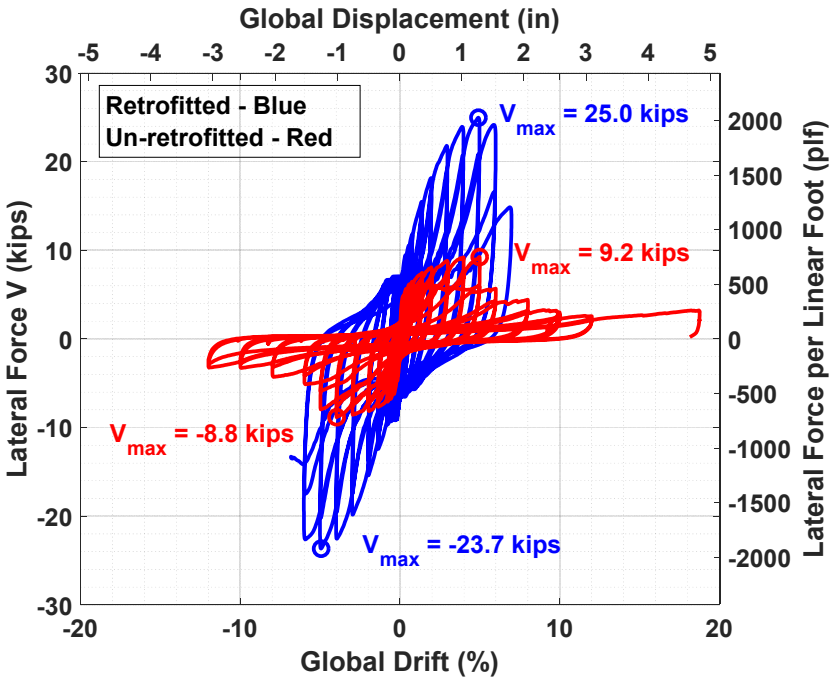

Figure 4.51 Specimens A-2 and A-5: comparison of *global* drift versus lateral strength hysteretic response for unretrofitted and retrofitted cripple walls.

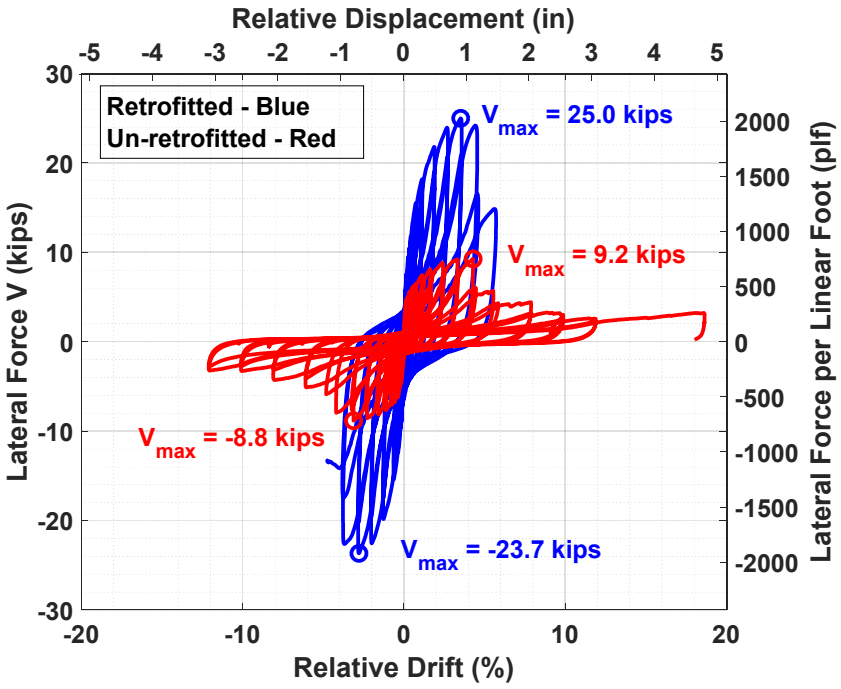

Figure 4.52 Specimens A-2 and A-5: comparison of *relative* drift versus lateral strength hysteretic response for unretrofitted and retrofitted cripple walls.

4.8 ENVELOPES OF HYSTERETIC RESPONSE

It is useful to assess the response of the cripple walls using overlays of the envelope extracted from the lateral force–lateral displacement hysteresis. These curves were obtained by extracting the strength at each drift amplitude throughout the loading protocol; only the leading cycles of each cycle group were considered. Figures 4.53 to 4.56 show key comparisons of the cripple walls using the envelopes of each specimen's hysteresis. Both the push and pull loading is displayed in the same quadrant for ease of comparison. Figure 4.53 compares the effect of the different top boundary conditions. It is evident that top boundary condition B and top boundary condition C had a very similar response. Both of these cripple walls had significantly higher strength than the cripple wall with top boundary condition A. This can be attributed to the built-up corners, which top boundary condition A did not have. Also notable are the reduction in strength and stiffness consistently observed in the pull direction, the amplitude of which is consistent irrespective of boundary condition. Figure 4.54 compares bottom boundary condition "a" and bottom boundary condition "b", which shows that there are significantly higher strengths achieved with bottom boundary condition "b" compared with bottom boundary condition "a". This is attributed to the bearing of the stucco on the foundation whereas bottom boundary condition "a" has the stucco positioned such that it is outboard of the foundation and is free to rotate.

Figure 4.55 shows the envelopes of the existing and retrofitted pair of specimens. As discussed earlier, the added retrofit drastically increased the strength and stiffness of the cripple wall. Lastly, Figure 4.56 shows the envelopes of the cripple walls with different anchorage conditions. The cripple wall with the typical anchorage condition (with the sill plate fastened to the foundation with anchor bolts) was significantly stronger than the cripple wall with a wet set sill plate. For all of the specimens, higher strengths were achieved when pushed on rather than pulled on. This is due to the push loading being the initial direction of loading; as a result, the strength of the cripple walls nominally degrades before being pulled to the same target displacement in the opposing direction.

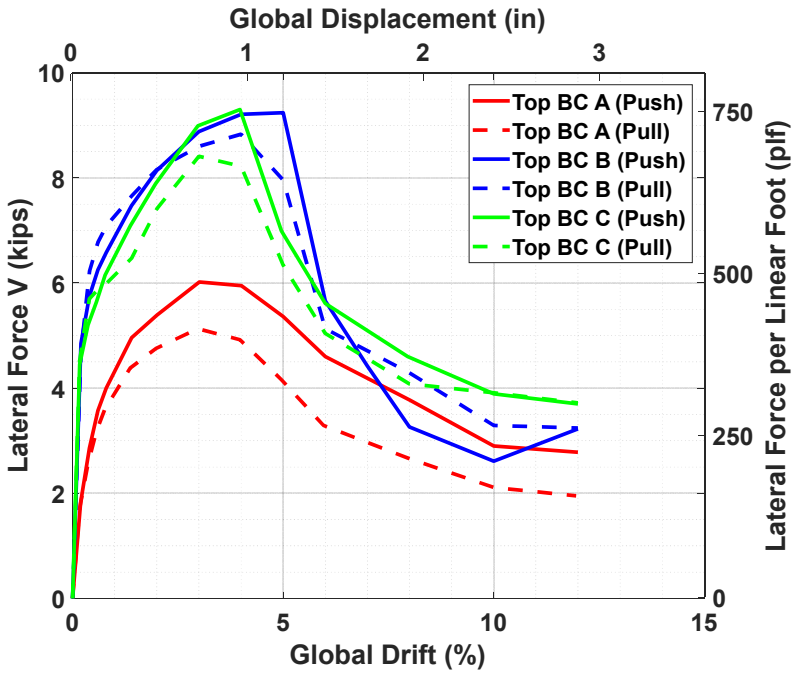

Figure 4.53 **Specimens A-1, A-2, and A-5: comparison of envelopes of *global* drift versus lateral strength hysteretic response for top boundary conditions.**

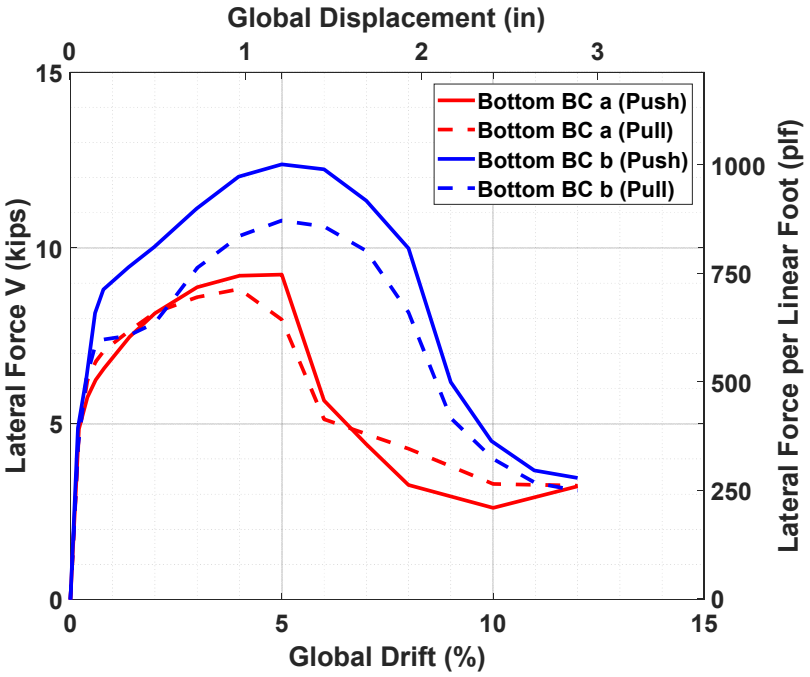

Figure 4.54 **Specimens A-2 and A-4: comparison of envelopes of *global* drift versus lateral strength hysteretic response for top boundary conditions.**

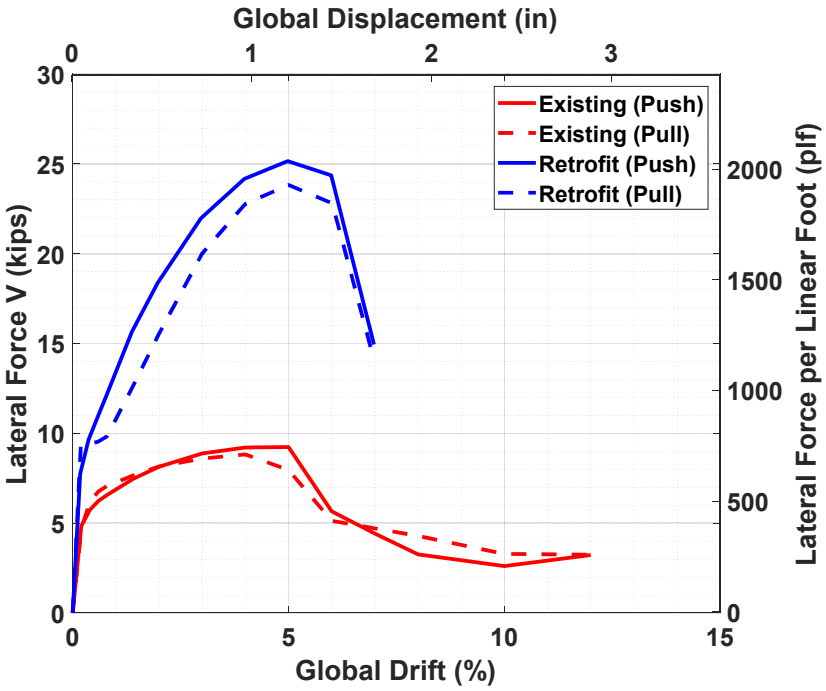

Figure 4.55 **Specimens A-2 and A-5: comparison of envelopes of *global* drift versus lateral strength hysteretic response for retrofit condition.**

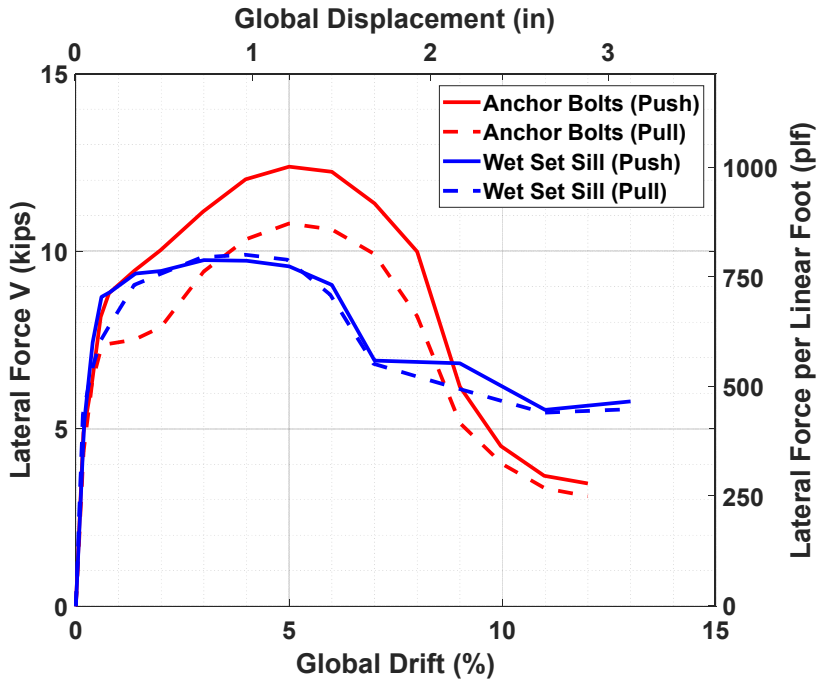

Figure 4.56 **Comparison of envelopes of *global* drift versus lateral strength hysteretic response for Top boundary conditions.**

4.9 HYSTERETIC ENERGY DISSIPATION

An important characteristic used to describe the seismic response of a cripple wall is the hysteretic energy dissipated by the cripple wall during loading. This may be calculated by summing the area of the hysteretic loops in both push and pull loading for each cycle level group. Note that the hysteretic energy dissipated was calculated for the leading and the trailing cycles in both the push and pull directions of loading. Figures 4.57 through 4.60 plots the cumulative energy dissipated versus drift for both the relative and global responses. These responses differed largely, depending on whether or not the cripple wall slid on the foundation as the friction between the sill plate and the foundation dissipated a significant amount of energy.

Figure 4.57 compares the dissipated energy considering different top boundary conditions. The cumulative energy dissipated by both top boundary condition B and top boundary condition C is very similar. The energy dissipated was over twice that of top boundary condition A when looking at the global response and over 60% greater when looking at the relative response. Figure 4.58 compares the bottom boundary conditions. At low-amplitude drift levels, the responses were very similar, but then they began to diverge strongly. The bearing of the stucco on the foundation, associated with bottom boundary condition “b” and the increased sliding of the cripple wall, were responsible for the larger values of energy dissipated. Figure 4.59 compares the existing and retrofitted specimens. As expected, the added retrofit dissipates much more energy than the existing specimen due to the increased number of fasteners connecting the plywood to the framing. There is over a 150% increase in cumulative energy dissipated for the global response and over a 400% increase in cumulative energy dissipated for the relative response when the specimen has been retrofitted. Note: the retrofitted cripple wall would have continued to dissipate even more energy had the test not ended prematurely. Finally, Figure 4.60 compares the cumulative energy dissipated for the two different anchorage conditions. The energy dissipated for the relative response is nearly identical but is significantly different when looking at the global response. This shows how much energy is dissipated due to the sill plate displacement relative to the foundation.

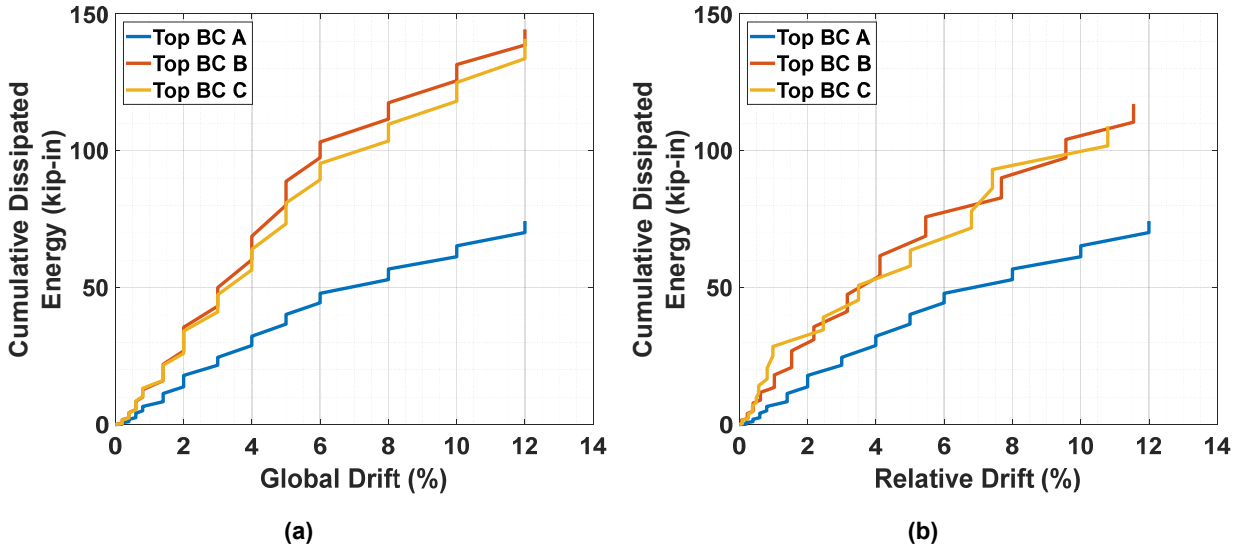

(a) (b)

Figure 4.57 **Comparison of cumulative energy dissipated for cripple walls with *different top boundary conditions*: (a) global response; and (b) relative response.**

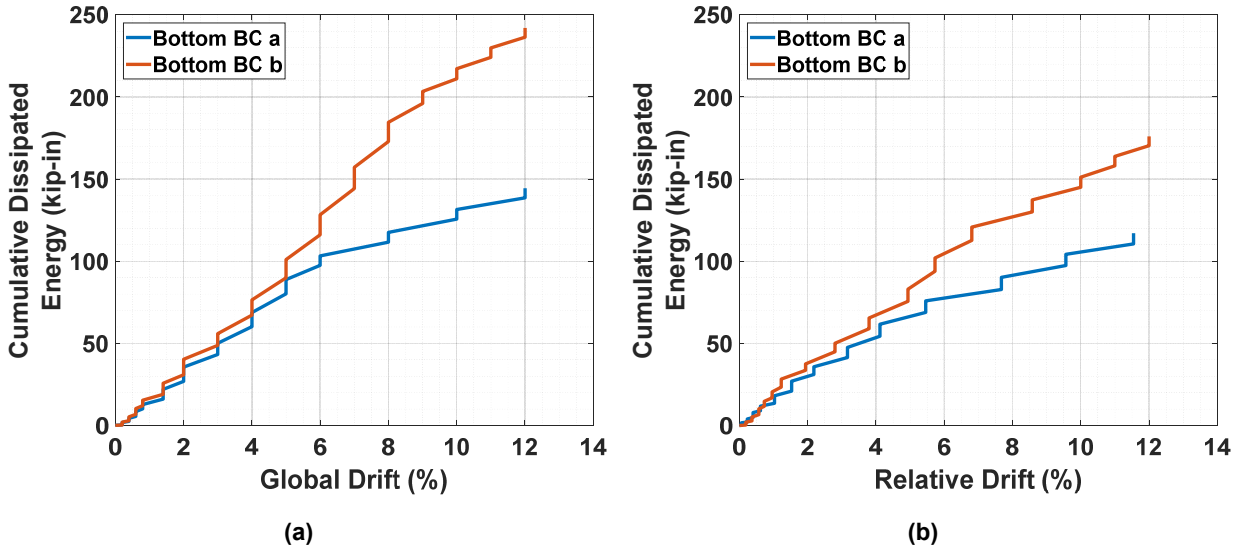

(a) (b)

Figure 4.58 **Comparison of cumulative energy dissipated for cripple walls with *different bottom boundary conditions*: (a) global response; and (b) relative response.**

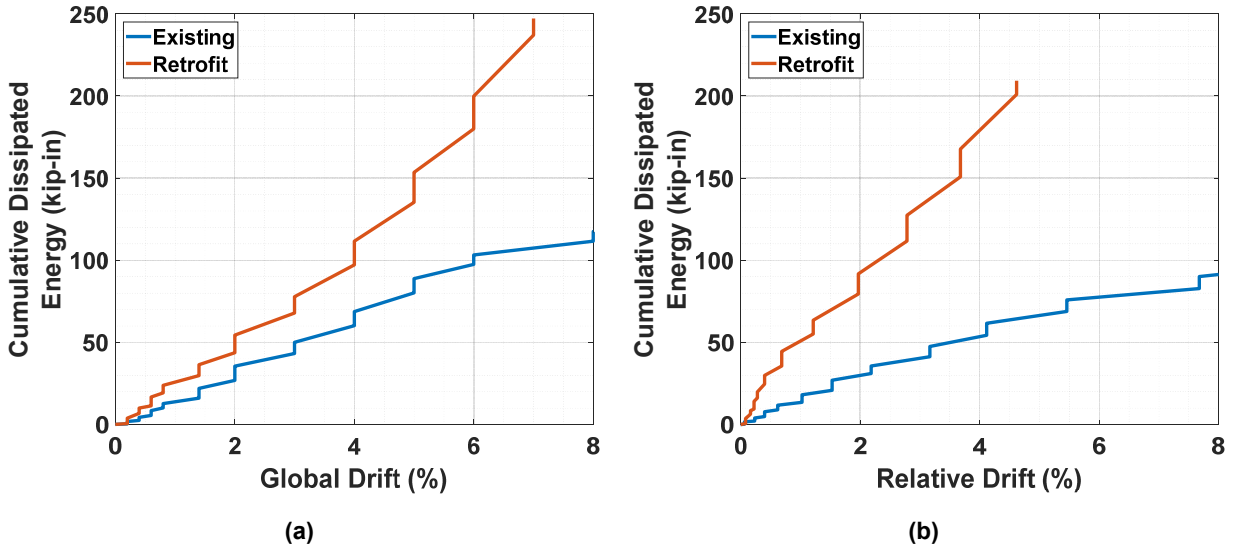

Figure 4.59 **Comparison of cumulative energy dissipated for existing and retrofitted cripple walls: (a) global response; and (b) relative response.**

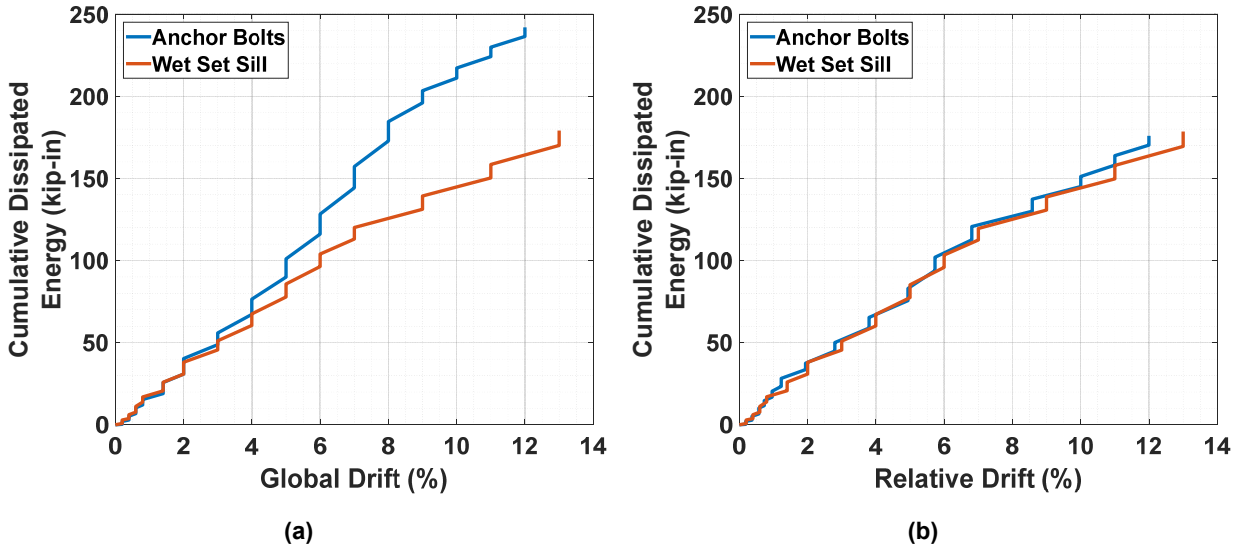

Figure 4.60 **Comparison of cumulative energy dissipated for cripple walls with different anchorage conditions: (a) global response; and (b) relative response.**

4.10 RESIDUAL DISPLACEMENT

As the cripple walls were cyclically loaded, they accumulated residual deformation. Residual deformation is an effective measure to evaluate the structural performance of a cripple wall under

seismic excitation. In addition, residual deformation represents the final state of a structure after an earthquake, thus making it a concern for homeowners as the aesthetic and structural performance of the dwelling are both affected. The residual displacement of the cripple walls was measured at the end of each displacement cycle level and can be defined as the amount of displacement in the cripple wall measured when there is no lateral force being imposed on the cripple wall. As the amplitude of the displacement was increased, the residual displacement increased to the point where it became visible, even prior to the cripple walls achieving full strength.

Figure 4.61 shows the global residual displacement of the cripple walls after the 1.4% drift cycle group. Global residual displacement refers to not only the residual displacement of the cripple wall itself, but also to the residual displacement of the sill plate relative to the foundation. Figure 4.62 shows the relative residual displacement of the cripple walls after the 1.4% drift cycle group. The relative residual displacement accounts for only the deformation sustained in the cripple wall, excluding any deformation of the sill plate relative the foundation. For convenience, the relative residual displacement will be referred to as residual displacement. This measurement is a better indicator of the structural performance of the cripple wall as it only accounts for the residual deformation of the cripple wall.

There were variations in the alignment of the sill plate connection to the foundation because of the use of oversized (1/4-in.) anchor bolt holes. The global residual displacement was between 0.2 in. and 0.28 in. or 0.8% to 1.2% drift. The range of values increased significantly when comparing the residual displacement. They varied from 0.04 to 0.28 in. or 0.2% to 1.1%. Specimen A-5 (retrofitted cripple wall) only had 0.04-in. of relative residual displacement, while Specimen A-6 (wet set sill) had 0.28 in. of residual displacement. With the added retrofit, the increased strength caused the cripple wall to have large displacements of the sill plate relative to the foundation; therefore, less of the imposed displacement was carried by the wall itself. The cripple wall with a wet set sill plate had no displacement of the sill plate relative to the foundation, so all of the residual displacement was carried by only the wall.

It is more useful to compare the residual displacements in the cripple walls at the same relative drift amplitude. Figure 4.63 shows the residual displacement of each cripple wall at 1.4% relative drift. Since the cripple walls never displaced to exactly 1.4% relative drift before unloading, the residual displacement at 1.4% relative drift was linearly interpolated from the residual displacement at the cycle group right before and right after the 1.4% relative drift mark. Note: the range in residual displacement significantly decreased to 0.18 to 0.21 in. or 0.7% to 0.8% drift. This excludes the cripple wall with the wet set sill plate, which had a residual displacement of 0.26 in. It is evident that despite the differences in boundary conditions and retrofit conditions, the cripple walls maintained fairly consistent residual deformation at low drift amplitudes.

Figure 4.64 shows the global residual displacement of the cripple walls at peak strength. These values range from 0.55 in. to 0.94 in. Excluding the retrofitted cripple wall and bottom boundary condition “b”, the range narrows to 0.55 to 0.67 in. When looking at the residual displacement, the retrofitted cripple wall had the lowest residual displacement; see Figure 4.65.

This large variation was due to the increased amount of displacement of the sill plate relative to the foundation for the retrofitted cripple wall. There was also a dramatic decrease for the cripple wall with bottom boundary condition “b” for the same reason (0.95 in. to 0.66 in.). This specimen had the largest amount of relative drift at peak strength, which can be attributed to the

bearing of the stucco on the foundation that caused the furring nails to lose connection with the framing or the stucco face at lower drift amplitudes, thus causing increased residual displacement. The ranges of residual displacement for all of the other cripple walls is fairly uniform, from 0.51 in. to 0.59 in., with the wet set sill specimen at the upper end of that range. The cripple wall with the wet set sill also had bottom boundary condition “b”, causing increased residual displacement at peak strength.

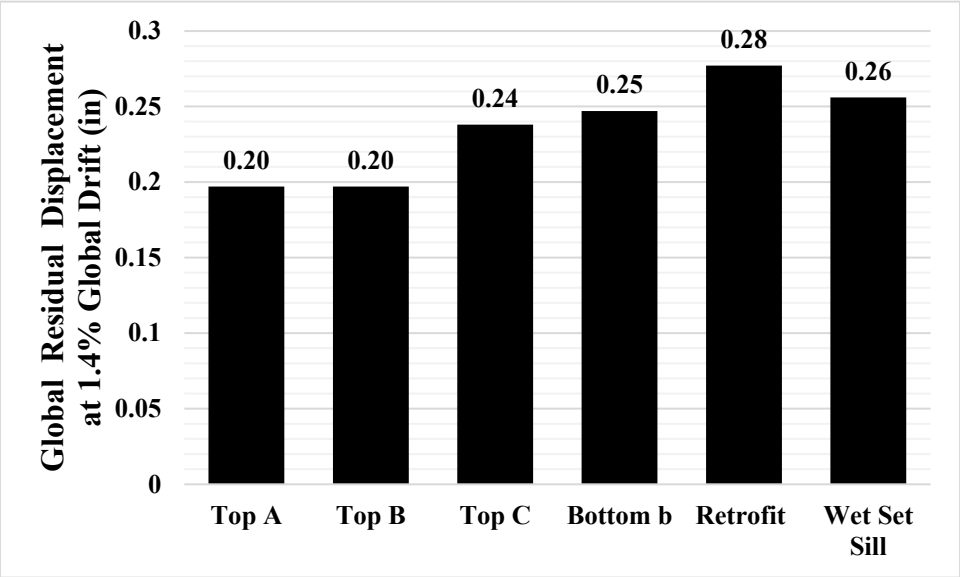

Figure 4.61 ***Global*** **residual displacement of cripple walls at the end of the 1.4% global drift cycle group.**

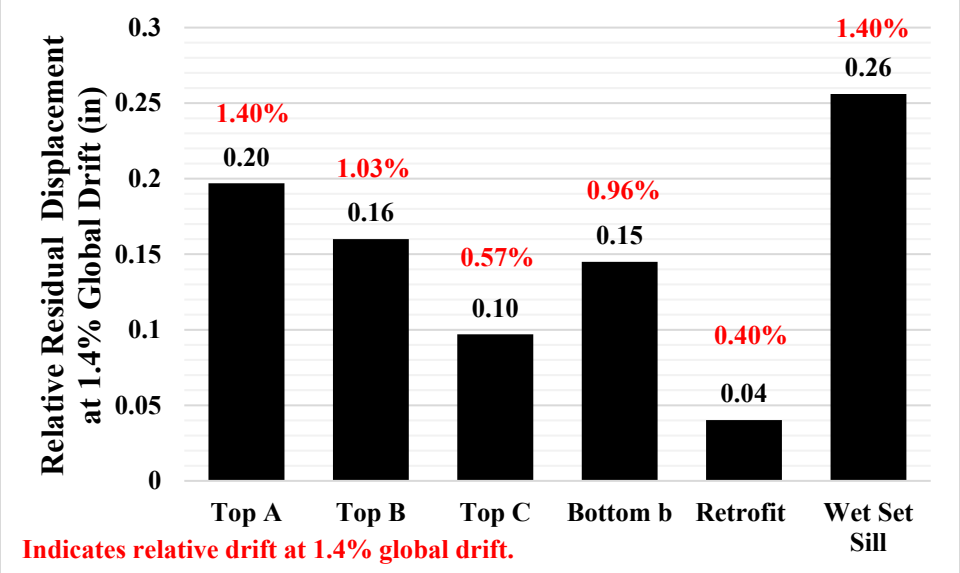

Figure 4.62 ***Relative*** **residual displacement of cripple walls at the end of the 1.4% global drift cycle group.**

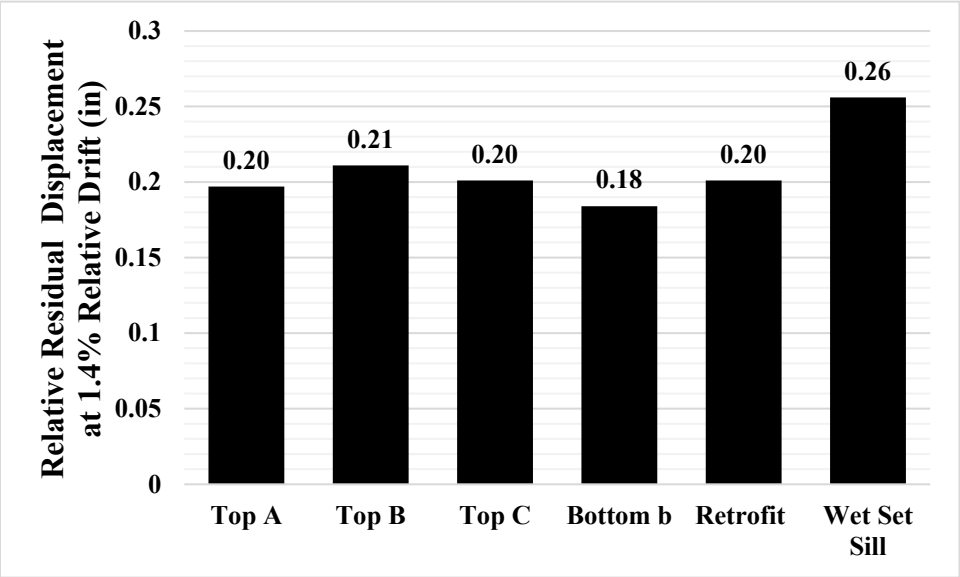

Figure 4.63 ***Relative*** **residual displacement of cripple walls at the end of the 1.4% relative drift cycle, linearly interpolated.**

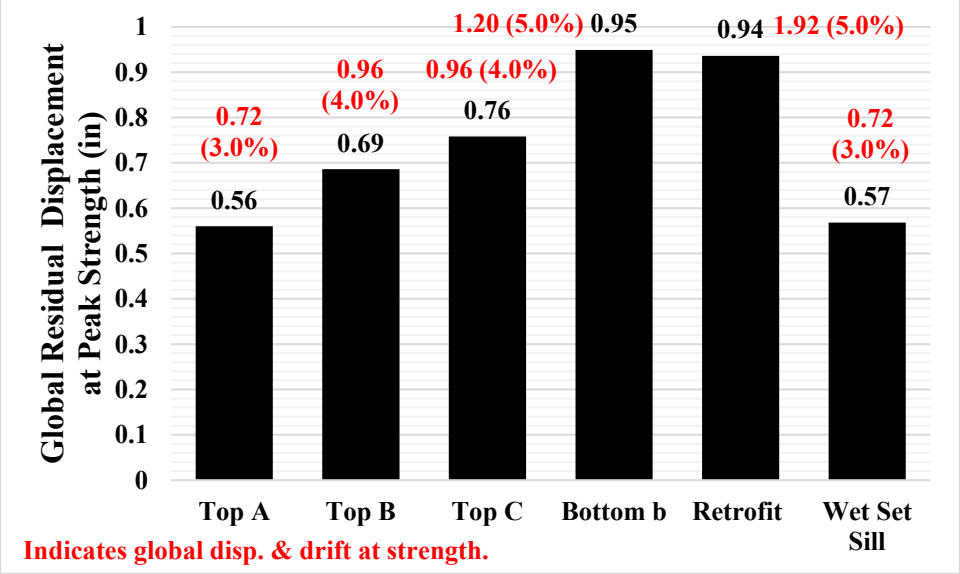

Figure 4.64 ***Global*** **residual displacement of cripple walls at the end of the peak strength drift cycle group.**

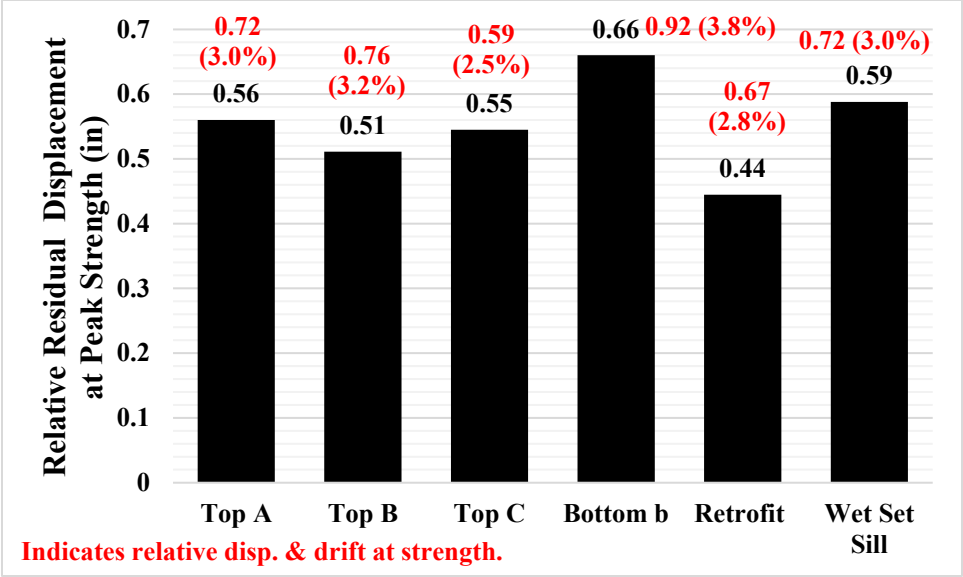

Figure 4.65 ***Relative*** **residual displacement of cripple walls at the end of the peak strength drift cycle group.**

4.11 VERTICAL LOAD CORRECTION

Using four hydraulic jacks, the vertical load was applied vertically with two 4 in. × 4 in. × 3/8 in. HSS members acting as point loads. The load was measured with four axial load cells, one for each rod. The connection of the rods to the hydraulic jacks was engineered such that they were only able to rotate, thereby creating a pinned connection at the ceiling of the strong floor, as described earlier. As the cripple walls displace, the applied vertical load will develop a horizontal component that needs to be included in the horizontal force being applied (and measured by the lateral actuator) to the cripple wall. Since the horizontal component opposed the measured lateral force, the corrected lateral force would reduce the measured lateral force. The vertical load experienced by the cripple wall is also reduced due to the displacement of the cripple wall but to a negligible degree, particularly for the Phase 1 shorter (2-ft-tall) cripple walls.

Figure 4.66 shows the setup for the application of the vertical load, and Figure 4.67 shows the geometry of the vertical load and lateral load as the cripple wall displaces. Overall, the correction for the lateral load was a reduction in the range of 0–3% for all cycles. During the monotonic push, the correction would be a reduction in the range of 0–5%. Note: all results presented in the prior sections have accounted for these corrections. The equations for the corrected lateral load and corrected vertical load are as follows:

$$V_{actual} = V_{measured} - P_{rod,x} = V_{measured} - P_{rod}\sin(\theta_{rod}),$$

$$P_{actual} = P_{rod,y} = P_{rod}\cos(\theta_{rod}), \text{ where } \theta_{rod} = \sin^{-1}\frac{\Delta}{L_{rod}}$$

The vertical load for all specimens was 450 plf. This corresponds to a 5-kip load being applied between the four hydraulic jacks after the weight of the horizontal load transfer beam, laminated wood beam, and HSS sections had been considered. Throughout the displacement

cycles, the vertical load applied by the jacks would oscillate. These oscillations are shown in Figure 4.68. For all cripple walls, the vertical loads fluctuated from 1.0–1.2 kips over their entire loading protocol. The maximum vertical load experienced was 5.7 kips for Specimen A-2 and the lowest vertical load was 4.3 kips for Specimen A-1.

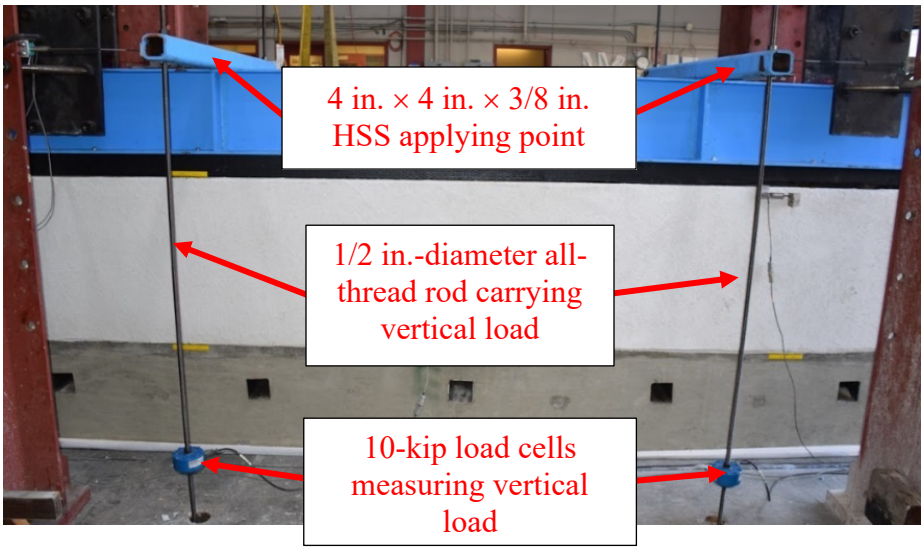

Figure 4.66 Vertical load setup.

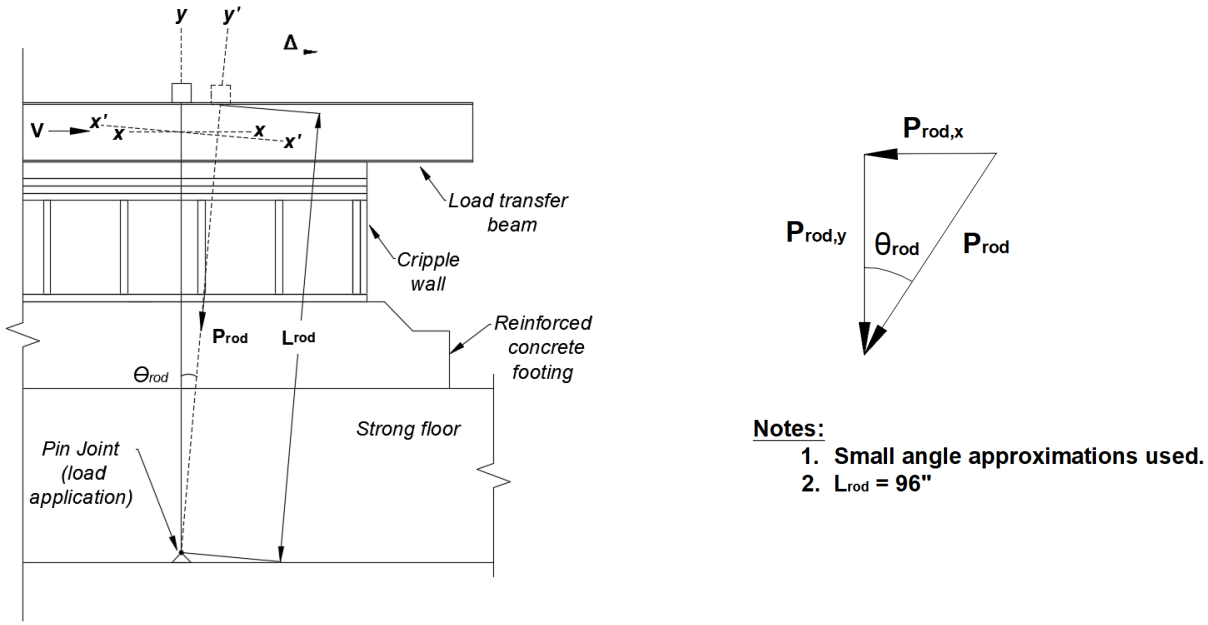

Figure 4.67 Schematic of displaced geometry for lateral load correction.

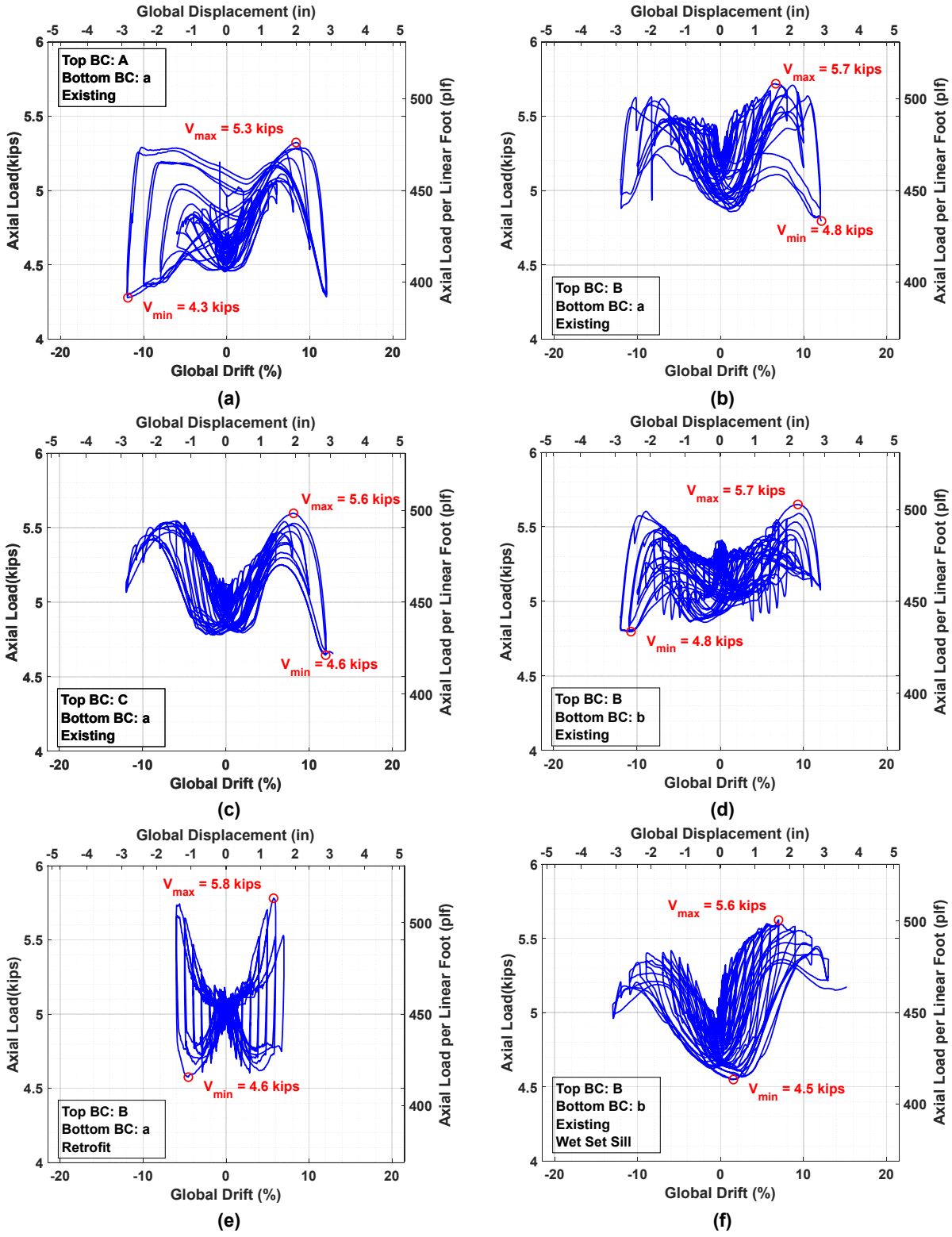

Figure 4.68 Vertical load versus global drift for all Phase 1 specimens: (a) Specimen A-1; (b) Specimen A-2; (c) Specimen A-3 (d) Specimen A-4; (e) Specimen A-5; and (f) Specimen A-6.

5 DAMAGE CHARACTERISTICS

5.1 OVERVIEW

This chapter presents the physical damage characteristics as they evolved during the cyclic testing of each cripple wall specimen tested in Phase 1. Tracking the physical damage of cripple walls is key to determining the structural integrity of a cripple wall after a seismic event. Stucco cracking, nail withdrawal/rotation, plywood panel tearing, and rotation, as well as uplift and splitting of framing members were observed. Damage documentation was taken via hand notes and high-resolution photographs, as well as examination of video footage following testing. For all drift ratio levels, photographs of damage were taken at the initial push and initial pull at each drift amplitude. In addition, from the 0.2% to the 1.4% drift ratio levels, photographs were taken at the end of the cycle grouping for the purpose of recording the state of damage at zero-imposed lateral load, as well photographic documentation of the residual displacement that accrued in the cripple walls. The ability to relate the physical damage of a cripple wall to its lateral strength is critical in determining what repairs are required to fix the aesthetic and structural elements of a cripple wall and its superstructure. This chapter will be broken into sections based on the damage to each of the six cripple walls.

5.2 DAMAGE CHARACTERISTICS FROM 0.0% TO 1.4% DRIFT RATIO LEVEL (SERVICE-LEVEL RANGE)

Understanding the physical damage characteristics of cripple walls at low-level drift amplitudes is important to be able to make distinctions between what is a serviceable structure and what is a structure requiring repairs to become serviceable again. In this section, the service-level drift is denoted as amplitudes prior to and including 1.4% global drift of the cripple wall. The damage characteristics of each of the six cripple wall specimens at these drift amplitude cycles will be described and shown. In addition, photographs of the original structure are presented to illustrate the initial state of the structure prior to testing.

5.2.1 Specimen A-1: 0.0% to 1.4% Drift Ratio Level

Figure 5.1 shows the initial state of Specimen A-1 constructed without any end-wall continuity, i.e., no additional continuity of finish was incorporated. There were no built-up corners compared to the other five cripple walls tested in Phase 1. In addition, this cripple wall contained the most widely spaced furring nails at the cripple wall top plate of any of the other specimens. The framing and stucco attachment details of Specimen A-1 match those of cripple walls tested in the UC Davis testing program within the CUREE Caltech-Woodframe Project [Chai et al. 2002]. Figure 5.1(a)

shows the exterior face of the cripple wall, while Figure 5.1(b) shows the interior face of the cripple wall. Views of the corners are shown in Figure 5.1(c) and (d).

Figure 5.2(a) to (f) show the damage state of Specimen A-1 at 1.4% drift amplitude. At this low-level amplitude, no cracks had yet formed on the stucco face. On the interior of the wall, the studs began to uplift and exhibit slight rotation. This uplift and rotation can be seen in the connection of the studs to the sill plate as well as the connection to the top plates. The most noticeable damage characteristics are as follows: the 1/4 in. of relative slip between stucco and foundation face at the base of the cripple wall and the 1/8 in. of relative slip between the stucco and framing at the top of the cripple wall. From an exterior view, the lack of cracking on the specimen would indicate that at this point there was minimal-to-no structural damage to the wall.

Figure 5.3 shows the initial state of Specimen A-2 prior to testing. The primary difference between Specimen A-1 versus Specimen A-2 is the change in the boundary conditions. Specimen A-2 utilized an extra top plate to allow for two rows of a denser furring nail arrangement. This provides the extra 1-1/2 in. of wall height compared with Specimen A-1, which contained only a double top plate. In addition, Specimen A-2 incorporated built-up corners, featuring two 2 × 4 corner studs and a 2 × 4 flat stud. In addition, the finishes wrapped 6 in. around the corner; see Figure 5.3(c). The stucco finish was outboard of the foundation, while the face of the horizontal sheathing boards was flush with the foundation face. Specimen A-2 had top boundary condition B and bottom boundary condition “c”; see Figure 5.3(a); note that a crack had already formed on the face of the stucco prior to testing.

5.2.2 Specimen A-2: 0.0% to 1.4% Drift Ratio Level

Figure 5.4(a) to (f) show the damage state of Specimen A-2 at 1.4% drift amplitude. At this drift level, a new vertical crack began forming at the base of the stucco but had not yet propagated up the entire stucco face. In addition, both the north and south corners of the wall exhibited extensive cracking. Figure 5.4(e) and (f) shows that most of the cracks were concentrated at the bottom, close to the corner, and ran vertically, but additional cracks formed on corner faces that propagated diagonally across the face. These cracks began forming at drift amplitudes as low as 0.2% and extended at larger drift amplitudes. Figure 5.4(c) shows that the stucco had slipped 1/4 in. relative to the stucco, and that the stucco had detached from the foundation; a gap had begun to form between the stucco and the foundation face. This occurred as the furring nails began to detach from sheathing board and framing members. Like Specimen A-1, the studs began to rotate and uplift. At the top of the cripple wall, the slip between the sheathing and framing was negligible.

(a)

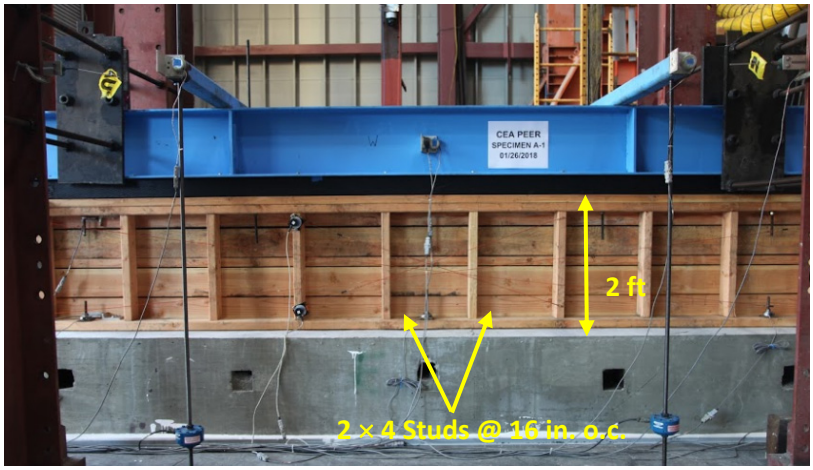

(b)

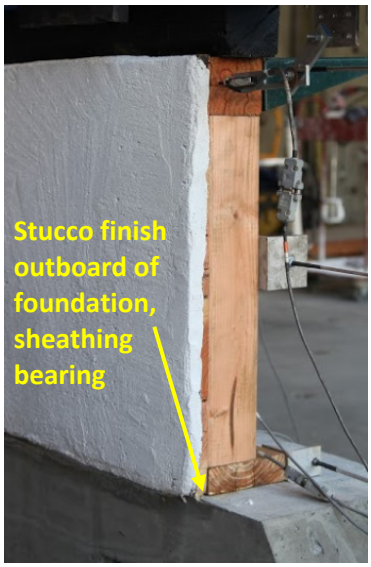

(c)

(d)

Figure 5.1 **Specimen A-1 pre-test photographs with top boundary condition A and bottom boundary condition "a": (a) exterior elevation; (b) interior elevation; (c) exterior north-end corner view; and (d) interior north-end corner view.**

Figure 5.2 Specimen A-1 damage state at -1.4% drift @ Δ = -0.336 in.: (a) exterior elevation; (b) interior elevation; (c) bottom of exterior wall displacement; (d) south top exterior and corner view; (e) north exterior and corner view; and (f) top of wall displacement.

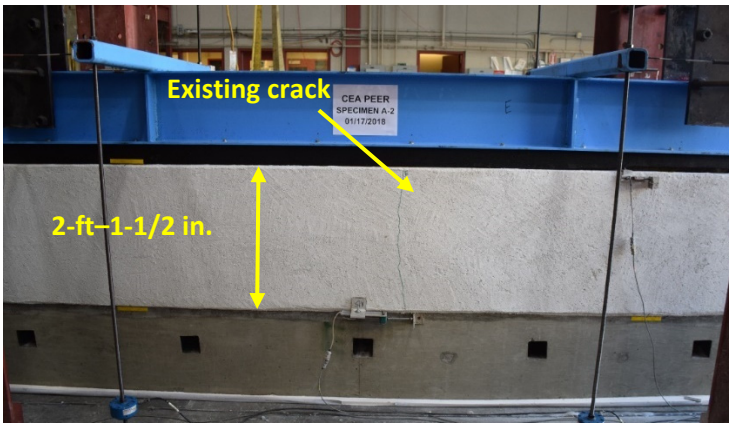

(a)

(b)

(c)

(d)

Figure 5.3 **Specimen A-2 pre-test photographs with existing top boundary condition B, bottom boundary condition "a": (a) exterior elevation of cripple wall; (b) interior elevation of cripple wall; (c) north-end exterior and corner view; and (d) north-end interior and corner view.**

(a)

(b)

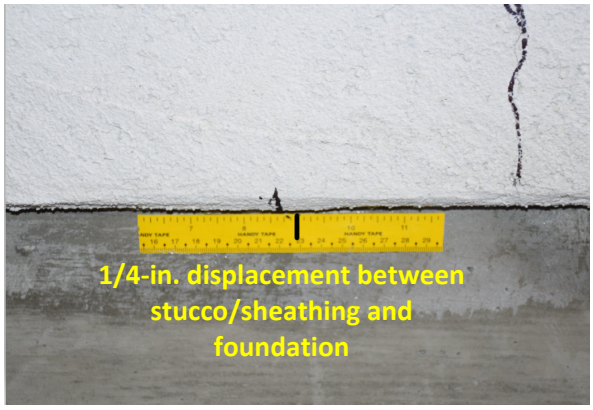

(c)

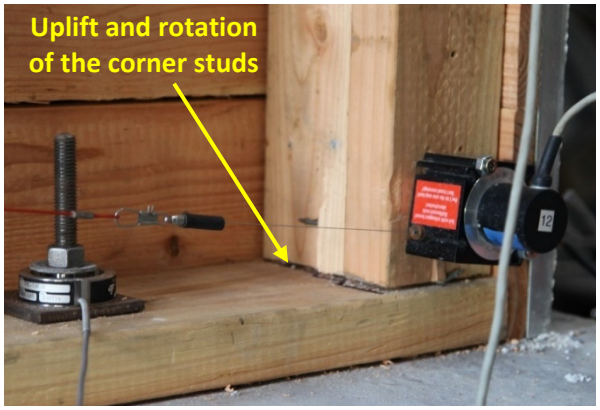

(d)

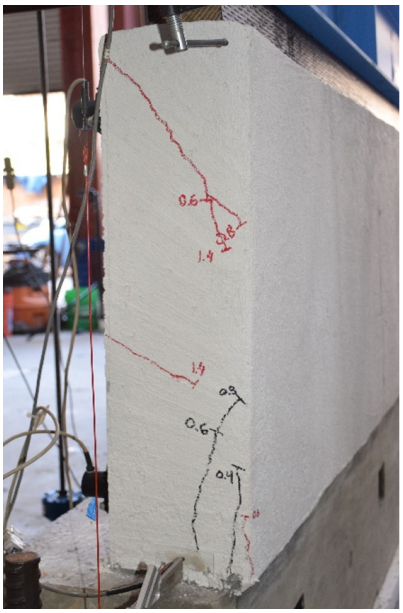

(e)

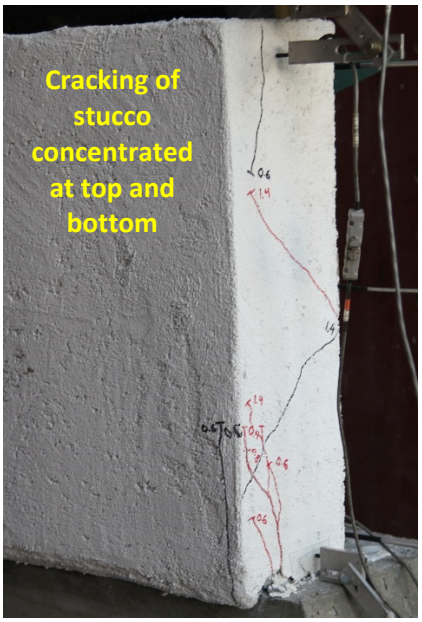

(f)

Figure 5.4 **Specimen A-2 damage state at -1.4% drift @ Δ = -0.336 in.: (a) exterior elevation; (b) top of exterior wall; (c) bottom of exterior wall; (d) bottom corner of south-end interior; (e) north-end exterior corner view; and (f) north-end interior corner view.**

5.2.3 Specimen A-3: 0.0% to 1.4% Drift Ratio Level

The photographs in Figure 5.5 show the initial state of Specimen A-3 prior to testing. Specimen A-3 has a C-shape configuration, which extended the corner finishes from 6 in. for Specimen A-2 to 30 in for Specimen A-3. The triple top plate and furring nail arrangement remained the same as in the previous test. The stucco on the exterior face is outboard of the foundation, while the sheathing boards bear on the foundation. For the return walls, both the stucco and sheathing boards bear on the foundation; see Figure 5.5(c). Two anchor bolts were added to each return wall section.

Figure 5.6(a) to (f) show the damage state of Specimen A-3 at 1.4% drift amplitude. At this drift level, no cracks had yet formed on the exterior face of the stucco besides a small crack running diagonally from the top of the cripple wall to the corner on the north. Many cracks started propagating vertically at the corners; see Figure 5.6(d) and (e). Similar to the previous specimen, these cracks started at the 0.2% drift amplitude and continued to extend in subsequent cycles of increased drift amplitude. Note: no cracks appeared on the face of either return walls. Figure 5.6(c) shows that stucco-to-foundation slip of 3/8 in. occurred, which is higher than the previous test; however, unlike the previous test, the slip of the sheathing relative to the framing did not occur. The continued reduction of relative displacement between the sheathing and framing is attributed to the presence of extended corners (end return walls), which offered additional resistance. This is demonstrated by the 50% reduction in slip. The return walls showed significant uplift and slight rotation in the studs; see Figure 5.6(d).

(a)

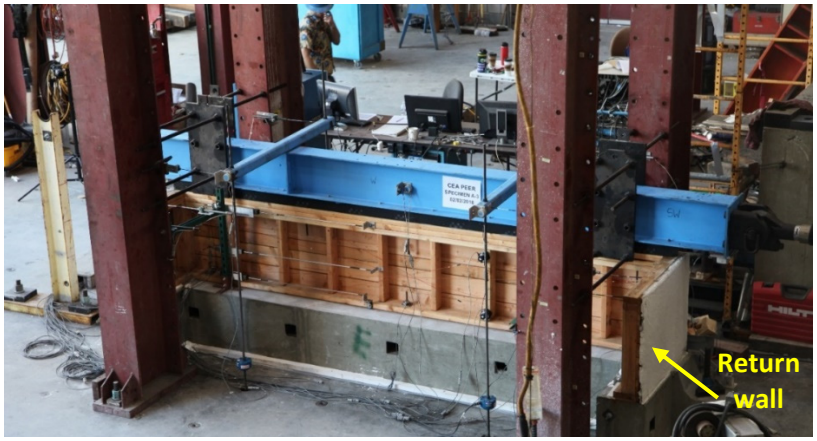

(b)

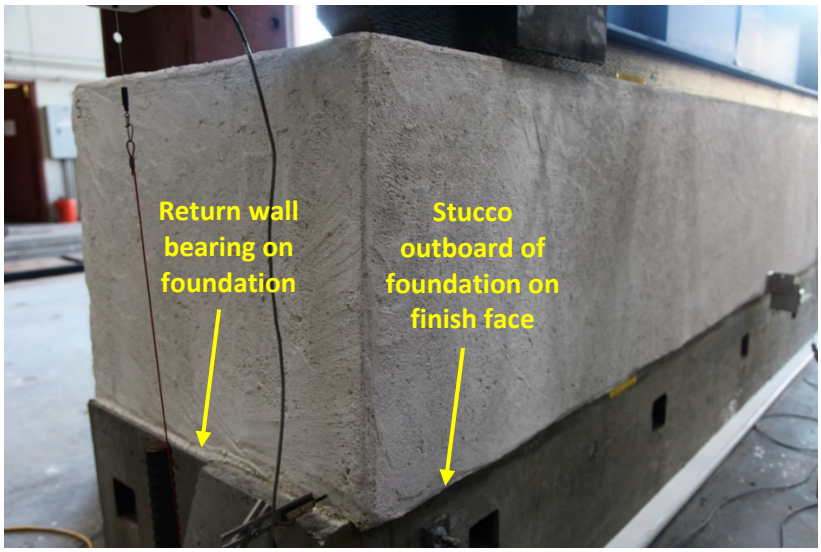

(c)

Figure 5.5 **Specimen A-3 pre-test photographs with existing top boundary condition C and bottom boundary condition "a": (a) exterior elevation of cripple wall; (b) isometric view of interior cripple wall; and (c) isometric view of south-end return wall.**

(a)

(b)

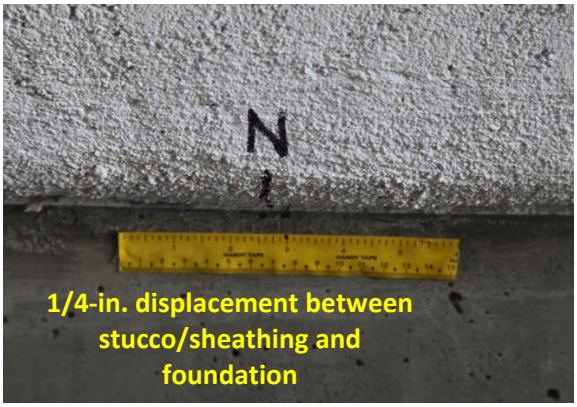

(c)

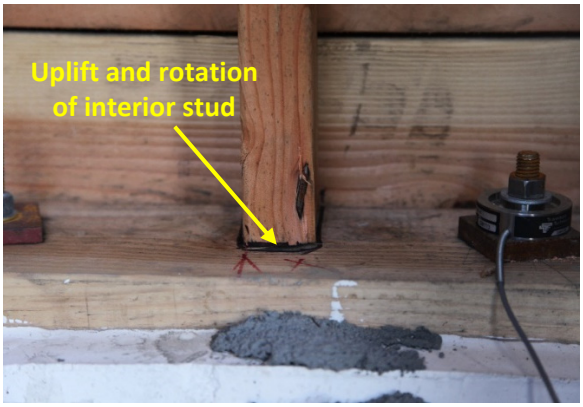

(d)

(e)

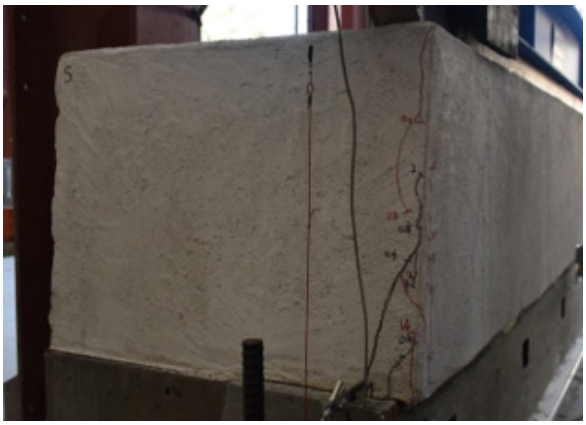

(f)

Figure 5.6 Specimen A-3 damage state at -1.4% drift @ Δ = -0.336 in.: (a) exterior elevation; (b) top of the exterior wall; (c) bottom of exterior wall; (d) bottom of interior wall; (e) north-end of exterior corner; and (f) south-end of exterior corner.

5.2.4 Specimen A-4: 0.0% to 1.4% Drift Ratio Level

Photographs in Figure 5.7 show the initial state of Specimen A-4 prior to testing. Specimen A-4 has the same construction details as Specimen A-2; however, the location of the cripple wall is centered on the middle of the foundation. Denoted as bottom boundary condition “b”, both the stucco finish and the horizontal sheathing boards bore down on the foundation. While this condition is not as common in the California housing stock where the stucco finish runs outboard of the foundation, the bearing of the stucco was expected to cause significant differences in the response and visual damage of the cripple wall.

Figure 5.8(a) to (f) show the damage of Specimen A-4 at 1.4% drift amplitude. At this drift level, cracks had started to propagate vertically on the exterior face of the stucco; see Figure 5.8(a). As with the two previous specimens, significant cracking occurred, concentrated around the corners of the wall. The response of Specimen A-4 varied slightly, which showed greater vertical and diagonal cracking on the corner faces compared to the previous two cripple walls. Even at this low drift amplitude, 1/8 in. of uplift was experienced at the end of cripple wall; see Figure 5.8(d).

Across the entire wall, the seal between the stucco and foundation had broken, and a gap had begun to form at the base of the wall. On the interior, there was uplift of the studs but no visible rotation of the studs. This is due to the entire wall bearing on the foundation and thus resisting movement more evenly than the cripple walls, which had no bearing resistance from the stucco due to it being outboard of the foundation. As with the all specimens tested, there was a 1/4-in. slip between the stucco and the foundation at the base of the wall. Different from the previous specimens was the relative slipping that occurred at the top of the cripple wall. As shown in Figure 5.8(b), there was insignificant slip between the sheathing and framing, which was present in previous tests but was typically less than 1/8 in.; this was the first instance that showed slip between the stucco finish and the horizontal sheathing. Again, this is due to the stucco finish bearing down on the foundation. As the cripple wall displaced, the bearing caused the furring nails to rotate and pull away from the sheathing boards, leading to a relative slip between the stucco and sheathing.

(a)

(b)

(c)

(d)

Figure 5.7 Specimen A-4 pre-test photographs with existing top boundary condition C and bottom boundary condition "b": (a) isometric view of cripple wall exterior face; (b) interior elevation of cripple wall; (c) north-end exterior corner view; and (d) north-end interior corner view.

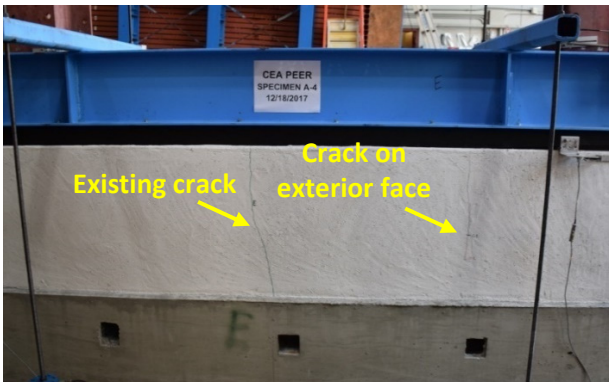

(a)

(b)

(c)

(d)

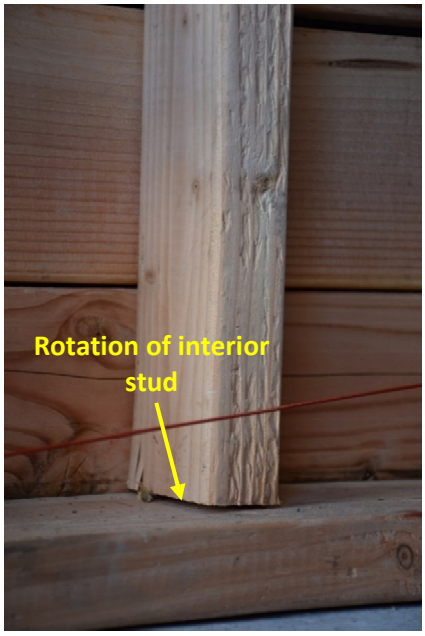

(e)

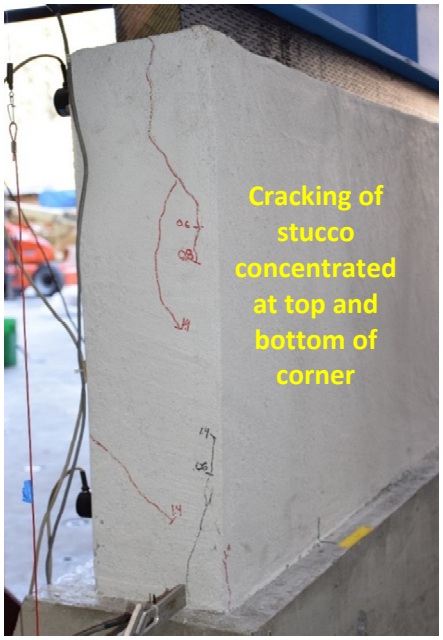

(f)

Figure 5.8 Specimen A-4 damage state at -1.4% drift (Δ = -0.336 in.): (a) exterior elevation; (b) top of exterior wall; (c) bottom of exterior wall; (d) bottom of north-end exterior corner; (e) bottom of interior wall; and (f) north-end of exterior corner.

5.2.5 Specimen A-5: 0.0% to 1.4% Drift Ratio Level

Photographs in Figure 5.9 show the initial state of Specimen A-5 prior to testing. Specimen A-5 has the same boundary conditions as the Specimen A-2 but was retrofitted. The retrofit consisted of 100% bracing of 15/32-in. plywood panels. Each panel was 4 ft long and ran from the sill plate to the top of the middle top plate. As described in Chapter 3, additional studs and blocking were placed on the interior of the cripple wall to allow for connection of the plywood panels. The plywood was connected with 8d common hot-dipped galvanized nails at 4 in. on center over the edge and 12 in. on center over the field. In addition, two anchor bolts were added to decrease the spacing from the typical 64 in. on center, as is with the previous cripple walls, to 32 in. on center. The retrofit detail conforms to the ATC-110 design guidelines. As shown in Figure 5.9(a), a vertical crack had formed along the face of the stucco prior to testing, and that ~one-fourth of the nails were slightly overdriven between 1/16 and 1/8 in.; see Figure 5.9(e).

Figure 5.10(a) to (f) shows the damage state of Specimen A-5 at 1.4% drift amplitude. At this drift level, no additional cracks formed on the face of stucco. There was a large reduction in the amount of cracking at the corners of the cripple wall compared to Specimens A-2 through A-4; see Figure 5.10(f). This could be because much of the work resisting displacement was due to the retrofit strategy instead of the finish materials bearing on the foundation at both ends of the specimen, as was the case with Specimen A-2. As with Specimen A-2, there was a 1/4-in. slip between the stucco and the foundation, as well as disconnect between the stucco and the foundation at the base of the cripple wall. At the top of the cripple wall, a 3/16-in. displacement between the sheathing and framing formed, which is the largest seen in any of the previous tests. This is due to the framing members being significantly stiffened by the attachment of the plywood panels on the interior face. On the interior face, small slips between the plywood panels had started to form as the plywood panels began to rotate. The 1/8-in. gap between abutting plywood panels remained; therefore, the wood structural panels had not yet begun to bear down on each other. Figure 5.10(e) shows that some of the nails were slightly overdriven and had started to pull through the plywood. For the other nails that attached the plywood to framing, minimal rotation or pulling through was visible at this drift level.

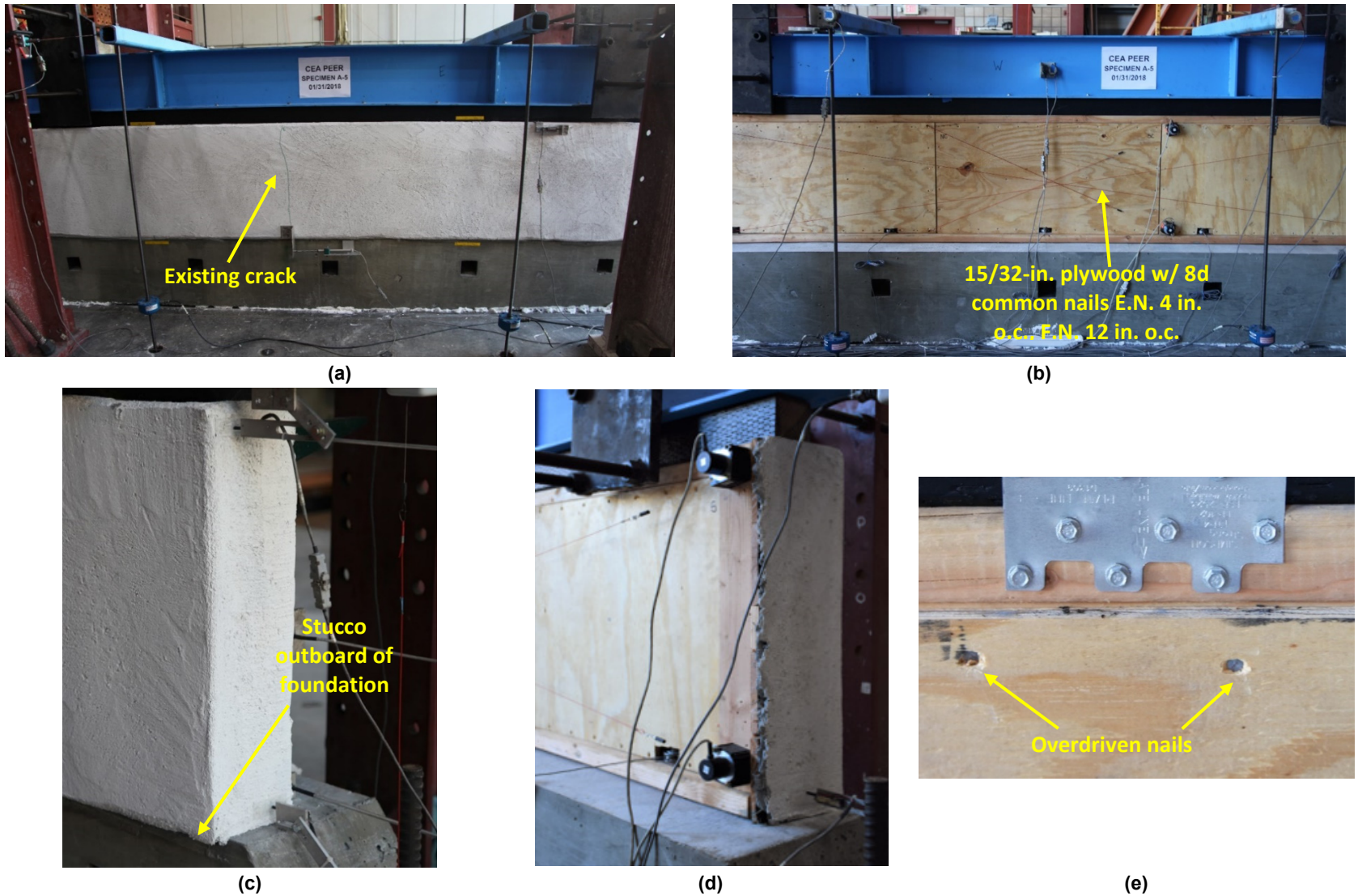

Figure 5.9 Specimen A-5 (retrofitted) pre-test photographs with top boundary condition B and bottom boundary condition "a": (a) exterior elevation; (b) interior elevation; (c) exterior north-end corner view; (d) interior north-end corner view; and (e) close-up of plywood nailing at top of wall.

(a)

(b)

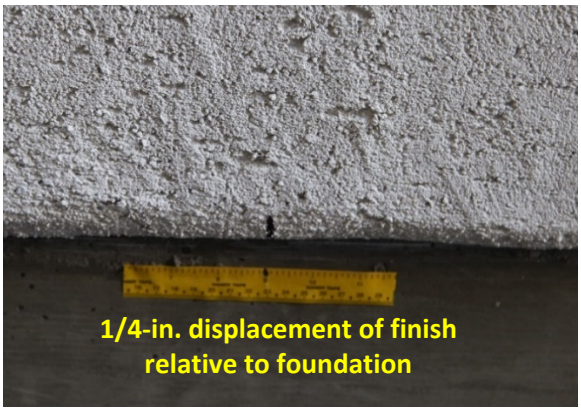

(c)

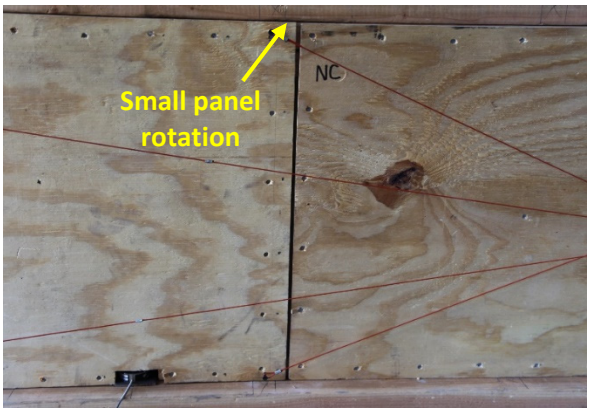

(d)

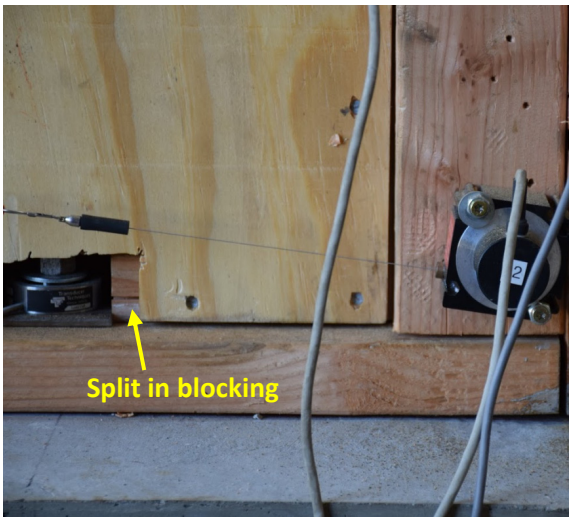

(e)

(f)

Figure 5.10 Specimen A-5 damage state at +1.4% drift @ Δ = +0.336 in.: (a) exterior elevation; (b) top of exterior wall; (c) bottom of exterior wall; (d) plywood panel joint; (e) close-up of top of the south-end interior wall; and (f) north-end exterior corner.

5.3.6 Specimen A-6: 0.0% to 1.4% Drift Ratio Level

The photographs in Figure 5.11 show the initial state of Specimen A-6 prior to testing, which has the same boundary conditions as Specimen A-4 but with the addition of a wet set sill plate. The wet set sill plate is a nominal 2 × 6, construction-grade redwood member, which is different from the #2 Douglas Fir sill plates used in all other cripple walls. As described in Chapter 3, the wet set sill plate was embedded 1 in. into the center of the foundation when the foundation was being cast; see Figure 5.11(c). Because of this embedment, there remained only 1/2 in. of sill plate to attach the furring nails into, whereas the furring nails would typically be driven into the center of the 1-1/2 in. sill plates as was done with other specimens. All finish material bore down on the top of the foundation.

Figure 5.12(a) to (f) show the damage state of Specimen A-5 at 1.4% drift amplitude. At this drift level, extensive cracking had begun to form on the face of the stucco. These cracks started as early as 0.4% drift and continued to propagate vertically along the face of the stucco. These cracks began both at the top and the bottom of the cripple wall but eventually would run vertically across the entire cripple wall face as drift amplitudes increased. As was found for Specimen A-4, a 1/4-in. slip occurred between the base of the stucco and the foundation; unlike Specimen A-4, there was less slip between the sheathing and the stucco and no slip between the stucco finish and the sheathing.

The increased presence of surface stucco cracks and lack of displacement between the stucco and sheathing are due to the inability for the wet set sill plate to slip. At this drift amplitude, the sill plate of Specimen A-4 had displaced 1/10 in. relative to its foundation. With a wet set sill, an appreciable resistance to sliding is created, thus the imposed lateral displacements propagated in the form of more extensive cracking on the stucco face. Figure 5.12(e) and (f) show that single vertical cracks had formed at the bottom corners of the cripple wall. The reduction in corner cracks between this Specimens A-4 and A-6 is again due to the lack of sill slip. As with Specimen A-4, the stucco finish bearing condition caused an 1/8-in. uplift on the corner of the wall and separated the connection between the base of the stucco and top of the foundation.

(a)

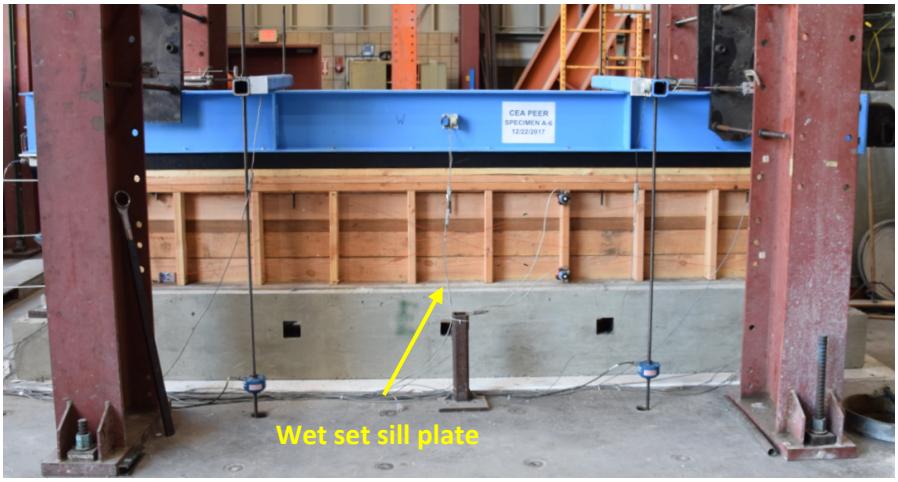

(b)

(c)

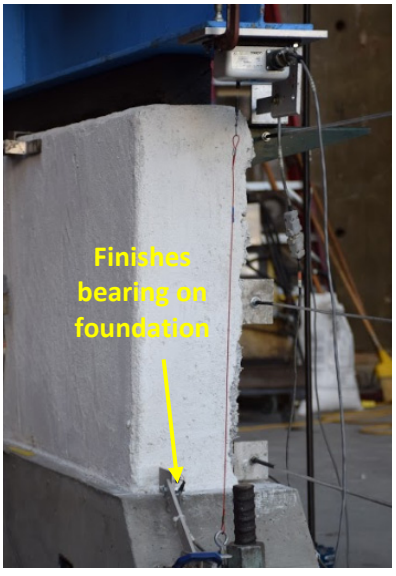

(d)

Figure 5.11 **Specimen A-6 (wet set sill plate) pre-test photographs with top boundary condition B and bottom boundary condition "b": (a) exterior elevation; (b) interior elevation; (c) interior south-end corner view; and (d) interior north-end corner view.**

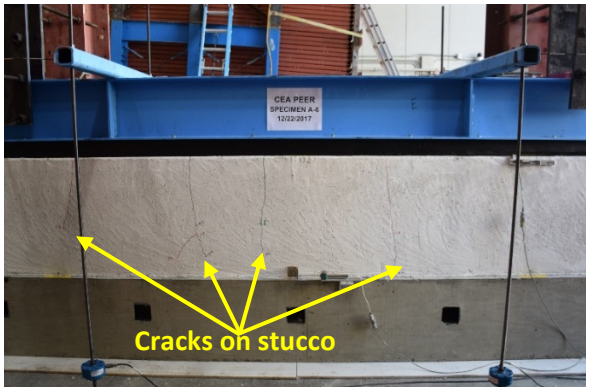

(a)

(b)

(c)

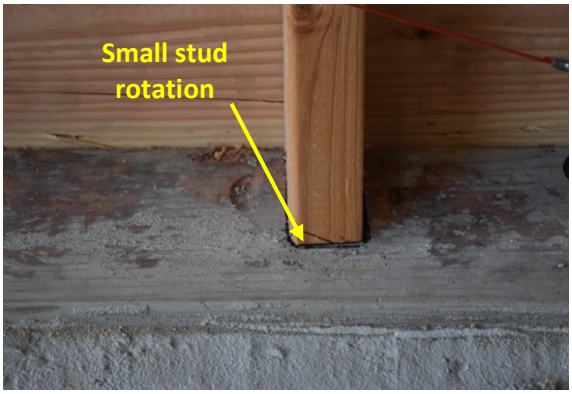

(d)

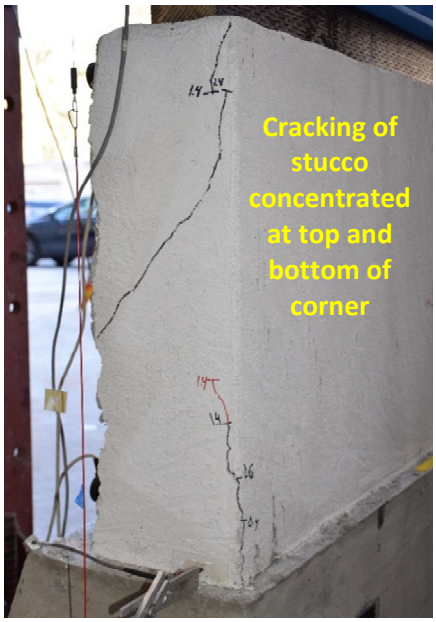

(e)

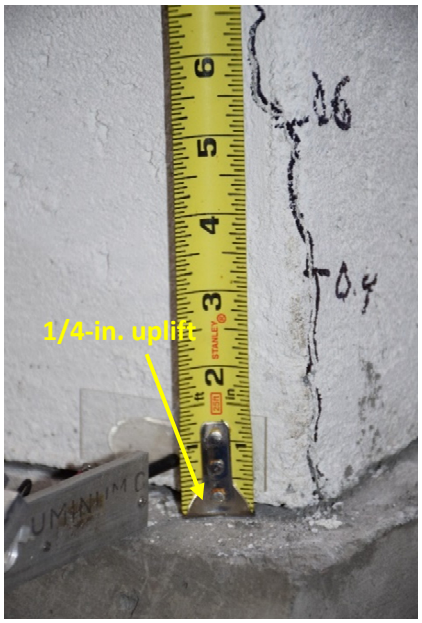

(f)

Figure 5.12 Specimen A-6 damage state at -1.4% drift (Δ = -0.336 in.): (a) exterior elevation; (b) top of exterior wall; (c) bottom of exterior wall; (d) close-up of stud; (e) south-end exterior corner; and (f) close-up of south-end exterior corner.

5.4 DAMAGE CHARACTERISTICS AT LATERAL STRENGTH

Beyond the low levels of drift, another key damage state occurs when the lateral strength of each cripple wall is reached. Thus, the damage features presented in this section occurred following attainment of the lateral strength of the cripple walls. Beyond this point, larger imposed drifts resulted in a loss of load capacity. By examining the damage states at this level, insight into how and why failure is occurring in a cripple wall is possible. Note: the lateral strength for the six cripple walls tested in Phase 1 occurred between global drift ratios of 3.0 to 5.0% and relative drift ratios of 2.0 to 4.3%. The relative drift is defined as the drift of the cripple wall only and does not include the displacement of the sill plate relative to the foundation.

5.4.1 Specimen A-1 Lateral Strength

Figure 5.13(a) to (f) show the damage state of Specimen A-1 at lateral strength, which occurred at 3% global and relative drift in both the push and pull directions. Due to its lower capacity, Specimen A-1 did not experience any sill slip relative to the foundation. At strength, there were still no visible cracks on the face of the stucco. Figure 5.13(e) shows a 3/16-in. separation between the stucco and sheathing. This occurred as the furring nails (a) began to detach from the framing and work their way out of the sheathing (nail withdrawal) and/or (b) the furring nails had detached from the stucco (nail head pullout). Nail withdrawal or nail head pullout is dependent on how well the furring nails were fastened to the metal reinforcement mesh and how well they were fastened to the sheathing. Whichever condition has the least capacity will occur first. Note: only 1/8 in. of the 1-1/2-in. furring nails would be driven into the framing; the nails are furred out 1/4 in. and penetrate through the 7/8 in.-thick horizontal sheathing. The slip between the base of the stucco and the foundation increased to 1/2 in., and a gap between the stucco and foundation face became more pronounced. Figure 5.13(f) shows that at the top of the cripple wall there was a 1/4-in. relative displacement between the stucco finish and the sheathing, as well as a 1/4-in. relative displacement between the sheathing and framing. In addition, a small gap opened up between the sheathing and framing, indicating that the small amount of embedment of the furring nails into the framing was gone. On the interior of the cripple walls, the uplift of the studs was more pronounced, while the rotation of the studs was similar to that experienced at the service-level drift. Some of the studs began splitting at both the connection to the sill plate and top plate. Lastly, cracks had begun to form on the ends of the sheathing boards and were concentrated near the location where the boards were nailed to the studs.

(a)

(b)

(c)

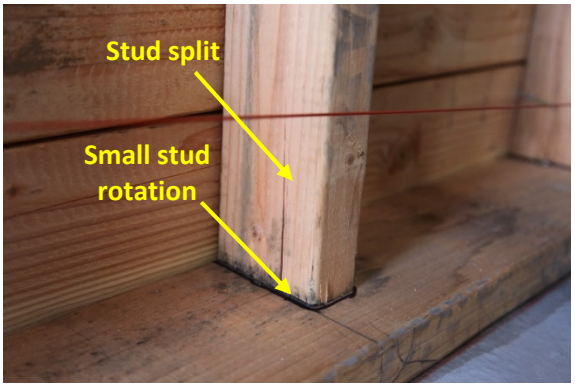

(d)

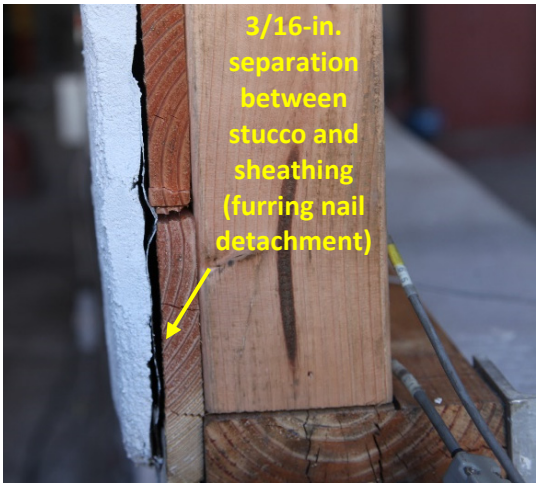

(e)

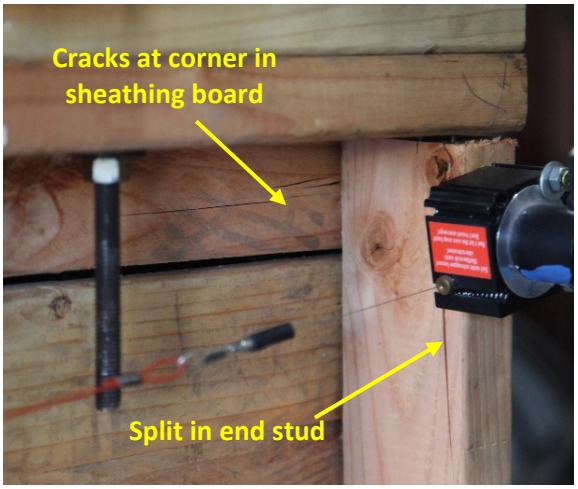

(f)

Figure 5.13 Specimen A-1 damage state at lateral strength @ +3% drift, Δ = +0.72 in.: (a) exterior elevation; (b) top of the exterior wall; (c) bottom of exterior wall; (d) close-up of stud; (e) north-end corner of wall; and (f) close-up of top of south-end interior corner.

5.4.2 Specimen A-2 Lateral Strength

Figure 5.14(a) to (f) show the damage state of Specimen A-2 at lateral strength. The lateral strength occurred at 5% global drift in the push loading direction and 4% in the pull loading direction. The subsequent relative drift was 4.3% in the push direction and 3.1% in the pull direction. At peak strength, additional vertical cracks began propagating along the face of the stucco. The formation of a 1/2-in. gap formed at the base of the stucco; see Figure 3.14(c) and (e). At this point, although the stucco had detached from the furring nails at the base, in some cases the furring nails remained attached to the stucco, but as expected they had pulled out significantly from the sheathing. This same gap is not evident at the top of the cripple wall because of the increased pullout resistance due to the significantly denser furring nail arrangement on the upper top plates. The displacement of the stucco at the base and the foundation increased to 7/8 in., while the only apparent relative displacement at the top of the cripple wall was 1/4-in. displacement between the stucco and sheathing; see Figure 5.14(d). This is due to the rotation of the furring nails at the top of the wall. At the exterior corners, major cracking ran in all directions and was heavily concentrated at the corner edge. Crushing and spalling of the stucco was extensive at the corner faces due to the heavy bearing sown of the stucco finish on the foundation. On the interior face, some of the studs split at the connection to the sill plate. In addition, a slight lateral movement occurred on the studs. This lateral movement can be attributed to the horizontal sheathing and stucco finish moving out laterally. The cause of this lateral movement is due to the nails being pulled out as they rotate back and forward during each cycle.

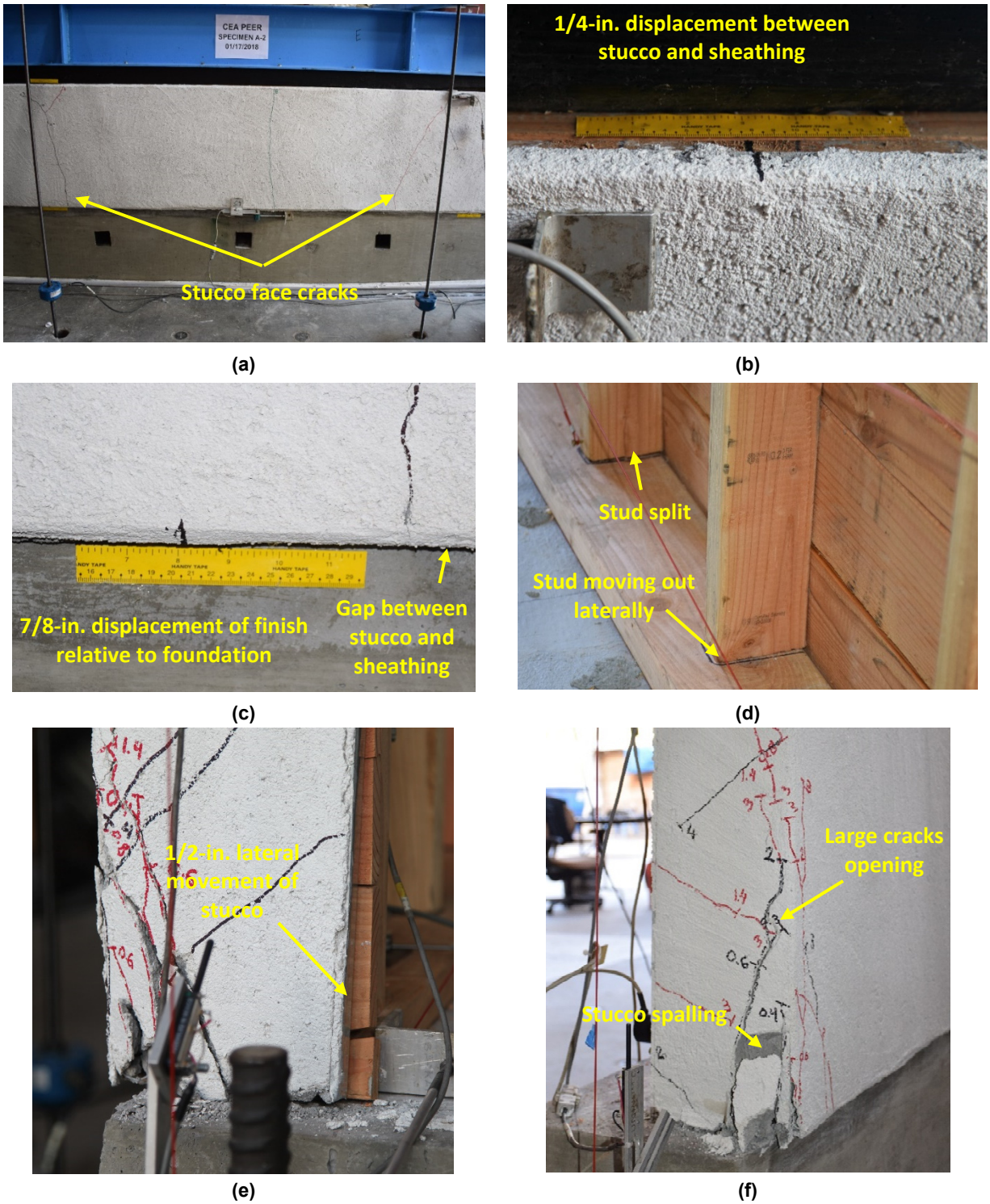

Figure 5.14 Specimen A-2 damage state at lateral strength @-4% drift, Δ = -0.96 in.: (a) exterior elevation; (b) top of exterior wall; (c) bottom of exterior wall; (d) close-up of studs; (e) close-up of north-end corner; and (f) close-up of bottom south-end exterior corner.

5.4.3 Specimen A-3 Lateral Strength

Figure 5.15(a) to (f) show the damage state of Specimen A-3 at lateral strength. The lateral strength occurred at 4% global drift in the push loading direction and 3% in the pull loading direction. The subsequent relative drift was 2.9% in the push direction and 2.0% in the pull direction. At peak strength, cracks propagated vertically along the face of the stucco. As seen in Figure 5.15(c), the displacement between the base of the stucco and the foundation had increased to 1 in., and a large gap formed between the stucco and the foundation face, meaning that the furring nails were completely detached from the stucco along bottom of the stucco face. At the corners, this is further demonstrated by the large cracks running vertically from the base of the stucco. In addition to the vertical cracks at the corners, diagonal cracks formed and propagated along the face of the return walls. At the top of the cripple wall, the displacement between the sheathing and framing remained static, and there was no evidence of displacement between the stucco and sheathing. This is both due to (a) the dense furring nail arrangement on the upper top plates and (b) the extended corner return walls resisting these relative displacements. As shown in Figure 5.15(e), a gap formed at the base of the return walls as the furring nails began detaching from the stucco. On the interior of the wall, a more pronounced uplift of the studs occurred. Again, some of the studs split near the connection to the sill plate [see Figure 5.15(b)], and splitting occurred in the south return wall sill plate due to the rocking motion of the return walls during cyclic loading.

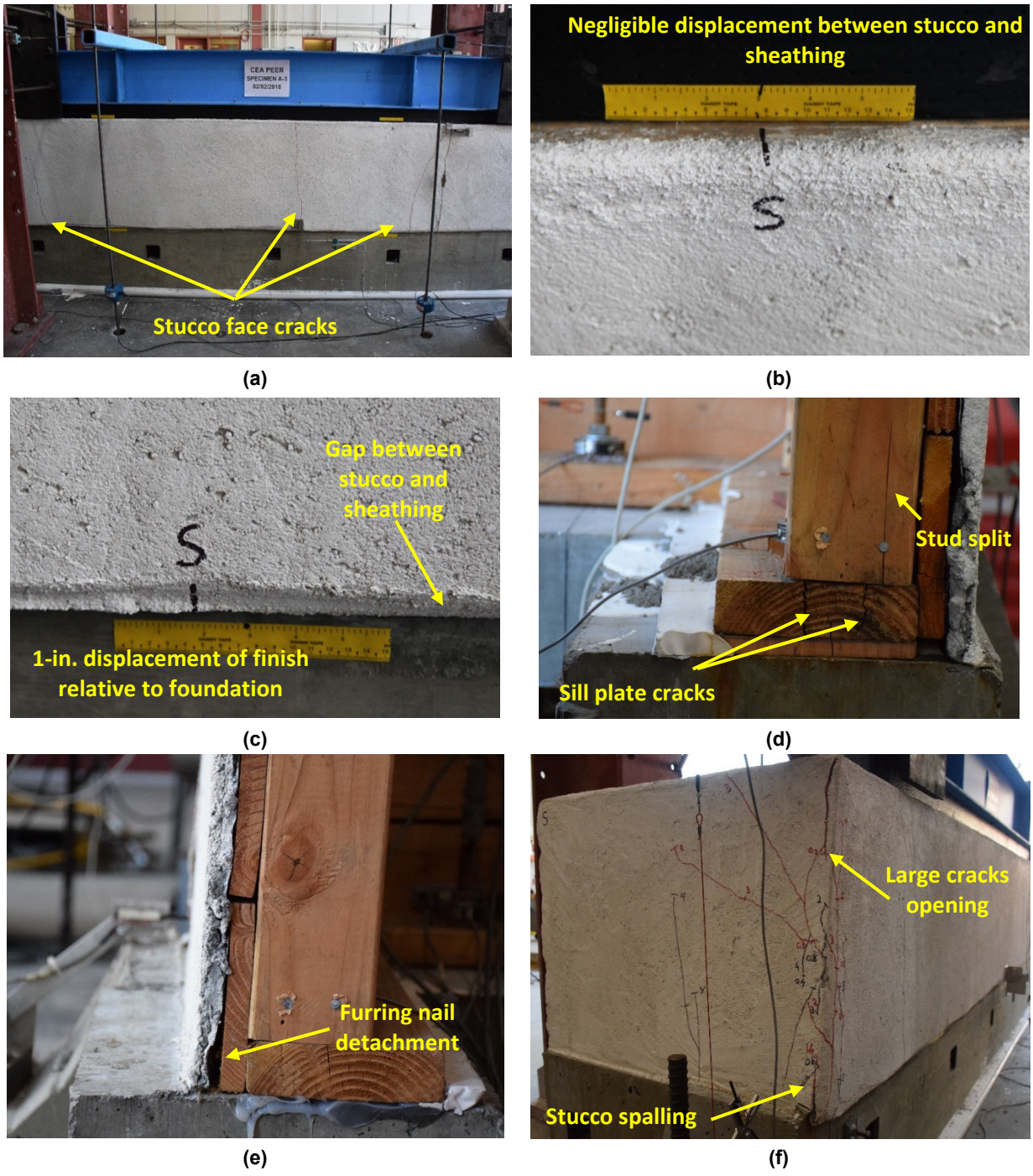

Figure 5.15 Specimen A-3 damage state at lateral strength @ +4% drift, Δ = +0.96: (a) exterior elevation; (b) top of exterior wall (c) bottom of exterior wall; (d) close-up of south-end wall; (e) close-up of north-end corner of wall; and (f) north-end exterior corner.

5.4.4 Specimen A-4 Lateral Strength

Figure 5.16(a) to (f) show the damage state of Specimen A-4 at lateral strength. The lateral strength occurred at 5% global drift in the push loading direction and 5% in the pull loading direction. The subsequent relative drift was 3.9% in the push direction and 3.5% in the pull direction. At the peak strength, an additional crack in the stucco formed, running from the top of the cripple wall to the base. The displacement between the base of the stucco and the foundation increased to 3/4 in. Figure 5.16(e) shows that large cracks had opened up near the bottom at the corner of the wall, indicating that the stucco was moving out laterally away from the sheathing, which is supported by noting that the furring nails became detached from the stucco at the base of the wall. Because the stucco was bearing on the foundation, the rotation was inhibited (unlike the previous specimens). This led to an increased capacity of the cripple wall and drift at peak because the separation between the stucco finish and the sheathing occurred as a lateral movement of the stucco away from the sheathing or an uplift of the stucco. The stucco nails detached primarily from the metal reinforcement in the stucco but more readily than the previous tests; many of the furring nails pulled away from the sheathing boards. At the top of the cripple wall, a 1/4-in. slip occurred between the stucco and the sheathing, and a 1/4-in. slip occurred between the sheathing and framing. Both the nails in the sheathing and the furring nails exhibited significant rotations, leading to these displacements. Figure 5.16(f) shows that at the exterior on the corners, extensive cracking occurred both vertically and diagonally. In addition, significant crushing and spalling of the stucco was evident on the corner faces. On the interior, the uplift of the studs was more pronounced, and there was no visible rotation of the studs.

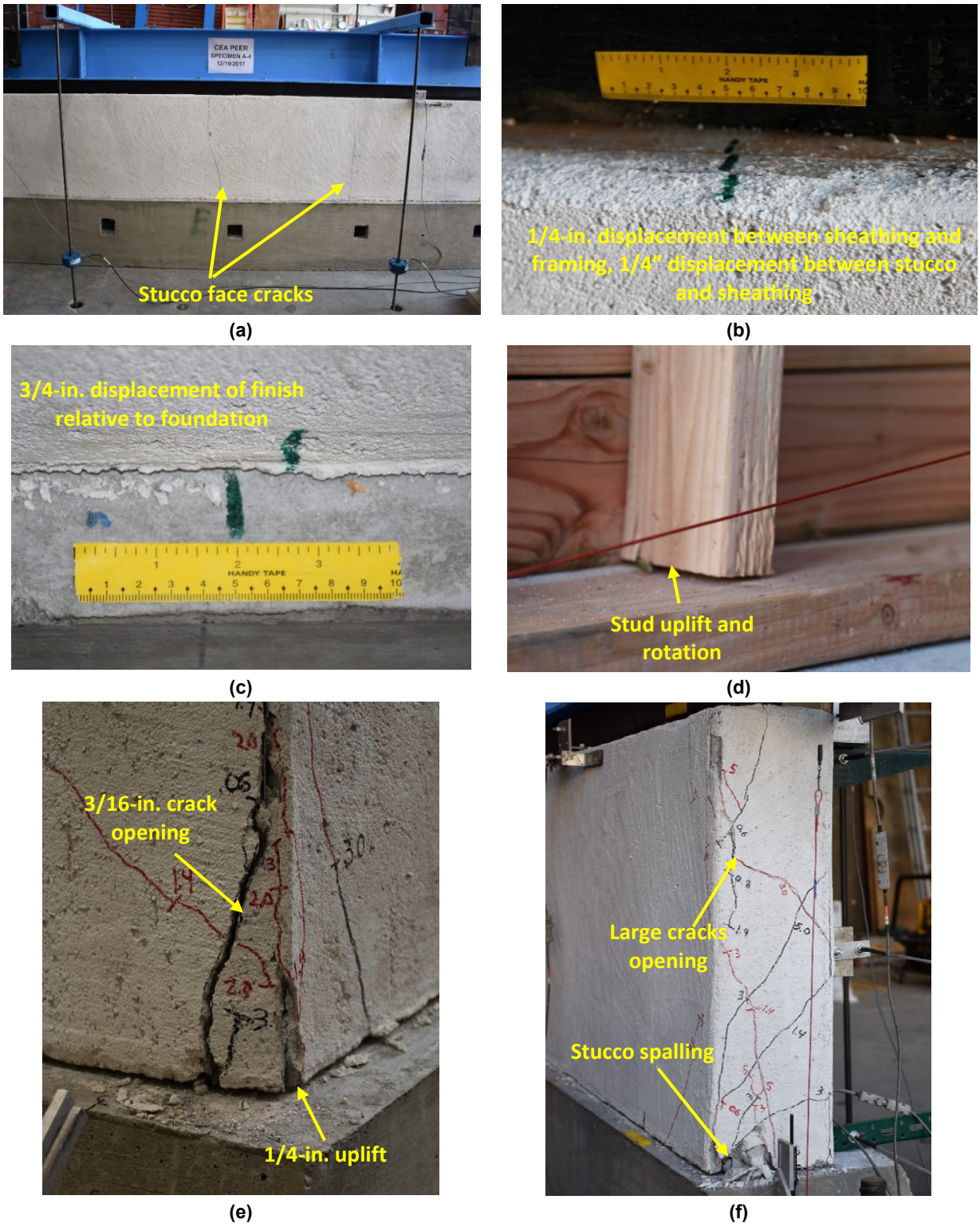

Figure 5.16 Specimen A-4 damage state at lateral strength @-5% drift, Δ = -1.20 in.: (a) exterior elevation; (b) top of exterior wall; (c) bottom of exterior wall; (d) close-up of stud; (e) close-up of exterior south-end corner; and (f) north-end exterior corner.

5.4.5 Specimen A-5 Lateral Strength

Figure 5.17(a) to (f) show the damage state of Specimen A-5 at lateral strength. The lateral strength occurred at 5% global drift in the push loading direction and 5% in the pull loading direction. The subsequent relative drift was 3.6% in the push direction and 2.8% in the pull direction. At strength, multiple cracks began propagating vertically from across the entire face of the stucco. The slip between the stucco base and the foundation increased to almost 5/8 in., which is around half of total displacement imposed on the wall. Again, this correlated to a complete detachment of stucco from the sheathing at the base of the wall. Most of this detachment came in the form of the furring nails detaching from the metal reinforcement in the stucco. As shown in Figure 5.17(e), significant uplift (3/8 in.) occurred at the ends of the cripple walls. The uplift exhibited here is the first to occur with bottom boundary condition "c" and can be attributed to strength of the connecting plywood panels, causing the sill plate to bend. At the top of the cripple wall, there was a 3/16-in. relative displacement between the sheathing and the framing, which is due to the increased stiffness of the framing from the plywood attachment resisting displacement.

Figure 5.17(f) shows the damage state of the interior at the corner. Uplift of the corner studs, uplift of the sill plate, splitting of the added blocking that the plywood is nailed to, and pulling through of the nails attaching the plywood panels to the blocking are all evident. In addition, the slip between the plywood panels is more pronounced as the panel rotations increased. All nails on the plywood panels began to either pull out or pull through. Any nail that was slightly overdriven fell into the latter category; the other nails fall into both categories. The majority of nails pulling out were located at the base where they caused the blocking to split, thus freeing the nails. Both the pulling out and pulling through of the nails is attributed to the back and forward rotation of the nails during each cycle.

Figure 5.17 **Specimen A-5 damage state at lateral strength @ +5% drift, Δ = +1.20 in.: (a) exterior elevation; (b) top of exterior wall; (c) bottom of exterior wall; (d) close-up of plywood panel joint; (e) close-up of south-end exterior corner; and (d) bottom of south-end interior wall corner.**

5.4.6 Specimen A-6 Lateral Strength

Figure 5.18(a) to (f) show the damage state of Specimen A-6 at lateral strength. The lateral strength occurred at 3% global drift in both the push and pull directions. The subsequent relative drift was 3% in the push loading direction and 3% in the pull loading direction. Because of the wet set sill condition, slip never occurred between the sill plate and the foundation. At peak strength, some

additional cracks formed on the face of the stucco, but many cracks were apparent at the service-level drift. At the base of the stucco, the displacement between the stucco and the foundation increased to 3/4 in., which is equal to the entire imposed displacement. As with previous cripple walls, this indicated that the stucco and sheathing had detached from one another; see Figure 5.18(c). Not only is the slip apparent, but it can be seen that the stucco is slightly uplifted from the foundation, and the distance between the stucco face and the measuring tape began to shrink. The displacement between the stucco and sheathing at the top of the cripple wall was 1/4 in., and a 1/4-in. displacement between the sheathing and the framing occurred as well. This is the same amount of displacement as seen in Specimen A-4, which had a similar bottom boundary condition.

Gaps also formed at the two interfaces because of the inhibited rotation of the stucco. Due to the stucco-bearing condition, the movement of the stucco finish was positioned laterally away from the sheathing and uplifting at the corners. At peak strength, the uplift was as much as 3/8 in. at the corners; see Figure 5.18(e). With the stucco uplift on one side, there was subsequent crushing and spalling of the stucco on the opposite side. Cracks formed on the stucco in every direction on the corner faces. On the interior face, the wet set sill plate remained completely intact. Large cracks formed in the studs where the single 8d nails were toe-nailed from the stud into the sill plate. In addition, slight rotation in the studs became apparent, which was due to the lack of symmetry in the toenailing of the studs into the sill plate.

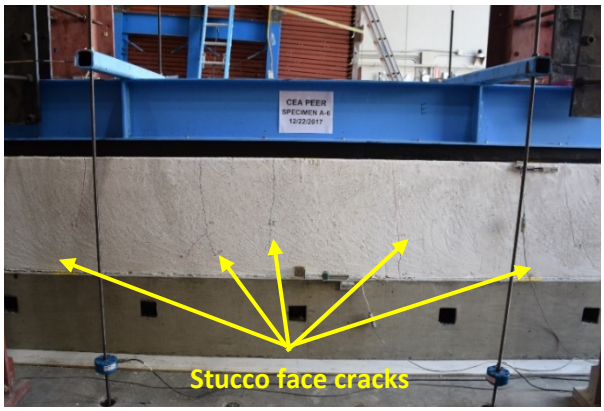

(a)

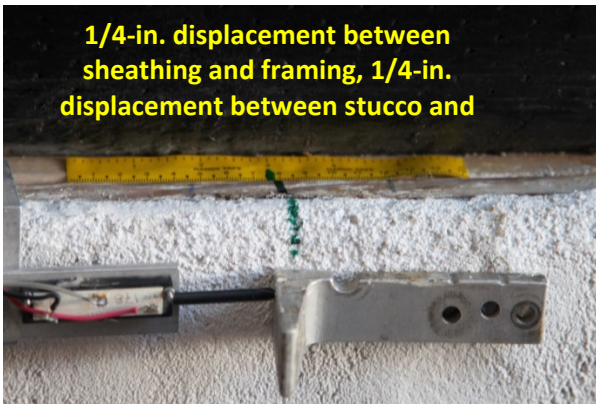

(b)

(c)

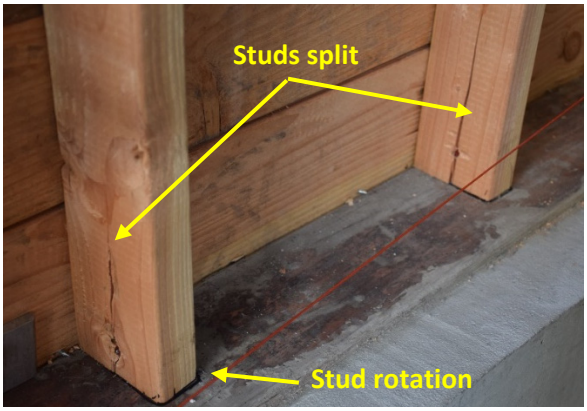

(d)

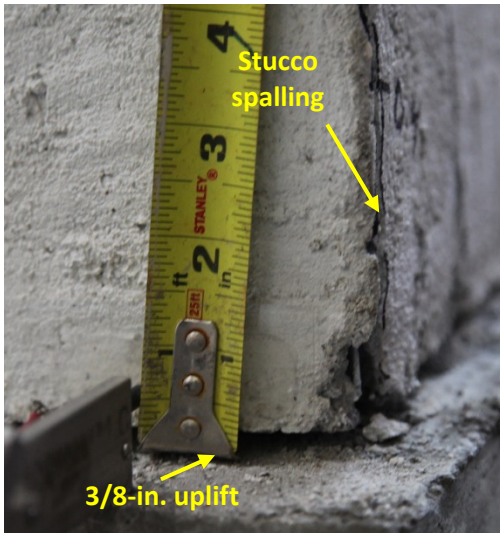

(e)

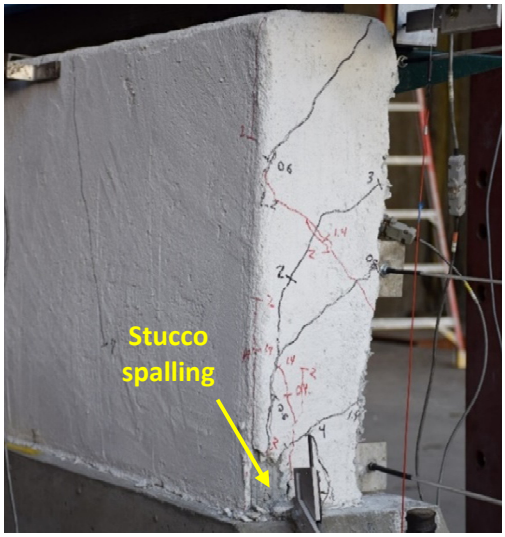

(f)

Figure 5.18 Specimen A-6 damage state at lateral strength @ +3% drift, Δ = +0.72 in.: (a) exterior elevation; (b) top of exterior wall; (c) bottom of exterior wall; (d) close-up of studs and sill plate; (e) close-up of south-end of exterior corner; and (f) north-end exterior corner.

5.5 POST-PEAK DAMAGE CHARACTERISTICS

The damage state at 20% residual strength or an 80% drop below lateral strength offers some insight into the incipient failure mode of the wall. Note: not all of the cripple walls dropped 80% in peak strength, which will be addressed below. When an 80% loss of strength in the cripple wall occurred, the loading protocol called for a monotonic push to be imposed for the subsequent drift amplitude. At this point, sufficient post-peak strength and residual-strength characteristics have been defined for the wall.

5.5.1 Specimen A-1 Post-Peak Performance

Figure 5.19(a) to (d) shows the damage state of Specimen A-1 at +12% drift. The damage state at 12% correlates closer to a 60% drop in peak strength as opposed to an 80% drop in lateral strength. At this stage, the stucco was only connected to the top plate and top row of furring nails on the studs. From Figure 5.19(c) and (d), it is evident that almost all of the furring nails remained attached to the sheathing and pulled away the metal reinforcement in the stucco. The displacement between the stucco and sheathing at the top of the cripple wall was 1/4 in., and a 1/4-in. displacement between the sheathing and the framing occurred as well. In addition, pronounced gaps occurred at the interface of the stucco and sheathing, as well as sheathing and framing. At this point, the stucco provided negligible lateral resistance. The source of capacity was due to the stacking of the horizontal sheathing boards bearing on the foundation. As shown in Figure 5.19(c), the gaps between all but the top sheathing board had closed. Cracks formed on the corners of the sheathing boards where the nails were located. Figure 5.20 shows the cripple wall in its residual state at the end of testing after a 5.0-in. monotonic push. There was a residual displacement of 4.90 in. once the load was removed.

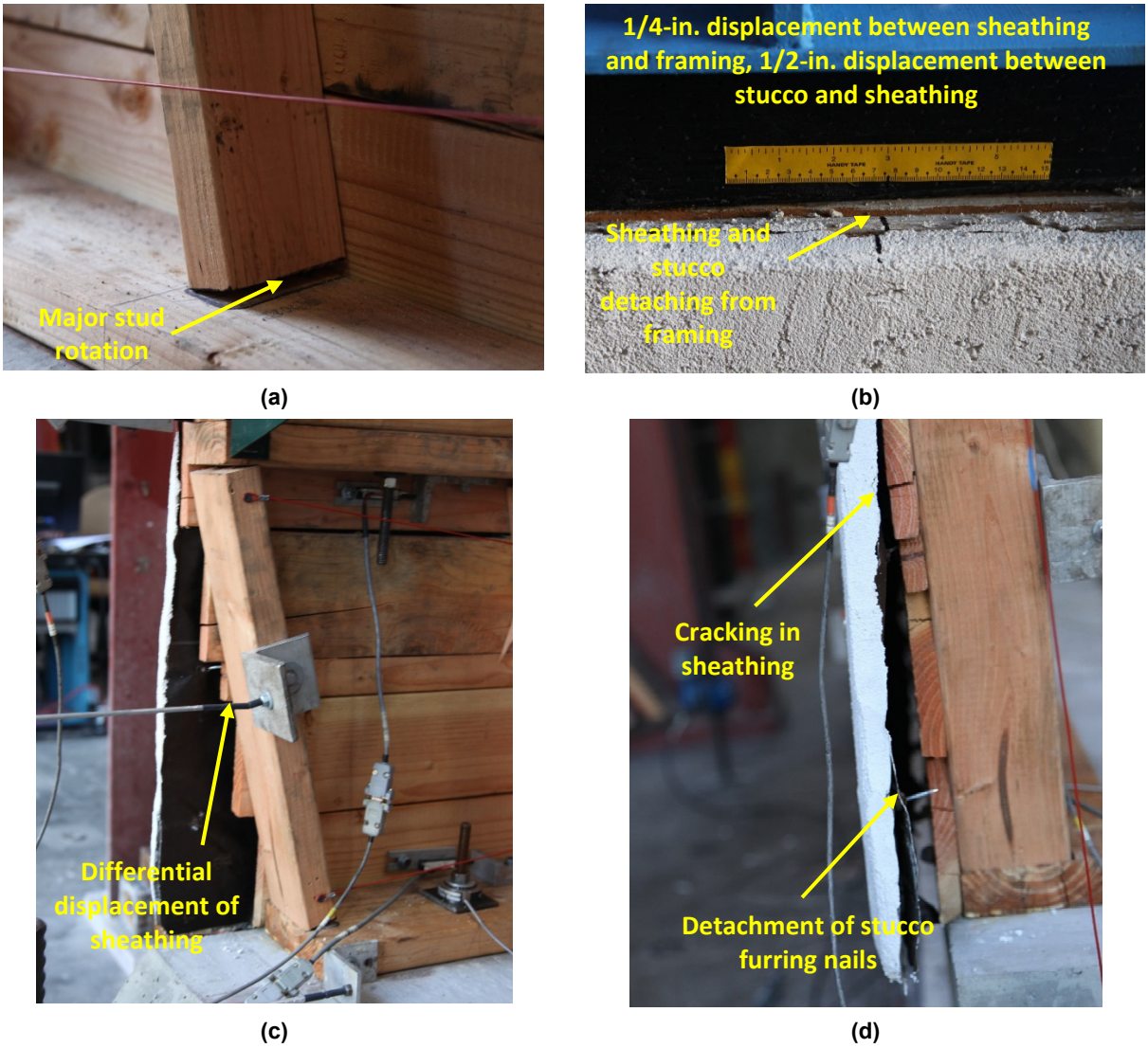

Figure 5.19 Specimen A-1 damage state at 60% post-peak reduction of lateral strength @ +12% drift, Δ = +2.88 in.: (a) close-up of studs and sill plate; (b) exterior top of the wall; (c) north-end interior corner; and (d) north-end bottom of corner.

(a)

(b)

(c)

(d)

Figure 5.20 **Specimen A-1 post-test photographs at lateral load = 0 kips, residual displacement = +4.90 in. @ +20.4% drift: (a) exterior elevation of cripple wall; (b) interior elevation of cripple wall; (c) north-end exterior corner view: and (d) south-end interior corner view.**

5.5.2 Specimen A-2 Post-Peak Performance

Figure 5.21(a) to (d) shows the damage state of Specimen A-2 at +12% drift. Specimen A-2 never exhibited an 80% drop in lateral strength. The damage state at 12% correlates closer to a 70% drop in peak strength. The stucco detached completely over the majority of the wall. The only attachment was at the dense furring nail arrangement at top. Figure 5.21(d) shows extensive movement of the stucco away from the sheathing at the base, as well as around a 1/4 in. of movement of the sheathing board away from the framing. Much of the stucco had spalled off of the corners, coming off in large chunks. Most of the sheathing boards on the corners split. A 3/8-in. gap formed between the top two sheathing boards, which was due to the top sheathing board being fastened to the top plates, while the other sheathing boards were attached to the studs. Like the other specimens, the capacity of the wall is attributed the sheathing boards stacking on each other and bearing on the foundation. Figure 5.22 shows the cripple wall in its residual state at the end of testing after a 4.5-in. monotonic push. There was a residual displacement of 3.45 in. once the load was removed.

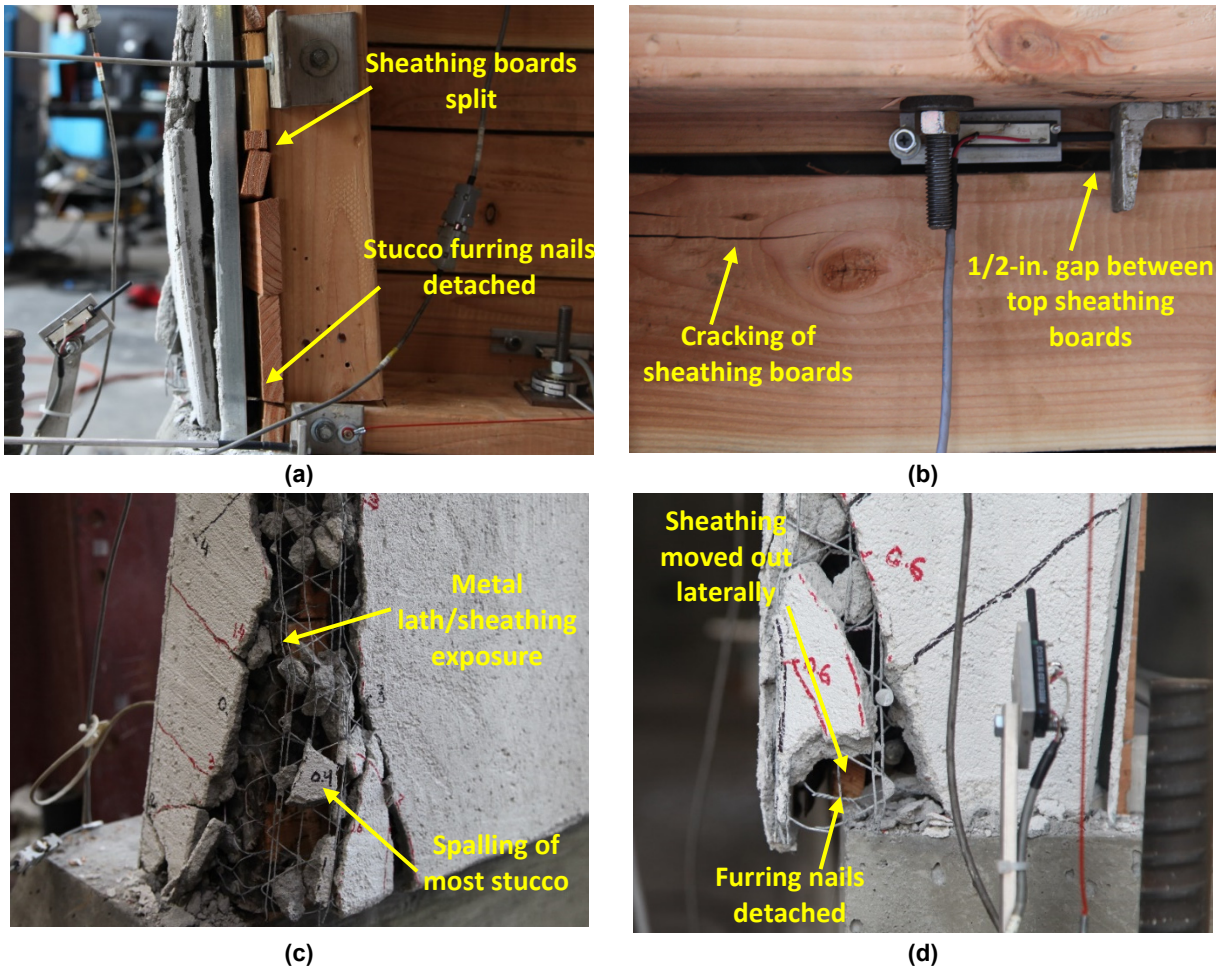

Figure 5.21 **Specimen A-2 damage state at 70% post-peak reduction of lateral strength @ +12% drift, Δ = +2.88 in.: (a) north-end of interior corner bottom; (b) close-up of top of interior wall; (c) south-end of exterior bottom corner; and (d) north-end of bottom corner.**

(a)

(b)

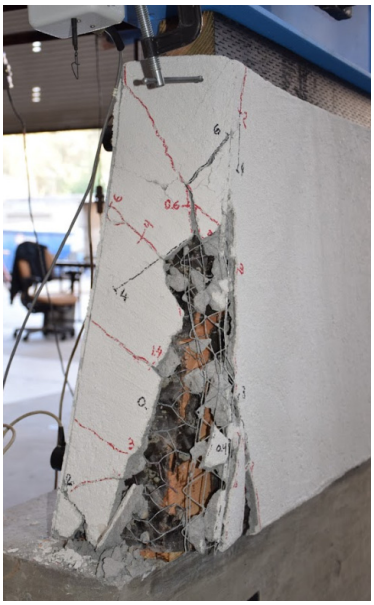

(c)

(d)

Figure 5.22 **Specimen A-2 post-test photographs at lateral load = 0 kips, residual displacement = +3.45 in @ +14.4% drift: (a) exterior elevation of cripple wall; (b) interior elevation of cripple wall; (c) south-end exterior corner view; and (d) north-end interior view.**

5.5.3 Specimen A-3 Post-Peak Performance

Figure 5.23(a) to (d) shows the damage state of Specimen A-3 at -12% drift; Specimen A-3 never exhibited an 80% drop in lateral strength. The damage state at 12% correlates closer to a 60% drop in peak strength. Extensive horizontal cracks propagated across the return walls, and a massive gap occurred between the return wall and stucco face. Again, the only attachment of the stucco on the face was to the top plates. The face stucco acted as a rigid body that provided little lateral resistance. Like Specimen A-2, the sheathing boards stacked on top of each other, providing the majority of the remaining strength in the wall. This stacking caused the sheathing nails to pull away from the framing; see Figure 5.23(d). The studs on the return walls rotated markedly; see Figure 5.23(b). Figure 5.24 shows the cripple wall in its residual state at the end of testing after a 5.0-in. monotonic push. There was a residual displacement of 4.51 in. once the load was removed.

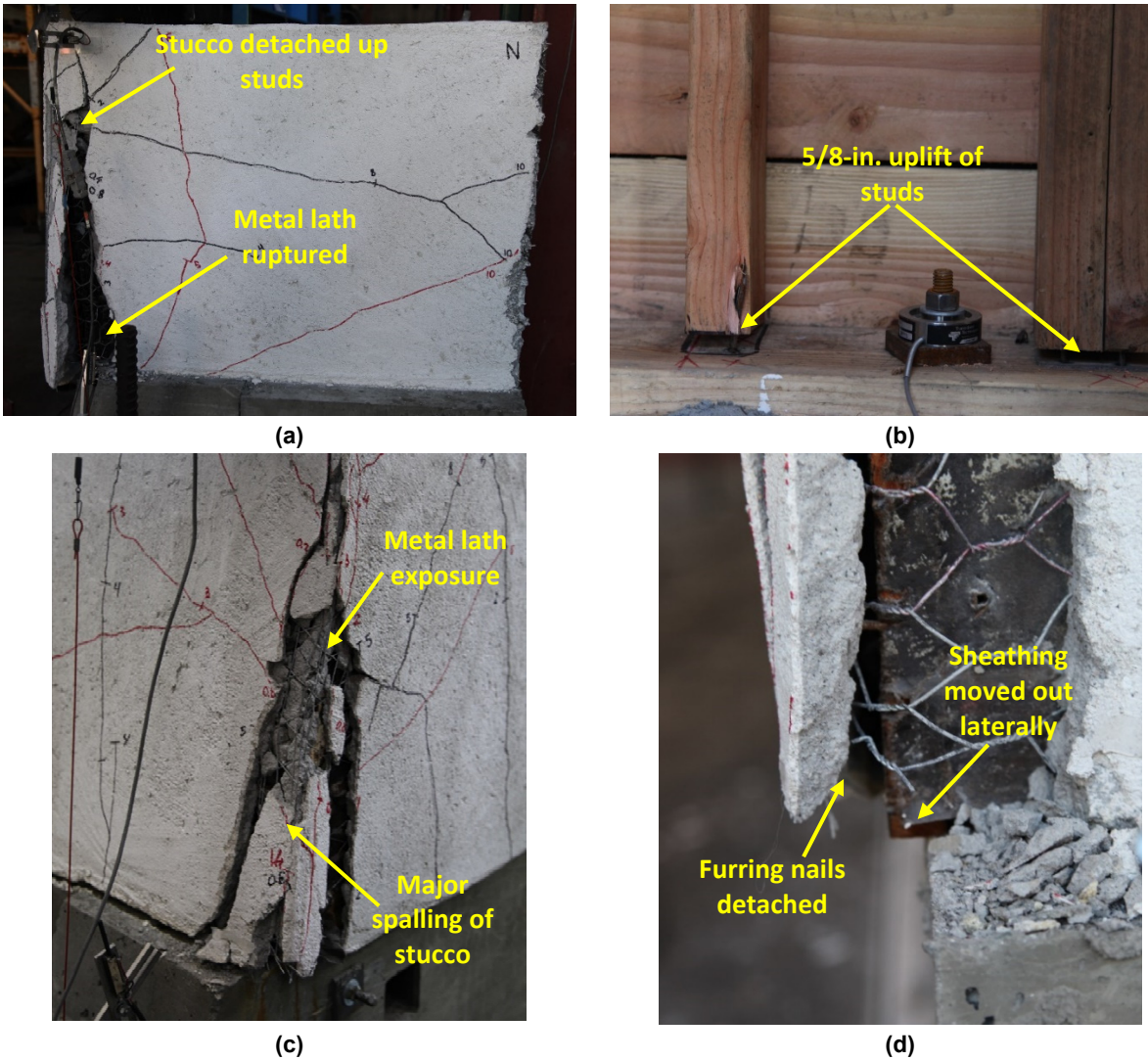

Figure 5.23 **Specimen A-3 damage state at 60% post-peak reduction of lateral strength @ -12% drift, Δ = -2.88 in.: (a) exterior view of north-end return wall; (b) interior of bottom of south-end return wall; (c) bottom of south-end exterior corner; and (d) bottom of north-end corner.**

(a)

(b)

(c)

(d)

Figure 5.24 **Specimen A-4 damage state at 80% post-peak reduction of lateral strength @-12% drift, Δ = -2.88 in.: (a) exterior elevation (b) bottom of north-end interior corner; (c) north-end exterior corner; and (d) top-down view of exterior.**

5.5.4 Specimen A-4 Post-Peak Performance

Figure 5.25(a) to (d) shows the damage state of Specimen A-4 at -12% drift. Specimen A-4 achieved an 80% loss of strength before the monotonic push was implemented. Because of the stucco-bearing condition, the stucco detached from both the bottom and top of the wall (unlike the previous three specimens); see Figure 5.25(c) and (d). At this point, the stucco provided almost no lateral resistance. In addition, there was a complete detachment of the stucco at the corners and splitting of many of the sheathing boards; see Figure 5.25(b). Like the previous three tests, the majority of the lateral resistance can be attributed to the bearing of the sheathing boards on the foundation. Figure 5.26 shows the cripple wall in its residual state at the end of testing after a 4.7-in. monotonic push. There was a residual displacement of 3.43 in. once the load was removed.

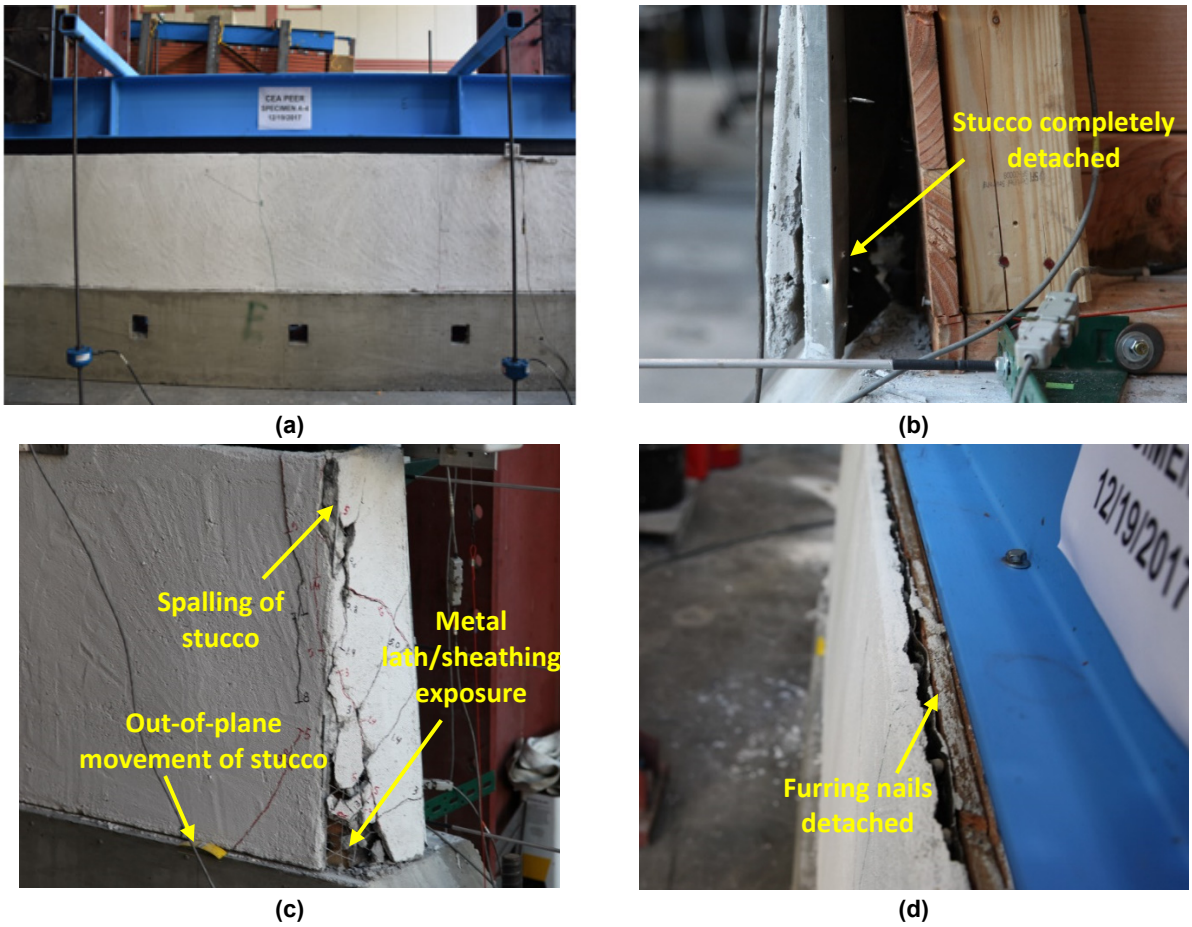

Figure 5.25 **Specimen A-4 damage state at 80% post-peak reduction of lateral strength @ -12% drift, Δ = -2.88 in.: (a) exterior elevation; (b) bottom of north-end interior corner; (c) north-end exterior corner; and (d) bottom of north-end corner.**

(a)

(b)

(c)

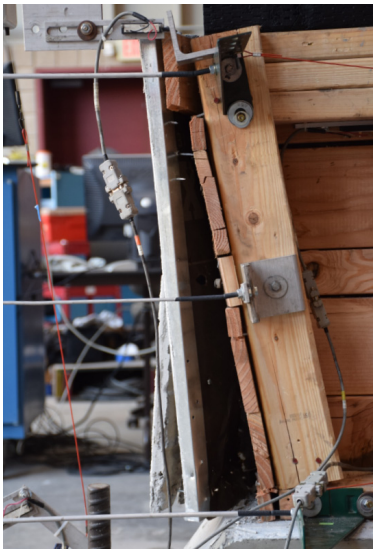

(d)

Figure 5.26 **Specimen A-4 post-test photographs at lateral load = 0 kips, residual displacement = +3.43 in. @ +14.3% drift: (a) exterior elevation of cripple wall; (b) interior elevation of cripple wall; (c) north-end exterior corner view; and (d) north-end interior view.**

5.5.5 Specimen A-5 Post-Peak Performance

Figure 5.27(a) to (d) shows the damage state of Specimen A-5 at -11% drift. The data for this test stopped being accurately recorded at 7% drift amplitude due to the loss of the control displacement potentiometer; however, higher amplitudes were imposed to obtain a visual of the damage state of the failed wall. All plywood panels almost completely detached (only two to three nails remained attached) on the top, bottom, and one side, providing no lateral resistance. The south-end plywood panel remained attached by only two nails; see Figure 5.27(a). Most of the nails at the top had ripped through or pulled through the plywood. At the bottom of the plywood panels, many of the nails pulled out of the block, and much of the blocking was either uplifted out of the sill plate or split where the plywood was nailed. The corner flat studs split due to the abutment of the plywood. The damage to the stucco had the same characteristics as Specimen A-2, the existing condition replica. Figure 5.28 shows the cripple wall in its residual state at the end of testing after the end of the 11% drift cycle group. After the wall was unloaded at -11% drift (-2.64 in.), a residual displacement of -1.74 in. remained.

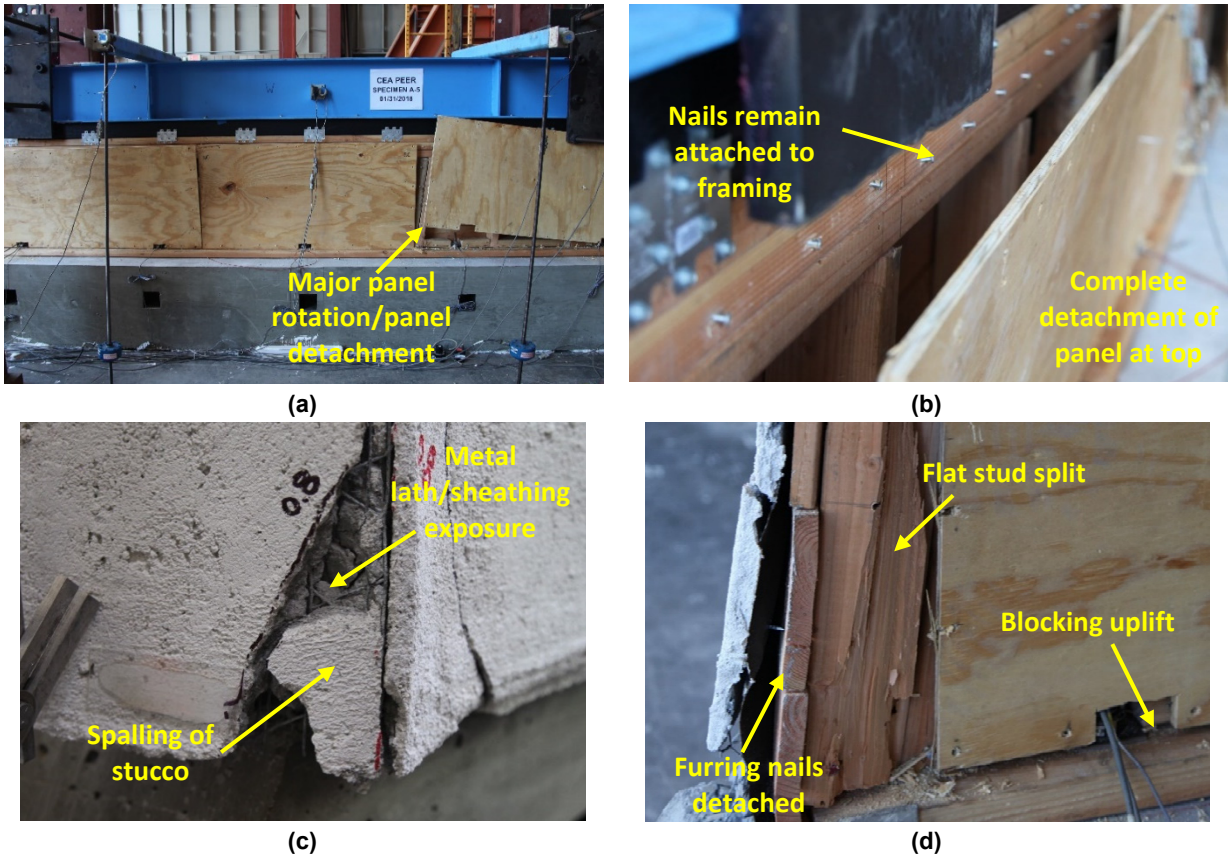

Figure 5.27 **Specimen A-5 damage state at 80% post-peak reduction of lateral strength @ -11% drift, Δ = -2.64 in.: (a) interior elevation; (b) top-down view of interior; (c) close-up of exterior south-end corner; and (d) close-up of interior north-end corner.**

(a)

(b)

(c)

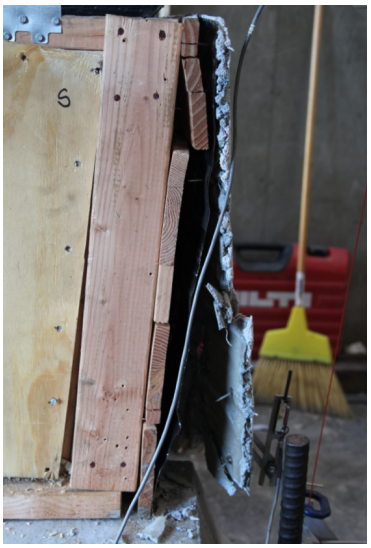

(d)

Figure 5.28 **Specimen A-5 post-test photographs at lateral load = 0 kips, residual displacement = -1.74 in. @ -7.3% drift: (a) exterior elevation of cripple wall; (b) interior elevation of cripple wall; (c) north-end exterior corner view; and (d) south-end interior corner view.**

5.5.6 Specimen A-6 Post-Peak Performance

Figure 5.29(a) to (d) shows the damage state of Specimen A-6 at +13% drift. This wet set sill specimen never dropped under half of its peak capacity. This is due to the sheathing boards bearing on the foundation, which at large displacements closed up the gaps between the bottom sheathing boards, causing the sheathing boards to work as a unit and provide increased lateral resistance; see Figure 5.29(d). Due to the top sheathing board being nailed to the top plates instead of the studs, a 3/16-in. gap formed between the upper two sheathing boards. At the corners, the stucco spalled off in large chunks, and the entire stucco face detached from the cripple wall along the sill plate and studs; see Figure 5.24(c). Partial attachment of the stucco remained at the top plates. The studs exhibited large rotations as well as uplifting. Figure 5.30 shows the cripple wall in its residual state at the end of testing after a 4.32-in. monotonic push. There was a residual displacement of 4.22 in. once the load was removed.

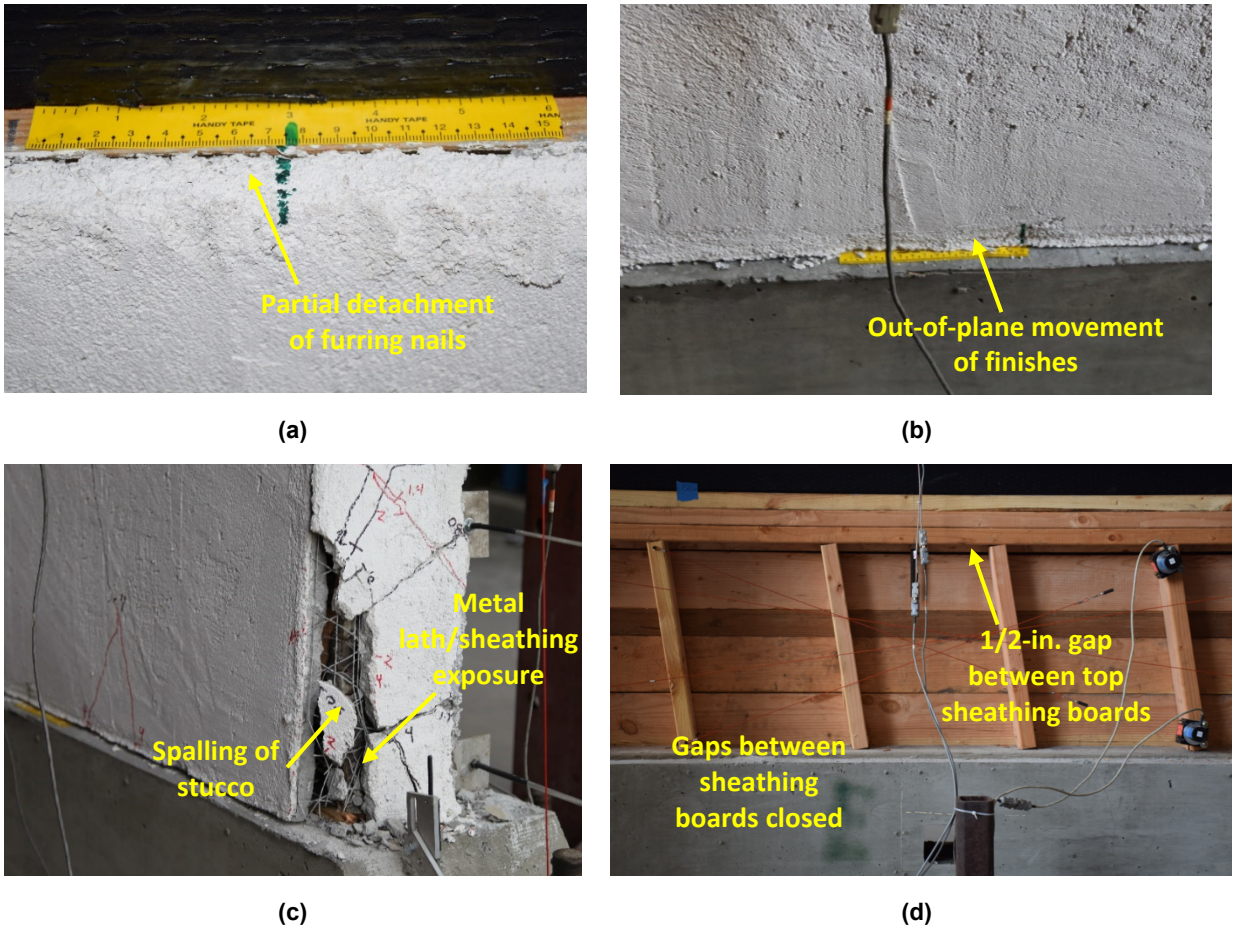

Figure 5.29 **Specimen A-6 damage state at 40% post-peak reduction of lateral strength @ +13% drift, Δ = +3.12 in.: (a) close-up of top of exterior wall; (b) close-up of the bottom of the exterior wall; (c) the north-end bottom of the exterior corner; and (d) the interior of the wall.**

(a)

(b)

(c)

(d)

Figure 5.30 **Specimen A-6 post-test photographs at lateral load = 0 kips and residual displacement = +4.22 in. @+17.6% drift: (a) exterior elevation of cripple wall; (b) interior elevation of cripple wall; (c) exterior north-end corner view; and (d) interior north-end view.**

5.6 FAILURE MODES

Ultimately, all of the cripple walls failed in the same manner. As the displacement increased, the furring nails connecting the stucco to the framing moved out laterally, ultimately disconnecting from the framing. This is where softening prior to lateral strength occurred. The furring nails are 1-1/2 in. in length and were embedded 1/4 in. into the stucco and 7/8 in. into the horizontal sheathing boards. This leaves around 3/8 in. of embedment into the framing of the wall as opposed to a stucco-only condition, which would have furring nails embedded around 1-1/4 in. into the framing. The shorter embedment led to the furring nails pulling out of the framing at smaller drift amplitudes, thus forcing the load to transfer from the framing to the sheathing boards to the stucco finish instead of directly from the framing to the stucco finish. The result is an overall softening around the peak strength.

In general, at strength the furring nails would begin tearing out of the stucco at the base and sides of the wall where there was a more distance between furring nails. The exception to this is Specimen A-1 with top boundary condition A, which had the same furring nail spacing at the top and bottom, leading to the furring nails tearing away more uniformly over the entire wall. The large drops in lateral strength observed in all the walls occurred when many of the furring nails had torn away from the stucco. At this point there was no load transfer from the sheathing to the stucco, so the stucco essentially rotated as a rigid body as the wall displaced. The additional capacity left in the walls was mainly attributed to the horizontal sheathing boards bearing on the concrete. At large displacements, the gaps between the sheathing boards closed, and the boards stacked on one another. With no room to move down due to the bearing on the foundation, the sheathing was forced to move upward, causing the nails connecting boards to the frame to rotate and pullout. This behavior was attributed to a significant amount of strength at the large post-peak displacements and why an 80% drop in lateral strength for any of the walls was rare.

6 CONCLUSIONS

Quantifying the performance of retrofitted and unretrofitted single-family wood-frame houses has become increasingly important in California due to the high seismicity of the state and the often-poor seismic resiliency of some portions of the housing stock. From field observations of past earthquakes, it has been found that inadequate lateral bracing of both cripple walls and sill bolting are the primary reasons for failures of residential homes even in the event of moderate earthquakes. While methods to retrofit weak cripple walls and improve sill anchorage have been developed, the improvement in performance with retrofit have observed only limited experimental quantification. In addition, little knowledge is available to characterize the performance of houses with existing cripple walls and sill anchorages.

To this end, this report presents Phase 1 of an experimental investigation to study the seismic performance of retrofitted and existing cripple walls with sill anchorage. Paralleled by a large-component test program conducted at UC Berkeley [Cobeen et al. 2020], the present study involves the first of multiple phases of small-component tests conducted at UC San Diego. Details representative of era-specific construction are the primary focus in the present effort. Parameters examined are cripple wall height, finish materials, gravity load, boundary conditions, and anchorage, with emphasis on pre-1960s construction. This report addresses the first phase of testing, which consisted of six specimens.

Specifically, the parameters examined in Phase 1 were: boundary conditions (on the top, bottom, and ends of the walls), anchorage conditions, and retrofit conditions. The six cripple walls tested were nominally 12 ft long × 2 ft high and finished with stucco over horizontal lumber sheathing. The loading history and applied vertical load remained constant for all six specimens. Observations regarding the effects of the various conditions considered in this phase are summarized below.

6.1 GENERAL OBSERVATIONS

- The hysteresis of all specimens was generally stable with no abrupt brittle failure; as anticipated, the strength and stiffness of the unretrofitted (existing) specimens were much smaller than the specimen when retrofitted; and
- The relative drift ratios at strength were fairly consistent for all specimens, ranging from 2.8%–4.3% with the exception of the cripple wall containing a return wall, which had a 2.0% relative drift ratio at peak loading in the pull direction. The global drift ratio at strength for all specimens fell between 3% and 5%.

6.2 BOUNDARY CONDITIONS

- The implementation of an extended corner return, i.e., denoted as top boundary condition C, had little effect on the lateral strength of the cripple wall when compared with top boundary condition B;
- The cripple wall without built-up corners, i.e., top boundary condition A, had 60% of the strength and 50% of the secant stiffness associated with drift at 80% strength of the cripple wall than top boundary condition B. In addition, the cumulative energy dissipated by the cripple walls with built-up ends was twice that of the cripple wall without;
- When the stucco finish was constructed such that it bore directly on the foundation, an additional 25% increase in the lateral strength of the cripple wall was observed; however, there were more significant relative displacements between the framing and sheathing as well as the sheathing and stucco finish compared with cripple walls with the stucco finish outboard of the foundation. In the cases where the stucco finish was outboard, the relative displacement between the stucco and sheathing tended to be very small, while the relative displacement between the sheathing and the framing tended to be large. There were insignificant changes in the stiffness between cripple walls with all the stucco bearing and the stucco outboard of the foundation;
- Larger residual drifts were observed when the stucco finish bore directly on the foundation. The residual drift for cripple walls with and without built-up corners was nearly the same; and
- The implementation of a denser furring nail arrangement at the top of the cripple walls as well as a built-up corner (top boundary condition B and top boundary condition C) provided a dramatic increase in the stiffness and lateral strength of a cripple wall compared with top boundary condition A, featuring a furring nail arrangement absent in this emulation of the stucco-finish continuity to the upper floor. This denser furring nail arrangement at the top of the cripple wall provided a more accurate representation of the continuity of the stucco running from the cripple wall up through the superstructure of the house.

6.3 RETROFIT CONDITION

- There was a 270% increase in strength of the retrofitted cripple wall as compared with the unretrofitted cripple wall;
- The secant stiffness at drift associated with 80% strength increased by over 130% with the addition of the retrofit;
- The drift capacity of the cripple walls was not significantly affected by the addition of the retrofit;
- The cumulative energy dissipated by the retrofitted cripple wall was doubled when regarding the global response and four times when regarding the relative

response. This is due to the increased number of fasteners attaching the plywood panel to the cripple wall framing; and

- The residual displacement was the same regardless of the retrofit condition upon completion of the lower-amplitude drift cycles. At strength, the retrofitted cripple wall had a smaller residual drift than unretrofitted specimens.

6.4 ANCHORAGE CONDITION

- With the presence of oversized anchor bolt holes, sliding of the sill plate relative to the concrete foundation occurred for these specimens until anchor bolt bearing on the sill plate occurred. As such, significant portions of the imposed drift were taken up by sliding of the sill plate on the concrete foundation, so much so that it became important to present the global lateral response that included the sill slip and the relative lateral response that omitted the sill slip. It is worth noting that the smooth trowel finished footings may divert from finished concrete footings of this vintage, thus offering reduced contribution to sliding;
- The use of a wet set sill plate instead of a traditional sill plate with anchor bolts resulted in an 18% decrease in strength. This loss of capacity may be partially due to the reduced area of the sill for attaching the furring nails to the sill plate, causing the furring nails to detach from the sill plate more easily during loading. The location of the mudsill for a wet set sill configuration is investigated in a later stage of this test program;
- The wet set sill plate did not displace nor damage the surrounding concrete during loading; and
- At low drift levels, the cumulative energy dissipated was similar for the anchored and wet set sill conditions. More energy was dissipated at larger amplitude drift levels due to the movement of the sill plate relative to the foundation. Not taking this displacement into account, the cumulative energy dissipation was nearly identical, regardless of the anchorage condition.

6.5 DAMAGE CHARACTERISTICS

- Cracking of the stucco was minimal on the face of the cripple walls not detailed with finish around the ends (corners). When corners were present on the cripple walls, significant cracking propagated vertically and diagonally at the corners, even at low drift amplitudes (0.2% to 1.4% drift amplitude). In addition, when corners were detailed with additional finish, vertical cracks also appeared on the exterior stucco face at the same low drift amplitudes. The extent of cracking and crack widths increased as the imposed drift increased. For cripple walls with corner conditions at large drift amplitudes, crushing and spalling of the stucco was observed, in particular at the interface with the concrete foundation;

- After strength was attained, the lateral resistance contribution from the stucco was greatly reduced due to loss of its connection to the sheathing and framing members (i.e., furring nail detachment). Upon continued lateral drift, however, the horizontal sheathing boards began to provide increased lateral resistance for those conditions when the sheathing boards were bearing on the footing. At very large drift amplitudes, the gaps between all sheathing boards (except for the sheathing board attached to the top plates) closed up, and the sheathing started bearing on each other, which resisted the lateral displacement of the cripple wall, causing a significant retention of the lateral strength of the cripple wall up to large drift amplitudes;
- The stucco finish provided the majority of the stiffness and lateral strength of the cripple walls in all unretrofitted cases. Following attainment of the wall's lateral capacity, the strength of the cripple wall decreased mostly due to the detachment of the stucco from the furring nails but also from the detachment of the furring nails from the sheathing and framing members. As drift amplitudes increased, the stucco finish was pushed out laterally at the base of the cripple wall from the sheathing and framing members as the furring nails detached. At larger drift amplitudes, the stucco finish only retained its connection to the top plates, providing very little lateral strength to the wall specimen;
- Failure of the retrofitted cripple wall was primarily attributed to sheathing nail head pull through and/or nail withdrawal along the edges of the plywood panels, especially along the top plate and sides. At the bottom of the plywood panels, nails withdrew from the framing as added blocking split at large displacements. Some tearing of the nails through the plywood panels (edge tear-out) was observed at the corners; and
- In the cases where the stucco finish was bearing on the foundation, more significant cracking on the face of the stucco was observed in the retrofitted wall.

The current report is the first in a series of four reports. In the subsequent reports, discussion, results, and conclusions of the remaining twenty-two tests are presented.

REFERENCES

Aira J.R., Arriaga F., Iniguez-Gonzalez G., Crespo J. (2014). Static and kinetic friction coefficients of Scots pine (Pinus Sylvestris L.), parallel and perpendicular to grain direction, *Materiales de Construcción*, 64(315):e030, doi: 10.3989/mc.2014.03913.

Anderson T. (2015). Anderson-Niswander Archives, JPEG file (December), Anderson-Niswander Construction. Oakland, CA.

ATC (2014). *ATC-110: Plan for Development of a Pre-Standard for Evaluation and Retrofit of Wood Light-Frame Dwellings*, Applied Technology Council, Redwood City, CA.

Arnold A.E., Uang C.-M., Filiatrault F. (2003). Cyclic behavior and repair of stucco and gypsum woodframe walls: Phase I. *CUREE Publication No. EDA-03*, Department of Structural Engineering, University of California, San Diego, CA, 268 pgs.

AWC (2018). National design specification for wood construction, *ANSI/AWC NDS-2018*, American Wood Council, Washington, D.C.

ASTM (2006). *ASTM C207-06 Standard Specification for Hydrated Lime for Masonry Purposes*, American Standards for Testing Methods, West Conshohocken, PA.

Chai Y.-H., Hutchinson T.C., Vukazich S.M. (2002). Seismic behavior of level and stepped cripple walls, *CUREE Publication No. W-17*, Division of Civil and Environmental Engineering, University of California, Davis. Davis, CA.

Chai Y.H., Hutchinson T.C., Vukazich S.M. (2003). Quasi-static reversed cyclic response of level and stepped cripple walls, ASCE, *J. Struct. Eng.*, 129(5): 567–575.

Cobeen K. (2019). Damage to stucco house in Trona, CA from 2019 Ridgecrest earthquake, Photograph, JPEG file, Trona, CA.

Cobeen K., Mahdavifar V., Hutchinson T.C., Schiller B. Welch D., Kang G.S., Bozorgnia Y. (2020). Large-component seismic testing for existing and retrofit single-family wood-frame dwellings, *PEER Report No. 2020/20*, Pacific Earthquake Engineering Research Center, University of California, Berkeley, CA.

Cook H. (2006). Seismic retrofit for cripple walls, *https://www.jlconline.com/how-to/framing/seismic-retrofit-for-cripple-walls_o*.

EERI (1996). Northridge Earthquake reconnaissance report, Vol. 2. Earthquake Spectra, January 1996. Supplement C to Vol. 11.

NAHB Research Center, Inc. (1994). *Assessment of Damage to Residential Buildings Caused by the Northridge Earthquake*. US Department of Housing and Urban Development, Washington, D.C., 87 pgs.

NAHB Research Center, Inc. (2001). *Review of Structural Materials and Methods for Home Building in the United States: 1900 to 2000*, Department of Housing and Urban Development., Washington, D.C., 40 pgs.

FEMA (1997). *NEHRP Guidelines for the Seismic Rehabilitation of Buildings, FEMA Publication 273*, Federal Emergency Management Agency, Washington, D.C.

FEMA (2015). *Earthquake Strengthening of Cripple Walls in Wood-Frame Dwellings, FEMA DR-4193-RA2*, Federal Emergency Management Agency, Washington, D.C.

FEMA (2018). *Vulnerability-Base Seismic Assessment and Retrofit of One- and Two-Family Dwellings, FEMA P-1100*, Vol. 1 – Prestandard, Federal Emergency Management Agency, Washington, D.C.

Gatto K., Uang C.-M. (2002). Cyclic response of woodframe shearwalls: loading protocol and rate of loading effects, *CUREE Publication No. W-13*, Department of Structural Engineering, University of California, San Diego. CA.

Hall J.F. (Ed.) (1994). Northridge earthquake January 17, 1994, preliminary reconnaissance report, *Earthquake Engineering Research Institute 94-01*, Oakland, CA.

IBHS (1995). *A Homeowner's Guide to Earthquake Retrofit*, Institute for Business and Home Safety, Tampa, FL, pg. 42.

ICBO (1927). *Uniform Building Code*, International Conference of Building Officials, Whittier, CA.

ICBO (1943). *Uniform Building Code*, International Conference of Building Officials, Whittier, CA.

ICBO (1946). *Uniform Building Code*, International Conference of Building Officials, Whittier, CA.

Kang G.S., Mahin S.A. (2014). PEER preliminary notes and observations on the August 24, 2014, South Napa earthquake, *PEER Report No. 2014/13*, Pacific Earthquake Engineering Research Center, University of California, Berkeley, CA.

Krawinkler H., Parisi F., Ibarra L., Ayoub A., Medina R. (2001). Development of a testing protocol for wood frame structures. *CUREE Publication No. W-02*, Department of Civil and Environmental Engineering, Stanford University. Stanford, CA.

Mahin S.A. (1991). The Loma Prieta earthquake: implications of structural damage, *Proceedings, 2nd International Conferences on Recent Advances in Geotechnical Earthquake Engineering and Soil Dynamics*, St. Louis, MO.

Perry S., Cox D., Jones L., Bernknopf R., Goltz J., Hudnut, K., Mileti D., Ponti D. Porter K., Reichle M., Seligson H., Shoaf K., Treiman J., Wein A. (2008). The ShakeOut earthquake scenario: A story that that southern Californians are writing, *U.S. Geological Survey Circular 1324* and *California Geological Survey Special Report 207*, 16 pg., *http://pubs.usgs.gov/circ/1324/*.

Portland Cement Association (1941). *Portland Stucco Cement*. Provided by Building Technology Heritage Library Association for Preservation Technology, Springfield, IL.

Rabinovici S., Ofodire N. (2017). *California Earthquake Authority South Napa Home Impact Study*. California Earthquake Authority, Sacramento, CA.

Schiller B., Hutchinson T.C., Cobeen, K. (2020). Cripple wall small-component test program: Dry specimens, *PEER Report*, Pacific Earthquake Engineering Research Center, University of California, Berkeley, CA.

Reis E. (2020). Development of index buildings, *PEER Report*, Pacific Earthquake Engineering Research Center, University of California, Berkeley, CA.

Reis E. (2020). Project technical summary, *PEER Report*, Pacific Earthquake Engineering Research Center, University of California, Berkeley, CA.

Reitherman R., Cobeen K. (2003). Design documentation of woodframe project index buildings, *CUREE Publication No. W-29*, Consortium of Universities for Research in Earthquake Engineering, Richmond, CA

Schiller B., Hutchinson T.C., Cobeen K. (2020). Cripple wall small-component test program: Dry specimens, *PEER Report No. 2020/17*, Pacific Earthquake Engineering Research Center, University of California, Berkeley, CA.

Schiller B., Hutchinson T.C., Cobeen K. (2020). Cripple wall small-component test program: Wet specimens II, *PEER Report No. 2020/18*, Pacific Earthquake Engineering Research Center, University of California, Berkeley, CA.

Schiller B., Hutchinson T.C., Cobeen K. (2020). Cripple wall small-component test program: Comparisons, *PEER Report No. 2020/19*, Pacific Earthquake Engineering Research Center, University of California, Berkeley, CA.

Shepherd R., Delos-Santos E.O. (1991). An investigation of retrofitted cripple walls, *Bull. Seismol. Soc. Am*., 81(5): 2111–2126.

Steiner M.R. (1993). Experimental testing of cripple wall retrofits using plywood and oriented strand board. An independent study supervised by R. Shepherd.

U.S. Census Bureau (2000). *https://www.census.gov/census2000/.*

Zareian F., Lanning J. (2020). Development of testing protocol for cripple walls, *PEER Report No. 2020/15,* Pacific Earthquake Engineering Research Center, University of California, Berkeley, CA.

APPENDIX A MATERIAL PROPERTIES

Appendix A includes four sections: lumber moisture content readings (A.1), stucco compressive strengths (A.2), loading protocols (A.3), and nail strength (A.4). Discussion of these sections is provided in Chapter 3.

A.1 LUMBER MOISTURE CONTENT

For all cripple walls constructed, the moisture content of the wood was recorded. The moisture content was measured using an Dr. Meter MD912 digital moisture meter, which is a pin meter with a resolution of 0.5% and accuracy of +/- 0.5%. A picture of the moisture content reader used for the project can be seen in Figure A.5. Understanding the moisture content of wood is important as drier wood has higher strength properties than fresh or moist wood. For all cripple walls, the moisture content was from 4–12% immediately prior to testing. The moisture content was considerably higher when the lumber was first purchased but dried out significantly before testing, especially after the application of the stucco finish. The moisture content was read on five various places on a piece of lumber–top, bottom, middle, and sides–and then repeated on four additional pieces of the same type of lumber. The results were recorded and are displayed in Table A.3 along with the date of recording and averages for each type of lumber.

Figure A.1 MD912 digital moisture content reader in use.

Table A.1 Moisture content readings of Phase 1 lumber used in construction.

CONSTRUCTION PHASE 1							
LUMBER SECTION	**MOISTURE CONTENT READINGS (%)**					**AVERAGE**	**DATE**
2x6 Redwood Sill WS	4.9					4.9	11/21/2017
2x6 #2 Douglas Fir	18.3	23.3	23.5	19.2	22.7	21.40	11/21/2017
2x4 #2 Douglas Fir	22.5	23.8	20.8	22.8	28	23.58	11/21/2017
1x6 Construction Douglas Fir	15	17.3	11	7.8	20.2	14.26	11/21/2017

TEST 1 SPECIMEN A4							
LUMBER SECTION	**MOISTURE CONTENT READINGS (%)**						**DATE**
2x6 #2 Douglas Fir	12.3					12.30	12/18/2017
2x4 #2 Douglas Fir	7.8	8.6	10.1	5.5	6.6	7.72	12/18/2017
1x6 Construction Douglas Fir	3.5	4.5	4.9	7.1	6.2	5.24	12/18/2017

TEST 2 SPECIMEN A6							
LUMBER SECTION	**MOISTURE CONTENT READINGS (%)**						**DATE**
2x6 Redwood Sill WS	2.4					2.40	12/22/2017
2x4 #2 Douglas Fir	4.9	8.7	8.8	6.9	6.9	7.24	12/22/2017
1x6 Construction Douglas Fir	3.4	3.7	4.7	6.3	5.4	4.70	12/22/2017

TEST 3 SPECIMEN A2							
LUMBER SECTION	**MOISTURE CONTENT READINGS (%)**						**DATE**
2x6 #2 Douglas Fir	11					11.00	1/18/2018
2x4 #2 Douglas Fir	8.4	7.7	7.5	9.8	10.2	8.72	1/18/2018
1x6 Construction Douglas Fir	7.5	7.4	8	6.2	6.8	7.18	1/18/2018

TEST 4 SPECIMEN A1							
LUMBER SECTION	**MOISTURE CONTENT READINGS (%)**						**DATE**
2x6 #2 Douglas Fir	12.2					12.20	1/26/2018
2x4 #2 Douglas Fir	8.4	10.3	6.7	8.8	8.2	8.48	1/26/2018
1x6 Construction Douglas Fir	5.6	5.9	9.1	4.3	6.5	6.28	1/26/2018

TEST 5 SPECIMEN A5							
LUMBER SECTION	**MOISTURE CONTENT READINGS (%)**						**DATE**
2x6 #2 Douglas Fir	9.2					9.20	1/31/2018
2x4 #2 Douglas Fir	8.3	7.3	6.5	6.5	9.3	7.58	1/31/2018
1x6 Construction Douglas Fir	3.4	6.2	4.8	4.6	7	5.20	1/31/2018

TEST 6 SPECIMEN A3							
LUMBER SECTION	**MOISTURE CONTENT READINGS (%)**						**DATE**
2x6 #2 Douglas Fir	8.7					8.70	2/2/2018
2x4 #2 Douglas Fir	6.3	9.9	10.1	5.3	8.2	7.96	2/2/2018
1x6 Construction Douglas Fir	3.2	6.2	5	4.8	4.7	4.78	2/2/2018

A.2 STUCCO COMPRESSIVE STRENGTH

During the stucco application process, 2-in. × 4-in. test cylinders were filled with the stucco mix to be tested later for quality control. For each layer of stucco (scratch coat, brown coat, and finish coat), there were 12 samples taken. Three cylinders of each layer were tested on the day of Test 1, three cylinders of each layer were tested on the day of Test 2, and then the final six cylinders of each layer were tested after Test 6. Table A.2 presents the data of all tests. Within this table is the average compressive strength of each layer on the day tested and the average compressive strength of all the samples taken for each layer regardless of day tested. For the scratch coat, the average compressive strength was 1142 psi, for the brown coat, the average compressive strength was 1109 psi, and for the finish coat, the average compressive strength was 630 psi. Since the composition of the scratch coat and the brown coat are the sample, there compressive strength values should be comparable. The difference between the two can be largely contributed the increased curing time of the scratch coat versus the curing time of the brown coat. The finish coat is expected to be weaker than the scratch coat and brown coats weaker due to the increased amount of hydrated lime used in the mix.

The details of the stucco mix and application are presented below. The stucco-mix details and application procedure are derived from the 1943 Uniform Building Code [ICBO 1943] as well as recommendations from the Portland Cement Association journal, *Portland Cement Stucco*, from 1941 [Portland Cement Association 1941]; see Figure A.2. The stucco mix and application are meant to closely mimic common building practices of pre-1945. A licensed contractor was responsible for the application of the stucco. The amount of water used for each batch of stucco was up to the discretion of the contractor and kept uniform for each batch. Each batch contained the following proportions: one-part cement, three parts sand, and 1/5-parts hydrated lime, and a water content between 0.50 and 0.55.

Portland Cement Plaster (Stucco) Mix

Recommendations:

Mixing Ratios:

- 1 part Portland Type I Cement
- 3 parts sand (well graded, clean sand (70-90% passing No. 8 sieve)
- 1/5 part hydrated lime **(3/5 part hydrated lime for finish coat)**
- Sufficient clean water to become workable (needs to be measured/consistent for all batches)

Procedure:

- Mix cement and dry sand
- Mix in hydrated lime
- Once uniformly mixed, measure water and add to mix
- Once mortar is workable, record amount of water used

Notes:

- Scratch coat must be the same as brown coat (mix and procedure)
- All mixes must remain consistent for all stucco applications
- Brown coat, scratch coat, and finish coat shall be kept moist for 48 hours after application
- 48 hours required before application of brown coat
- 7 days required before application of finish coat
- *Finish coat must be smooth troweled finish (NOT a standard sand or other textured finish)*
- 3 days required for curing of finish coat

Figure A.2 Stucco mix details [Portland Cement Association 1941].

Table A.2 Compressive strengths of stucco.

Construction Phase 1						
Layer	**Cylinder Label**	**Test Date**	**Days after install**	**Axial Load (kips)**	**Compressive Strength (psi)**	**Average Compressive Strength Per Test (psi)**
Scratch	DOT (Test1-A4)	12/18/2017	21	3.49	1111	997
Installed on:	DOT (Test1-A4)	12/18/2017	21	3.25	1035	
11/27/2017	DOT (Test1-A4)	12/18/2017	21	2.65	844	
	DOT (Test2-A6)	12/22/2017	25	3.93	1252	1103
	DOT (Test2-A6)	12/22/2017	25	3.15	1003	
	DOT (Test2-A6)	12/22/2017	25	3.31	1054	
	After Test6-A3	1/29/2018	62	3.19	1016	1235
	After Test6-A3	1/29/2018	62	4.62	1471	
	After Test6-A3	1/29/2018	62	3.73	1188	
	After Test6-A3	1/29/2018	62	3.91	1245	
	After Test6-A3	1/29/2018	62	3.4	1083	
	After Test6-A3	1/29/2018	62	4.41	1404	
Average Compressive Strength (psi)					**1142**	
Brown	DOT (Test1-A4)	12/18/2017	17	3.19	1016	918
Installed on:	DOT (Test1-A4)	12/18/2017	17	2.73	869	
12/1/2017	DOT (Test1-A4)	12/18/2017	17	2.73	869	
	DOT (Test2-A6)	12/22/2017	21	3.26	1038	1104
	DOT (Test2-A6)	12/22/2017	21	3.39	1080	
	DOT (Test2-A6)	12/22/2017	21	3.75	1194	
	After Test6-A3	1/29/2018	58	3.25	1035	1246
	After Test6-A3	1/29/2018	58	4.74	1510	
	After Test6-A3	1/29/2018	58	3.75	1194	
	After Test6-A3	1/29/2018	58	3.1	987	
	After Test6-A3	1/29/2018	58	3.28	1045	
	After Test6-A3	1/29/2018	58	4.61	1468	
Average Compressive Strength (psi)					**1109**	
Finish	DOT (Test1-A4)	12/18/2017	10	1.39	443	448
Installed on:	DOT (Test1-A4)	12/18/2017	10	1.34	427	
12/8/2017	DOT (Test1-A4)	12/18/2017	10	1.49	475	
	DOT (Test2-A6)	12/22/2017	14	1.79	570	641
	DOT (Test2-A6)	12/22/2017	14	2.14	682	
	DOT (Test2-A6)	12/22/2017	14	2.11	672	
	After Test6-A3	1/29/2018	51	2.31	736	716
	After Test6-A3	1/29/2018	51	2.14	682	
	After Test6-A3	1/29/2018	51	2.54	809	
	After Test6-A3	1/29/2018	51	2.17	691	
	After Test6-A3	1/29/2018	51	2.32	739	
	After Test6-A3	1/29/2018	51	2.01	640	
Average Compressive Strength (psi)					**630**	

A.3 LOADING PROTOCOLS

The following section presents a graph and table of the loading protocol for Specimen A-2 through A-6. The loading protocol for Specimen A-1 is discussed in Section 3.9. Overall, the initial loading protocol was the same for each specimen. Variations occurred at later drift levels, depending on the rate of post-peak strength degradation of the individual specimen. As noted in Section 2.4, all cripple walls underwent the same loading protocol up until the specimen realized a loss greater than 60% of its measured lateral strength. At this point, each subsequent drift level was increased by 2%, rather than 1%. If the 60% loss in strength did not occur, each drift level would remain at an increase of 1% per cycle grouping. The loading protocol would progress until an 80% loss in strength was realized. At this point, a monotonic push would be conducted, typically to a global drift of 20%. The amplitude of the monotonic push might vary slightly depending on instrumentation constraints. The first cripple wall tested, Specimen A-4, did not have a monotonic push initiated at the end of the loading protocol because this specific loading protocol was not being implemented, a practice that was included later for subsequent specimens. The loading protocol for Specimen A-5 ends after the 7% drift cycle due to linear transducer controlling displacement being disturbed on the 9% drift cycle, causing the cripple wall to be pushed to around 13% drift; see Figures A.3–A.7 and Tables A.3–A.7.

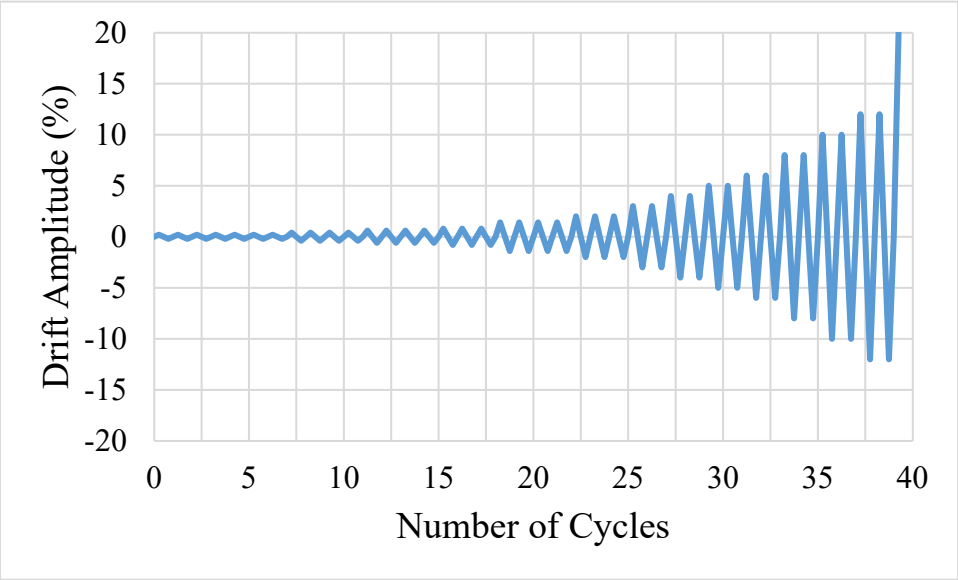

Figure A.3 Specimen A-2 loading protocol.

Table A.3 Specimen A-2 loading protocol.

Cycle Group #	Drift (%)	Amplitude (in)	# of Cycles per Group	Loading Rate (in/sec)	Time per Cycle (sec)	Total Time per Cycle Group (sec)
1	0.2	0.048	7	0.0064	30	210
2	0.4	0.096	4	0.0128	30	120
3	0.6	0.144	4	0.0192	30	120
4	0.8	0.192	3	0.0256	30	90
5	1.4	0.336	3	0.0448	30	90
6	2	0.48	3	0.064	30	90
7	3	0.72	2	0.096	30	60
8	4	0.96	2	0.128	30	60
9	5	1.2	2	0.16	30	60
10	6	1.44	2	0.192	30	60
11	8	1.92	2	0.256	30	60
12	10	2.4	2	0.16	60	120
13	12	2.88	2	0.192	60	120
14	Mono	5	--	0.333	60	60

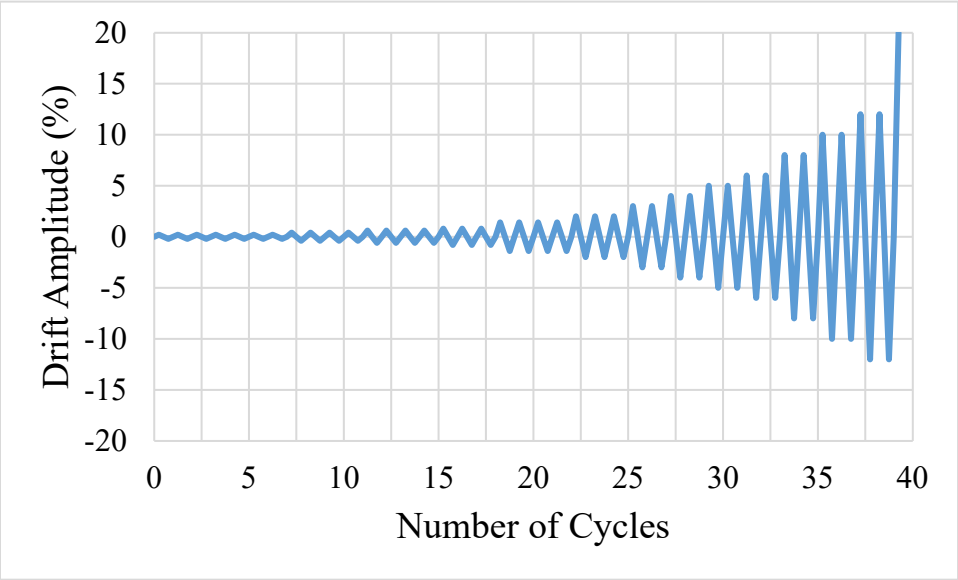

Figure A.4 Specimen A-3 loading protocol.

Table A.4 Specimen A-3 loading protocol.

Cycle Group #	Drift (%)	Amplitude (in)	# of Cycles per Group	Loading Rate (in/sec)	Time per Cycle (sec)	Total Time per Cycle Group (sec)
1	0.2	0.048	7	0.0064	30	210
2	0.4	0.096	4	0.0128	30	120
3	0.6	0.144	4	0.0192	30	120
4	0.8	0.192	3	0.0256	30	90
5	1.4	0.336	3	0.0448	30	90
6	2	0.48	3	0.064	30	90
7	3	0.72	2	0.096	30	60
8	4	0.96	2	0.128	30	60
9	5	1.2	2	0.16	30	60
10	6	1.44	2	0.192	30	60
11	8	1.92	2	0.256	30	60
12	10	2.4	2	0.16	60	120
13	12	2.88	2	0.192	60	120
14	Mono	5	--	0.333	60	60

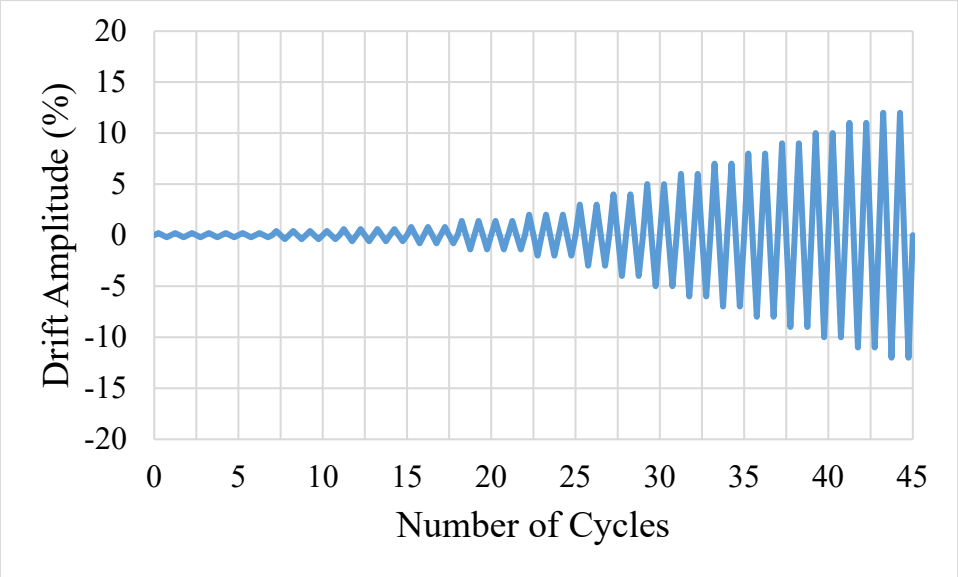

Figure A.5 Specimen A-4 loading protocol.

Table A 5 Specimen A-4 loading protocol.

Cycle Group #	Drift (%)	Amplitude (in)	# of Cycles per Group	Loading Rate (in/sec)	Time per Cycle (sec)	Total Time per Cycle Group (sec)
1	0.2	0.048	7	0.0064	30	210
2	0.4	0.096	4	0.0128	30	120
3	0.6	0.144	4	0.0192	30	120
4	0.8	0.192	3	0.0256	30	90
5	1.4	0.336	3	0.0448	30	90
6	2	0.48	3	0.064	30	90
7	3	0.72	2	0.096	30	60
8	4	0.96	2	0.128	30	60
9	5	1.2	2	0.16	30	60
10	6	1.44	2	0.192	30	60
11	7	1.68	2	0.224	30	60
12	8	1.92	2	0.256	30	60
13	9	2.16	2	0.288	30	60
14	10	2.4	2	0.16	60	120
15	11	2.64	2	0.176	60	120
16	12	2.88	2	0.192	60	120
17	Mono	5	--	0.333	60	60

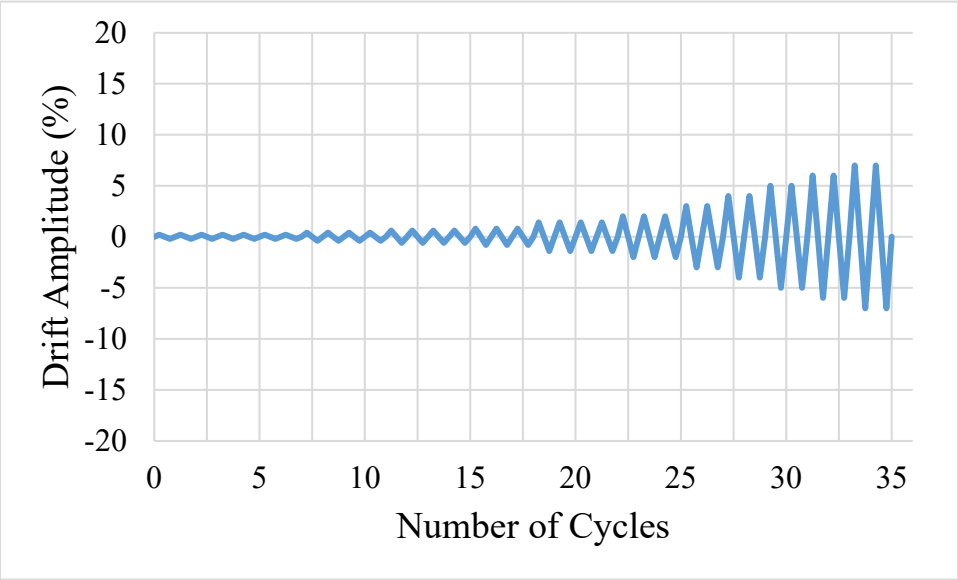

Figure A.6 Specimen A-5 loading protocol.

Table A.6 Specimen A-5 loading protocol.

Cycle Group #	Drift (%)	Amplitude (in)	# of Cycles per Group	Loading Rate (in/sec)	Time per Cycle (sec)	Total Time per Cycle Group (sec)
1	0.2	0.048	7	0.0064	30	210
2	0.4	0.096	4	0.0128	30	120
3	0.6	0.144	4	0.0192	30	120
4	0.8	0.192	3	0.0256	30	90
5	1.4	0.336	3	0.0448	30	90
6	2	0.48	3	0.064	30	90
7	3	0.72	2	0.096	30	60
8	4	0.96	2	0.128	30	60
9	5	1.2	2	0.16	30	60
10	6	1.44	2	0.192	30	60
11	7	1.68	2	0.224	30	60

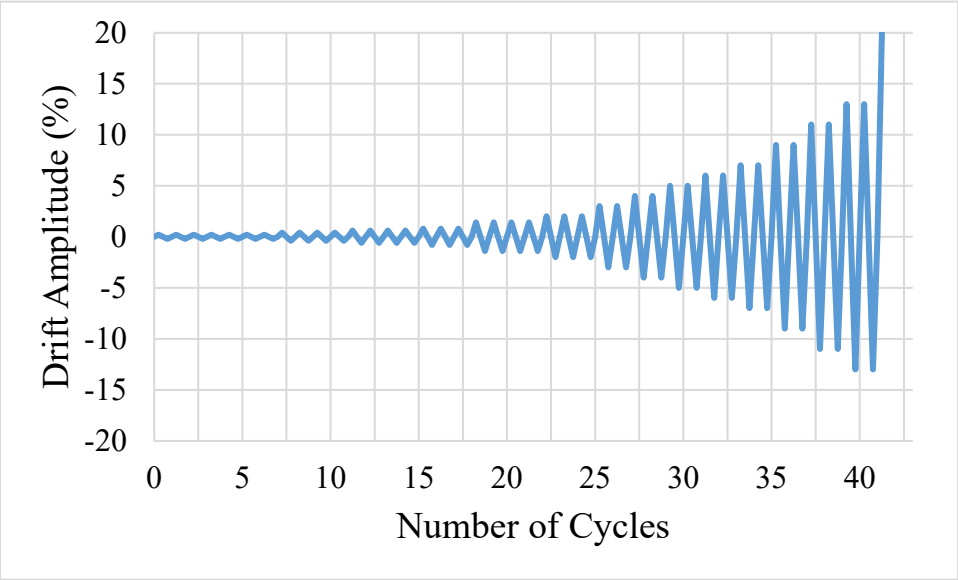

Figure A.7 Specimen A-6 loading protocol.

Table A.7 Specimen A-6 loading protocol.

Cycle Group #	Drift (%)	Amplitude (in)	# of Cycles per Group	Loading Rate (in/sec)	Time per Cycle (sec)	Total Time per Cycle Group (sec)
1	0.2	0.048	7	0.0064	30	210
2	0.4	0.096	4	0.0128	30	120
3	0.6	0.144	4	0.0192	30	120
4	0.8	0.192	3	0.0256	30	90
5	1.4	0.336	3	0.0448	30	90
6	2	0.48	3	0.064	30	90
7	3	0.72	2	0.096	30	60
8	4	0.96	2	0.128	30	60
9	5	1.2	2	0.16	30	60
10	6	1.44	2	0.192	30	60
11	7	1.68	2	0.224	30	60
13	9	2.16	2	0.288	30	60
14	11	2.64	2	0.176	60	120
15	13	3.12	2	0.208	60	120
16	Mono	5	--	0.333	60	60

A.4 NAIL STRENGTH

Per ASTM F1575-95, three-point bending tests were performed on nails used to construct the cripple wall specimens. Each type of nail was tested five times. The three types of nails tested are 16-penny common nails, 10-penny common nails, and 8-penny, hot-dipped galvanized, common nails. The support distance used for nails in the bending test is 1.5 in. Figure A.8 shows the test setup used for the bending test. Figures A.9 through A.11 show the force-displacement curves for each of the nails. The equivalent yield stress was determined using an offset of 5% diameter of the nail. Test results are shown in Table A.8.

Figure A.8 Three-point bending test setup.

Table A.8 Three-point nail bending test results as per *ASTM F1575-95*.

Nail Type	Diameter d (in)	Section Modulus S (in^3)	P_y (lbf)	$\sigma_{yb} = M_y/S$
8d Common	0.134	0.0004010	110.8	103.6
10d Common	0.148	0.0005403	143.8	99.8
16d Common	0.165	0.0007487	223.4	111.9

Note: $S = d^3/6$ and $M_y = P_y * s_{bp}/4$ with $s_{pb} = 1.5$ in. for all tests.

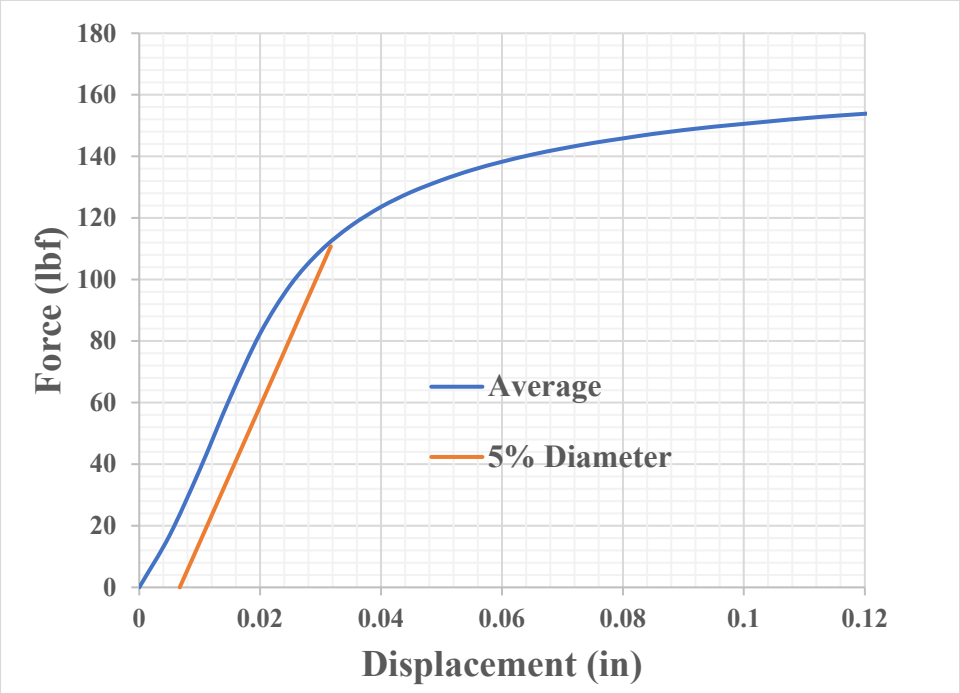

Figure A.9 8d common nail 3-point bending test force-displacement.

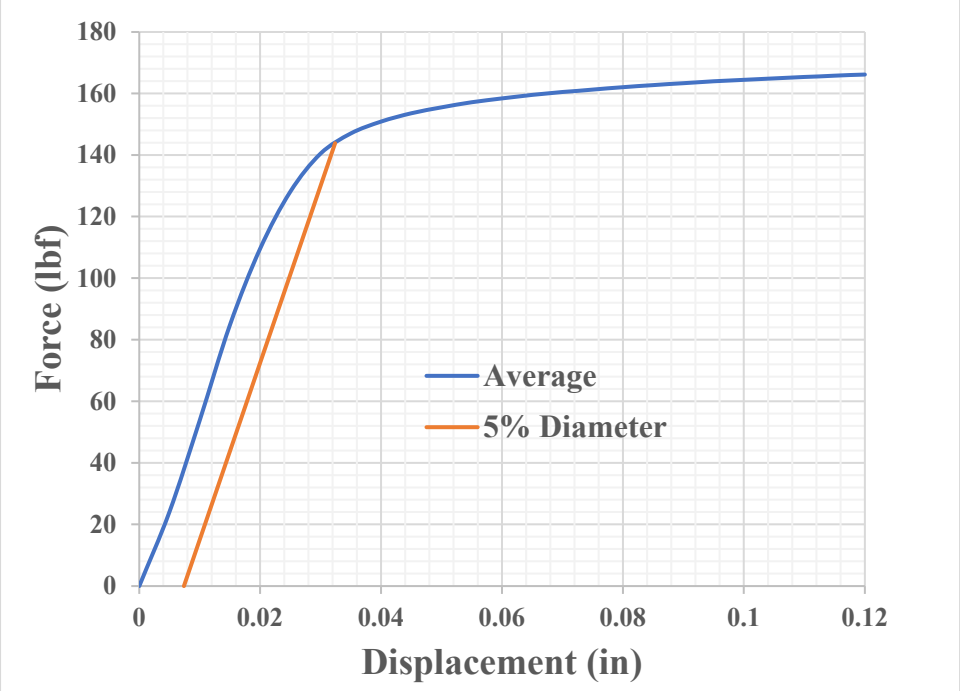

Figure A.10 10d common nail 3-point bending test force-displacement.

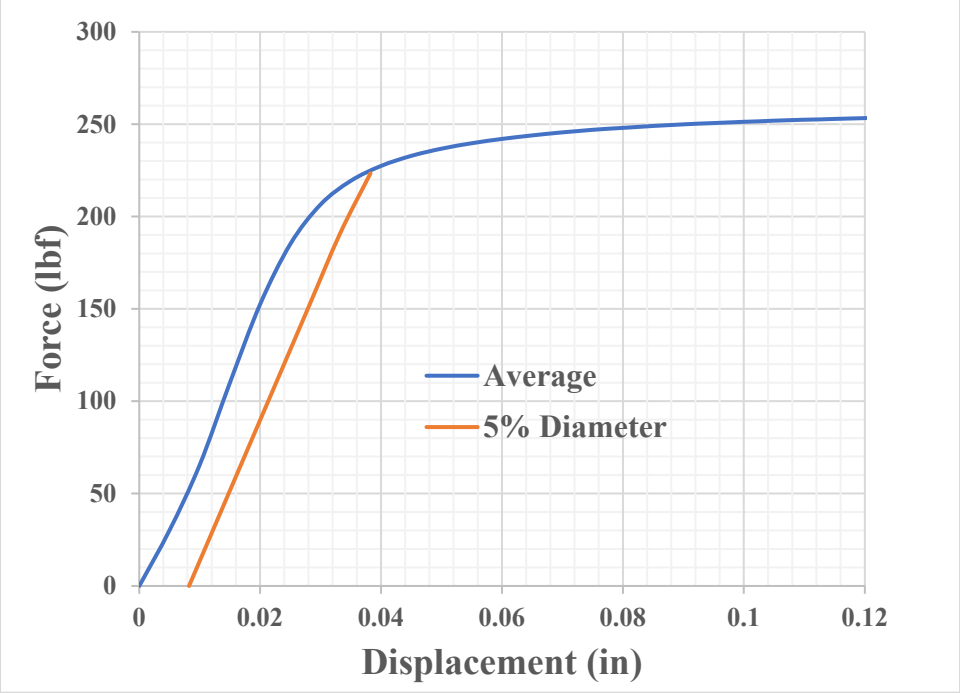

Figure A.11 16d common nail 3-point bending test force-displacement.

APPENDIX B TEST SETUP

Appendix B includes the instrumentation plans for the test program. Discussion of this section is provided in Chapter 3.

B.1 INSTRUMENTATION DRAWINGS

The instrumentation drawings for most tests in Phase 1 were identical. The exceptions were Specimens A-3, A-5, and A-6. Specimen A-3 had additional instrumentation channels to measure displacements of the return walls (top boundary condition C), and Specimen A-5 had two additional channels to measure loads from the added anchor bolts. Lastly, Specimen A-6 did not have any anchor bolts (wet set sill plate), so no channels were used to measure anchor bolt loads.

B.2.1 Specimens A-1, A-2, and A-4: Instrumentation Drawings

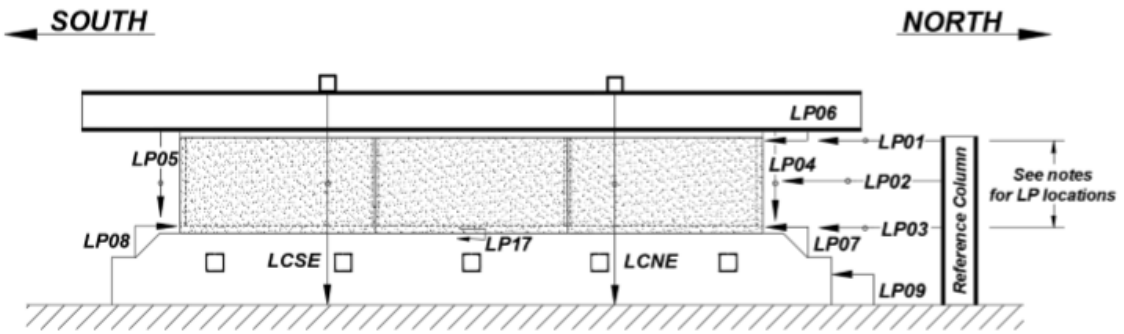

Notes:

1. LP01, LP02, and LP03 measure lateral displacement with LP01 attached to middle of second top plate, LP02 attached to middle of stud, and LP03 attached to middle of sill plate.
2. LP04 and LP05 measure the uplift at each end of the wall.
3. LP06 monitors the slip between the horizontal transfer beam and the upper top plate.
4. LP07 and LP08 monitor the slip between the footing and the sill plate.
5. LP09 monitors the slip of the footing.
5. LCNE and LCSE monitor the axial load on the East Side of the wall.
6. LP17 monitors displacement of stucco relative to the footing.

Instrumentation Elevation (E1)
Stucco Face
2' Tall Cripple Wall

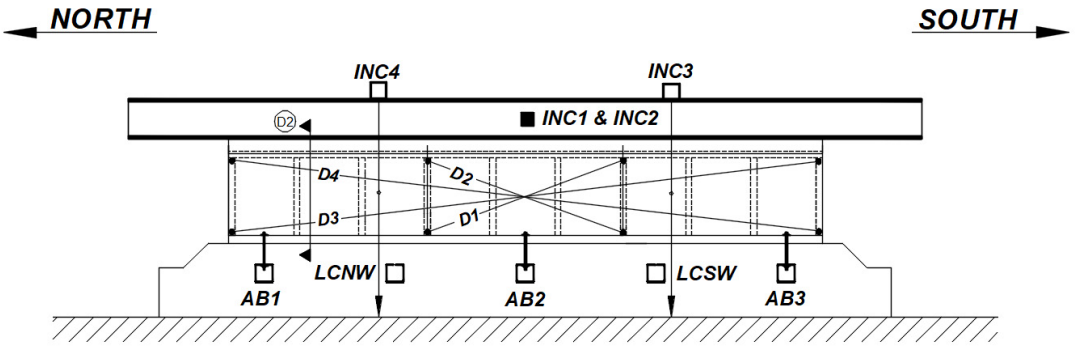

Notes:

1. AB1-AB3 are instrumented with 2" Ø Donut Load Cells measuring uplift loads.
2. Pairs of strength potentiometers are mounted on framing studs or plywood panels for retrofit cases.
3. INC1 measures longitudinal rotation of load transfer beam. INC2 measures the transverse rotation of the load transfer beam.
4. INC3 and INC4 measure the rotation of the transverse beams where axial load is applied.
5. LCNW and LCSW monitor the axial load on the West Side of the wall.

Instrumentation Elevation (E2)
Framing Face
2' Tall Cripple Wall

Figure B.1 Specimens A-1, A-2, and A-4 instrumentation.

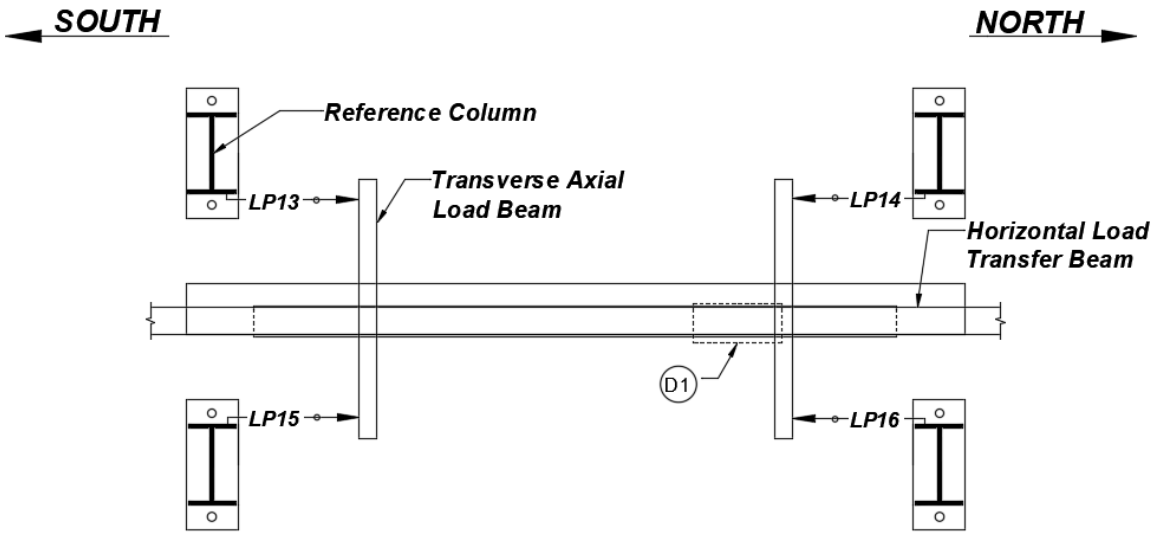

Notes:
1. LP13 - LP16 monitor the displacement of the transverse axial load beams.

Instrumentation Plan View (P1)
2' Tall Cripple Wall

Notes:
1. LP10 monitors the differential displacement between the stucco and the top plate.

Instrumentation Detail (D1)
Stucco Detachment

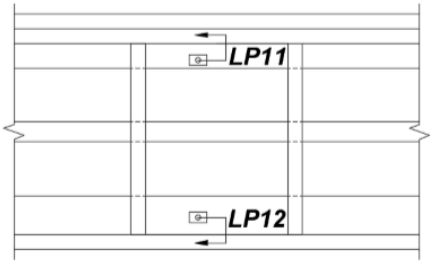

Notes:
1. LP11 and LP12 monitor the siding slip.

Instrumentation Detail (D2)
Siding

Figure B.1 (continued).

B.2.2 Specimen A-3 Instrumentation Drawings

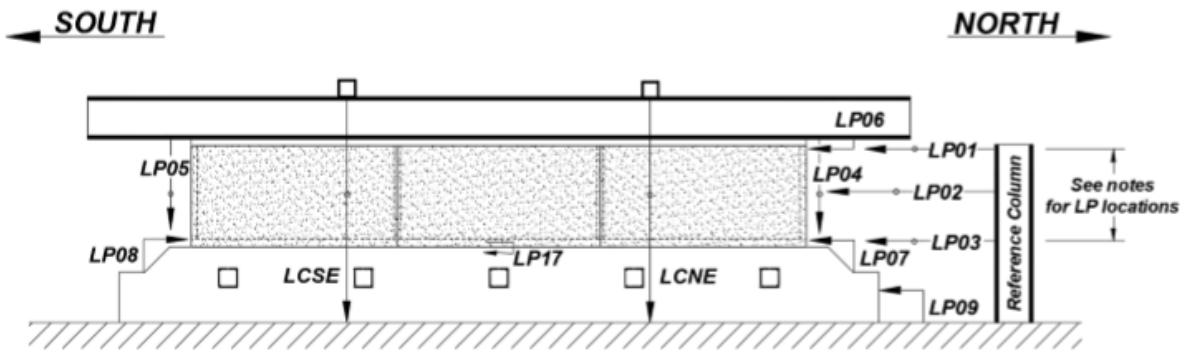

Notes:

1. LP01, LP02, and LP03 measure lateral displacement with LP01 attached to middle of second top plate, LP02 attached to middle of stud, and LP03 attached to middle of sill plate.
2. LP04 and LP05 measure the uplift at each end of the wall.
3. LP06 monitors the slip between the horizontal transfer beam and the upper top plate.
4. LP07 and LP08 monitor the slip between the footing and the sill plate.
5. LP09 monitors the slip of the footing.
5. LCNE and LCSE monitor the axial load on the East Side of the wall.
6. LP17 monitors displacement of stucco relative to the footing.

Instrumentation Elevation (E1)
Stucco Face
2' Tall Cripple Wall

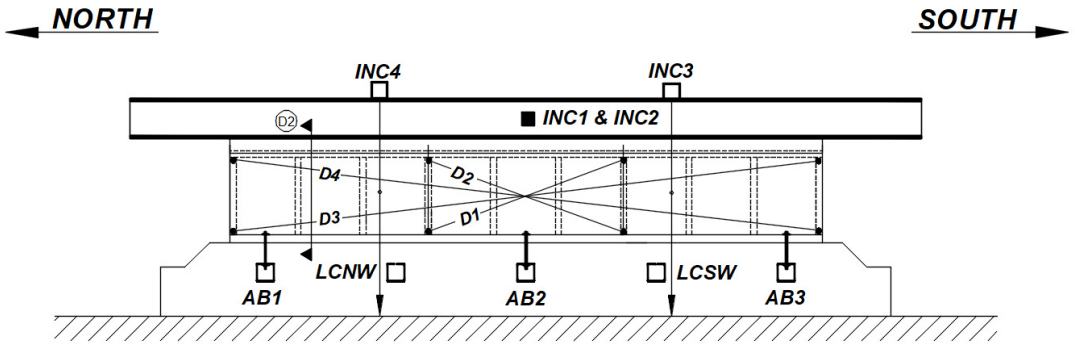

Notes:

1. AB1-AB3 are instrumented with 2" Ø Donut Load Cells measuring uplift loads.
2. Pairs of strength potentiometers are mounted on framing studs or plywood panels for retrofit cases.
3. INC1 measures longitudinal rotation of load transfer beam. INC2 measures the transverse rotation of the load transfer beam.
4. INC3 and INC4 measure the rotation of the transverse beams where axial load is applied.
5. LCNW and LCSW monitor the axial load on the West Side of the wall.

Instrumentation Elevation (E2)
Framing Face
2' Tall Cripple Wall

Figure B.2 Specimen A-3 instrumentation.

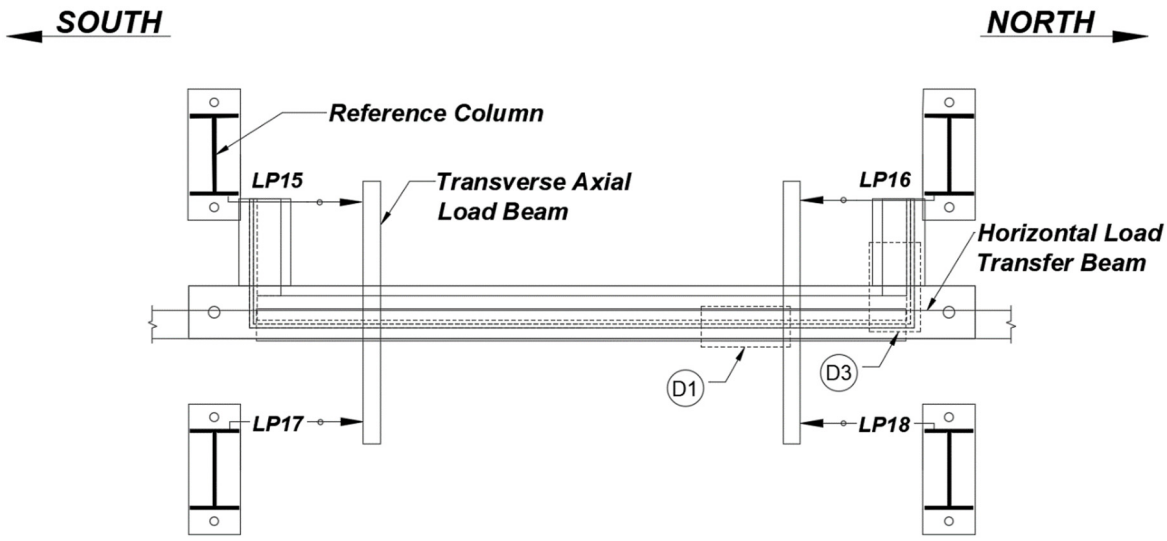

Notes:

1. LP15 - LP19 monitor the displacement of the transverse axial load beams.

Instrumentation Plan View (P1)
2' Tall Cripple Wall

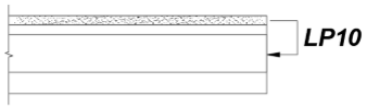

Notes:

1. LP10 monitors the differential displacement between the stucco and the top plate.

Instrumentation Detail (D1)
Stucco Detachment

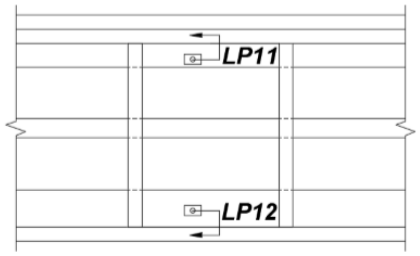

Notes:

1. LP11 and LP12 monitor the siding slip.

Instrumentation Detail (D2)
Siding

Figure B.2 (continued).

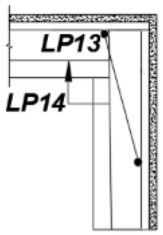

Notes:

1. LP13 monitors the displacement of the of the wall relative to the return wall.
2. LP14 monitors the displacement of the top plates for the wall and the wall return.

Instrumentation Detail (D3)
Top Boundary Condition C Corner

Figure B.2 (continued).

B.2.3 Specimen A-5 Instrumentation Drawings of Test 5

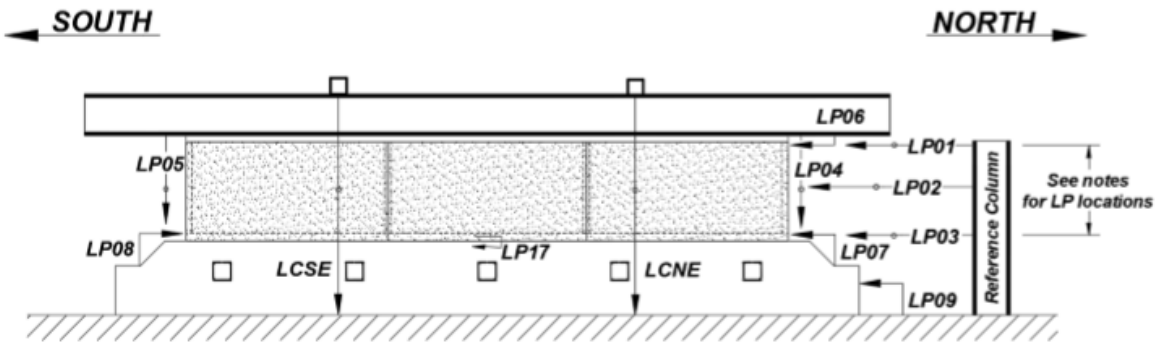

Notes:

1. LP01, LP02, and LP03 measure lateral displacement with LP01 attached to middle of second top plate, LP02 attached to middle of stud, and LP03 attached to middle of sill plate.
2. LP04 and LP05 measure the uplift at each end of the wall.
3. LP06 monitors the slip between the horizontal transfer beam and the upper top plate.
4. LP07 and LP08 monitor the slip between the footing and the sill plate.
5. LP09 monitors the slip of the footing.
5. LCNE and LCSE monitor the axial load on the East Side of the wall.
6. LP17 monitors displacement of stucco relative to the footing.

Instrumentation Elevation (E1)
Stucco Face
2' Tall Cripple Wall

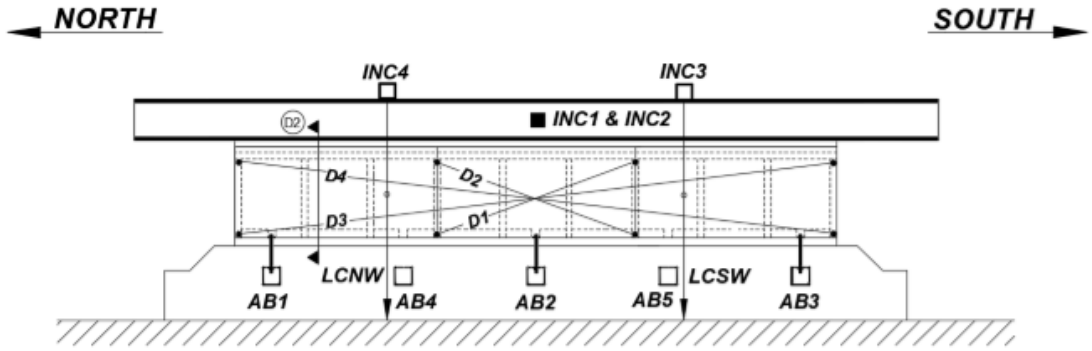

Notes:

1. AB1-AB5 are instrumented with 2" Ø Donut Load Cells measuring uplift loads.
2. Pairs of strength potentiometers are mounted on framing studs or plywood panels for retrofit cases.
3. INC1 measures longitudinal rotation of load transfer beam. INC2 measures the transverse rotation of the load transfer beam.
4. INC3 and INC4 measure the rotation of the transverse beams where axial load is applied.
5. LCNW and LCSW monitor the axial load on the West Side of the wall.

Instrumentation Elevation (E2)
Framing Face
2' Tall Cripple Wall

Figure B.3 Specimen A-5 instrumentation for Test 5.

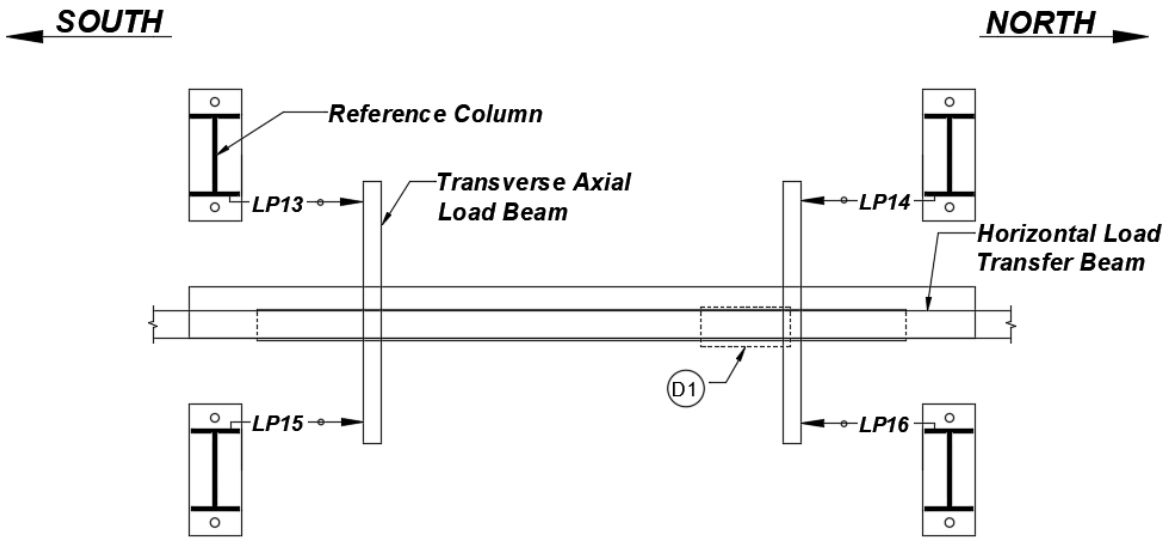

Notes:

1. LP13 - LP16 monitor the displacement of the transverse axial load beams.

Instrumentation Plan View (P1)
2' Tall Cripple Wall

Notes:

1. LP10 monitors the differential displacement between the stucco and the top plate.

Instrumentation Detail (D1)
Stucco Detachment

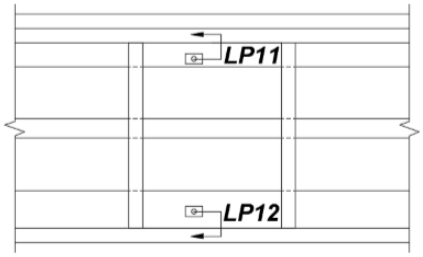

Notes:

1. LP11 and LP12 monitor the siding slip.

Instrumentation Detail (D2)
Siding

Figure B.3 (continued).

B.2.4 Specimen A-6 Instrumentation Drawings

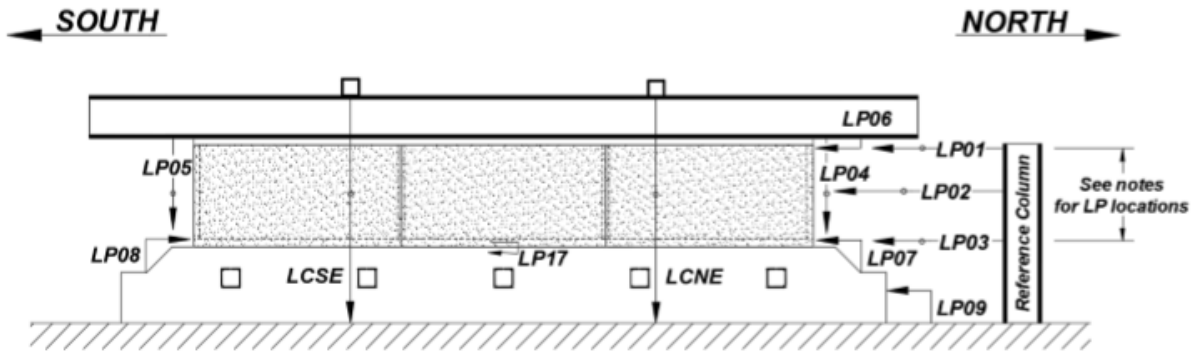

Notes:

1. LP01, LP02, and LP03 measure lateral displacement with LP01 attached to middle of second top plate, LP02 attached to middle of stud, and LP03 attached to middle of sill plate.
2. LP04 and LP05 measure the uplift at each end of the wall.
3. LP06 monitors the slip between the horizontal transfer beam and the upper top plate.
4. LP07 and LP08 monitor the slip between the footing and the sill plate.
5. LP09 monitors the slip of the footing.
5. LCNE and LCSE monitor the axial load on the East Side of the wall.
6. LP17 monitors displacement of stucco relative to the footing.

Instrumentation Elevation (E1)
Stucco Face
2' Tall Cripple Wall

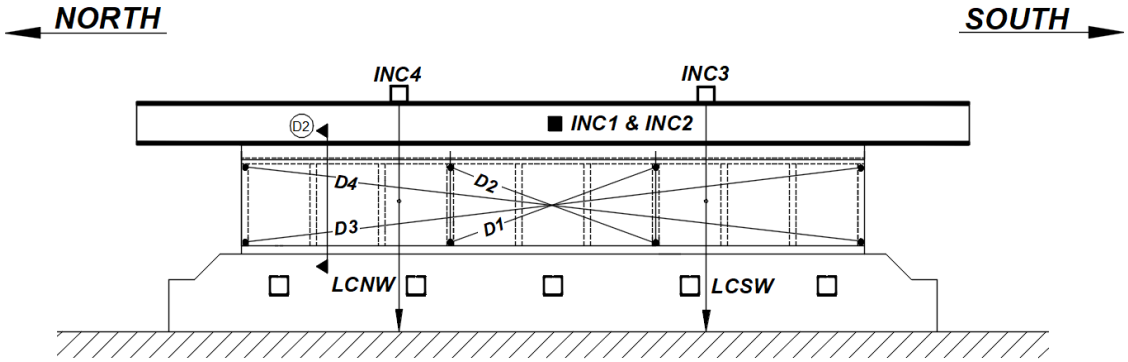

Notes:

1. Pairs of strength potentiometers are mounted on framing studs or plywood panels for retrofit cases.
2. INC1 measures longitudinal rotation of load transfer beam. INC2 measures the transverse rotation of the load transfer beam.
3. INC3 and INC4 measure the rotation of the transverse beams where axial load is applied.
4. LCNW and LCSW monitor the axial load on the West Side of the wall.

Instrumentation Elevation (E2)
Framing Face
2' Tall Cripple Wall

Figure B.4 Specimens A-6 instrumentation.

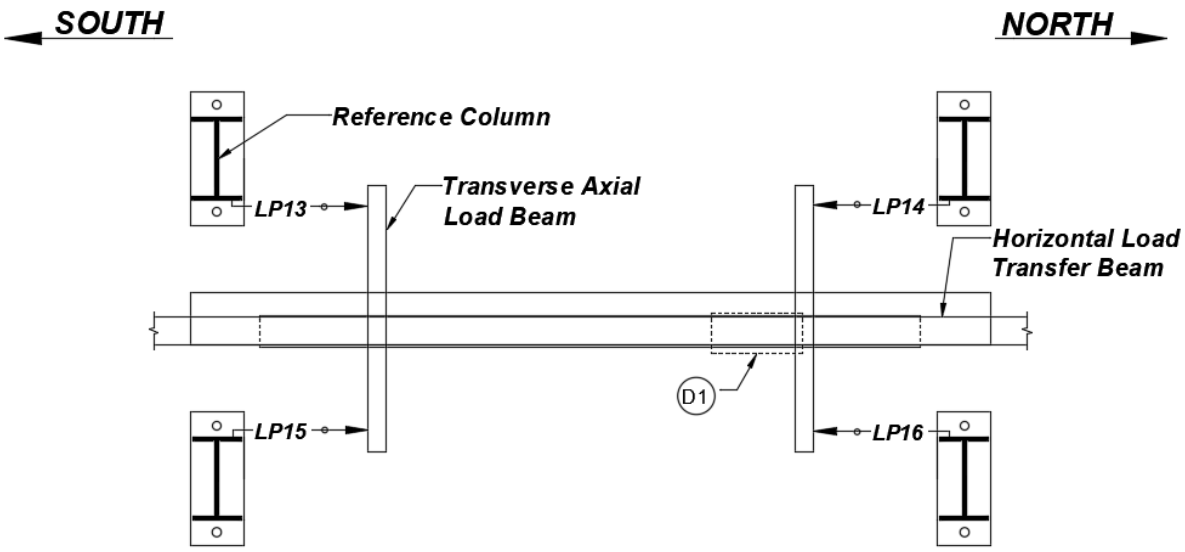

Notes:
1. LP13 - LP16 monitor the displacement of the transverse axial load beams.

Instrumentation Plan View (P1)
2' Tall Cripple Wall

Notes:
1. LP10 monitors the differential displacement between the stucco and the top plate.

Instrumentation Detail (D1)
Stucco Detachment

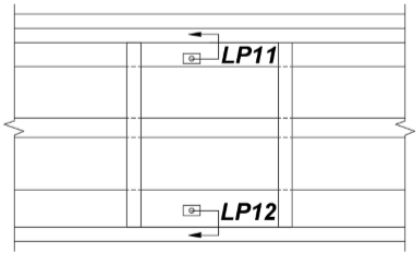

Notes:
1. LP11 and LP12 monitor the siding slip.

Instrumentation Detail (D2)
Siding

Figure B.4 (continued).

APPENDIX C TEST RESULTS

Appendix C includes four sections: anchor bolt load measurements (C.1), diagonal distortion measurements (C.2), uplift measurements (C.3), and sheathing board displacement measurements (C.4). Discussion of these sections is provided in Chapter 4.

C.1 ANCHOR BOLT MEASUREMENTS

Tension in anchor bolts were measured with 10-kip donut load cells placed on top of the square plate washers. A spherical washer was placed on top of the load cell and fastened with a nut. For un-retrofitted cripple walls, three anchor bolts were used, spaced at 64 in. on center. The anchor bolt layout for these cripple walls can be seen in Figure 4.35. For retrofitted cripple walls, additional anchor bolts were added per the ATC-110 retrofit guidelines. Specimen A-3, the cripple wall with a return wall, contained two additional anchor bolts on each return wall. For Specimens A-1 and A-4, the anchor bolts were tensioned between 4 and 5 kips. This was reduced to tensioning of around 1 kip per anchor bolt for Specimens A-2 and A-5. The last cripple wall tested in Phase 1, Specimen A-3, started with around 0.2 kips of tension in each anchor bolt, which became the standard tensioning for all tests in subsequent phases. This is meant to mimic a hand-tightened amount of tension commonly observed in the field for older homes.

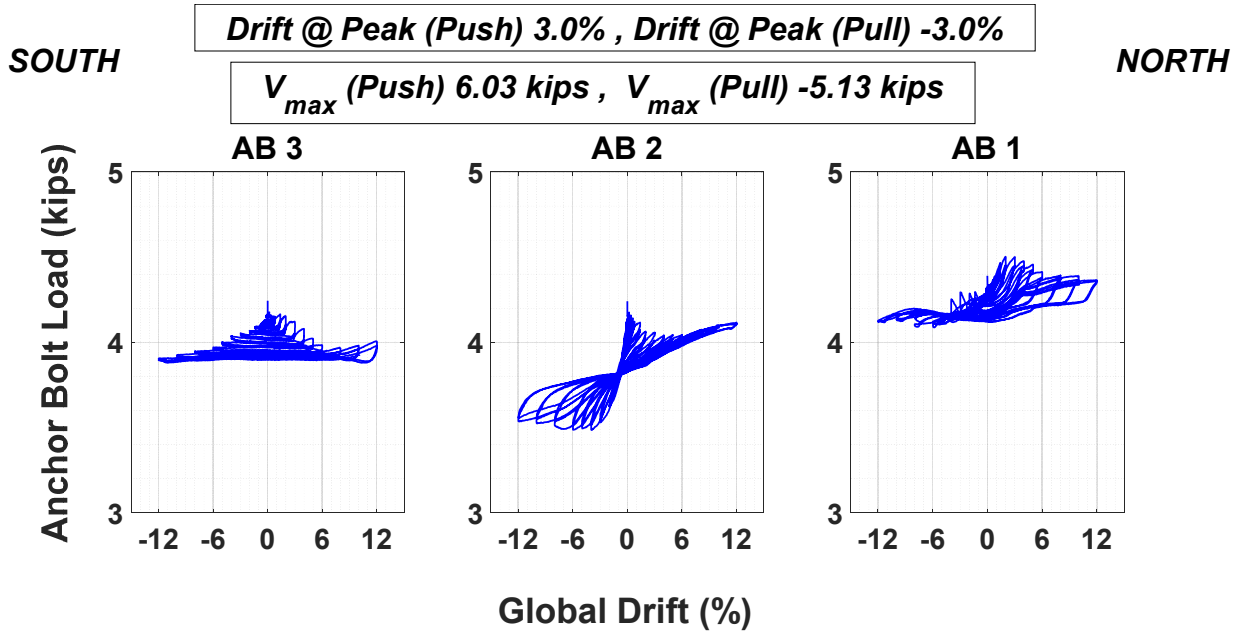

Figure C.1 Specimen A-1 anchor bolt loads versus global drift.

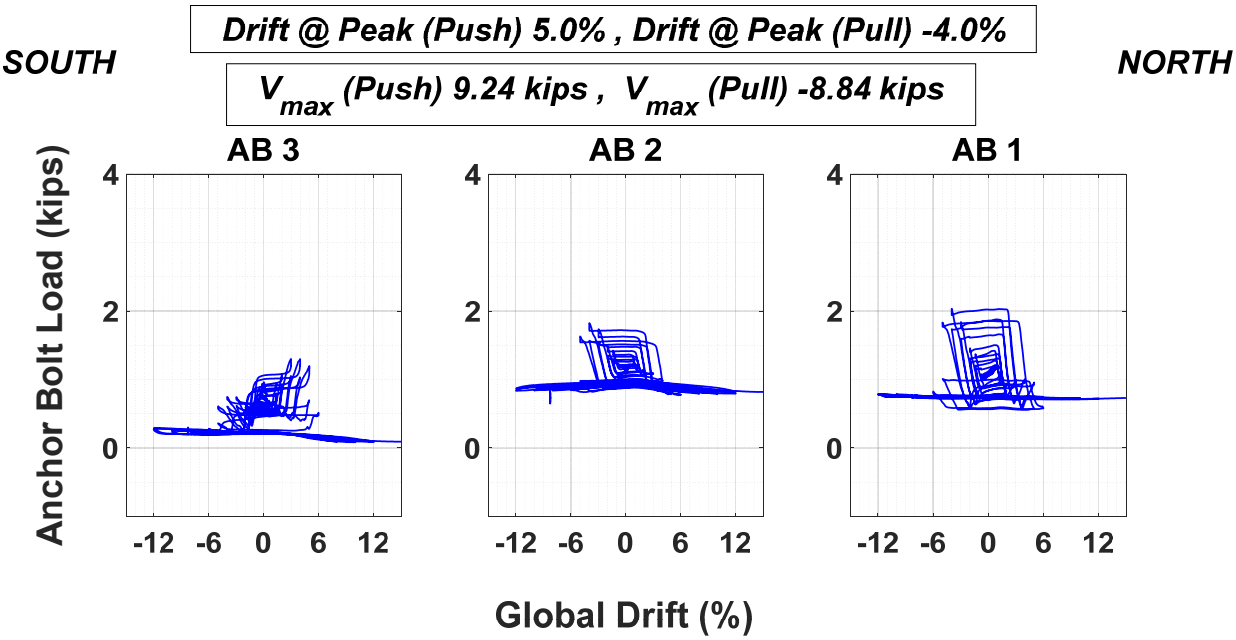

Figure C.2 Specimen A-2 anchor bolt loads versus global drift.

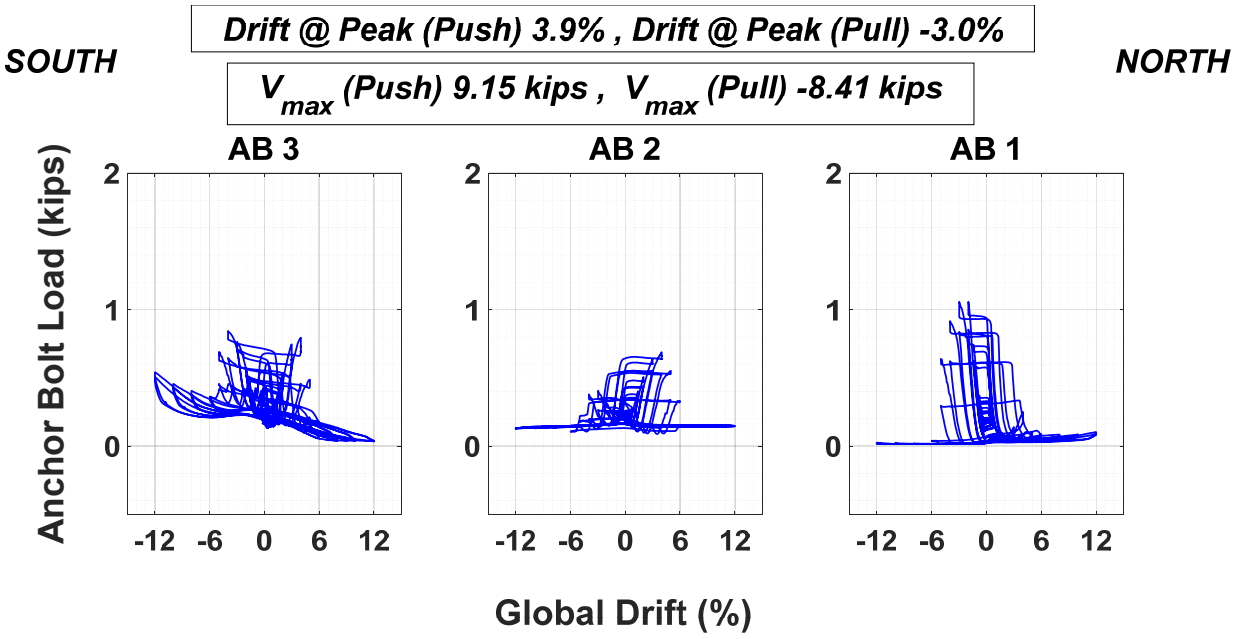

Figure C.3 Specimen A-3 anchor bolt loads versus global drift.

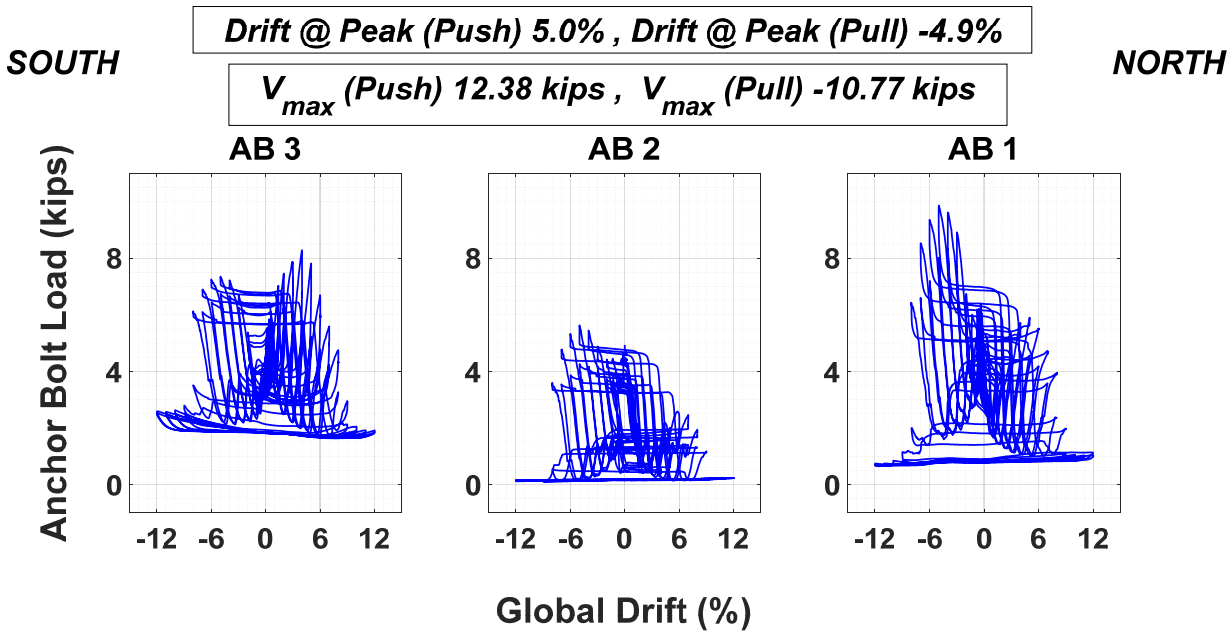

Figure C.4 Specimen A-4 anchor bolt loads versus global drift.

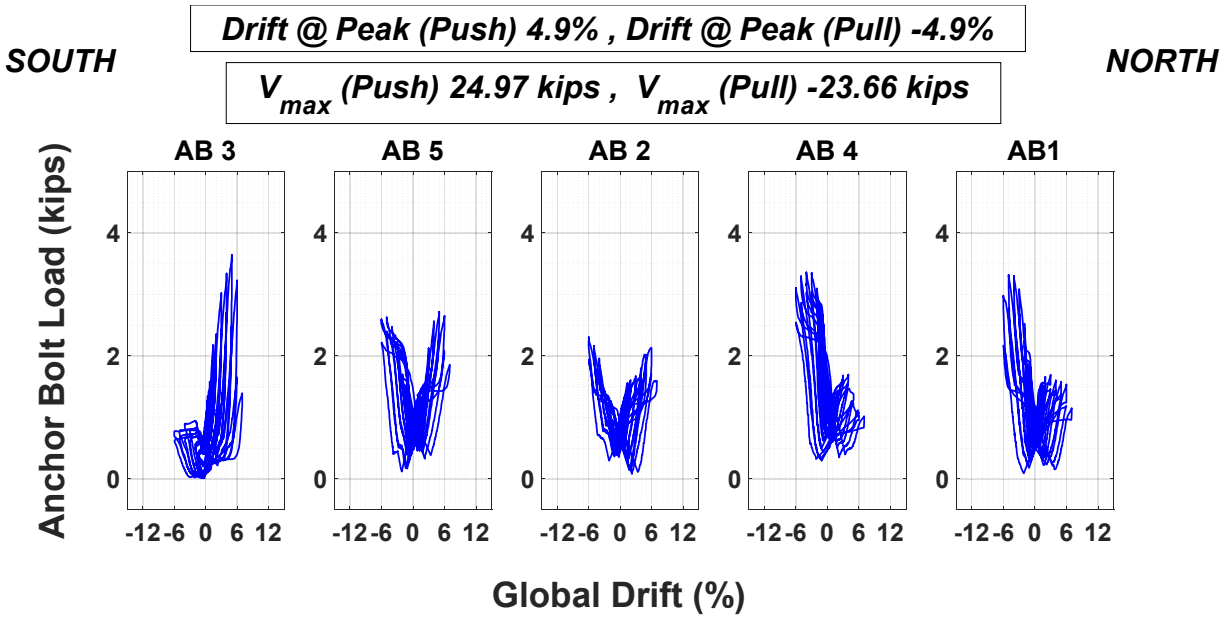

Figure C.5 Specimen A-5: anchor bolt loads versus global drift.

C.2 DIAGONAL DISTORTION MEASUREMENTS

Two pairs of linear displacement potentiometers were used to measure the diagonal distortion of the cripple walls during testing. One pair, shown in Figure C.6 and denoted as D1 and D2, measured the distortion of the middle third of the cripple wall. These are referred to as the inner diagonal measurements. The other pair, denoted as D3 and D4, measured the distortion across the entire cripple wall. These are referred to as the outer diagonal measurements. The diagonal measurements are useful in determining the amount of shear distortion experienced by the cripple wall during testing. When coupled with the uplift measurements, LP04 and LP05, the amount of lateral displacement of the cripple wall can be resolved and compared to the measured lateral displacement. Figure C.7 gives a schematic for the how the resolved lateral displacements from diagonal and uplift measurements were derived.

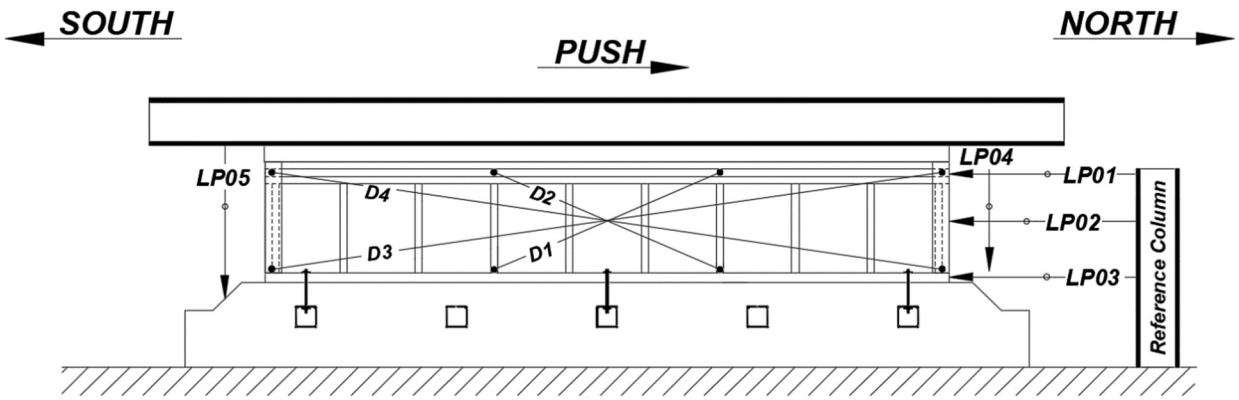

Figure C.6 **Diagonal, end uplift, and lateral displacement potentiometer schematic.**

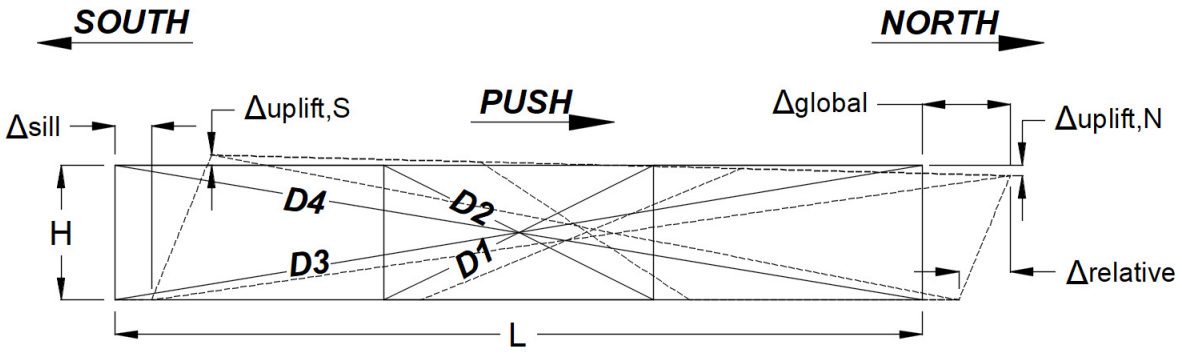

Figure C 7 **Deformed cripple wall with measurements used for resolving lateral displacement from diagonal and uplift measurements.**

The resolved lateral displacement from the diagonal and end uplift potentiometer measurements is as follows:

Undeformed diagonal lengths

$$L_{D30} = L_{D40} = \sqrt{L^2 + H^2}$$

$$L_{D10} = L_{D20} = \sqrt{\left(\frac{L}{3}\right)^2 + H^2}$$

$$where, \quad L = horizontal\ distance\ between\ D3\ and\ D4,$$
$$H = vertical\ distance\ between\ D3\ and\ D4$$

Diagonal measurement relationship

$$D1 = L_{D1} - L_{D10}$$
$$D2 = L_{D2} - L_{D20}$$
$$D3 = L_{D3} - L_{D30}$$
$$D4 = L_{D4} - L_{D40}$$

$$where, \quad D1, D2, D3, and\ D4\ are\ the\ diagonal\ measurements$$
$$and\ L_{D1}, L_{D2}, L_{D3}, and\ L_{D4}\ are\ the\ deformed\ lengths\ of\ the\ diagonals$$

Assume the uplift is linear across the entire wall. Therefore, the uplift at locations of D1, D2, D3, and D4 measurements can be linearly interpolated:

$$\Delta_{uplift}(x) = \Delta_{uplift,N} + \frac{\left(\Delta_{uplift,S} - \Delta_{uplift,N}\right)}{L + 2L_{end}}(x)$$

$where\ L_{end}$
$= horiztonal\ distance\ from\ the\ uplift\ measurement\ to\ the\ outside\ diagonal\ measurement$

$$For\ D1: \quad x = \frac{2L}{3} + L_{end} \ \therefore \Delta_{uplift,D1} = \Delta_{uplift,N} + \frac{\left(\Delta_{uplift,S} - \Delta_{uplift,N}\right)}{L + 2L_{end}} * \left(\frac{2L}{3} + L_{end}\right)$$

$$For\ D2: \quad x = \frac{L}{3} + L_{end} \ \therefore \Delta_{uplift,D2} = \Delta_{uplift,N} + \frac{\left(\Delta_{uplift,S} - \Delta_{uplift,N}\right)}{L + 2L_{end}} * \left(\frac{L}{3} + L_{end}\right)$$

$$For\ D3: \quad x = L + L_{end} \ \therefore \Delta_{uplift,D3} = \Delta_{uplift,N} + \frac{\left(\Delta_{uplift,S} - \Delta_{uplift,N}\right)}{L + 2L_{end}} * \left(L + L_{end}\right)$$

$$For\ D4: \quad x = L_{end} \ \therefore \Delta_{uplift,D4} = \Delta_{uplift,N} + \frac{\left(\Delta_{uplift,S} - \Delta_{uplift,N}\right)}{L + 2L_{end}} * \left(L_{end}\right)$$

$where\ \Delta_{uplift,N}\ is\ measured\ from\ LP04\ and\ \Delta_{uplift,S}\ are\ measured\ from\ LP05$

Deformed diagonal lengths (sample calculation for D1)

$$L_{D1} = \sqrt{\left(\frac{L}{3} - \Delta_{relative}\right)^2 + \left(H + \Delta_{uplift,D1}\right)^2}$$

$$L_{D2} = \sqrt{\left(\frac{L}{3} + \Delta_{relative}\right)^2 + \left(H + \Delta_{uplift,D2}\right)^2}$$

$$L_{D3} = \sqrt{\left(L - \Delta_{relative}\right)^2 + \left(H + \Delta_{uplift,D3}\right)^2}$$

$$L_{D4} = \sqrt{\left(L + \Delta_{relative}\right)^2 + \left(H + \Delta_{uplift,D4}\right)^2}$$

$where\ \Delta_{relative}\ is\ positive\ in\ the\ push\ direction\ and\ negative\ in\ the\ pull\ direction$

Vertical component of uplift measurements

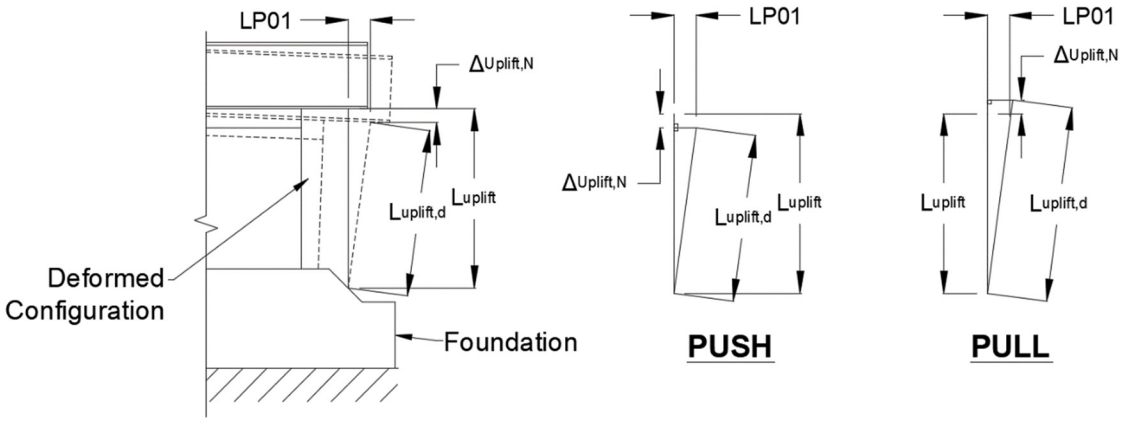

Figure C.8 Schematic for resolving end of wall uplift.

$Let, \quad L_{uplift} = length\ of\ uplift\ measurement\ string,\ L_{uplift,d} = deformed\ length\ of\ uplift\ measurement\ string$

Push loading

$$L_{uplift,d} = L_{uplift} + LP04$$

$$L_{uplift,d}^2 = \left(L_{uplift} - \Delta_{uplift,S}\right)^2 + LP01^2$$

$$\Rightarrow \left(L_{uplift} + LP04\right)^2 = \left(L_{uplift} - \Delta_{uplift,S}\right)^2 + LP01^2$$

$$\Rightarrow \left(L_{uplift} - \Delta_{uplift,S}\right)^2 = \left(L_{uplift} + LP04\right)^2 - LP01^2$$

$$\therefore \Delta_{uplift,S} = L_{uplift} - \sqrt{\left(L_{uplift} + LP04\right)^2 - LP01^2}$$

$$\therefore \Delta_{uplift,N} = L_{uplift} - \sqrt{\left(L_{uplift} + LP05\right)^2 - LP01^2}$$

Pull loading

$$L_{uplift,d} = L_{uplift} + LP04$$

$$L_{uplift,d}^2 = \left(L_{uplift} + \Delta_{uplift,S}\right)^2 + LP01^2$$

$$\Rightarrow \left(L_{uplift} + LP04\right)^2 = \left(L_{uplift} + \Delta_{uplift,S}\right)^2 + LP01^2$$

$$\Rightarrow \left(L_{uplift} + \Delta_{uplift,S}\right)^2 = \left(L_{uplift} + LP04\right)^2 - LP01^2$$

$$\therefore \Delta_{uplift,S} = \sqrt{\left(L_{uplift} + LP04\right)^2 - LP01^2} - L_{uplift}$$

$$\therefore\ \Delta_{uplift,N}\ =\ \sqrt{\left(L_{uplift}+LP05\right)^2-LP01^2}-L_{uplift}$$

Solving for relative displacements as a function of uplift and diagonal measurements

$$D1=\ \ L_{D1}-L_{D10}\ \Rightarrow D1=\ \sqrt{\left(\frac{L}{3}+\Delta_{relative}\right)^2+\left(H+\Delta_{uplift,D1}\right)^2}\ -\sqrt{\left(\frac{L}{3}\right)^2+H^2}$$

$$\Rightarrow D1+\sqrt{\left(\frac{L}{3}\right)^2+H^2}=\ \sqrt{\left(\frac{L}{3}+\Delta_{relative}\right)^2+\left(H+\Delta_{uplift,D1}\right)^2}$$

$$\Rightarrow D1^2+2D1\sqrt{\left(\frac{L}{3}\right)^2+H^2}+\left(\frac{L}{3}\right)^2+H^2=\ \left(\frac{L}{3}+\Delta_{relative}\right)^2+\left(H+\Delta_{uplift,D1}\right)^2$$

$$\Rightarrow D1^2+2D1\sqrt{\left(\frac{L}{3}\right)^2+H^2}+\left(\frac{L}{3}\right)^2+H^2-\left(H+\Delta_{uplift,D1}\right)^2=\ \left(\frac{L}{3}+\Delta_{relative}\right)^2$$

$$\Rightarrow\ \sqrt{D1^2+2D1\sqrt{\left(\frac{L}{3}\right)^2+H^2}+\left(\frac{L}{3}\right)^2+H^2-\left(H+\Delta_{uplift,D1}\right)^2}=\frac{L}{3}+\Delta_{relative}$$

Resolved lateral displacements as a function of the uplift and diagonal measurements

$$\therefore\ \Delta_{relative}=\ \sqrt{D1^2+2D1\sqrt{\left(\frac{L}{3}\right)^2+H^2}+\left(\frac{L}{3}\right)^2+H^2-\left(H+\Delta_{uplift,D1}\right)^2}\ -\frac{L}{3}\quad for\ D1$$

$$\therefore\ \Delta_{relative}=\ \frac{L}{3}-\sqrt{D2^2+2D2\sqrt{\left(\frac{L}{3}\right)^2+H^2}+\left(\frac{L}{3}\right)^2+H^2-\left(H+\Delta_{uplift,D2}\right)^2}\quad for\ D2$$

$$\therefore\ \Delta_{relative}=\ \sqrt{D3^2+2D3\sqrt{L^2+H^2}+L^2+H^2-\left(H+\Delta_{uplift,D3}\right)^2}\ -L\quad for\ D3$$

$$\therefore\ \Delta_{relative}=\ L-\sqrt{D2^2+2D2\sqrt{L^2+H^2}+L^2+H^2-\left(H+\Delta_{uplift,D4}\right)^2}\quad for\ D4$$

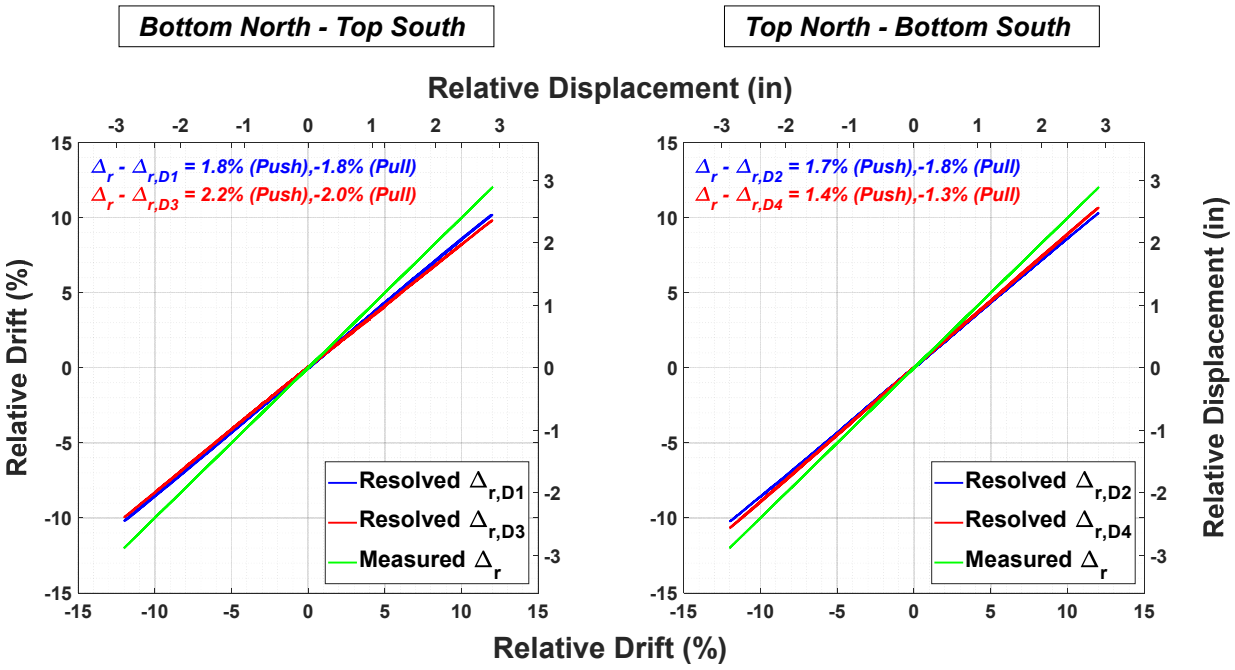

Figure C.9 Specimen A-1 resolved relative drift from diagonal measurements in one direction versus measured relative drift.

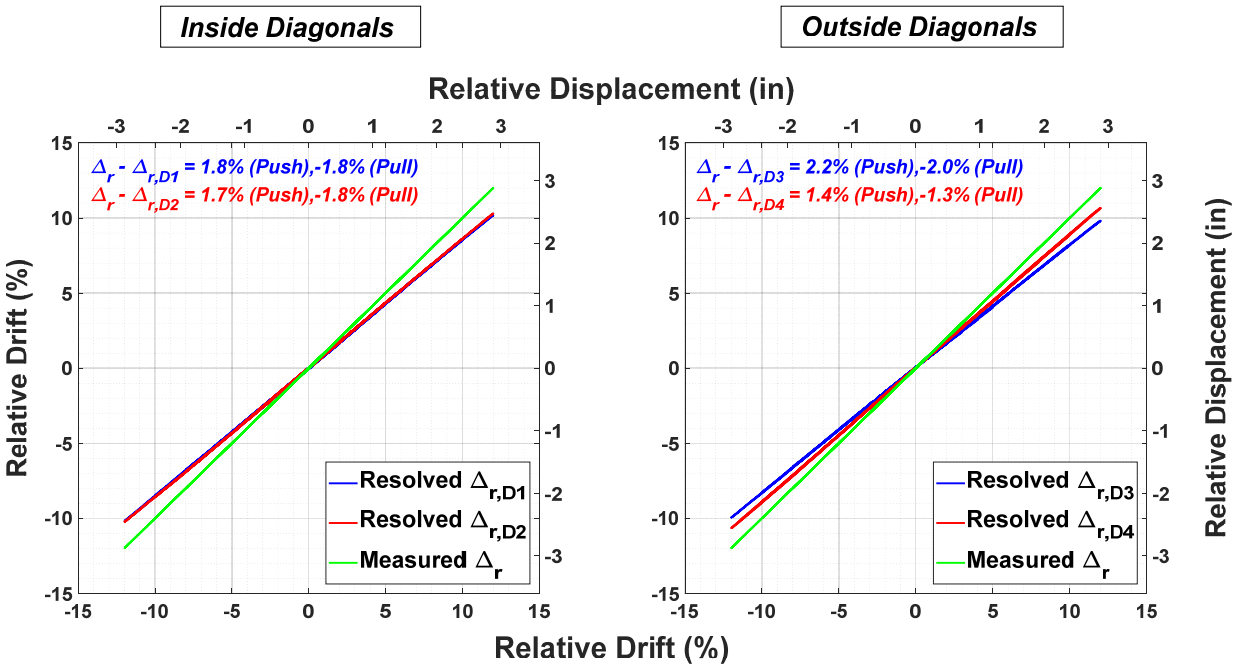

Figure C.10 Specimen A-1 resolved relative drift from diagonal measurements (outside and inside diagonals) versus measured relative drift.

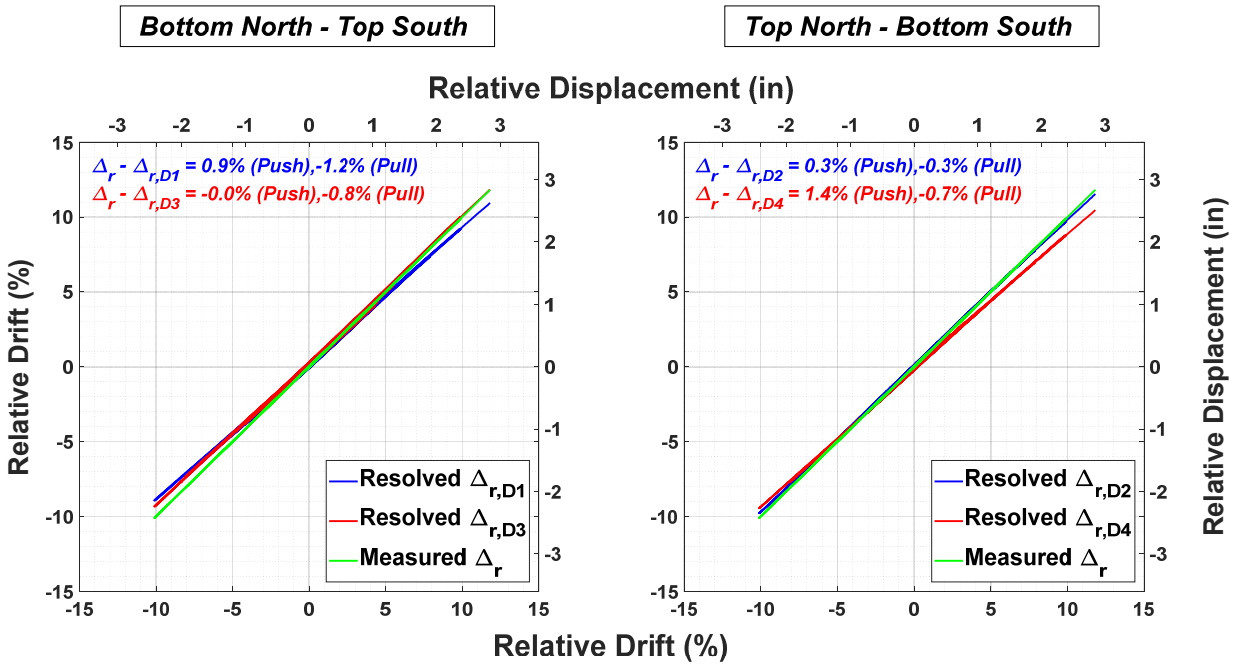

Figure C.11 Specimen A-2 resolved relative drift from diagonal measurements in one direction versus measured relative drift.

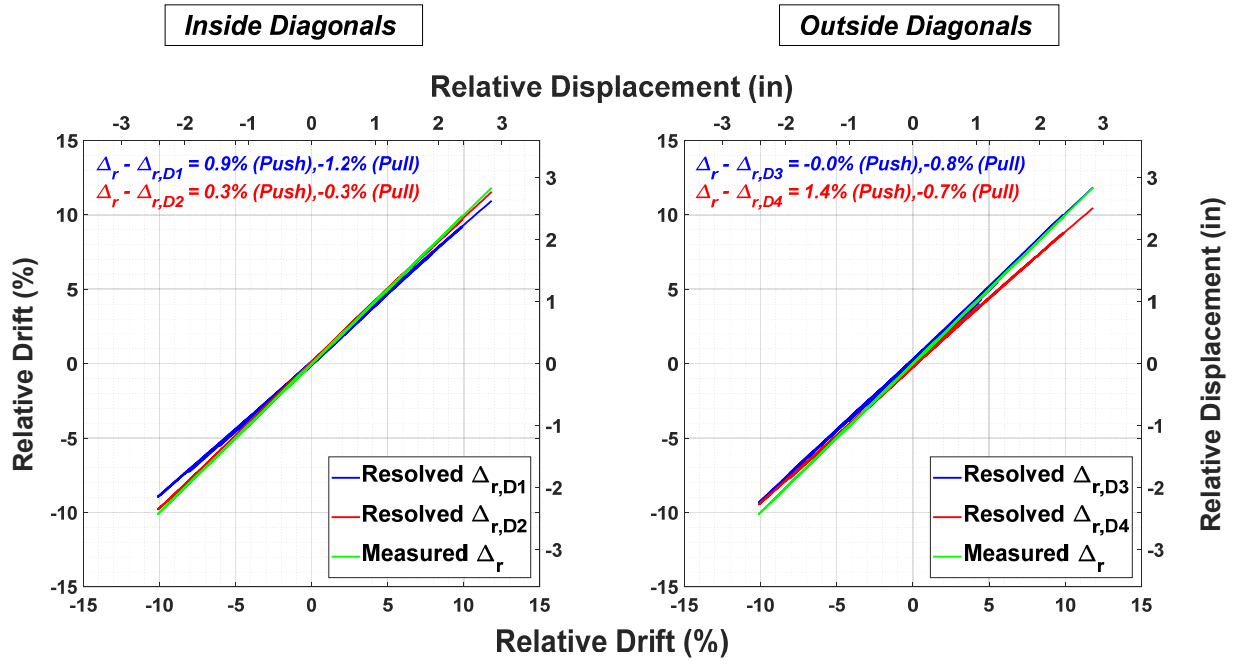

Figure C.12 Specimen A-2 resolved relative drift from diagonal measurements (outside and inside diagonals) versus measured relative drift.

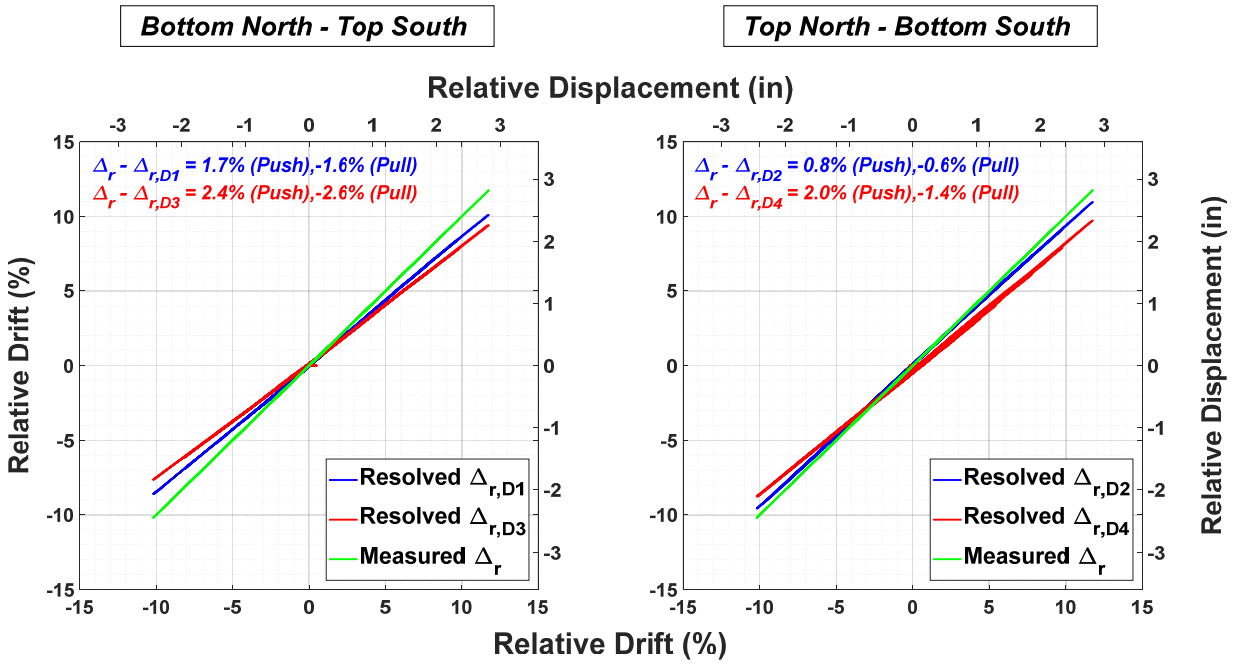

Figure C.13 Specimen A-3 resolved relative drift from diagonal measurements in one direction versus measured relative drift.

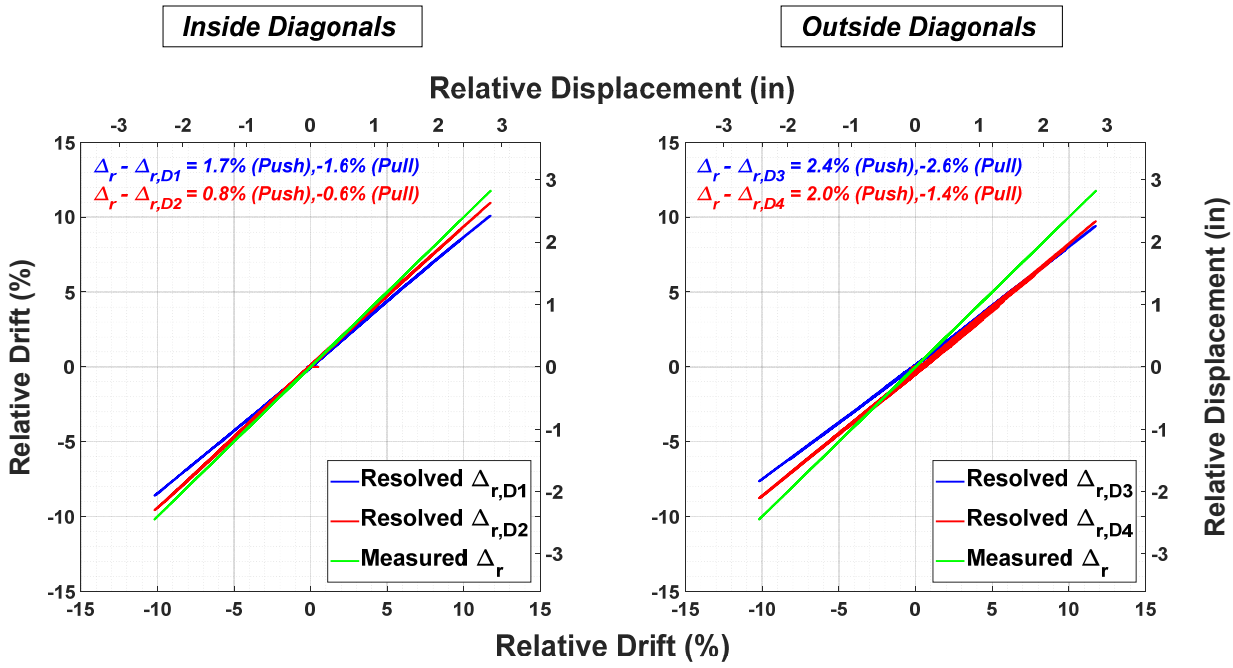

Figure C.14 Specimen A-3 resolved relative drift from diagonal measurements (outside and inside diagonals) versus measured relative drift.

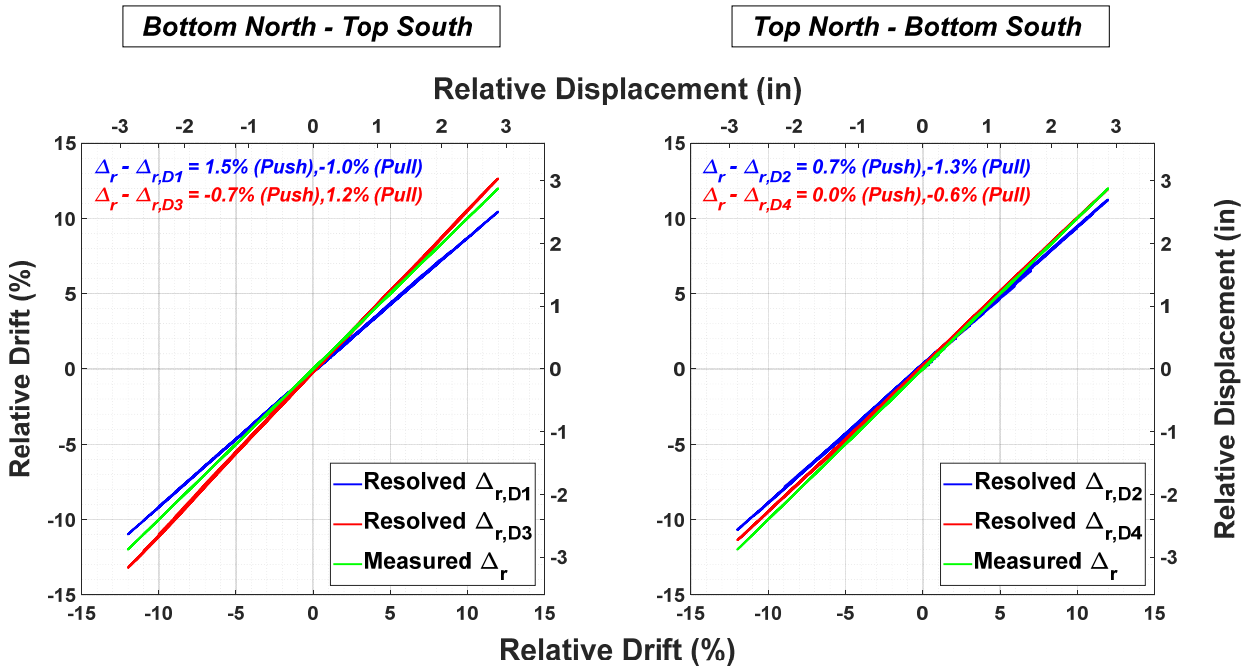

Figure C.15 Specimen A-4 resolved relative drift from diagonal measurements in one direction versus measured relative drift.

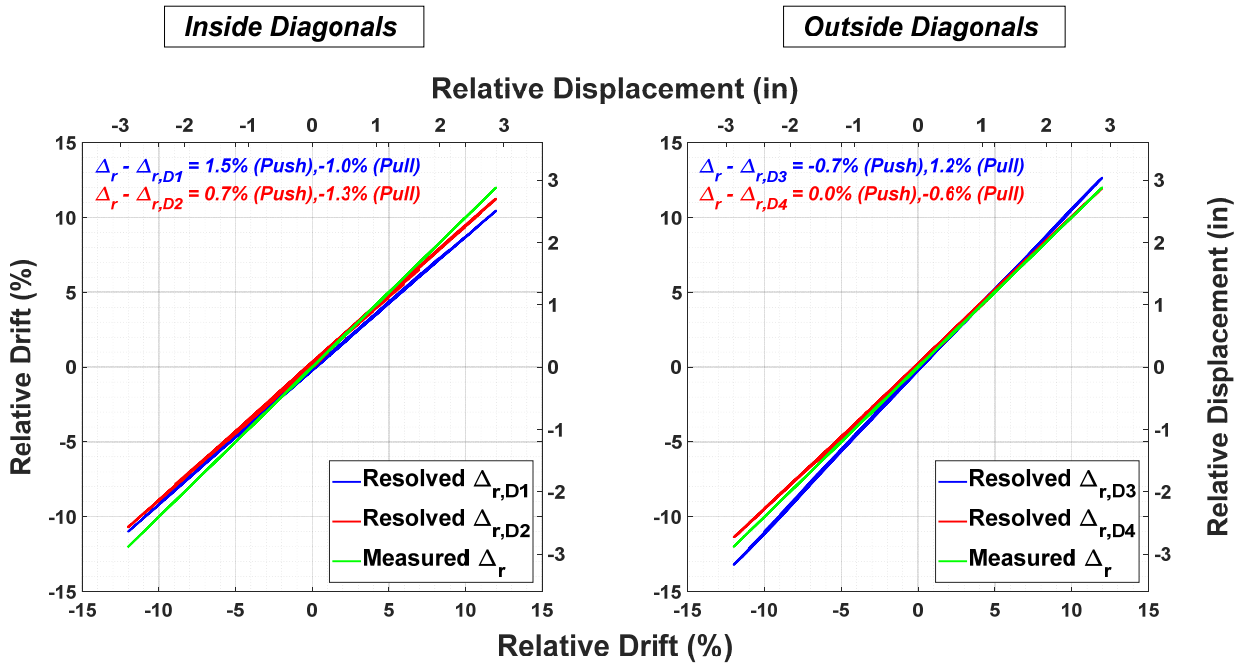

Figure C.16 Specimen A-4 resolved relative drift from diagonal measurements (outside and inside diagonals) versus measured relative drift.

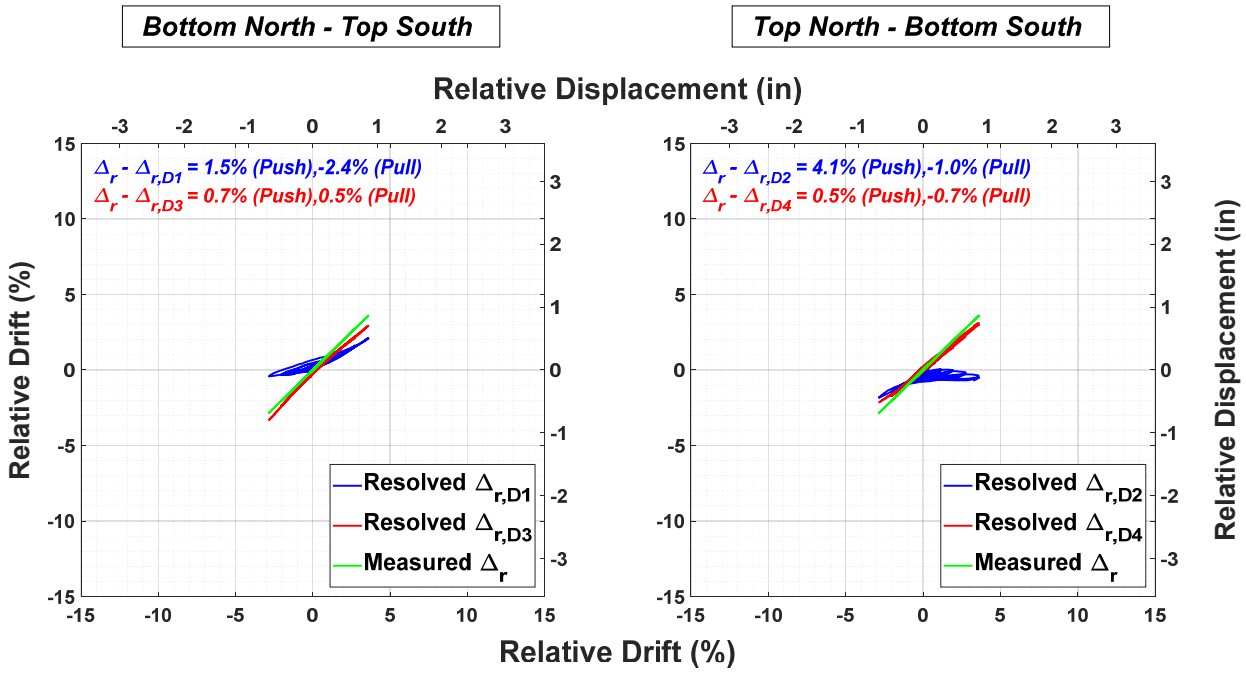

Figure C.17 Specimen A-5 resolved relative drift from diagonal measurements in one direction versus measured relative drift.

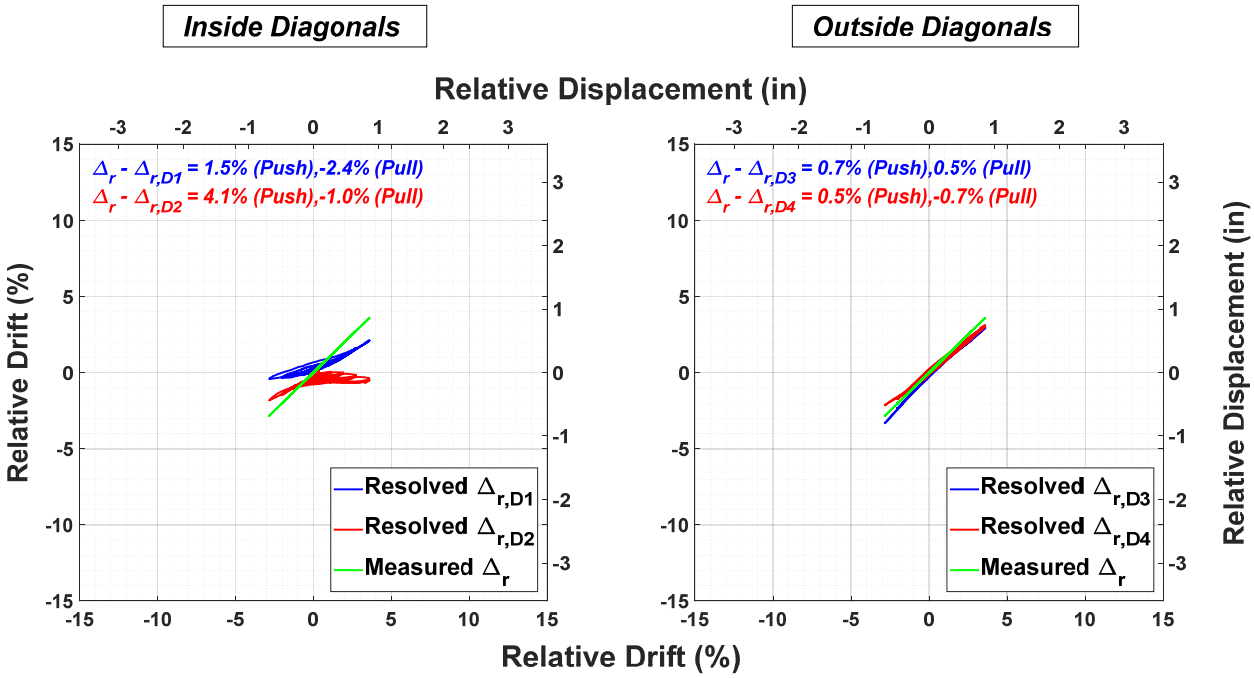

Figure C.18 Specimen A-5 resolved relative drift from diagonal measurements (outside and inside diagonals) versus measured relative drift.

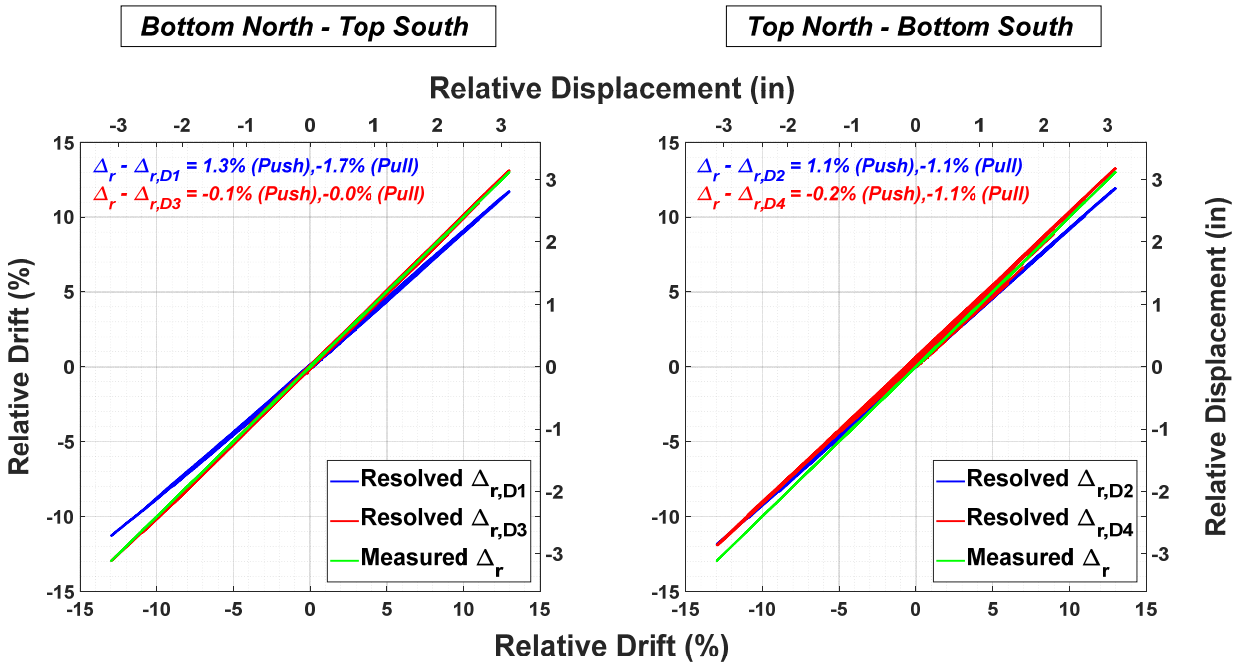

Figure C.19 Specimen A-6 resolved relative drift from diagonal measurements in one direction versus measured relative drift.

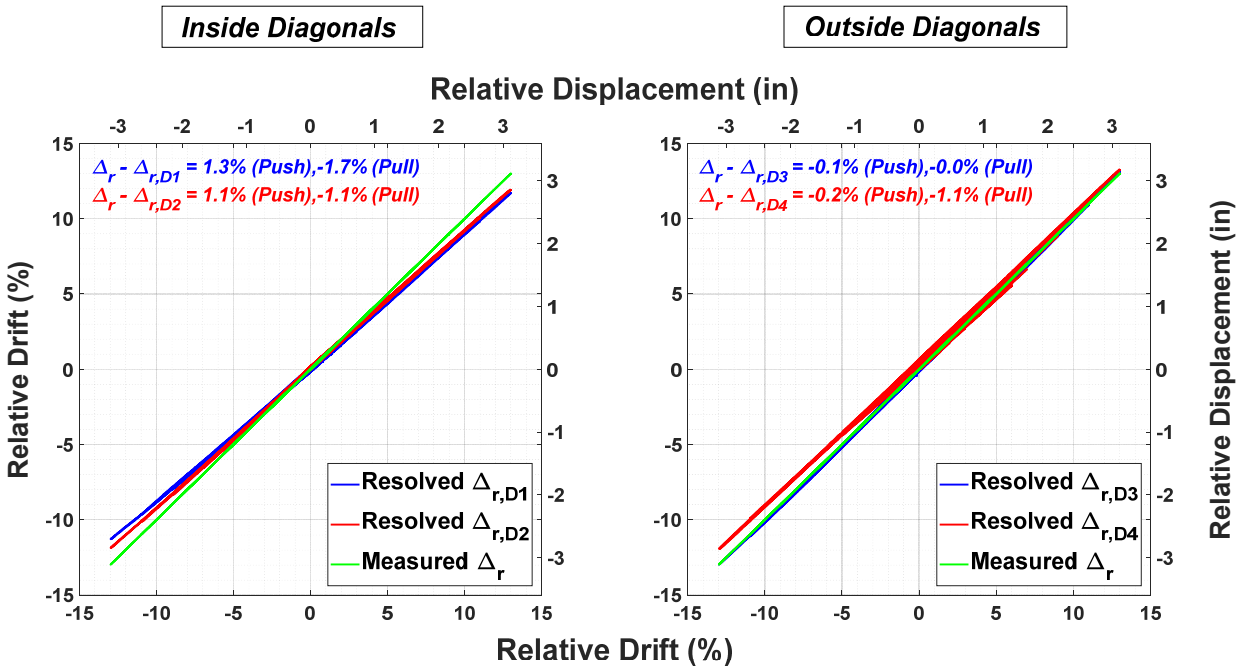

Figure C.20 Specimen A-6 resolved relative drift from diagonal measurements (outside and inside diagonals) versus measured relative drift.

C.3 UPLIFT MEASUREMENTS

Two linear potentiometers were used to measure the uplift at both ends of the cripple wall. These potentiometers were attached to the foundation and the steel load transfer beam. The calculations for determining the uplift of the cripple walls is shown in the previous section as the uplift measurements were factored into calculating the resolved relative displacement from the diagonal measurements.

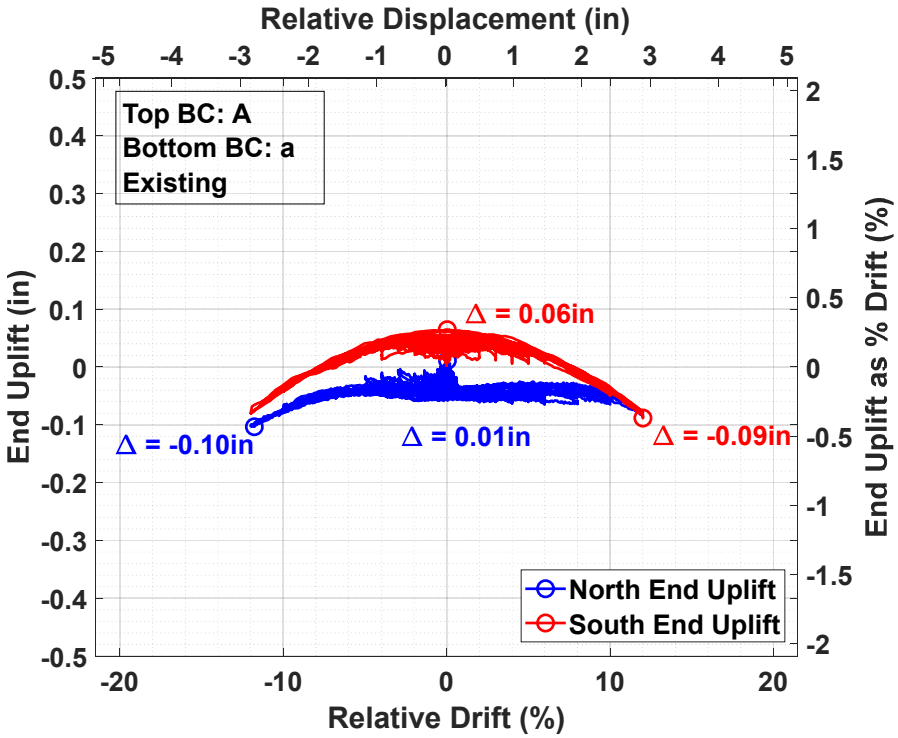

Figure C.21 Specimen A-1 end uplift versus relative drift.

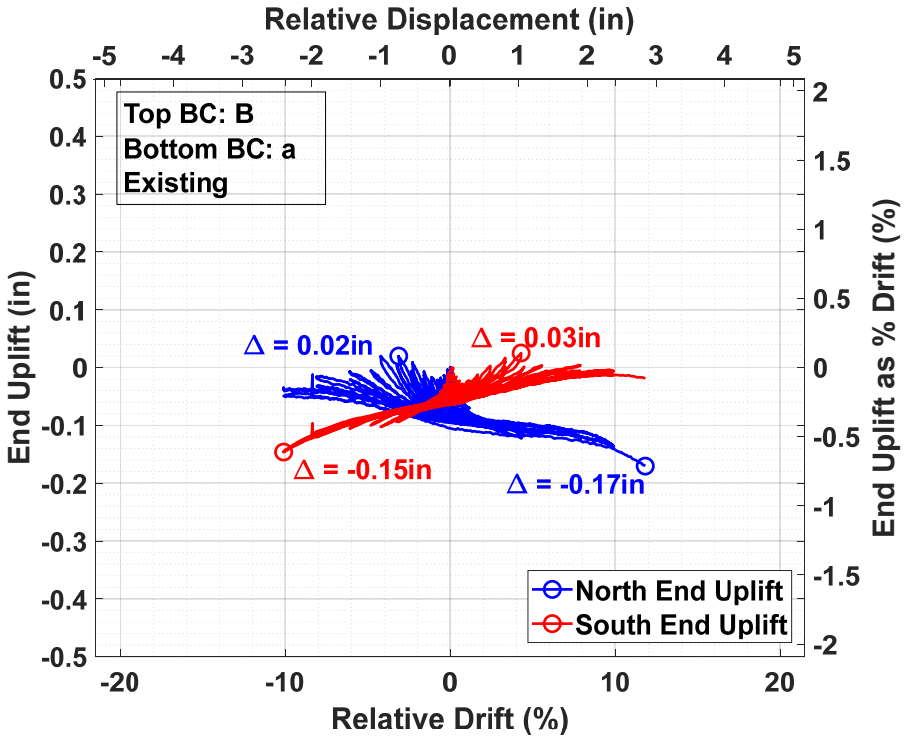

Figure C.22 Specimen A-3 end uplift versus relative drift.

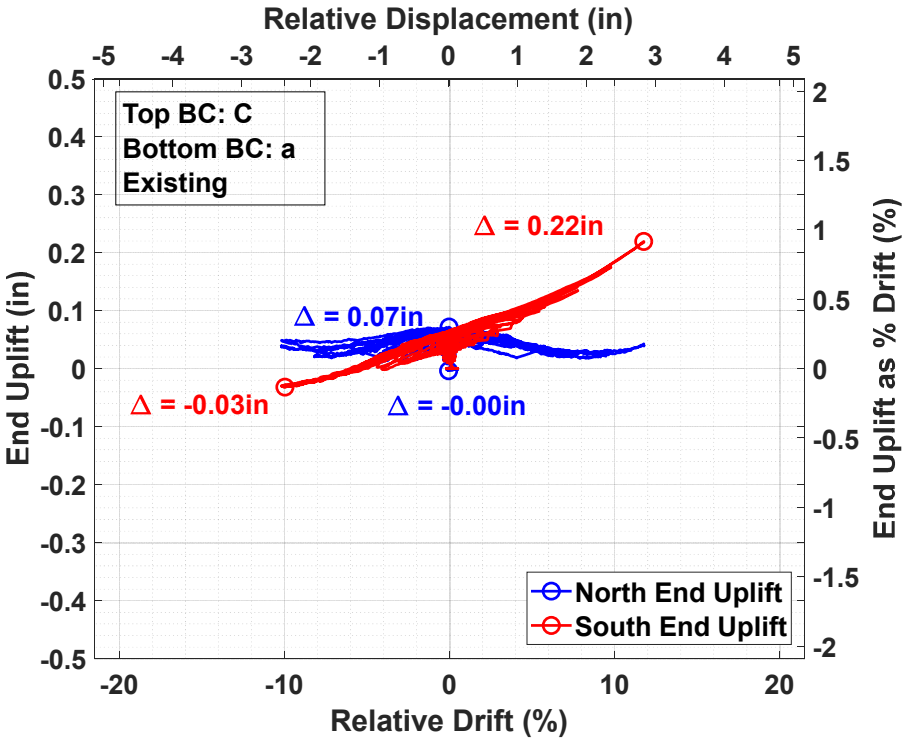

Figure C.23 Specimen A-3 end uplift versus relative drift.

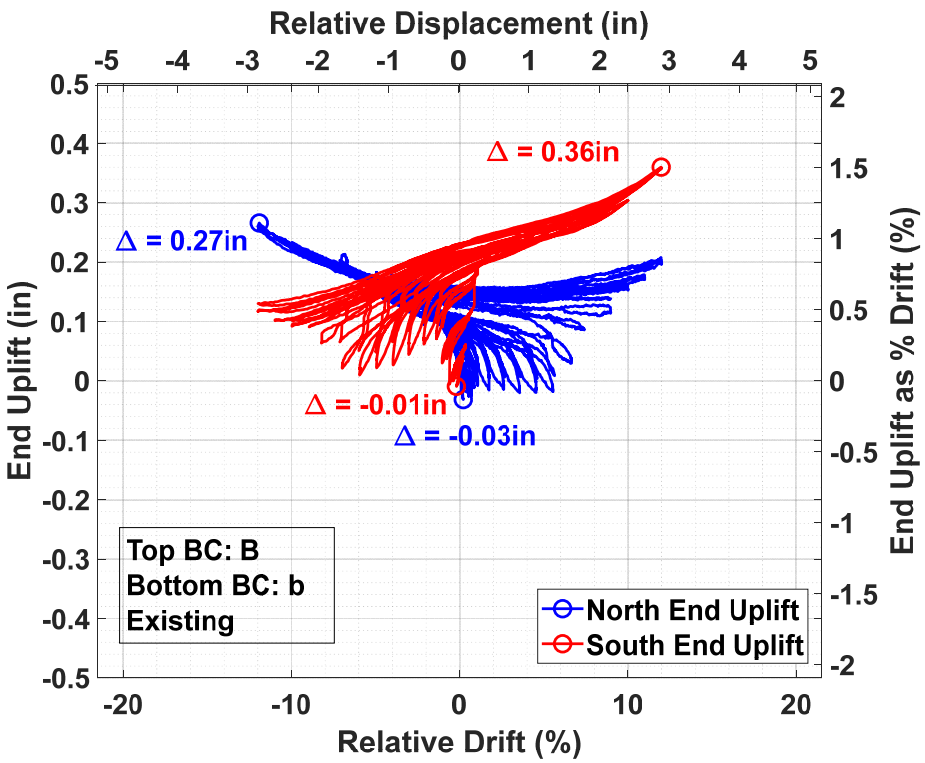

Figure C.24 Specimen A-4 end uplift versus relative drift.

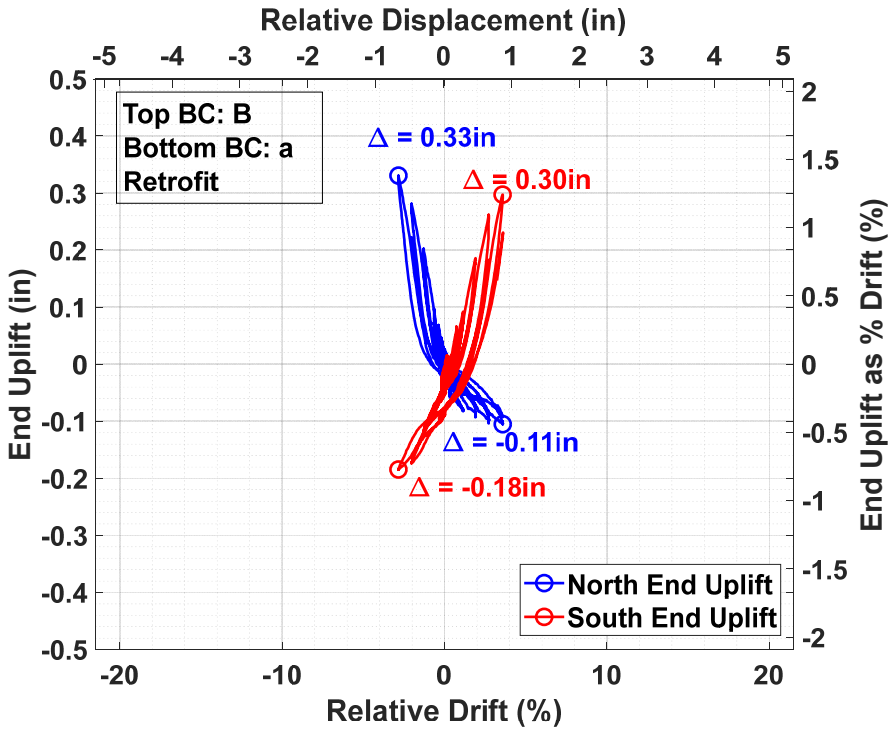

Figure C.25 Specimen A-5 end uplift versus relative drift.

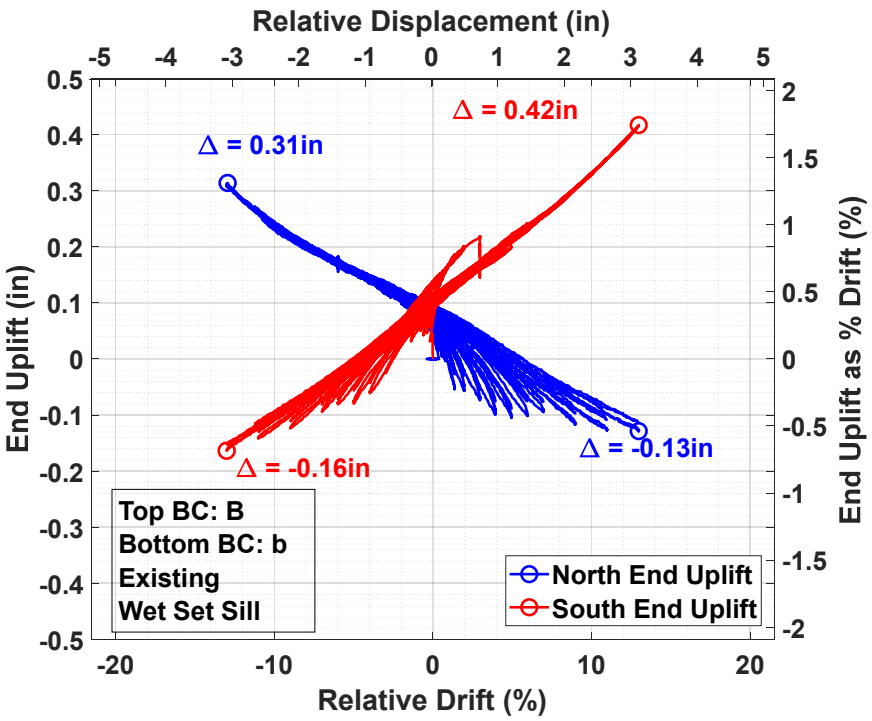

Figure C.26 Specimen A-6 end uplift versus relative drift.

C.4 SHEATHING BOARD MEASUREMENTS

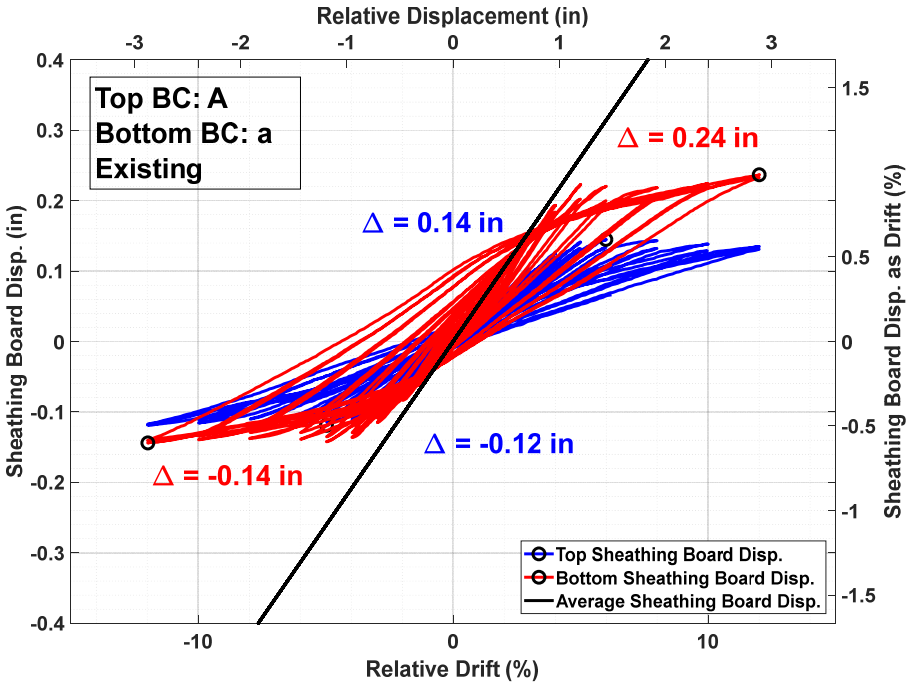

Figure C.27 Specimen A-1 top and bottom sheathing board displacements versus relative drift.

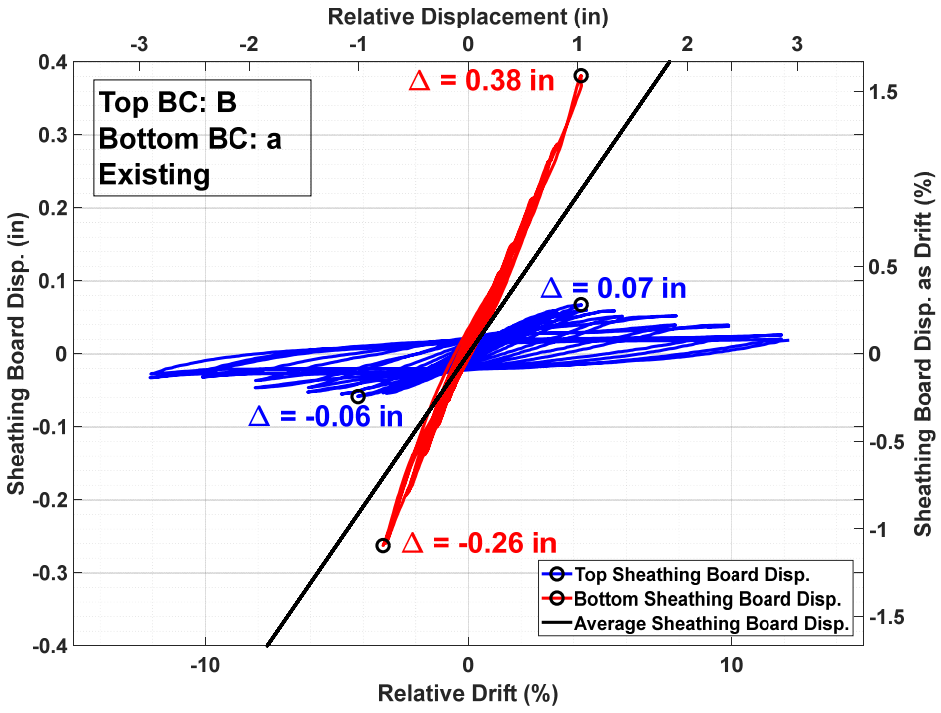

Figure C.28 Specimen A-2 top and bottom sheathing board displacements versus relative drift.

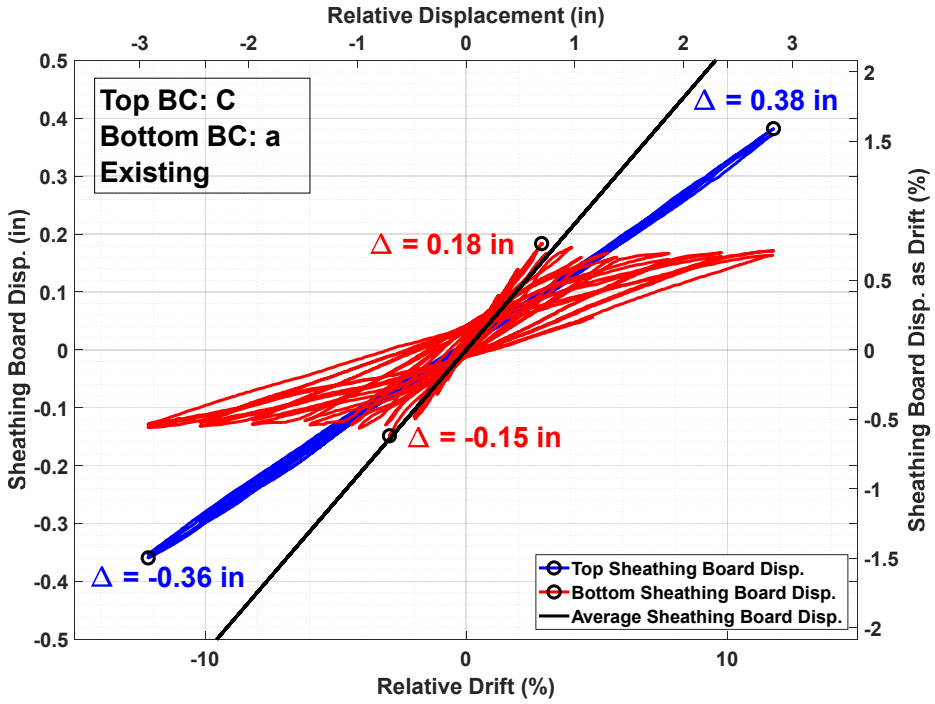

Figure C.29 Specimen A-3 top and bottom sheathing board displacements versus relative drift.

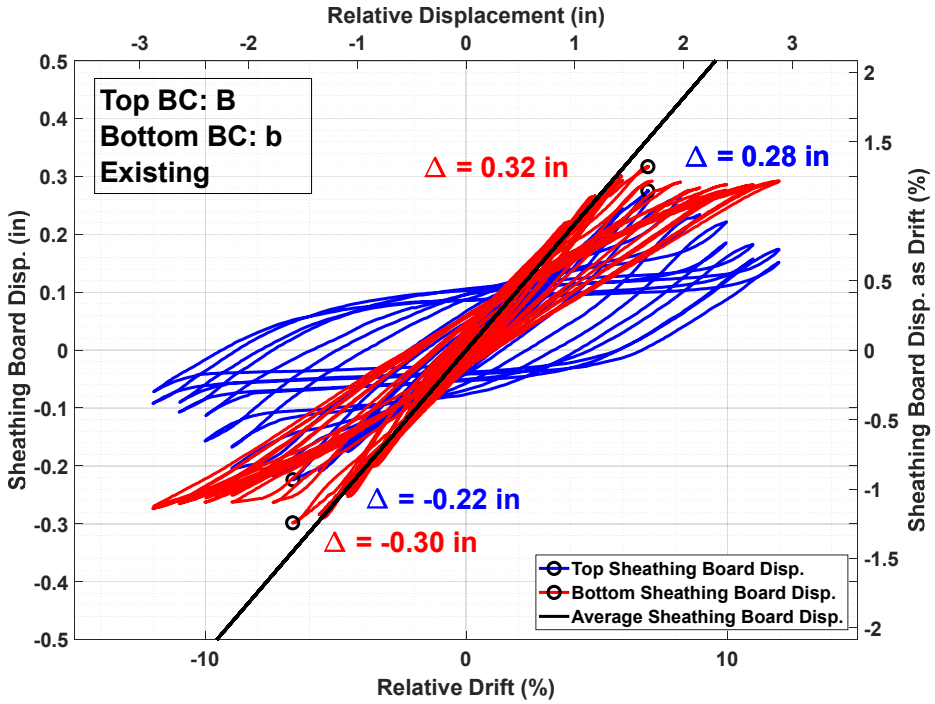

Figure C.30 Specimen A-4 top and bottom sheathing board displacements versus relative drift.

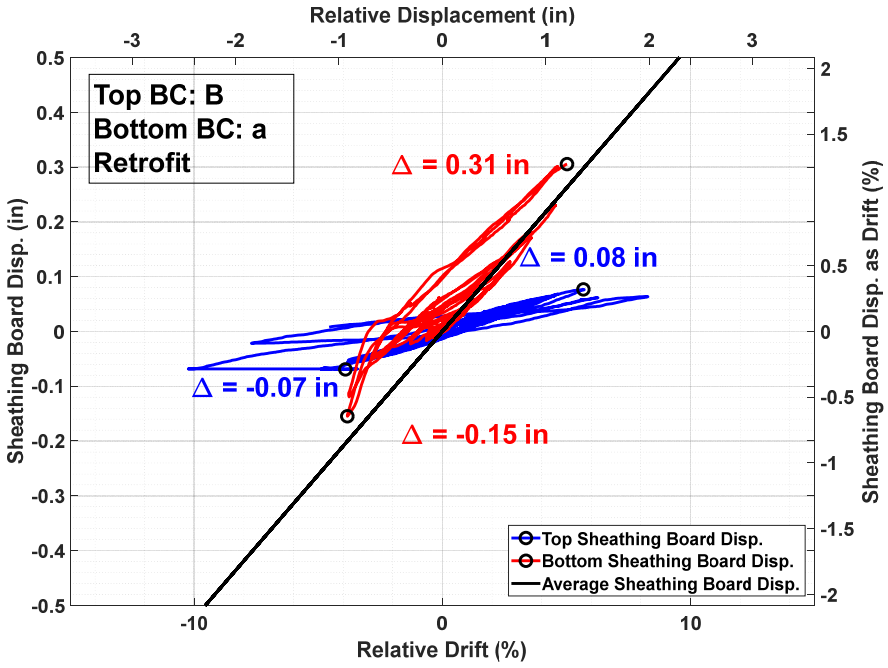

Figure C.31 Specimen A-5 top and bottom sheathing board displacements versus relative drift.

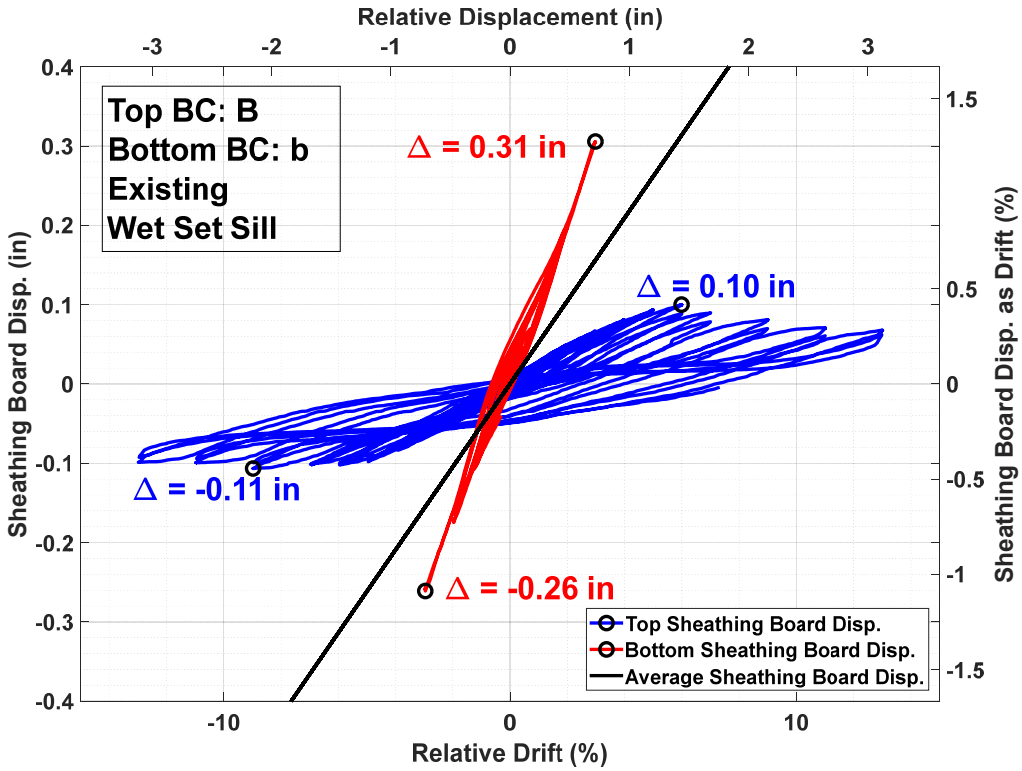

Figure C.32 Specimen A-6 top and bottom sheathing board displacements versus relative drift.

The Pacific Earthquake Engineering Research Center (PEER) is a multi-institutional research and education center with headquarters at the University of California, Berkeley. Investigators from over 20 universities, several consulting companies, and researchers at various state and federal government agencies contribute to research programs focused on performance-based earthquake engineering.

These research programs aim to identify and reduce the risks from major earthquakes to life safety and to the economy by including research in a wide variety of disciplines including structural and geotechnical engineering, geology/seismology, lifelines, transportation, architecture, economics, risk management, and public policy.

PEER is supported by federal, state, local, and regional agencies, together with industry partners.

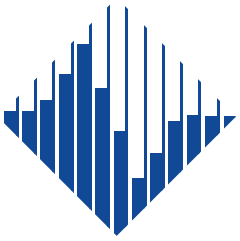

PEER Core Institutions

University of California, Berkeley (Lead Institution)
California Institute of Technology
Oregon State University
Stanford University
University of California, Davis
University of California, Irvine
University of California, Los Angeles
University of California, San Diego
University of Nevada, Reno
University of Southern California
University of Washington

PEER reports can be ordered at https://peer.berkeley.edu/peer-reports or by contacting

Pacific Earthquake Engineering Research Center
University of California, Berkeley
325 Davis Hall, Mail Code 1792
Berkeley, CA 94720-1792
Tel: 510-642-3437
Email: peer_center@berkeley.edu

ISSN 1547-0587X